AEDC-TR-73-171

cy.2

THREE-PARTICLE COLLISION INTEGRALS FOR THERMAL CONDUCTIVITY, VISCOSITY AND SELF-DIFFUSION OF A GAS OF HARD SPHERICAL MOLECULES. PART II CALCULATIONS.

D. T. Gillespie
Earth and Planetary Sciences Division
Naval Weapons Center
China Lake, California 93555

and

J. V. Sengers
Institute for Molecular Physics
University of Maryland
College Park, Maryland 20742

November 1973

Final Report for Period September 1, 1970 – June 30, 1972

Approved for public release; distribution unlimited.

Prepared for

ARNOLD ENGINEERING DEVELOPMENT CENTER
AIR FORCE SYSTEMS COMMAND
ARNOLD AF STATION, TENNESSEE 37389

NOTICES

When U. S. Government drawings specifications, or other data are used for any purpose other than a definitely related Government procurement operation, the Government thereby incurs no responsibility nor any obligation whatsoever, and the fact that the Government may have formulated, furnished, or in any way supplied the said drawings, specifications, or other data, is not to be regarded by implication or otherwise, or in any manner licensing the holder or any other person or corporation, or conveying any rights or permission to manufacture, use, or sell any patented invention that may in any way be related thereto.

Qualified users may obtain copies of this report from the Defense Documentation Center.

References to named commercial products in this report are not to be considered in any sense as an endorsement of the product by the United States Air Force or the Government.

APPROVAL STATEMENT

This technical report has been reviewed and is approved.

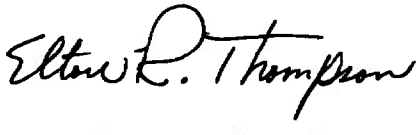

ELTON R. THOMPSON
Research and Development Division
Directorate of Technology

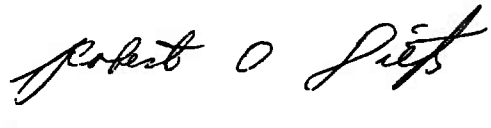

ROBERT O. DIETZ
Director of Technology

UNCLASSIFIED

SECURITY CLASSIFICATION OF THIS PAGE *(When Data Entered)*

REPORT DOCUMENTATION PAGE	READ INSTRUCTIONS BEFORE COMPLETING FORM
1 REPORT NUMBER: AEDC-TR-73-171	2. GOVT ACCESSION NO. / 3 RECIPIENT'S CATALOG NUMBER
4. TITLE *(and Subtitle)*: THREE-PARTICLE COLLISION INTEGRALS FOR THERMAL CONDUCTIVITY, VISCOSITY, AND SELF-DIFFUSION OF A GAS OF HARD SPHERICAL MOLECULES. PART II: CALCULATIONS	5. TYPE OF REPORT & PERIOD COVERED: Final Report-September 1, 1970, to June 30, 1972 / 6 PERFORMING ORG. REPORT NUMBER
7. AUTHOR(s): Gillespie, D. T., Naval Weapons Center; Sengers, J. V., University of Maryland	8. CONTRACT OR GRANT NUMBER(s): F40600-69-C-0002, F40600-72-C-0002, F40600-73-C-0006
9. PERFORMING ORGANIZATION NAME AND ADDRESS: Institute for Molecular Physics, University of Maryland, College Park, MD 20742	10. PROGRAM ELEMENT, PROJECT, TASK AREA & WORK UNIT NUMBERS
11. CONTROLLING OFFICE NAME AND ADDRESS: Arnold Engineering Development Center (XON), Arnold Air Force Station, TN 37389	12. REPORT DATE: November 1973 / 13. NUMBER OF PAGES: 226
14. MONITORING AGENCY NAME & ADDRESS *(If different from Controlling Office)*: Arnold Engineering Development Center (DYR), Arnold Air Force Station, TN 37389	15. SECURITY CLASS. *(of this report)*: UNCLASSIFIED / 15a. DECLASSIFICATION/DOWNGRADING SCHEDULE
16. DISTRIBUTION STATEMENT *(of this Report)*: Approved for public release; distribution unlimited.	
17. DISTRIBUTION STATEMENT *(of the abstract entered in Block 20, if different from Report)*	
18. SUPPLEMENTARY NOTES: Available in DDC.	
19 KEY WORDS *(Continue on reverse side if necessary and identify by block number)*: gases; binary systems; transport properties; particle collisions; diffusion; viscosity; thermal conductivity; self diffusion	
20. ABSTRACT *(Continue on reverse side if necessary and identify by block number)*: In order to predict the first density corrections to the transport properties of gases, it is necessary to consider collision integrals that account for the effects of collisions among three molecules. For a gas of hard spherical molecules such three-particle collision integrals can be decomposed into collision integrals associated with sequences of one, two,	

DD FORM 1 JAN 73 1473 EDITION OF 1 NOV 65 IS OBSOLETE

UNCLASSIFIED

SECURITY CLASSIFICATION OF THIS PAGE *(When Data Entered)*

20, Continued

three, and four successive collisions among three molecules, as shown in AEDC-TR-72-142. In the present technical report we calculate these three-particle collision integrals for the coefficients of thermal conductivity, viscosity, and self-diffusion.

PREFACE

The research reported herein was sponsored by the Arnold Engineering Development Center (AEDC), Air Force Systems Command (AFSC). The research was conducted at the Institute for Molecular Physics of the University of Maryland from September 1, 1970 to June 30, 1971 under contract F40600-69-C-0002 and from July 1, 1971 to June 30, 1972 under contract F40600-72-C-0002. The technical report was prepared during the period from September 1, 1972 to April 30, 1973 under contract F40600-73-C-0006. The Air Force project monitor for this project was Elton R. Thompson, AEDC (DYR). A major part of the computer time was supported by the Computer Science Center of the University of Maryland. The major part of the research was conducted, while Dr. D. T. Gillespie was a postdoctoral research associate at the Institute for Molecular Physics of the University of Maryland. The manuscript was submitted for publication May 15, 1973.

During this research effort the authors have benefitted from stimulating discussions with Dr. M. H. Ernst, Professor J. R. Dorfman, Dr. W. R. Hoegy, I-Jeng Chu Liu and Professor E. G. D. Cohen.

Part I of this series is documented in Technical Report AEDC-TR-72-142, Arnold Engineering Development Center, Tennessee, September, 1972.

The reproducibles used in the reproduction of this report were supplied by the authors.

TABLE OF CONTENTS

TABLE OF CONTENTS (Cont.)

Page

LIST OF TABLES

LIST OF TABLES (Cont.)

LIST OF FIGURES

LIST OF FIGURES (Cont.)

Figure

LIST OF FIGURES (Cont.)

Figure

CHAPTER I

INTRODUCTION

1.1 Objective

This report is concerned with the problem of calculating the transport properties of moderately dense gases. For one-component gases the transport properties of interest are: the coefficient of thermal conductivity λ, the coefficient of shear viscosity η and the coefficient of self-diffusion, D. For brevity we shall follow the literature in referring to these transport coefficients simply as thermal conductivity λ, viscosity η and self-diffusion D.

The theory predicts that the first density correction to the transport coefficients of a gas can be represented by a term linear in the density n[†]. Thus

$$\begin{aligned} \lambda &= \lambda_0 + \lambda_1 n + \cdots , \\ \eta &= \eta_0 + \eta_1 n + \cdots , \\ nD &= D_0 + D_1 n + \cdots . \end{aligned} \tag{1.1}$$

In this report we express the density as the number of molecules n per unit volume. The mass density ρ is related to the number density n by $\rho = nm$, where m is the mass of the individual molecules.

The coefficients λ_0, η_0 and D_0 represent the transport properties in the limit of low densities; in practice they are adequate at atmospheric and subatmospheric pressures. A description of the dynamic behavior of low density gases is based on the Boltzmann equation. The transport coefficients λ_0, η_0 and D_0 are then obtained by solving the linearized Boltzmann equation according to a procedure introduced by

† For a bibliography see: M. H. Ernst, L. K. Haines and J. R. Dorfman, Rev. Mod. Phys. 41, 296 (1969).

Chapman and Enskog [1,2]. The approximate nature of the Boltzmann equation is twofold. First, the Boltzmann equation considers only uncorrelated *binary* collisions. As a consequence the transport properties λ_0, η_0 and D_0 of the dilute gas are determined by collision integrals involving the dynamics of collisions between two molecules alone. The Boltzmann equation also neglects the interaction range σ of the molecules relative to mean free path. Thus the flux of energy, momentum and mass is wholly attributed to the flux associated with the free motion of the molecules *between* collisions.

In this report we focus our attention on the calculation of the coefficients λ_1, η_1 and D_1 that determine the first density corrections to the transport properties. These new coefficients cannot be obtained from the Boltzmann equation itself, and we need to consider appropriate corrections to the Boltzmann equation in order to account for the dense gas effects. In view of the complexity of this task we shall restrict ourselves in this report to a calculation of these coefficients for a gas of hard spherical molecules with diameter σ and mass m.

The coefficients λ_1 and η_1 are to be regarded as the sum of two terms. First, they contain a contribution $\lambda_1^{KU} + \lambda_1^{UK}$ and $\eta_1^{KU} + \eta_1^{UK}$, respectively, due to the difference in position of *two* molecules during a collision; this effect was neglected in the Boltzmann equation. Secondly, λ_1 and η_1 contain a contribution λ_1^{KK}, η_1^{KK} that accounts for the correlations in the positions and velocities of the molecules due to successive collisions among *three* molecules [3].

$$\lambda_1 = \lambda_1^{KK} + \lambda_1^{KU} + \lambda_1^{UK} \quad , \quad \eta_1 = \eta_1^{KK} + \eta_1^{KU} + \eta_1^{UK} \quad . \tag{1.2}$$

The contributions $\lambda_1^{KU} + \lambda_1^{UK}$ and $\eta_1^{KU} + \eta_1^{UK}$ are well known for a gas of hard spheres. They are proportional to the dilute gas values of the transport properties and were rederived in Part I [3].

$$\lambda_1^{KU} + \lambda_1^{UK} = \frac{4}{5}\pi\sigma^3\lambda_0 \quad , \quad \eta_1^{KU} + \eta_1^{UK} = \frac{8}{15}\pi\sigma^3\eta_0 \quad . \tag{1.3}$$

These terms incorporate the transfer of energy and momentum between two molecules *during* a collision; this transfer is often referred to as collisional transfer [1]. Since there is no collisional transfer of mass, the first density correction D_1 to the self-diffusion is to be attributed completely to collisions among three molecules.

For a gas of hard spheres the initial density dependence of the transport properties can thus be written as

$$\begin{aligned} \lambda &= \lambda_0 + \{\tfrac{4}{5}\pi\sigma^3\lambda_0 + \lambda_1^{KK}\}\, n \quad , \\ \eta &= \eta_0 + \{\tfrac{8}{15}\pi\sigma^3\eta_0 + \eta_1^{KK}\}\, n \quad , \\ nD &= D_o + D_1 n \quad . \end{aligned} \tag{1.4}$$

In a previous technical report, Part I of this series [3], we have demonstrated how the coefficients λ_1^{KK}, η_1^{KK} and D_1 are determined by sets of three-particle collision integrals that are related to various types of collision sequences involving three molecules. It is the purpose of the present report to show how one may evaluate these three-particle collision integrals. Based on this work we shall present tables of the contributions to the transport properties from the various three-particle collision sequences.

1.2 Molecular Collision Sequences

Before entering into a detailed discussion of the three-particle collision integrals, we want to familiarize the reader with the types of molecular collisions that are to be considered in the calculation of the transport properties.

For a calculation of the coefficients λ_0, η_0 and D_0 in (1.4) it is sufficient to consider the dynamics of a binary collision between *two* molecules. For the sake of the discussion we represent such a binary collision schematically by the diagram in Fig. 1. The lines in this diagram represent the trajectories of the centers of the molecules, and the circles represent the molecules themselves at the instant of contact. Just as in Part I [3], we adopt again the convention that in all figures the time increases when the diagrams are read from bottom to top as indicated by arrows on the particle lines. Thus $\vec{v}_1$ and $\vec{v}_2$

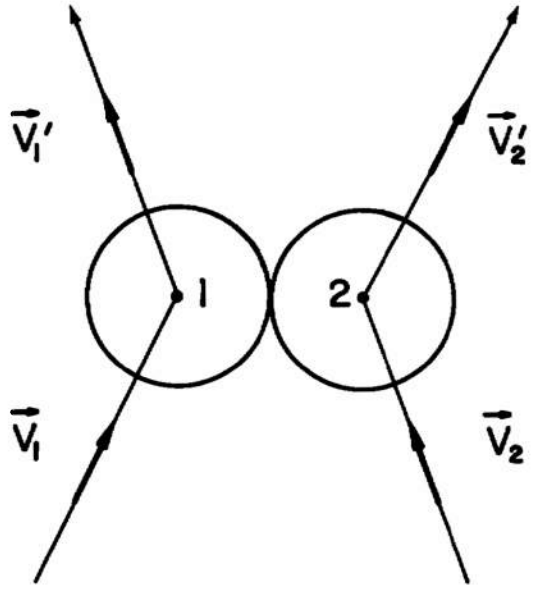

Figure 1. Schematic representation of a binary collision between molecules 1 and 2. The lines represent trajectories of the centers of the molecules and the circles depict the molecules themselves at the time of contact.

in Fig. 1 are the velocities of molecules 1 and 2 *before* the collision and $\vec{v}_1'$ and $\vec{v}_2'$ the velocities *after* the collision. The transport properties in the dilute gas limit are determined by collision integrals whose integrands depend only on the velocities $\vec{v}_1$, $\vec{v}_2$ and $\vec{v}_1'$, $\vec{v}_2'$ before and after a binary collision. For a gas of hard spheres these binary collision integrals were discussed extensively in earlier technical reports [4,5] and they will be summarized in Section 2.1.

The transport coefficients λ_1^{KK}, η_1^{KK} and D_1 are determined by collision integrals whose integrands depend on the molecular velocities before, between and after successive collisions among three molecules. As a result, the three-particle collision integrals can be represented by collision diagrams in very much the same way as the binary collision integrals were represented by the diagram of Fig. 1.

A preliminary analysis and evaluation of three-particle collision integrals was made earlier by Sengers [4,6,7]. This, and subsequent work reported in AEDC-TR-71-51 [5], showed it to be advantageous to make a distinction between "genuine triple collisions" and "successive binary collisions".

We define a genuine triple collision as a collision during which more than one pair of molecules lie inside each other's interaction range. Now, in a gas of hard spheres, the duration of an individual binary collision is negligibly brief compared to the time between successive collisions; therefore, genuine triple collisions would never *physically* occur in such a gas. Nevertheless, genuine triple collisions *will* play a very significant role in our considerations here. The reason is that the Boltzmann equation, from which the dilute, hard sphere gas, transport coefficients λ_0, η_0 and D_0 are calculated,

considers *all* binary collisions, including those in which the region occupied by the colliding pair of molecules is already partly occupied by a third molecule. This latter type of collision is evidently a "genuine triple collision", in the sense defined above. Thus, in correcting the Boltzmann equation results, it is necessary to assess and subtract out the contributions of these physically forbidden genuine triple collisions. The situation here is very much analogous to that in equilibrium statistical mechanics, wherein the ideal gas equation of state is corrected by assessing and subtracting out contributions from physically forbidden excluded volume configurations [8].

In so considering genuine triple collisions in a gas of hard sphere molecules, we find it convenient to introduce several new notions. We shall say that two hard spheres whose centers are separated by a distance *equal to* σ are "colliding", and two hard spheres whose centers are separated by a distance *less than* σ are "overlapping". We define an "overlap collision" to be a collision between two molecules which occurs while at least one of the two molecules is overlapping with a third molecule. We further distinguish between a "single-overlap collision" and a "double-overlap collision", according to whether the third molecule overlaps with just one or with both of the colliding molecules. The notion of overlap collision was introduced in earlier technical reports [3,5,9]. Such overlap collisions are evidently genuine triple collisions. They may be regarded as accounting for "excluded volume" effects, or, in the language of Part I, for the "statistical correlations" [3].

We have previously demonstrated [3,5,9] that the coefficients λ_1^{KK}, η_1^{KK} and D_1 can be decomposed into a series of four terms

$$\lambda_1^{KK} = \sum_{\mu=1}^{4} \lambda_{1\mu} , \quad \eta_1^{KK} = \sum_{\mu=1}^{4} \eta_{1\mu} , \quad D_1 = \sum_{\mu=1}^{4} D_{1\mu} . \tag{1.5}$$

For each transport coefficient, the terms in (1.5) are related to the dynamics of one, two, three and four successive collisions among three molecules. We represent the various collision sequences by diagrams in Figs. 2-5, just as the diagram in Fig. 1 was used to represent the collision sequence related to the dilute gas values λ_0, η_0 and D_0. The lines in Figs. 2-5 represent again the trajectories of the centers of the molecules, while the circles depict the molecules themselves at the time of a collision. The explicit formulas for the three-particle collision integrals will be introduced in the next chapter. In this chapter we restrict ourselves to an explanation of the various collision sequences that enter into a calculation of the coefficients $\lambda_{1\mu}$, $\eta_{1\mu}$, and $D_{1\mu}$.

The first terms (μ=1) in the expression (1.5) account for binary collisions in which *both* colliding molecules are overlapping with a third molecule (double-overlap collisions). Such a double-overlap collision is shown schematically in Fig. 2. The corresponding collision integrals contain the dynamics of only one binary collision, but do account for excluded volume effects due to the presence of a third molecule. We have shown in earlier reports [3,5,9] that these double-overlap collisions are precisely the collisions incorporated in the Enskog theory, and they yield

$$\lambda_{11} = -\frac{5}{12}\pi\sigma^3\lambda_0 , \quad \eta_{11} = -\frac{5}{12}\pi\sigma^3\eta_0 , \quad D_{11} = -\frac{5}{12}\pi\sigma^3 D_0 . \tag{1.6}$$

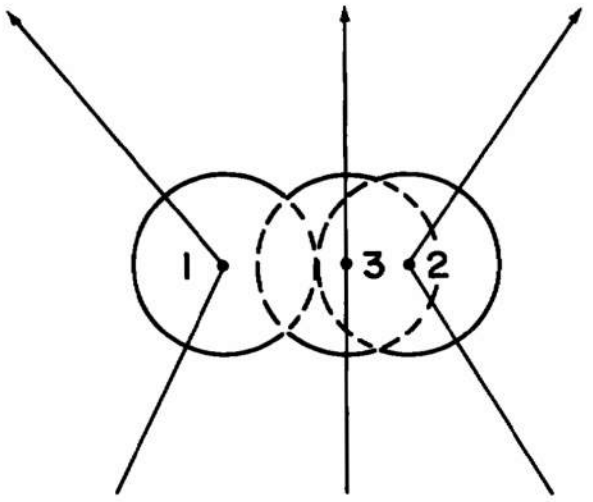

Figure 2. Schematic representation of a double-overlap collision. When molecules 1 and 2 are colliding, molecule 3 overlaps with both 1 and 2.

We emphasize that these "Enskog values" represent corrections to the dilute gas values due entirely to excluded volume effects.

The terms $\lambda_{1\mu}$, $\eta_{1\mu}$ and $D_{1\mu}$ for μ=2,3,4 constitute corrections to the Enskog theory due to sequences of, respectively, two, three and four successive collisions, as shown in Figs. 3-5. In each case, we consider a collision between molecules 1 and 2 at the bottom of the diagram, just as in Fig. 1. However, in contrast to Fig. 1, we now consider in addition the trajectories that account for the possible interactions with a third molecule 3.

The terms λ_{12}, η_{12}, D_{12} (μ=2) are related to sequences of *two* successive collisions of which at least one is a single-overlap collision. The three possible events of this type are shown in Fig. 3. The three events differ in that in Fig. 3a both collisions are single-overlap collisions, while in Fig. 3b only the earlier collision, and in Fig. 3c only the later collision, is a single-

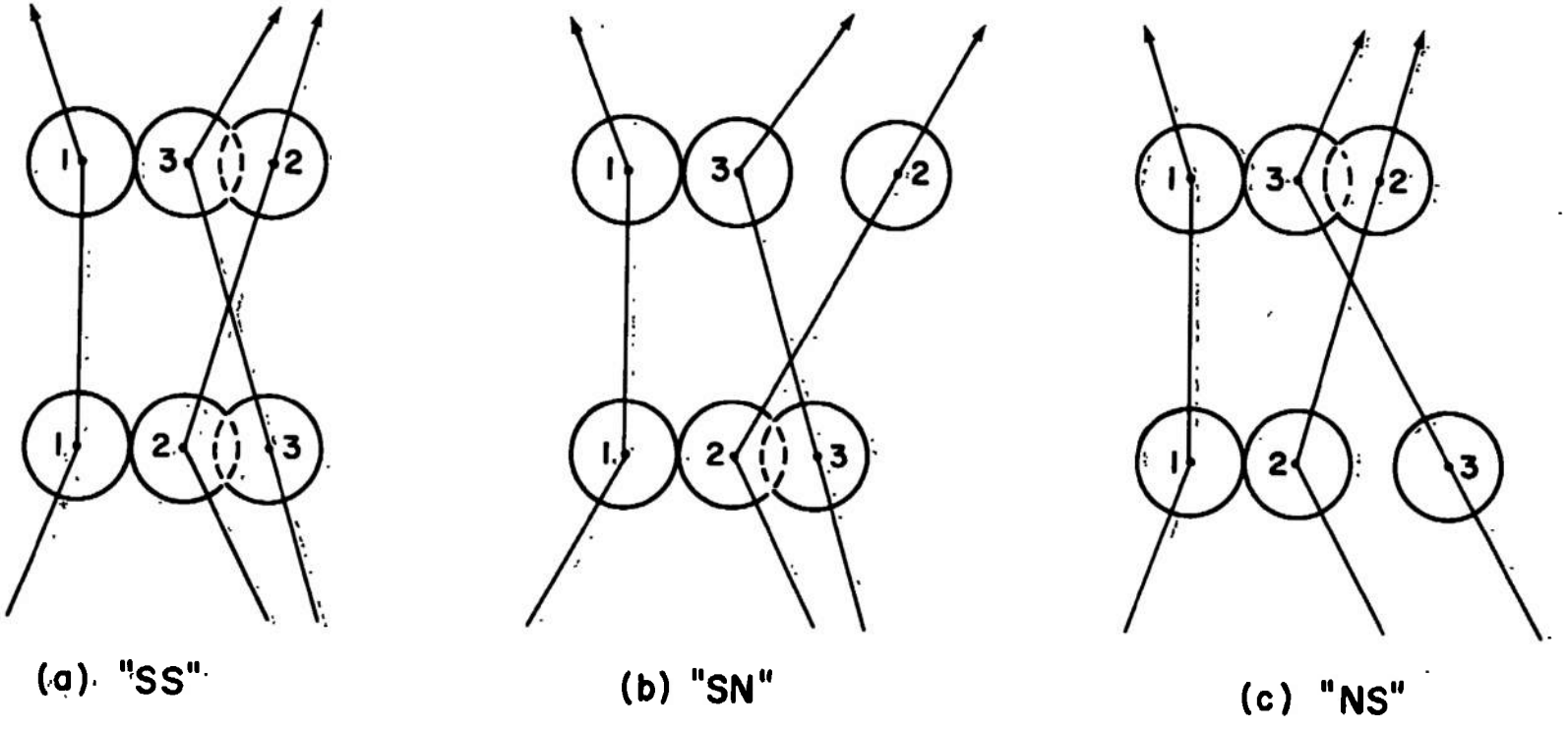

Figure 3. Sequences of two successive collisions among three molecules.

(a) Molecules 2 and 3 overlap at both collisions (SS-collision).

(b) Molecules 2 and 3 overlap at the earlier collision only (SN-collision).

(c) Molecules 2 and 3 overlap at the later collision only (NS-collision).

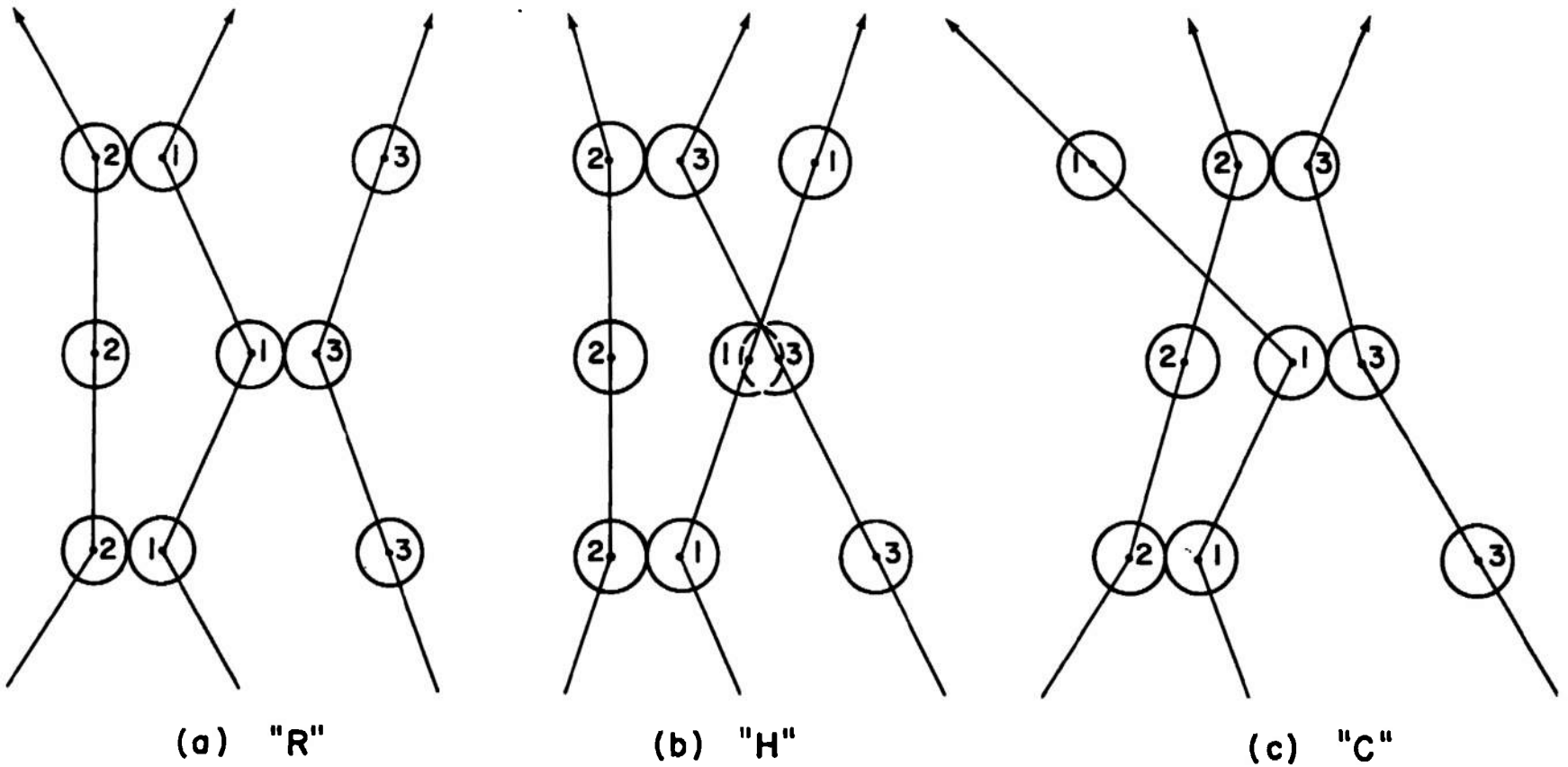

Figure 4. Sequences of three successive collisions among three molecules.

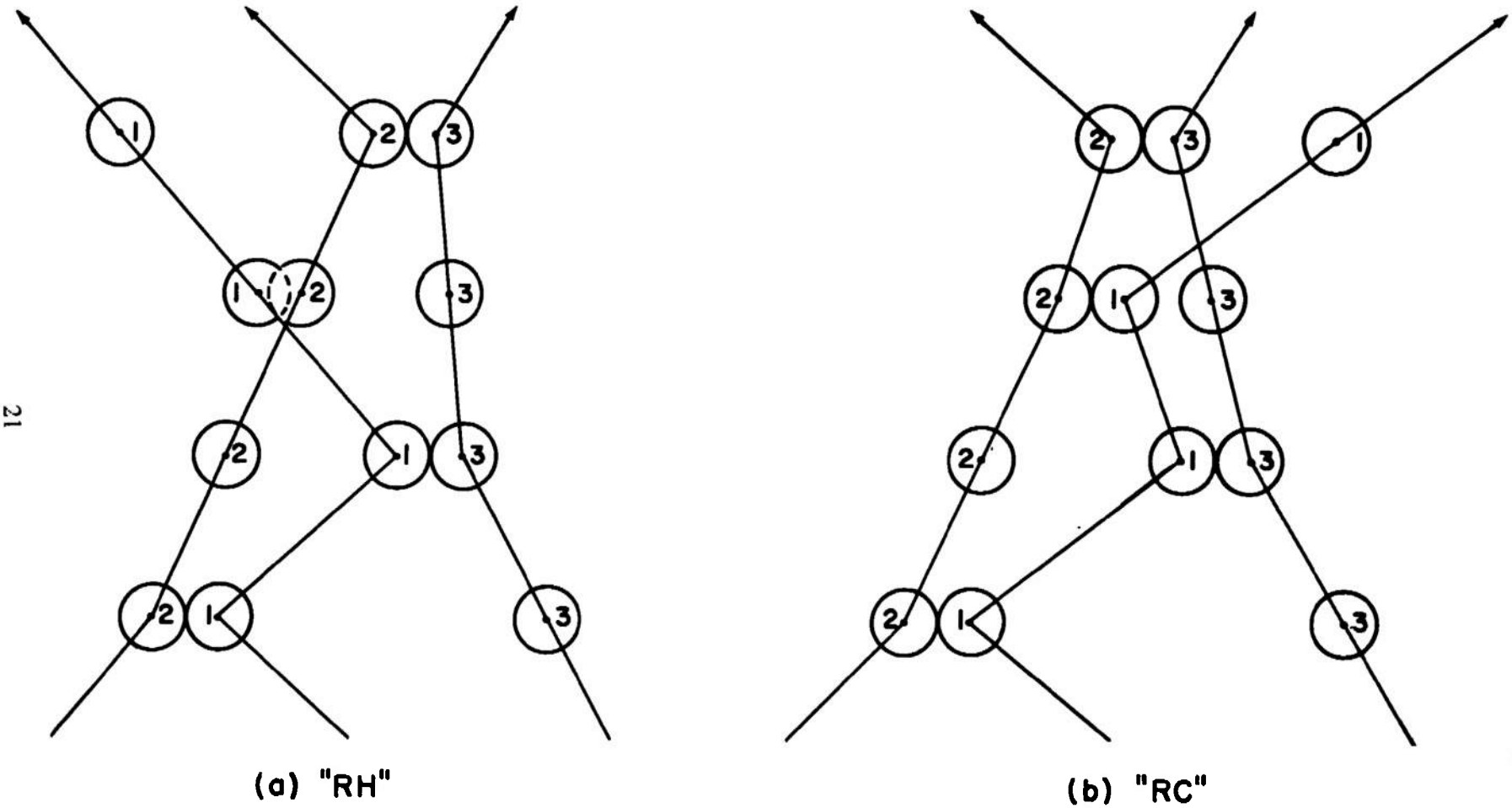

Figure 5. Sequences of four successive collisions among three molecules.

overlap collision. In Part I we have referred to these events as SS-collision (Fig. 3a), SN-collision (Fig. 3b) and NS-collision (Fig. 3c). These collision sequences account for a *combination* of excluded volume (overlap collisions) and dynamical (two successive collisions) effects.

The terms λ_{13}, η_{13}, D_{13} (μ=3) correspond to sequences of *three* successive collisions, shown in Fig. 4. In Part I we have referred to these sequences as recollisions (R), cyclic collisions (C) and hypothetical collisions (H). Note that in the diagram of Fig. 4b the intermediate collision between 1 and 3 is a "noninteracting" collision. That is, molecules 1 and 3 are indeed aimed to collide, but they pass through each other's interaction sphere and continue along the extension of their original trajectories. This noninteracting collision represents a dynamical screening effect due to the interfering presence of molecule 3. The sequences of Fig. 4 do *not* contain any overlap collisions, and they account for correlations that are of a purely dynamical nature [3,5,10].

Finally, the terms λ_{14}, η_{14}, D_{14} (μ=4) correspond to sequences of *four* successive collisons. The two collision sequences that need to be considered are shown in Fig. 5. Any other possible sequence of four successive collisions can be obtained from those shown in Fig. 5 by time reversal and/or suitable permutation of the particle numbers. These collision sequences, like those in Fig. 4, account for purely dynamical correlations. It can be shown that the expansion (1.5) for the coefficients λ_1, η_1 and D_1 terminates after sequences of four successive collisions [5,10,11].

1.3 Outline of Report

In this report we present calculations of the three-particle collision integrals that determine the coefficients λ_1^{KK}, η_1^{KK} and D_1 in the density expansion (1.4) of the transport properties. It is convenient to consider dimensionless three-particle collision integrals. For this purpose we define

$$\lambda_{1\mu}^* \equiv \frac{\lambda_{1\mu}}{\lambda_{11}} , \quad \eta_{1\mu}^* \equiv \frac{\eta_{1\mu}}{\eta_{11}} , \quad D_{1\mu}^* \equiv \frac{D_{1\mu}}{D_{11}} , \tag{1.7}$$

so that, in accordance with (1.5) and (1.6)

$$\begin{aligned} \lambda_1^{KK} &= -\frac{5}{12}\pi\sigma^3\lambda_0 \left[1 + \sum_{\mu=2}^{4} \lambda_{1\mu}^* \right] , \\ \eta_1^{KK} &= -\frac{5}{12}\pi\sigma^3\eta_0 \left[1 + \sum_{\mu=2}^{4} \eta_{1\mu}^* \right] , \\ D_1 &= -\frac{5}{12}\pi\sigma^3 D_0 \left[1 + \sum_{\mu=2}^{4} D_{1\mu}^* \right] . \end{aligned} \tag{1.8}$$

The terms $\lambda_{1\mu}^*$, $\eta_{1\mu}^*$ and $D_{1\mu}^*$ represent corrections to the Enskog theory due to sequences of 2(μ=2), 3(μ=3) and 4(μ=4) successive collisions among three molecules.

We shall proceed as follows. In Chapter II we formulate the three-particle collision integrals. The collision integrals corresponding to sequences of two successive collisions are then evaluated in Chapter III, those corresponding to sequences of three successive collisions are evaluated in Chapter IV, and the collision integrals

corresponding to sequences of four successive collisions are evaluated in Chapter V. The numerical results are compiled in tables of collision integrals collected in the Appendix at the end of this report; these tables are indicated by lower case roman numerals. For a survey and discussion of the results the reader is referred to Chapter VI.

CHAPTER II

FORMULATION OF COLLISION INTEGRALS

2.1 Binary Collision Integrals

The transport coefficients λ_0, η_0 and D_0 of the dilute gas are given by [3]

$$\lambda_0 = -\frac{1}{3kT^2}[\vec{A},\vec{A}]^{(2)} \quad , \quad \eta_0 = -\frac{1}{10kT}[\vec{\vec{B}},\vec{\vec{B}}]^{(2)} \quad , \quad D_0 = -\frac{1}{3}[\vec{C},\vec{C}]^{(\tilde{2})} \quad , \tag{2.1}$$

where k is Boltzmann's constant and T the temperature. The symbols $\vec{A}$ and $\vec{C}$ represent vector functions $\vec{A}(\vec{v})$, $\vec{C}(\vec{v})$, and $\vec{\vec{B}}$ a tensor function $\vec{\vec{B}}(\vec{v})$, of the molecular velocity $\vec{v}$; they are the solutions of the linearized Boltzmann equations†

$$\begin{aligned}
\int dx_2 \phi(v_2) \overline{T}_{12}\{\vec{A}(\vec{v}_1)+\vec{A}(\vec{v}_2)\} &= -\left(\frac{1}{2}mv_1^2-\frac{5}{2}kT\right)\vec{v}_1 \quad , \\
\int dx_2 \phi(v_2) \overline{T}_{12}\{\vec{\vec{B}}(\vec{v}_1)+\vec{\vec{B}}(\vec{v}_2)\} &= -mv_1\vec{\vec{v}}_1 \quad , \\
\int dx_2 \phi(v_2) \overline{T}_{12}\vec{C}(\vec{v}_1) &= -\vec{v}_1 \quad .
\end{aligned} \tag{2.2}$$

As in Part I, we use again the convention that the phase $\vec{x}_i=(\vec{v}_i,\vec{r}_i)$ represents the velocity $\vec{v}_i$ and position $\vec{r}_i$ of molecule i. The symbol $\vec{\vec{v}}_1\vec{v}_1$ indicates a traceless dyadic in the notation of Chapman and Cowling [1]. The Maxwell-Boltzmann factor $\phi(\vec{v}_i)$ is defined as

---

† The functions $\vec{A}$ and $\vec{\vec{B}}$ in this report are the same as those in AEDC-TR-72-142 [3], but differ by a factor kT from those used in some earlier reports [4,5] and publications [6,7,12].

$$\phi(v_i) = \left(\frac{m}{2\pi kT}\right)^{3/2} \exp\left[-\frac{mv_i^2}{2kT}\right] \quad . \tag{2.3}$$

The operator $\bar{T}_{12}$ is a binary collision operator introduced by Ernst et al. [13]; its definition and properties were discussed in detail in Part I. The square brackets with superscript 2 in (2.1) indicate *binary collision integrals*, defined as

$$[\vec{A},\vec{A}]^{(2)} = \frac{1}{2!}\int d\vec{v}_1 dx_2 \phi(v_1)\phi(v_2) \sum_{m=1}^{2} \vec{A}(\vec{v}_m) \cdot \bar{T}_{12} \sum_{n=1}^{2} \vec{A}(\vec{v}_n) \quad ,$$

$$[\vec{\vec{B}},\vec{\vec{B}}]^{(2)} = \frac{1}{2!}\int d\vec{v}_1 dx_2 \phi(v_1)\phi(v_2) \sum_{m=1}^{2} \vec{\vec{B}}(\vec{v}_m) : \bar{T}_{12} \sum_{n=1}^{2} \vec{\vec{B}}(\vec{v}_n) \quad , \tag{2.4}$$

$$[\vec{C},\vec{C}]^{(2)} = \frac{1}{2!}\int d\vec{v}_1 dx_2 \phi(v_1)\phi(v_2) \sum_{n=1}^{2} \vec{C}(\vec{v}_n) \cdot \bar{T}_{12} \vec{C}(\vec{v}_n) \quad .$$

For convenience we introduce the dimensionless quantities

$$\vec{W}_i = \left(\frac{m}{2kT}\right)^{1/2} \vec{v}_i ; \quad \vec{r}_i^{\,*} = \frac{\vec{r}_i}{\sigma} ; \quad \bar{T}_{12}^{*} = \sigma \left(\frac{m}{2kT}\right)^{1/2} \bar{T}_{12} \quad . \tag{2.5}$$

We also use dimensionless functions $\vec{A}^*$, $\vec{\vec{B}}^*$ and $\vec{C}^*$, defined by

$$\vec{A}(\vec{v}_i) = -\frac{15}{32\sigma^2}\sqrt{\frac{2}{\pi}}\, kT\, \vec{A}^*(\vec{W}_i) \quad ,$$

$$\vec{\vec{B}}(\vec{v}_i) = \frac{5}{8\sigma^2}\left[\frac{mkT}{\pi}\right]^{1/2} \vec{\vec{B}}^*(\vec{W}_i) \quad , \tag{2.6}$$

$$\vec{C}(\vec{v}_i) = \frac{3}{8\sigma^2}\sqrt{\frac{2}{\pi}}\, \vec{C}^*(\vec{W}_i) \quad .$$

The expressions (2.1) for λ_0, η_0 and D_0 may then be written as

$$\lambda_0 = \frac{75}{64\sigma^2}\left[\frac{k^3T}{m\pi}\right]^{1/2}\{\vec{A}^*,\vec{A}^*\}^{(2)} \quad ,$$

$$\eta_0 = \frac{5}{16\sigma^2}\left[\frac{mkT}{\pi}\right]^{1/2}\{\vec{B}^*,\vec{B}^*\}^{(2)} \quad , \qquad (2.7)$$

$$D_0 = \frac{3}{8\sigma^2}\left[\frac{kT}{m\pi}\right]^{1/2}\{\vec{C}^*,\vec{C}^*\}^{(\tilde{2})} \quad ,$$

where the curly brackets indicate dimensionless binary collision integrals,

$$\{\vec{A}^*,\vec{A}^*\}^{(2)} = -\frac{1}{(2\pi)^{7/2}}\int d\vec{W}_1 d\vec{W}_2 d\vec{r}_2^* e^{-(W_1^2+W_2^2)} \sum_{m=1}^{2}\vec{A}^*(\vec{W}_m)\cdot\bar{T}_{12}^*\sum_{n=1}^{2}\vec{A}^*(\vec{W}_n) \quad ,$$

$$\{\vec{B}^*,\vec{B}^*\}^{(2)} = -\frac{1}{(2\pi)^{7/2}}\int d\vec{W}_1 d\vec{W}_2 d\vec{r}_2^* e^{-(W_1^2+W_2^2)} \sum_{m=1}^{2}\vec{B}^*(\vec{W}_m):\bar{T}_{12}^*\sum_{n=1}^{2}\vec{B}^*(\vec{W}_n) \quad , \qquad (2.8)$$

$$\{\vec{C}^*,\vec{C}^*\}^{(\tilde{2})} = -\frac{2}{(2\pi)^{7/2}}\int d\vec{W}_1 d\vec{W}_2 d\vec{r}_2^* e^{-(W_1^2+W_2^2)} \sum_{n=1}^{2}\vec{C}^*(\vec{W}_n)\cdot\bar{T}_{12}^*\vec{C}^*(\vec{W}_n) \quad .$$

The functions $\vec{A}^*$, $\vec{B}^*$ and $\vec{C}^*$ are usually approximated by a finite sum of Sonine polynomials $S_n^{(k)}(x)$, defined in Table I.

$$\vec{A}^*(\vec{W}) = \sum_{k=1}^{N} a_k(N) S_{3/2}^{(k)}(W^2)\vec{W} \quad ,$$

$$\vec{B}^*(\vec{W}) = \sum_{k=0}^{N-1} b_k(N) S_{5/2}^{(k)}(W^2)\underline{\underline{\Omega}}\,\vec{W}\vec{W} \quad , \qquad (2.9)$$

$$\vec{C}^*(\vec{W}) = \sum_{k=0}^{N-1} c_k(N) S_{3/2}^{(k)}(W^2)\vec{W} \quad .$$

The coefficients $a_k(N)$, $b_k(N)$ and $c_k(N)$ of these expansions satisfy a set of linear equations [2,12]

Table I

Sonine Polynomials

$$\sum_{k=0}^{\infty} S_n^{(k)}(x)\,t^k = \frac{1}{(1-t)^{n+1}} \exp\left\{-\frac{xt}{1-t}\right\}$$

General: $$S_n^{(k)}(x) = \sum_{j=0}^{k} \frac{(-1)^j (k+n)!}{(j+n)!\ (k-j)!\ j!} x^j$$

k=0 $$S_n^{(0)}(x) = 1$$

k=1 $$S_n^{(1)}(x) = (n+1) - x$$

k=2 $$S_n^{(2)}(x) = \frac{(n+1)(n+2)}{2} - (n+2)x + \frac{1}{2}x^2$$

k=3 $$S_n^{(3)}(x) = \frac{(n+1)(n+2)(n+3)}{6} - \frac{(n+2)(n+3)}{2}x + \frac{(n+3)}{2}x^2 - \frac{1}{6}x^3$$

k=4 $$S_n^{(4)}(x) = \frac{(n+1)(n+2)(n+3)(n+4)}{24} - \frac{(n+2)(n+3)(n+4)}{6}x + \frac{(n+3)(n+4)}{4}x^2 - \frac{(n+4)}{6}x^3 + \frac{1}{24}x^4$$

Orthogonality relation:

$$\int_0^{\infty} x^n e^{-x} S_n^{(k)}(x)\ S_n^{(\ell)}(x)\,dx = \frac{(n+k)!}{k!}\,\delta_{k\ell}\ .$$

$$\sum_{k=1}^{N} a_k(N)\, a_{k\ell}^{(2)} = \delta_{\ell 1} \qquad (\ell=1,..,N) ,$$

$$\sum_{k=0}^{N-1} b_k(N)\, b_{k_\ell}^{(2)} = \delta_{\ell 0} \qquad (\ell=0,..,N-1) , \tag{2.10}$$

$$\sum_{k=0}^{N-1} c_k(N)\, c_{k\ell}^{(2)} = \delta_{\ell 0} \qquad (\ell=0,..,N-1) .$$

Here $\delta_{\ell m}$ is the Kronecker delta and $a_{k\ell}^{(2)}$, $b_{k\ell}^{(2)}$ and $c_{k\ell}^{(2)}$ are elements of matrices of binary collision integrals†:

$$a_{k\ell}^{(2)} = \{S_{3/2}^{(k)}(W^2)\vec{W} \ , \ S_{3/2}^{(\ell)}(W^2)\vec{W}\}^{(2)} ,$$

$$b_{k\ell}^{(2)} = \{S_{5/2}^{(k)}(W^2)\vec{W}\vec{W} \ , \ S_{5/2}^{(\ell)}(W^2)\vec{W}\vec{W}\}^{(2)} , \tag{2.11}$$

$$c_{k\ell}^{(2)} = \{S_{3/2}^{(k)}(W^2)\vec{W} \ , \ S_{3/2}^{(\ell)}(W^2)W\}^{(\tilde{2})}$$

The factor $(2\pi)^{-7/2}$ in the definition (2.8) of the dimensionless binary collision integrals was chosen so that $a_{11}^{(2)} = b_{00}^{(2)} = c_{00}^{(2)} = 1$. The binary collision integrals (2.11) are symmetric, i.e.

$$a_{k\ell}^{(2)} = a_{\ell k}^{(2)} \ ; \ b_{k\ell}^{(2)} = b_{\ell k}^{(2)} \ ; \ c_{k\ell}^{(2)} = c_{\ell k}^{(2)} . \tag{2.12}$$

We shall refer to the number N of Sonine polynomials retained in (2.9) as the order of the Sonine approximation used. Thus, inserting

---

† The matrix elements $a_{k\ell}^{(2)}$ and $b_{k\ell}^{(2)}$ used here are the same as the matrix elements $a_{k\ell}^{(0)}$ and $b_{k\ell}^{(0)}$ in AEDC-TR-69-68 [4,12],

(2.9)-(2.11) into (2.7), we have for the "N^{th} Sonine approximation" to the dilute gas transport coefficients,

$$\lambda_0(N) = \frac{75}{64\sigma^2}\left[\frac{k^3T}{m\pi}\right]^{1/2} a_1(N) \quad ,$$

$$\eta_0(N) = \frac{5}{16\sigma^2}\left[\frac{mkT}{\pi}\right]^{1/2} b_0(N) \quad , \tag{2.13}$$

$$D_0(N) = \frac{3}{8\sigma^2}\left[\frac{kT}{m\pi}\right]^{1/2} c_0(N) \quad .$$

The problem of calculating the transport properties in the dilute gas limit thus requires the calculation of the set of binary collision integrals (2.11). For a gas of hard spheres these matrix elements $a_{k\ell}^{(2)}$, $b_{k\ell}^{(2)}$ and $c_{k\ell}^{(2)}$ can be readily evaluated. They are equal to the coefficients of $s^k t^\ell$ in the expansions [14]:

$$\sum_{k=1}^{\infty}\sum_{\ell=1}^{\infty} a_{k\ell}^{(2)} s^k t^\ell = \{1-\tfrac{1}{2}(s+t)\}^{1/2} st(1-st)^{-3} - \frac{1}{4}\{1-\tfrac{1}{2}(s+t)\}^{-1/2} s^2t^2(1-st)^{-2} \quad , \tag{2.14a}$$

$$\sum_{k=0}^{\infty}\sum_{\ell=0}^{\infty} b_{k\ell}^{(2)} s^k t^\ell = \tag{2.14b}$$

$$= \{1-\tfrac{1}{2}(s+t)\}^{1/2}(1+\tfrac{2}{3}st+\tfrac{1}{3}s^2t^2)(1-st)^{-4} - \tfrac{1}{3}\{1-\tfrac{1}{2}s+t)\}^{-1/2} st(1-st)^{-3}$$

$$- \frac{1}{48}\{1-\tfrac{1}{2}(s+t)\}^{-3/2} s^2t^2(1-st)^{-2} \quad ,$$

$$\sum_{k=0}^{\infty}\sum_{\ell=0}^{\infty} c_{k\ell}^{(2)} s^k t^\ell = \{1-\tfrac{1}{2}(s+t)\}^{1/2}(1+st)(1-st)^{-3} - \frac{1}{4}\{1-\tfrac{1}{2}(s+t)\}^{-1/2} st(1-st)^{-2} \quad . \tag{2.14c}$$

Table II

The Binary Collision Integrals $a_{k\ell}^{(2)}$, $b_{k\ell}^{(2)}$, $c_{k\ell}^{(2)}$

$a_{11}^{(2)} = +1$	$a_{12}^{(2)} = -\frac{1}{4}$	$a_{13}^{(2)} = -\frac{1}{32}$	$a_{14}^{(2)} = -\frac{1}{128}$
	$a_{22}^{(2)} = +\frac{45}{16}$	$a_{23}^{(2)} = -\frac{103}{128}$	$a_{24}^{(2)} = -\frac{59}{512}$
		$a_{33}^{(2)} = +\frac{5657}{1024}$	$a_{34}^{(2)} = -\frac{6783}{4096}$
			$a_{44}^{(2)} = +\frac{149749}{16384}$
$b_{00}^{(2)} = +1$	$b_{01}^{(2)} = -\frac{1}{4}$	$b_{02}^{(2)} = -\frac{1}{32}$	
	$b_{11}^{(2)} = +\frac{205}{48}$	$b_{12}^{(2)} = -\frac{163}{128}$	
		$b_{22}^{(2)} = +\frac{11889}{1024}$	
$c_{00}^{(2)} = +1$	$c_{01}^{(2)} = -\frac{1}{4}$	$c_{02}^{(2)} = -\frac{1}{32}$	
	$c_{11}^{(2)} = +\frac{59}{16}$	$c_{12}^{(2)} = -\frac{139}{128}$	
		$c_{22}^{(2)} = +\frac{8358}{1024}$	

Note: $a_{k\ell}^{(2)} = a_{\ell k}^{(2)}$; $b_{k\ell}^{(2)} = b_{\ell k}^{(2)}$; $c_{k\ell}^{(2)} = c_{\ell k}^{(2)}$

Table III

The Coefficients $a_k(N)$, $b_k(N)$, $c_k(N)$

N=1	$a_1(1)=1$	$b_0(1)=1$	$c_0(1)=1$
N=2	$a_1(2)=1.022727272$	$b_0(2)=1.014851485$	$c_0(2)=1.017241379$
	$a_2(2)=0.09090909091$	$b_1(2)=0.05940594059$	$c_1(2)=0.06896551724$
N=3	$a_1(3)=1.024818524$	$b_0(3)=1.015878912$	$c_0(3)=1.018689786$
	$a_2(3)=0.09678720258$	$b_1(3)=0.06231945009$	$c_1(3)=0.07306202215$
	$a_3(3)=0.01989514720$	$b_2(3)=0.00956957592$	$c_2(3)=0.01357698769$
N=4	$a_1(4)=1.025134456$		
	$a_2(4)=0.09761889723$		
	$a_3(4)=0.02183560672$		
	$a_4(4)=0.00606324830$		

For reasons that will become clear in Chapter III, we shall study in this report the viscosity and the self-diffusion up to the third Sonine approximation, and the thermal conductivity up to the fourth Sonine approximation. The binary collision integrals required for this analysis are listed in Table II, and the corresponding coefficients $a_k(N)$, $b_k(N)$ and $c_k(N)$, obtained by solving the simultaneous equations (2.10), are given in Table III.

The rate of convergence, as N increases, of the expansion (2.13) for the transport coefficients λ_0, η_0 and D_0 is well established [1,2]. From Table III it is seen that the second Sonine approximations $a_1(2)$, $b_0(2)$ and $c_0(2)$ modify the first approximation $a_1(1)=b_0(1)=c_0(1)=1$ by only a few percent.

2.2 Three-Particle Collision Integrals

The coefficients λ_1^{KK}, η_1^{KK} and D_1 in the density-expansion (1.4) for the transport properties are determined by three-particle collision integrals. In earlier technical reports we have presented two different methods for deriving these collision integrals. The method followed in AEDC-TR-71-51 was based on a geometrical analysis of the three-particle collision operator in the generalized Boltzmann equation [5,9]. In AEDC-TR-72-142 we presented a more algebraical derivation in which the three-particle collision operator was represented by a binary collision expansion [3]. Both methods yield the same results, and we obtained for the coefficients $\lambda_{1\mu}$, $\eta_{1\mu}$ and $D_{1\mu}$, defined in (1.5) [see equation (5.1) of Part I]

$$\lambda_1^{KK} = \sum_{\mu=1}^{4} \lambda_{1\mu} = \frac{1}{3kT^2} \sum_{\mu=1}^{4} [\vec{A},\vec{A}]_\mu^{(3)} \quad ,$$

$$\eta_1^{KK} = \sum_{\mu=1}^{4} \eta_{1\mu} = \frac{1}{10kT} \sum_{\mu=1}^{4} [\vec{\vec{B}},\vec{\vec{B}}]_\mu^{(3)} \quad , \tag{2.15}$$

$$D_1 = \sum_{\mu=1}^{4} D_{1\mu} = \frac{1}{3} \sum_{\mu=1}^{4} [\vec{C},\vec{C}]_\mu^{\tilde{(3)}} \quad .$$

Here $\vec{A}$, $\vec{\vec{B}}$ and $\vec{C}$ are the same functions as those in the expressions (2.1) for the dilute gas quantities λ_0, η_0 and D_0. However, the square brackets now indicate three-particle collision integrals defined as

(2.16)

$$[\vec{A},\vec{A}]_\mu^{(3)} = \frac{1}{3!}\int d\vec{v}_1 dx_2 dx_3 \phi(v_1)\phi(v_2)\phi(v_3) \sum_{m=1}^{3} \vec{A}(\vec{v}_m) \cdot T_\mu(123) \sum_{n=1}^{3} \vec{A}(\vec{v}_n) \quad ,$$

$$[\vec{\vec{B}},\vec{\vec{B}}]_\mu^{(3)} = \frac{1}{3!}\int d\vec{v}_1 dx_2 dx_3 \phi(v_1)\phi(v_2)\phi(v_3) \sum_{m=1}^{3} \vec{\vec{B}}(\vec{v}_m) : T_\mu(123) \sum_{n=1}^{3} \vec{\vec{B}}(\vec{v}_n) \quad ,$$

$$[\vec{C},\vec{C}]_\mu^{\tilde{(3)}} = \frac{1}{3!}\int d\vec{v}_1 dx_2 dx_3 \phi(v_1)\phi(v_2)\phi(v_3) \sum_{n=1}^{3} \vec{C}(\vec{v}_n) \cdot T_\mu(123) \vec{C}(\vec{v}_n) \quad .$$

The operators $T_\mu(123)$ (μ=1,2,3,4) are three-particle collision operators defined in Part I.

We introduce again dimensionless quantities as given by (1.7), (2.5), (2.6) and

$$T_\mu^*(123) = \sigma \left[\frac{m}{2kT}\right]^{1/2} T_\mu(123) \quad . \tag{2.17}$$

Using (1.6) and (2.7) we may thus write

$$\lambda_1^{KK} = -\frac{5}{12}\pi\sigma^3\lambda_0[1+\sum_{\mu=2}^{4}\lambda_{1\mu}^*] \quad ,$$

$$\eta_1^{KK} = -\frac{5}{12}\pi\sigma^3\eta_0[1+\sum_{\mu=2}^{4}\eta_{1\mu}^*] \quad , \tag{2.18}$$

$$D_1 = -\frac{5}{12}\pi\sigma^3 D_0[1+\sum_{\mu=2}^{4}D_{1\mu}^*] \quad ,$$

with

$$\lambda_{1\mu}^* = -\frac{\{\vec{A}^*;\vec{A}^*\}_\mu^{(3)}}{\{\vec{A}^*;\vec{A}^*\}^{(2)}} \quad , \quad \eta_{1\mu}^* = -\frac{\{\vec{B}^*;\vec{B}^*\}_\mu^{(3)}}{\{\vec{B}^*;\vec{B}^*\}^{(2)}} \quad , \quad D_1^* = -\frac{\{\vec{C}^*;\vec{C}^*\}_\mu^{(\tilde{3})}}{\{\vec{C}^*;\vec{C}^*\}^{(\tilde{2})}} \quad . \tag{2.19}$$

Here we have introduced dimensionless three-particle collision integrals defined as

$$\{\vec{A}^*;\vec{A}^*\}_\mu^{(3)} = \frac{3\sqrt{2}}{10\pi^6}\frac{1}{3!}\int d\vec{W}_1 d\vec{W}_2 d\vec{W}_3 d\vec{r}_2^* d\vec{r}_3^* e^{-(W_1^2+W_2^2+W_3^2)}$$

$$\times \sum_{m=1}^{3}\vec{A}^*(\vec{W}_m)\cdot T_\mu^*(123)\sum_{n=1}^{3}\vec{A}^*(\vec{W}_n) \quad ,$$

$$\{\vec{B}^*;\vec{B}^*\}_\mu^{(3)} = \frac{3\sqrt{2}}{10\pi^6}\frac{1}{3!}\int d\vec{W}_1 d\vec{W}_2 d\vec{W}_3 d\vec{r}_2^* d\vec{r}_3^* e^{-(W_1^2+W_2^2+W_3^2)} \tag{2.20}$$

$$\times \sum_{m=1}^{3}\vec{B}^*(\vec{W}_m) : T_\mu^*(123)\sum_{n=1}^{3}\vec{B}^*(\vec{W}_n) \quad ,$$

$$\{\vec{C}^*;\vec{C}^*\}_\mu^{(\tilde{3})} = \frac{3\sqrt{2}}{10\pi^6}\frac{1}{3!}\int d\vec{W}_1 d\vec{W}_2 d\vec{W}_3 d\vec{r}_2^* d\vec{r}_3^* e^{-(W_1^2+W_2^2+W_3^2)}$$

$$\times 2\sum_{n=1}^{3}\vec{C}^*(\vec{W}_n)\cdot T_\mu^*(123)\,\vec{C}^*(\vec{W}_n) \quad .$$

We may again represent the functions $\vec{A}^*$, $\vec{B}^*$ and $\vec{C}^*$ by the Sonine polynomial expansion (2.9). We then obtain for the coefficients λ_1^{KK}, η_1^{KK} and D_1 in the N^{th} Sonine approximation

$$\lambda_1^{KK}(N) = -\frac{5}{12}\pi\sigma^3\lambda_0(N)\left[1+\sum_{\mu=2}^{4}\lambda_{1\mu}^*(N)\right] ,$$

$$\eta_1^{KK}(N) = -\frac{5}{12}\pi\sigma^3\eta_0(N)\left[1+\sum_{\mu=2}^{4}\eta_{1\mu}^*(N)\right] , \qquad (2.21)$$

$$D_1(N) = -\frac{5}{12}\pi\sigma^3 D_0(N)\left[1+\sum_{\mu=2}^{4}D_{1\mu}^*(N)\right] ,$$

with

$$\lambda_{1\mu}^*(N) = -\frac{1}{a_1(N)}\sum_{k=1}^{N}\sum_{\ell=1}^{N} a_k(N)\,a_\ell(N)\,a_{k\ell,\mu}^{(3)} ,$$

$$\eta_{1\mu}^*(N) = -\frac{1}{b_0(N)}\sum_{k=0}^{N-1}\sum_{\ell=0}^{N-1} b_k(N)\,b_\ell(N)\,b_{k\ell,\mu}^{(3)} , \qquad (2.22)$$

$$D_{1\mu}^*(N) = -\frac{1}{c_0(N)}\sum_{k=0}^{N-1}\sum_{\ell=0}^{N-1} c_k(N)\,c_\ell(N)\,c_{k\ell,\mu}^{(3)} .$$

Here we have defined elements $a_{k\ell,\mu}^{(3)}$, $b_{k\ell,\mu}^{(3)}$ and $c_{k\ell,\mu}^{(3)}$ of matrices of three-particle collision integrals†

†The matrix elements $a_{k\ell,\mu}^{(3)}$ and $b_{k\ell,\mu}^{(3)}$ are related to the matrix elements $a_{k\ell}^{(1)}$ and $b_{k\ell}^{(1)}$ in AEDC-TR-69-68 [4,7,12] by

$$\sum_{\mu=1}^{4} a_{k\ell,\mu}^{(3)} = -\frac{8}{5}a_{k\ell}^{(1)} \quad \text{and} \quad \sum_{\mu=1}^{4} b_{k\ell,\mu}^{(3)} = -\frac{8}{5}b_{k\ell}^{(1)} .$$

$$a^{(3)}_{k\ell,\mu}=\{S^{(k)}_{3/2}(W^2)\vec{W}\ ,\ S^{(\ell)}_{3/2}(W^2)W\}^{(3)}_{\mu}\quad ,$$

$$b^{(3)}_{k\ell,\mu}=\{S^{(k)}_{5/2}(W^2)\vec{WW}\ ,\ S^{(\ell)}_{5/2}(W^2)\vec{WW}\}^{(3)}_{\mu}\quad , \tag{2.23}$$

$$c^{(3)}_{k\ell,\mu}=\{S^{(k)}_{3/2}(W^2)\vec{W}\ ,\ S^{(\ell)}_{3/2}(W^2)\vec{W}\}^{(\tilde{3})}_{\mu}\quad .$$

In earlier reports [3,5,9] we have shown that these matrices are symmetric in analogy with the result (2.12) for the binary collision matrices:

$$a^{(3)}_{k\ell,\mu}=a^{(3)}_{\ell k,\mu};\quad b^{(3)}_{k\ell,\mu}=b^{(3)}_{\ell k,\mu};\quad c^{(3)}_{k\ell,\mu}=c^{(3)}_{\ell k,\mu}\ . \tag{2.24}$$

2.3 Collision Integrals and Collision Diagrams

It is seen from (2.21)-(2.23) that we have to evaluate a set of three-particle collision integrals of the form $\{\psi,\chi\}^{(3)}_{\mu}$ and $\{\psi,\chi\}^{(\tilde{3})}_{\mu}$, where ψ and χ are functions of the dimensionless velocity $\vec{W}$. These integrals involve the dynamics of the three-particle collision sequences discussed in Section 1.2. However, in order to precisely specify the relationship between the collision integrals and the collision sequences, we use a diagrammatic notation which is a bit more abstract.

We first make a distinction between *interacting* collisions and *noninteracting* collisions. In an interacting collision between two molecules, the molecular velocities change according to the usual laws of mechanics. In a noninteracting collision the colliding molecules pass through each other's interaction sphere undeflected. A noninteracting collision may be decomposed into a noninteracting *penetrating*

collision, when the molecules enter each other's interaction sphere, followed by a period during which the two molecules are overlapping, followed in turn by a noninteracting *separating* collision, when the particles leave each other's interaction sphere. We shall continue to indicate the trajectories of the centers of the molecules by line diagrams as in Figs. 3-5. However, we shall indicate whether at a given instant two particles are penetrating, separating or overlapping by the notation presented in Fig. 2 of Part I [3].

As an example, consider the collision integrals related to sequences of *two* successive collisions. These "single-overlap" collision integrals can be formulated in terms of the SS-collision sequence and SN-collision sequence shown in Fig. 6. In both collision sequences the collision between 1 and 2 is followed after some time $\tau>0$ by a collision between 1 and 3. In Fig. 6a particles 2 and 3 overlap at both these collisions, as is indicated by the hash marks. In Fig. 6b particles 2 and 3 overlap at the time of the collision between 1 and 2, but, they leave each other's interaction sphere after some time τ', with $0<\tau'<\tau$, i.e., before the collision between 1 and 3 occurs. We use roman numerals to indicate *velocity regions* in the diagram of interest. Thus, $\vec{W}_i(I)$ represents the initial velocities, $\vec{W}_i(II)$ the velocities between the two collisions, and $\vec{W}_i(III)$ the final velocities, in the diagrams of Fig. 6. We shall use a similar notation to indicate the velocities in the sequences of three and four successive collisions.

In Part I we have shown that the collision integrals $\{\psi,\chi\}_2^{(3)}$ and $\{\psi,\chi\}_2^{\tilde{(3)}}$ corresponding to the single-overlap collisions may be written as

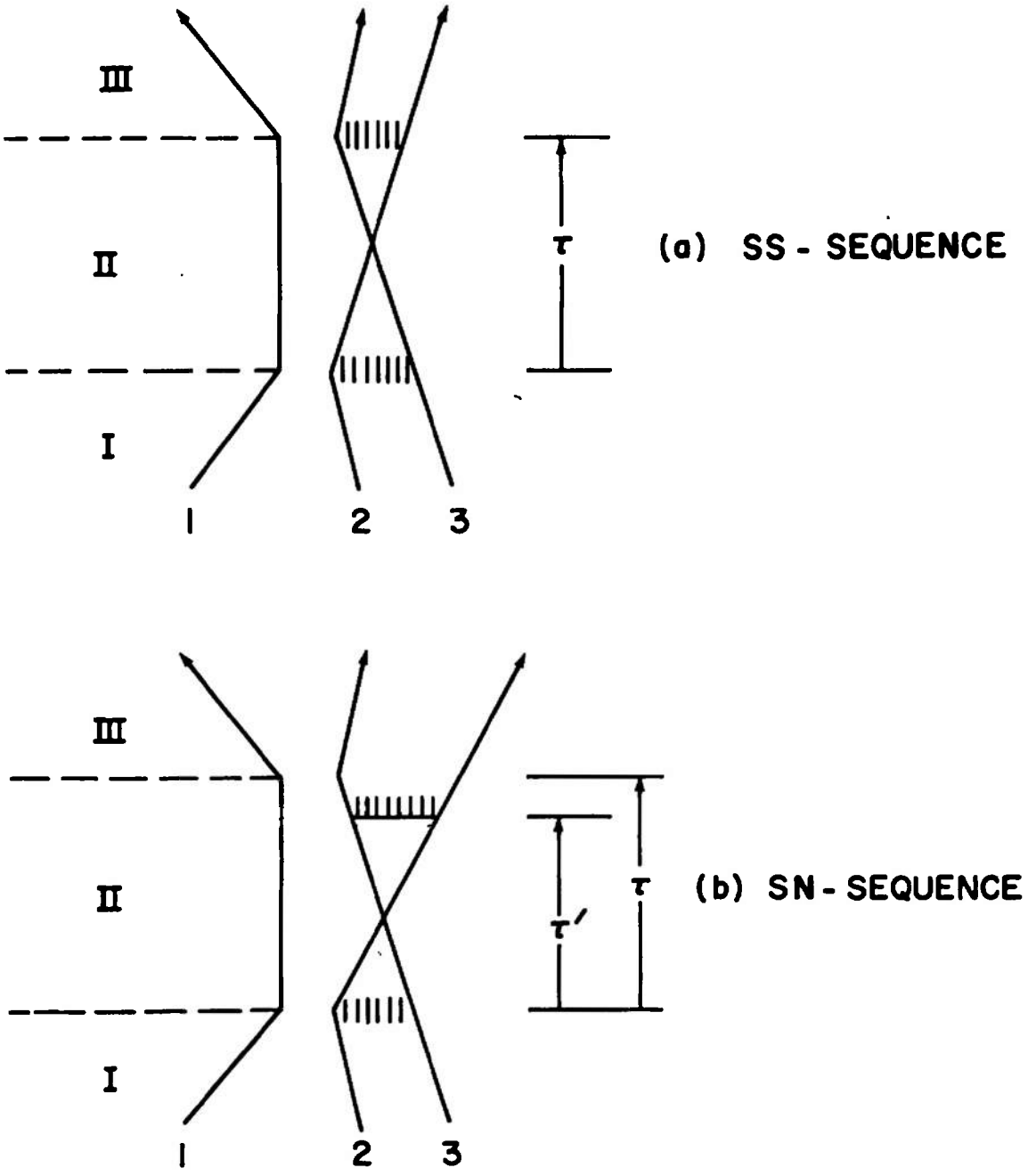

Figure 6. Diagrams representing the SS-collision and SN-collision.

$$\{\psi,\chi\}_2^{(3)}=\{\psi,\chi\}_{SS}^{(3)}+\{\psi,\chi\}_{SN}^{(3)}+\{\chi,\psi\}_{SN}^{(3)} \quad , \tag{2.25a}$$

$$\{\psi,\chi\}_2^{\tilde{(3)}}=\{\psi,\chi\}_{SS}^{\tilde{(3)}}+\{\psi,\chi\}_{SN}^{\tilde{(3)}}+\{\chi,\psi\}_{SN}^{\tilde{(3)}} \quad . \tag{2.25b}$$

The explicit formulae for these collision integrals are given by eqs. (5.16) and (5.21) of Part I [3]. In the terms of dimensionless quantities they may be written as

$$\{\psi,\chi\}_{SS}^{(3)}=\frac{3\sqrt{2}}{10\pi^6}\int_{\Omega_{SS}} d\Omega^* e^{-(W_1^2+W_2^2+W_3^2)} \tag{2.26a}$$

$$\times \sum_{m=1}^{3}\sum_{n=1}^{3}\{\psi_m(I)-\psi_m(II)\}^*\{\chi_n(III)-\chi_n(II)\} \quad ,$$

$$\{\psi,\chi\}_{SS}^{\tilde{(3)}}=\frac{3\sqrt{2}}{10\pi^6}\int_{\Omega_{SS}} d\Omega^* e^{-(W_1^2+W_2^2+W_3^2)} \tag{2.26b}$$

$$\times 2\{\psi_1(I)-\psi_1(II)\}^*\{\chi_1(III)-\chi_1(II)\} \quad ,$$

$$\{\psi,\chi\}_{SN}^{(3)}=\frac{3\sqrt{2}}{10\pi^6}\int_{\Omega_{SN}} d\Omega^* e^{-(W_1^2+W_2^2+W_3^2)} \tag{2.27a}$$

$$\times \sum_{m=1}^{3}\sum_{n=1}^{3}\{\psi_m(I)-\psi_m(II)\}^*\{\chi_n(III)-\chi_n(II)\} \quad ,$$

$$\{\psi,\chi\}_{SN}^{\tilde{(3)}}=\frac{3\sqrt{2}}{10\pi^6}\int_{\Omega_{SN}} d\Omega^* e^{-(W_1^2+W_2^2+W_3^2)} \tag{2.27b}$$

$$\times 2\{\psi_1(I)-\psi_1(II)\}^*\{\chi_1(III)-\chi_1(II)\} \quad .$$

Here we have abbreviated $\psi(\vec{W}_m(I))$ by $\psi_m(I)$, etc. The notation $\psi * \chi$ indicates the appropriate scalar product between the vector or tensor functions $\psi(\vec{W})$ and $\chi(\vec{W})$. The symbol $d\Omega^*$ represents a dimensionless volume element

$$d\Omega^* = d\vec{W}_1 d\vec{W}_2 d\vec{W}_3 d\hat{k}_1 d\vec{r}^*_{31} |\vec{W}_{21} \cdot \hat{k}_1| \quad , \tag{2.28}$$

where $\hat{k}_1 = \vec{r}^*_1 - \vec{r}^*_2$ and $\vec{r}^*_{31} = \vec{r}^*_3 - \vec{r}^*_1$ are the relative positions of the molecules at the instant of the first (1-2) collision. The velocities $\vec{W}_i$ *without* a velocity region designation are understood to represent the velocities just *after* the first collision:

$$\vec{W}_i \equiv \vec{W}_i(II) \text{ for } i=1,2,3 \quad . \tag{2.29}$$

The integrations in (2.26a) and (2.26b) are to be carried out over that subvolume Ω_{SS} of the 14-dimensional space spanned by the variables $\vec{W}_1$, $\vec{W}_2$, $\vec{W}_3$, $\hat{k}_1$ and $\vec{r}^*_{31}$, for which the SS-collision sequence can be dynamically realized. Similarly, the integrations in (2.27) are to be carried out over the subvolume Ω_{SN} of the same 14-dimensional space which corresponds to the dynamical requirements of the SN-collision sequence. Notice that the subvolumes Ω_{SS} and Ω_{SN} have no points in common.

The collision integrals $\{\psi,\chi\}^{(3)}$ and $\{\psi,\chi\}^{(\tilde{3})}$, associated with sequences of *three* successive collisions, are sums of three terms:

$$\{\psi,\chi\}_3^{(3)} = \{\psi,\chi\}_R^{(3)} + \{\psi,\chi\}_H^{(3)} + \{\psi,\chi\}_C^{(3)} \equiv \sum_{\nu=1}^{3} \{\psi,\chi\}_{3\nu}^{(3)} \quad , \tag{2.30a}$$

$$\{\psi,\chi\}_3^{(\tilde{3})} = \{\psi,\chi\}_R^{(\tilde{3})} + \{\psi,\chi\}_H^{(\tilde{3})} + \{\psi,\chi\}_C^{(\tilde{3})} \equiv \sum_{\nu=1}^{3} \{\psi,\chi\}_{3\nu}^{(\tilde{3})} \quad . \tag{2.30b}$$

Here the index ν refers to the R(ν=1), H(ν=2) and C(ν=3) diagrams in Fig. 7. These collision integrals are given by eqs. (5.25), (5.29), (5.32) and (5.35) of Part I [3] and read in dimensionless form

$$\{\psi,\chi\}_{3\nu}^{(3)}=(-1)^{\nu-1}\frac{3\sqrt{2}}{10\pi^6}\int_{\Omega_{3\nu}}d\Omega^* e^{-(W_1^2+W_2^2+W_3^2)} \tag{2.31a}$$

$$\times\sum_{m=1}^{3}\sum_{n=1}^{3}\{\psi_m(I)-\psi_m(II)\}*\{\chi_n(IV_\nu)-\chi_n(III_\nu)\}\quad,$$

$$\{\psi,\chi\}_{3}^{(\tilde{3})}=(-1)^{\nu-1}\frac{3\sqrt{2}}{10\pi^6}\int_{\Omega_{3\nu}}d\Omega^* e^{-(W_1^2+W_2^2+W_3^2)} \tag{2.31b}$$

$$\times\,2\sum_{n=1}^{3}\{\psi_n(I)-\psi_n(II)\}*\{\chi_n(IV_\nu)-\chi_n(III_\nu)\}\quad.$$

The symbols I, II, III_ν and IV_ν now refer to the velocity regions in the diagrams of Fig. 7. The integration element $d\Omega^*$ is the same as in (2.28), with $\vec{W}_1$, $\vec{W}_2$, $\vec{W}_3$ denoting the velocities, and $\hat{k}_1=\vec{r}_1^*-\vec{r}_2^*$, $\vec{r}_{31}^*=\vec{r}_3^*-\vec{r}_1^*$ denoting the relative positions, instantaneously after the first (1-2) collision. Notice that nothing precludes the integration volumes Ω_{31}, Ω_{32}, Ω_{33} from having non-empty intersections.

The collision integrals $\{\psi,\chi\}_4^{(3)}$ and $\{\psi,\chi\}_4^{(\tilde{3})}$, associated with sequences of *four* successive collisions can be decomposed as

$$\{\psi,\chi\}_4^{(3)}=[\{\psi,\chi\}_{RH}^{(3)}+\{\chi,\psi\}_{RH}^{(3)}]+[\{\psi,\chi\}_{RC}^{(3)}+\{\chi,\psi\}_{RC}^{(3)}]\equiv$$

$$\equiv\sum_{\nu=1}^{2}[\{\psi,\chi\}_{4\nu}^{(3)}+\{\chi,\psi\}_{4\nu}^{(3)}]\quad, \tag{2.32a}$$

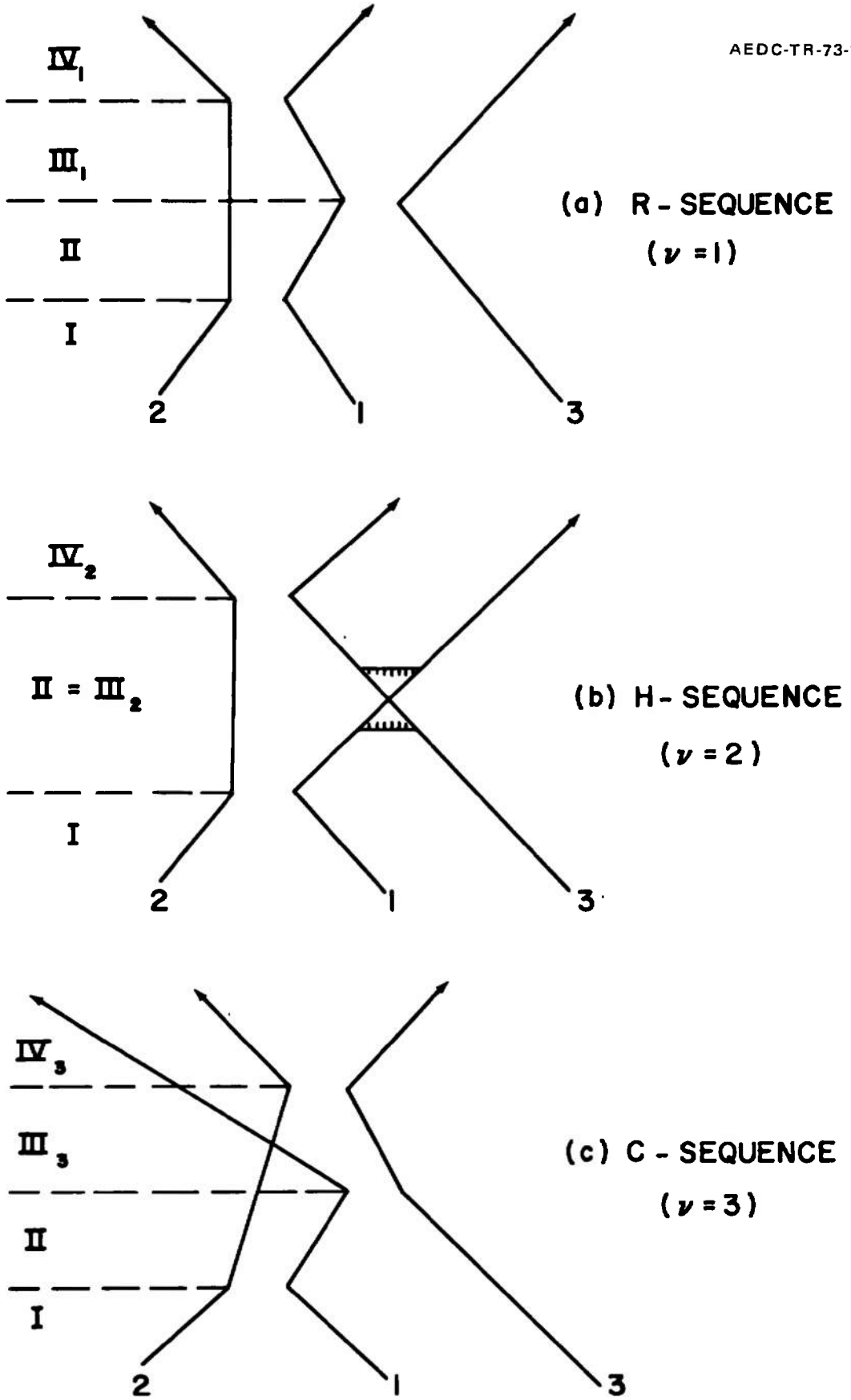

Figure 7. Diagrams representing the R-collision, H-collision, and C-collision.

$$\{\psi,\chi\}_4^{\tilde{(3)}} = [\{\psi,\chi\}_{RH}^{\tilde{(3)}} + \{\chi,\psi\}_{RH}^{\tilde{(3)}}] + [\{\psi,\chi\}_{RC}^{\tilde{(3)}} + \{\chi,\psi\}_{RC}^{\tilde{(3)}}] \equiv$$

$$\equiv \sum_{\nu=1}^{2} [\{\psi,\chi\}_{4\nu}^{\tilde{(3)}} + \{\chi,\psi\}_{4\nu}^{\tilde{(3)}}] \quad , \tag{2.32b}$$

where the index ν now refers to the RH(ν=1) and RC(ν=2) diagrams in Fig. 8. From eqs. (5.39) and 5.42) of Part I we conclude that they may be written as

$$\{\psi,\chi\}_{4\nu}^{(3)} = (-1)^{\nu} \frac{3\sqrt{2}}{10\pi^6} \int_{\Omega_{4\nu}} d\Omega^* e^{-(W_1^2+W_2^2+W_3^2)} \tag{2.33a}$$

$$\times \sum_{m=1}^{3} \sum_{n=1}^{3} \{\psi_m(\mathrm{I}) - \psi_m(\mathrm{II})\}^* \{\chi_n(V_\nu) - \chi_n(\mathrm{IV}_\nu)\} \quad ,$$

$$\{\psi,\chi\}_{4\nu}^{(3)} = (-1)^{\nu} \frac{3\sqrt{2}}{10\pi^6} \int_{\Omega_{4\nu}} d\Omega^* e^{-(W_1^2+W_2^2+W_3^2)} \tag{2.33b}$$

$$\times\ 2 \sum_{n=1}^{3} \{\psi_n(\mathrm{I}) - \psi_n(\mathrm{II})\}^* \{\chi_n(V_\nu) - \chi_n(\mathrm{IV}_\nu)\} \quad ,$$

where the integration variables, integration volumes and velocity regions now refer to the diagrams in Fig. 8.

We note that all collision sequences begin with an interacting collision between 1 and 2, which is followed by a collision between 1 and 3; the collision between 1 and 3 may either be an interacting collision (SS, SN, R, C, RH, RC) or a non-interacting penetrating collision (H). These first two collisions are represented schematically in Fig. 9. The initial velocities are $\vec{W}_1(\mathrm{I})$, $\vec{W}_2(\mathrm{I})$ and $\vec{W}_3(\mathrm{I})$; the integration variables $\vec{W}_1$, $\vec{W}_2$, $\vec{W}_3$ are the velocities after the first collision: $\vec{W}_1 = \vec{W}_1(\mathrm{II})$, $\vec{W}_2 = \vec{W}_2(\mathrm{II})$, $\vec{W}_3 = \vec{W}_3(\mathrm{II}) = \vec{W}_3(\mathrm{I})$. The vector $\hat{k}_1$ is the perihelion vector

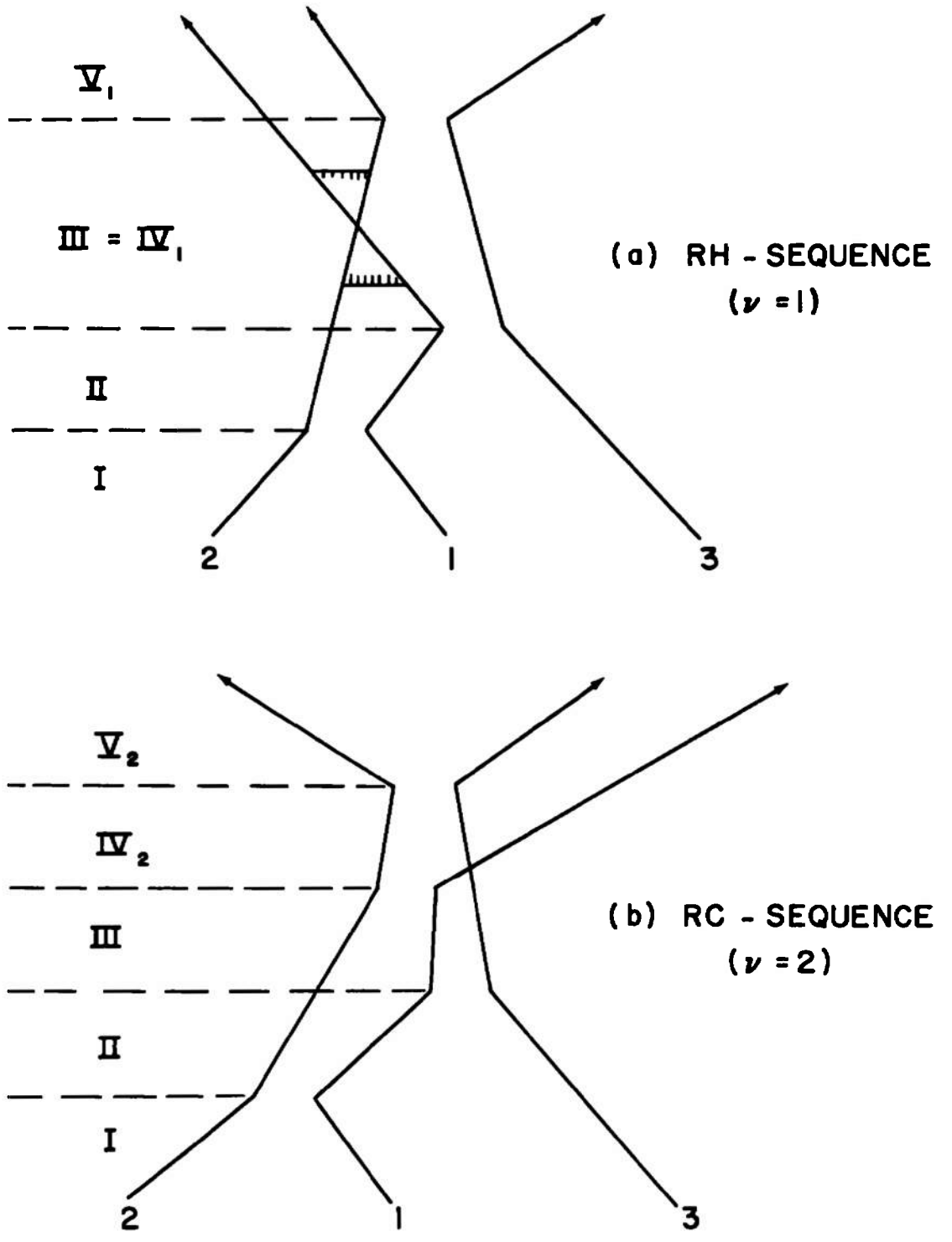

Figure 8. Diagrams representing the RH-collision and RC-collision.

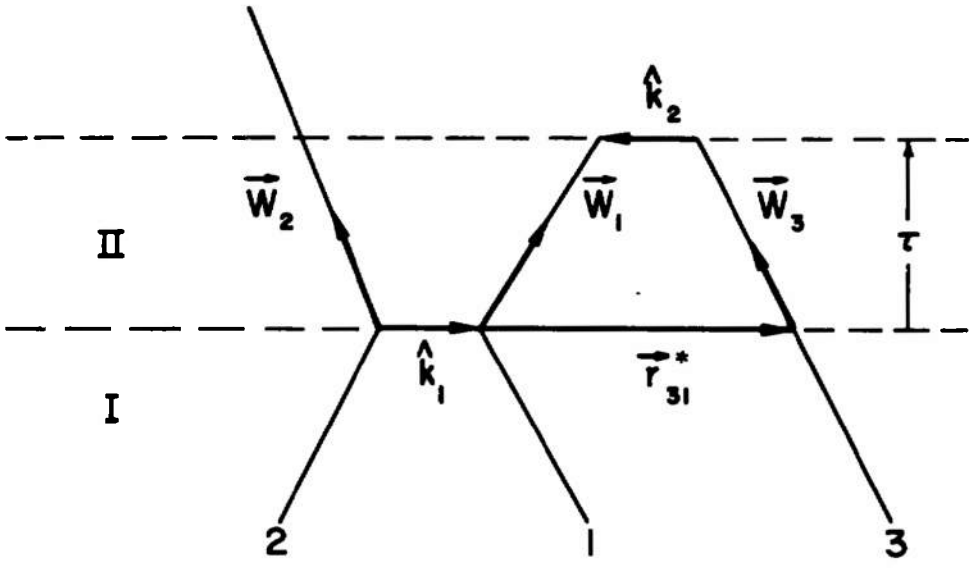

Figure 9. Schematic representation of the integration variables.

of the 1-2 collision. It will sometimes be convenient to replace the integration variables $\vec{r}^{\,*}_{31}$ by $\hat{k}_2$ and τ, where $\hat{k}_2$ is the perihelion vector of the 1-3 collision and τ the time between the two collisions. From Fig. 9 it is clear that these quantities are related by

$$-\hat{k}_2 = \vec{r}^{\,*}_{31} + \vec{W}_{31}\tau \quad , \tag{2.34a}$$

from which it follows that

$$dr^*_{31} = |\vec{W}_{31} \cdot \hat{k}_2| \, d\hat{k}_2 d\tau \quad . \tag{2.34b}$$

In all our calculations, we shall begin by making the transformation

$$\vec{W}_1, \vec{W}_2, \vec{W}_3 \rightarrow \vec{W}_0, \vec{W}_{21}, \vec{W}_{31} \quad , \tag{2.35}$$

where the new velocity variables are defined by

$$\left.\begin{aligned}\vec{W}_0 &= \tfrac{1}{3}(\vec{W}_1+\vec{W}_2+\vec{W}_3)\\ \vec{W}_{21} &= \vec{W}_2-\vec{W}_1\\ \vec{W}_{31} &= \vec{W}_3-\vec{W}_1\end{aligned}\right\} \quad \text{or} \quad \left\{\begin{aligned}\vec{W}_1 &= \vec{W}_0-\tfrac{1}{3}(\vec{W}_{21}+\vec{W}_{31})\\ \vec{W}_2 &= \vec{W}_0-\tfrac{1}{3}(\vec{W}_{31}-2\vec{W}_{21})\\ \vec{W}_3 &= \vec{W}_0-\tfrac{1}{3}(\vec{W}_{21}-2\vec{W}_{31})\end{aligned}\right. \quad . \tag{2.36}$$

Thus $\vec{W}_0$ is the velocity of the center of gravity of the three spheres, while $\vec{W}_{21}$ and $\vec{W}_{31}$ are the respective velocities of spheres 2 and 3 relative to sphere 1. The Jacobian of this transformation is unity, so that

$$d\vec{W}_1 d\vec{W}_2 d\vec{W}_3 = d\vec{W}_0 d\vec{W}_{21} d\vec{W}_{31} \quad . \tag{2.37}$$

Under this transformation the Maxwellian exponential in the integrands becomes

$$e^{-(W_1^2+W_2^2+W_3^2)} = e^{-(3W_0^2+E)} \quad , \tag{2.38}$$

where E depends only on $\vec{W}_{21}$ and $\vec{W}_{31}$ according to

$$E \equiv \tfrac{2}{3}(W_{21}^2+W_{31}^2-\vec{W}_{21}\cdot\vec{W}_{31}) \quad . \tag{2.39}$$

Since each collision conserves energy and momentum, E has the same value in all velocity regions: E=E(I)=E(II)=, etc.

Collecting the foregoing relations, we find that the common element appearing in the various triple collision integrals can be written as

$$d\Omega * e^{-(W_1^2+W_2^2+W_3^2)} =$$

$$= d\vec{W}_0 d\vec{W}_{21} d\vec{W}_{31} d\hat{k}_1 d\hat{k}_2 d\tau \, |\vec{W}_{21}\cdot\hat{k}_1| \, |\vec{W}_{31}\cdot\hat{k}_2| \, e^{-3W_0^2} e^{-E} \quad . \tag{2.40}$$

This form will be our starting point for the explicit calculations in the following sections, save for the following two minor exceptions: First, in the single-overlap calculations, it is convenient to retain the integration variable $\vec{r}^{*}_{31}$, and thus not introduce the transformation (2.34). Second, in a special calculation of the R-sequence, and in the calculations of the RH-and RC-sequences, it is convenient to introduce the further transformation $\vec{W}_{21} \rightarrow \vec{W}_{12}=-\vec{W}_{21}$.

All the three-particle collision integrals are seen to be 14-dimensional. However, since the integrands are isotropic functions of the vector variables, we are free to choose one of the vector variables as the Z-axis and another as defining the XZ-plane. The two vector variables chosen for this purpose will not be the same in all calculations. However, it is always true that this process is equivalent to performing *three* of the fourteen integrations. For when one vector is picked as the Z-axis, we are essentially integrating over the polar and azimuthal angles of that vector; similarly, when a second vector is picked to define the XZ plane, we are essentially integrating over the azimuthal angle of that vector. Hence, we shall always begin by choosing our coordinate system in this way, and *replacing* the angular integrations over the vector defining the Z-axis and the azimuthal integration over the vector defining the XZ-plane by the factor

$$(2\cdot 2\pi)(2\pi) = 8\pi^2 \quad . \tag{2.41}$$

Finally, the following definitions will be frequently employed

$$\Psi(I) \equiv \sum_{n=1}^{3} \psi_n(I) \equiv \sum_{n=1}^{3} \psi(\vec{W}_n(I)) \quad , \text{ etc. for II,III,...}$$

$$X(I) \equiv \sum_{n=1}^{3} \chi_n(I) \equiv \sum_{n=1}^{3} \chi(\vec{W}_n(I)) \quad , \text{ etc. for II,III,...} \tag{2.42}$$

CHAPTER III

SEQUENCES OF TWO SUCCESSIVE COLLISIONS (SINGLE-OVERLAP COLLISIONS)

3.1 Introduction

The collision integrals $\{\psi,\chi\}_2^{(3)}$ and $\{\psi,\chi\}_2^{\tilde{(3)}}$ are related to the SS- and SN-collision sequences shown in Fig. 6. Both collision sequences may be represented by the diagram of Fig. 10. In this diagram we require that molecules 2 and 3 are overlapping at the instant of the 1-2 collision, but we do not specify the time τ' at which the particles 2 and 3 separate. We shall refer to this diagram as the SO (single-overlap) diagram and to $\{\psi,\chi\}_2^{(3)}$ and $\{\psi,\chi\}_2^{\tilde{(3)}}$ as the SO (single-overlap) integrals. The SO-diagram in Fig. 10 reproduces the SS-collision sequence in Fig. 6a if $\tau'>\tau$ and it reproduces the SN-collision sequence in Fig. 6b if $\tau'<\tau$. It thus follows from (2.25)-(2.27) that we may write

$$\{\psi,\chi\}_2^{(3)}=-\frac{3\sqrt{2}}{10\pi^6}\int_{\Omega_{SO}} d\Omega\ e^{-(W_1^2+W_2^2+W_3^2)} \tag{3.1a}$$

$$\times\sum_{m=1}^{3}\sum_{n=1}^{3}[\{\psi_m(I)-\psi_m(II)\}*\{\chi_n(III)-\chi_n(II)\}$$

$$+\dot{\Theta}(\tau-\tau')\{\chi_m(I)-\chi_m(II)\}*\{\psi_n(III)-\psi_n(II)\}],$$

$$\{\psi,\chi\}_2^{\tilde{(3)}}=-\frac{3\sqrt{2}}{10\pi^6}\int_{\Omega_{SO}} d\Omega\ e^{-(W_1^2+W_2^2+W_3^2)} \tag{3.1b}$$

$$\times 2[\{\psi_1(I)-\psi_1(II)\}*\{\chi_1(III)-\chi_1(II)\}$$

$$+\ \Theta(\tau-\tau')\{\chi_1(I)-\chi_1(II)\}*\{\psi_1(III)-\psi_1(II)\}]\ ,$$

where

$$\theta(t)=1 \text{ for } t>0 \text{ and } \theta(t)=0 \text{ for } t<0, \tag{3.2}$$

and where the integration region Ω_{SO} now refers to the SO-diagram in Fig. 10. From now on we shall always use dimensionless quantities, and so we shall drop the asterisks in the dimensionless volume element $d\Omega^*$ and the dimensionless positions $\vec{r}_i^*$.

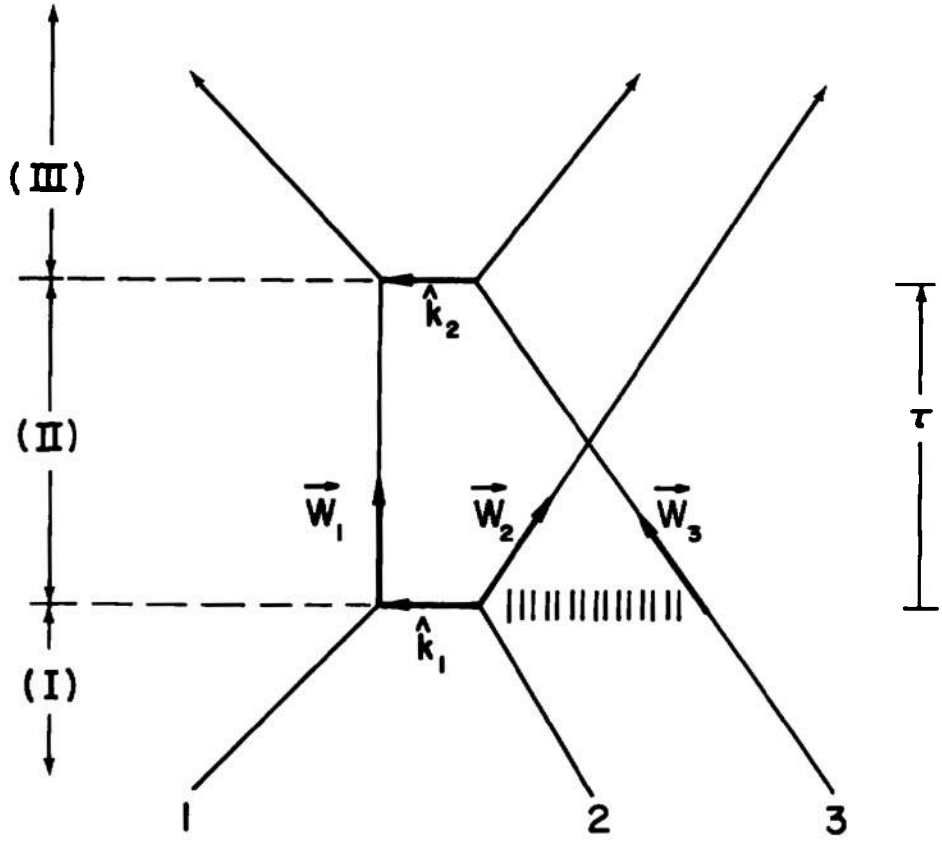

Figure 10. The SO-diagram associated with $\{\psi,\chi\}_2^{(3)}$ and $\{\psi,\chi\}_2^{\tilde{(3)}}$.

Since the two collision integrals $\{\psi,\chi\}_2^{(3)}$ and $\{\psi,\chi\}_2^{(\tilde{3})}$ refer to the same collision sequence, it is convenient to design a notation that covers both integrals. For any function $\alpha(\vec{W})$ and $\beta(\vec{W})$ we therefore define

$$(\alpha,\beta)_2 \equiv -\frac{3\sqrt{2}}{10\pi^6}\int_{\Omega_{SO}} d\Omega\ e^{-(W_1^2+W_2^2+W_3^2)}\,[\{\alpha(I)-\alpha(II)\}*\{\beta(III)-\beta(II)\} + \Theta(\tau-\tau')\{\beta(I)-\beta(II)\}*\{\alpha(III)-\alpha(II)\}] \quad . \tag{3.3}$$

We may then rewrite (3.1a) and (3.1b) as

$$\{\psi,\chi\}_2^{(3)} = (\Psi,X)_2 \quad , \tag{3.4a}$$

$$\{\psi,\chi\}_2^{\tilde{(3)}} = 2(\psi_1,\chi_1)_2 \quad , \tag{3.4b}$$

where $\Psi = \sum_{m=1}^{3}\psi_m$ and $X = \sum_{n=1}^{3}\chi_n$ as defined in (2.42).

As integration variables we choose the velocities $\vec{W}_0$, $\vec{W}_{21}$, $\vec{W}_{31}$ defined in (2.36) and the position vectors $\hat{k}_1$ and $\vec{r}_{31}$. The domains of integration of these variables are defined by the SO-diagram in Fig. 10. To obtain *specific limits* for the integrations, we consider the configuration of the particles in the rest frame of 1 just after the first collision. We take $\vec{W}_{21}$ in the +Z-direction and $\hat{k}_1$ in the XZ-plane as shown in Fig. 11; thus we have integrated trivially over the polar and azimuthal angles of $\vec{W}_{21}$ and the azimuthal angle of $\hat{k}_1$, yielding an overall factor $8\pi^2$ [see (2.41)]. The explicit limits of integration

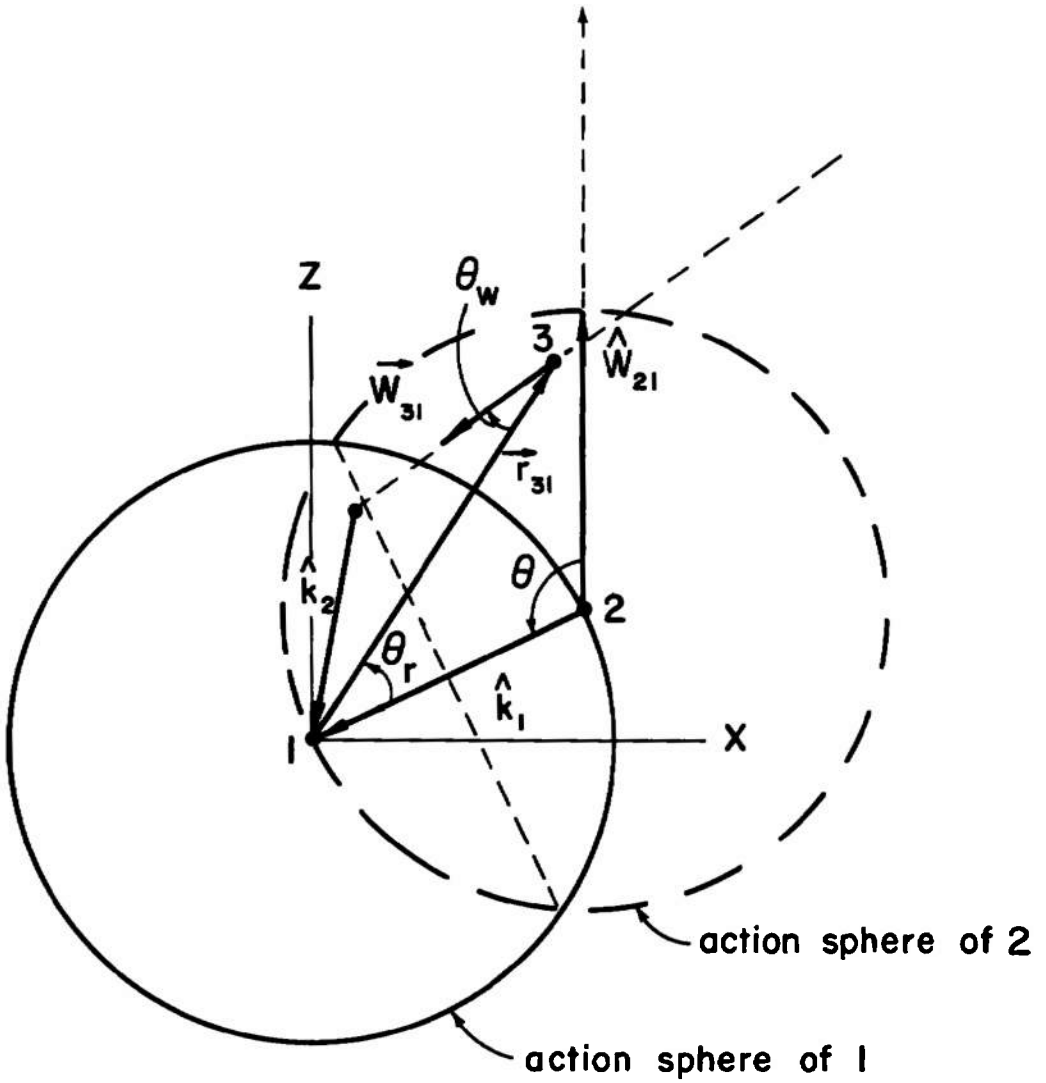

Figure 11. Schematic representation of the integration variables used in the calculation of the SO-integrals (=2). The figure shows the centers of 2 and 3 in the rest frame of 1 *just after* the first collision, with $\vec{W}_{12}$ in the Z-direction and $\hat{k}_1$ in the XZ-plane.

are now obtained simply by examining the constraints which are imposed on the geometry of Fig. 11 by the requirements of Fig. 10.

The variable $\vec{W}_0$ (not shown in Fig. 11) represents the velocity of the center of gravity and, hence, does not affect the relative motion of the particles; thus the components of $\vec{W}_0$ may assume all possible values. The magnitude of $\vec{W}_{21}$ is also unrestricted; the angles of $\vec{W}_{21}$ have already been integrated over in choosing $\vec{W}_{21}$ to lie along the Z-axis. If θ denotes the polar angle of $\hat{k}_1$ relative to the polar axis $\vec{W}_{21}$, then θ can vary from $\pi/2$ to π, so that $\cos\theta$ varies from -1 to 0; the azimuthal angle of $\hat{k}_1$ has already been integrated over in picking $\hat{k}_1$ to lie in the XZ-plane. With $\hat{k}_1$ fixed, we next choose $\vec{r}_{31}$ so that 3 lies anywhere *inside* the action sphere of 2 but *outside* the action sphere of 1. Denoting $\vec{r}_{31}$ by (r,θ_r,ϕ_r) with $-\hat{k}_1$ as the polar axis, then we see from Fig. 11 that ϕ_r can have any value between 0 and 2π, $\cos\theta_r$ any value between 1/2 and 1, and r any value between 1 and $2\cos\theta_r$. With $\vec{r}_{31}$ thus fixed, $\vec{W}_{31}$ must then be aimed to hit the action sphere of 1. Denoting $\vec{W}_{31}$ by (W_{31},θ_w,ϕ_w) with $-\vec{r}_{31}$ as the polar axis, we may deduce from Fig. 11 that the center of 3 will hit the action sphere of 1 provided that $\cos\theta_w$ lies between $\sqrt{1-r^{-2}}$ and 1; then ϕ_w may assume any value between 0 and 2π, while W_{31} may assume any value between 0 and ∞. These considerations allow us to write the SO-integral (3.3) in the following *explicit* 11-dimensional form†

---

† This collision integral was earlier derived in eq. (5-27) of AEDC-TR-71-51 [5].

$$(\alpha,\beta)_2 = -\frac{12\sqrt{2}}{5\pi^4}\int_{\infty}\int\int d^3\vec{W}_0 \int_0^{\infty} dW_{21} W_{21}^2 \int_{-1}^{0} d\cos\theta \int_0^{2\pi} d\phi_r \int_{1/2}^{1} d\cos\theta_r \int_1^{2\cos\theta_r} dr\, r^2$$

$$\times \int_0^{\infty} dW_{31} W_{31}^2 \int_0^{2\pi} d\phi_w \int_{\sqrt{1-r^{-2}}}^{1} d\cos\theta_w \, (-W_{21}\cos\theta) e^{-(3W_0^2+E)}$$

$$\times [\{\alpha(I)-\alpha(II)\}*\{\beta(III)-\beta(II)\}$$

$$+ \Theta(\tau-\tau')\{\beta(I)-\beta(II)\}*\{\alpha(III)-\alpha(II)\}] . \qquad (3.5)$$

The integration variables in (3.5) completely define the vectors $\vec{W}_0$, $\vec{W}_{21}$, $\vec{W}_{31}$, $\hat{k}_1$ and $\vec{r}_{31}$, but it is noted that the polar and azimuthal angles of these vectors are *not* all taken relative to the same frame. Thus, $\vec{W}_0$, $\vec{W}_{21}$ and $\hat{k}_1$ are all defined relative to a coordinate system with Z-axis along $\vec{W}_{21}$ and XZ-plane in the plane of $\vec{W}_{21}$ and $\hat{k}_1$; $\vec{r}_{31}$ is defined relative to a coordinate system with Z-axis along $-\hat{k}_1$; and $\vec{W}_{31}$ is defined relative to a coordinate system with Z-axis along $-\vec{r}_{31}$. However, by applying suitable rotation matrices, the components of $\vec{W}_0$, $\vec{W}_{21}$, $\vec{W}_{31}$, $\hat{k}_1$ and $\vec{r}_{31}$ can all be found relative to any desired frame and expressed explicitly in terms of the various integration variables in (3.5). The required rotation matrices are presented in Table IV. We shall return to this point later when we discuss the evaluation of the integrand.

In terms of the basic vectors $\vec{W}_0$, $\vec{W}_{21}$, $\vec{W}_{31}$, $\hat{k}_1$ and $\vec{r}_{31}$, all other quantities of interest can be calculated. Thus, the time τ is computed as the smaller (earlier) root of the quadratic equation

$$|\vec{r}_{31} + \vec{W}_{31}\tau|^2 = 1 \quad ,$$

Table IV

Rotation Matrices

Given two frames F and F', and a vector $\vec{v}$. Suppose Frame F' is obtained from Frame F by rotating frame F about axis i by an angle $+\theta$ [i.e., the rotation carries axis j toward axis k through an angle $|\theta|$, where ijk is a positive permutation of xyz]. Then if (x,y,z) are the components of $\vec{v}$ with respect to frame F, the components (x',y',z') with respect to frame F' are obtained by $\begin{pmatrix} x' \\ y' \\ z' \end{pmatrix} = R_i(\theta) \begin{pmatrix} x \\ y \\ z \end{pmatrix}$, where

$$R_x(\theta) = \begin{bmatrix} 1 & 0 & 0 \\ 0 & \cos\theta & \sin\theta \\ 0 & -\sin\theta & \cos\theta \end{bmatrix}$$

$$R_y(\theta) = \begin{bmatrix} \cos\theta & 0 & -\sin\theta \\ 0 & 1 & 0 \\ \sin\theta & 0 & \cos\theta \end{bmatrix}$$

$$R_z(\theta) = \begin{bmatrix} \cos\theta & \sin\theta & 0 \\ -\sin\theta & \cos\theta & 0 \\ 0 & 0 & 1 \end{bmatrix}$$

Note: $\cos(\pi-\theta) = -\cos\theta$ $\quad$ $\cos(-\theta) = \cos\theta$

$\sin(\pi-\theta) = \sin\theta$ $\quad$ $\sin(-\theta) = -\sin\theta$

while τ' is computed as the positive (future) root of

$$|\vec{r}_{32}+\vec{W}_{32}\tau'|^2 = 1 \quad (\vec{r}_{32} \equiv \hat{k}_1+\vec{r}_{31}, \quad \vec{W}_{32} \equiv \vec{W}_{31}-\vec{W}_{21}).$$

Carrying out the algebra, we find the explicit formulae

$$\tau = W_{31}^{-1} r(1-\varepsilon)\cos\theta_w \quad , \tag{3.6}$$

and

$$\tau' = W_{32}^{-1}\left[-\vec{r}_{32}\cdot\hat{W}_{32}+\sqrt{(\vec{r}_{32}\cdot\hat{W}_{32})^2+(1-r_{32}^2)}\right] \quad , \tag{3.7}$$

where

$$\varepsilon \equiv \sqrt{1-\frac{1-r^{-2}}{\cos^2\theta_w}} \quad . \tag{3.8}$$

The collision vector $\hat{k}_2$ is then given by

$$\hat{k}_2 = -\vec{r}_{31}-\vec{W}_{31}\tau = -r\left[\hat{r}_{31}+\hat{W}_{31}(1-\varepsilon)\cos\theta_w\right] \quad . \tag{3.9}$$

Finally, we need the velocities in regions I and III in order to evaluate the integrand in (3.5). The region I and region III velocities are obtained from the region II velocities $\vec{W}_0$, $\vec{W}_{21}$, $\vec{W}_{31}$ and the collision vectors $\hat{k}_1$ and $\hat{k}_2$ through the hard sphere collision formulae:

$$\left.\begin{aligned}
\vec{W}_0(\mathrm{I}) &= \vec{W}_0 & \vec{W}_0(\mathrm{III}) &= \vec{W}_0 \\
\vec{W}_{21}(\mathrm{I}) &= \vec{W}_{21}-2\vec{W}_{21}\cdot\hat{k}_1\hat{k}_1 & \vec{W}_{21}(\mathrm{III}) &= \vec{W}_{21}-\vec{W}_{31}\cdot\hat{k}_2\hat{k}_2 \\
\vec{W}_{31}(\mathrm{I}) &= \vec{W}_{31}-\vec{W}_{21}\cdot\hat{k}_1\hat{k}_1 & \vec{W}_{31}(\mathrm{III}) &= \vec{W}_{31}-2\vec{W}_{31}\cdot\hat{k}_2\hat{k}_2
\end{aligned}\right\} \tag{3.10}$$

Therefore, once we write down the components of the vectors $\vec{W}_0$, $\vec{W}_{21}$, $\vec{W}_{31}$, $\hat{k}_1$, $\hat{k}_2$ in some common frame, expressing these components in terms of the integration variables in (3.5), we may proceed to express the full integrands in terms of the integrating variables, provided of course that the functional forms of α and β are given.

In evaluating the integrand in (3.5), it will be observed that we always deal with *differences* in various functions of the velocities before and after a collision. For all the functions $\alpha(=\Psi,X,\psi,\chi)$ which we shall be dealing with, it turns out that these differences satisfy the proportionalities

$$\left.\begin{aligned} &\alpha(\vec{W}_0(I),\vec{W}_{21}(I),\vec{W}_{31}(I)) - \alpha(\vec{W}_0,\vec{W}_{21},\vec{W}_{31}) \propto \vec{W}_{21}\cdot\hat{k}_1 \quad , \\ &\text{and} \\ &\alpha(\vec{W}_0(III),\vec{W}_{21}(III),\vec{W}_{31}(III)) - \alpha(\vec{W}_0,\vec{W}_{21},\vec{W}_{31}) \propto \vec{W}_{31}\cdot\hat{k}_2 \quad . \end{aligned}\right\} \tag{3.11}$$

This property (3.11) is a consequence of the velocity-change equations (3.10) and the simple polynomial forms which are used for the functions ψ and χ. Because of this property, it is convenient to define the *primed* differences

$$\{\alpha(I)-\alpha(II)\}' \equiv \{\alpha(I)-\alpha(II)\}/\vec{W}_{21}\cdot\hat{k}_1, \tag{3.12a}$$

and

$$\{\alpha(III)-\alpha(II)\}' \equiv \{\alpha(III)-\alpha(II)\}/\vec{W}_{31}\cdot\hat{k}_2 \quad , \tag{3.12b}$$

for any function α of the velocities $\vec{W}_0$, $\vec{W}_{21}$, $\vec{W}_{31}$. Since from Fig. 11

$$\vec{W}_{21}\cdot\hat{k}_1 = W_{21}\cos\theta \ , \tag{3.13a}$$

and from (3.9) and Fig. 11

$$\vec{W}_{31}\cdot\hat{k}_2 = W_{31}r\varepsilon\cos\theta_w \ , \tag{3.13b}$$

we can replace the unprimed differences in (3.5) by the primed differences, provided we introduce into the integrand an overall factor of

$$(\vec{W}_{21}\cdot\hat{k}_1)(\vec{W}_{31}\cdot\hat{k}_2) = W_{21}W_{31}r\varepsilon\cos\theta\cos\theta_w \ . \tag{3.13c}$$

In addition we make the variable changes

$$\int_{-1}^{0} \cos^2\theta \ d\cos\theta \rightarrow \frac{1}{3}\int_{-1}^{0} d\cos^3\theta \ ,$$

$$\int_{1}^{2\cos\theta_r} r^3 dr \rightarrow \frac{1}{4}\int_{1}^{(2\cos\theta_r)^4} dr^4 \ ,$$

$$\int_{\sqrt{1-r^{-2}}}^{1} \cos\theta_w \ d\cos\theta_w \rightarrow \frac{1}{2}\int_{1-r^{-2}}^{1} d\cos^2\theta_w \ .$$

We thus conclude that expression (3.5) for the SO-integrals may be written as

$$(\alpha,\beta)_2 = \frac{1}{5\sqrt{2}\pi^4}\int_{\infty}\int\int d^3\vec{W}_0\, e^{-3W_0^2}\int_0^{\infty} dW_{21}W_{21}^4\int_0^{\infty} dW_{31}W_{31}^3\int_{-1}^{0} d\cos^3\theta$$

$$\times\int_0^{2\pi} d\phi_r\int_{1/2}^{1} d\cos\theta_r\int_1^{(2\cos\theta_r)^4} dr^4\int_0^{2\pi} d\phi_w\int_{1-r^{-2}}^{1} d\cos^2\theta_w\,\varepsilon e^{-E}$$

$$\times\left[\{\alpha(I)-\alpha(II)\}'*\{\beta(III)-\beta(II)\}'\right.$$

$$\left.+\,\theta(\tau-\tau')\{\beta(I)-\beta(II)\}'*\{\alpha(III)-\alpha(II)\}'\right] \quad . \tag{3.14}$$

In order to obtain the coefficients $\lambda_{12}^*(N)$, $\eta_{12}^*(N)$ and $D_{12}^*(N)$ as given by (2.22) we need to evaluate the matrix elements $a_{k\ell,2}^{(3)}$, $b_{k\ell,2}^{(3)}$ and $c_{k\ell,2}^{(3)}$. For the sake of simplicity we shall drop the $\mu=2$ designation in the matrix elements for the single-overlap collisions and write†

$$a_{k\ell,2}^{(3)} \equiv a_{k\ell}^{so}\ ;\quad b_{k\ell,2}^{(3)} = b_{k\ell}^{so}\ ;\quad c_{k\ell,2}^{(3)} = c_{k\ell}^{so} \quad . \tag{3.15}$$

From (2.23) and (3.4) we see that these matrix elements are given in terms of $(\alpha,\beta)_2$ by

$$a_{k\ell}^{so} = \left(\sum_{m=1}^{3} s_{3/2}^{(k)}(W_m^2)\vec{W}_m\ ,\ \sum_{n=1}^{3} s_{3/2}^{(\ell)}(W_n^2)\vec{W}_n\right)_2 \quad ,$$

$$b_{k\ell}^{so} = \left(\sum_{m=1}^{3} s_{5/2}^{(k)}(W_m^2)\vec{W}_m\vec{O}\vec{W}_m\ ,\ \sum_{n=1}^{3} s_{5/2}^{(\ell)}(W_n^2)\vec{W}_n\vec{O}\vec{W}_n\right)_2 \quad , \tag{3.16}$$

$$c_{k\ell}^{so} = 2\left(s_{3/2}^{(k)}(W_1^2)\vec{W}_1\ ,\ s_{3/2}^{(\ell)}(W_1^2)\vec{W}_1\right)_2 \quad .$$

---

† These matrix elements are related to the matrix elements $a_{k\ell}$, $b_{k\ell}$ and $c_{k\ell}$ in AEDC-TR-71-51 [5] by

$$a_{k\ell}^{so} = -a_{k\ell}\ ,\qquad b_{k\ell}^{so} = -b_{k\ell}\ ,\qquad c_{k\ell}^{so} = -c_{k\ell} \quad .$$

In a previous technical report [5] we have evaluated the four lowest order elements of the matrices of SO-collision integrals (3.16). These results enabled us to determine the coefficients $\lambda^*_{12}(N)$, $\eta^*_{12}(N)$ and $D^*_{12}(N)$ up to the second Sonine approximation N=2. The work indicated that the rate of convergence of the expansion (2.22) for the viscosity η^*_1 and self-diffusion D^*_1 is comparable to the rate of convergence of the expansion (2.13) for the dilute gas transport coefficients. However, the same conclusion could not be drawn for the thermal conductivity coefficient λ^*_1. In this report we shall evaluate all those matrix elements in (3.16) that are needed to evaluate the coefficients $\eta^*_{12}(N)$ and $D^*_{12}(N)$ up to the third Sonine approximation N=3, and the coefficient $\lambda^*_{12}(N)$ up to the fourth Sonine approximation N=4. We shall thus be able to establish the rate of convergence of the expansion (2.22) for all three transport coefficients.

In evaluating the matrix elements (3.16) we shall follow two different approaches. In the first approach we integrate analytically over $\vec{W}_0$ and $\vec{W}_{21}$ in (3.14), thus reducing $(\alpha,\beta)_2$ from an 11-dimensional integral form to a 7-dimensional integral form, and then we evaluate the various 7-dimensional integrals numerically using a Monte Carlo technique. In the second approach, we apply the Monte Carlo technique directly to the 11-dimensional form (3.14). The first approach yields fairly accurate results, but the algebraic complexities introduced as a result of the analytic integrations over $\vec{W}_0$ and W_{21} are so great that only the matrix elements for the first (N=1) and second (N=2) Sonine approximations can be calculated with reasonable effort. The second approach yields less accurate results, but is algebraically simpler so that the

computation of the higher order Sonine approximations can be effected. Clearly, this two-pronged approach will provide us with a strong check on the consistency of our calculations of the single-overlap contributions.

3.2 Reduction of Collision Integrals to a 7-Dimensional Form

When the explicit forms of the Sonine polynomials are inserted into (3.16) and use is made of the fact that $\sum_{n=1}^{3} \vec{W}_n = 3\vec{W}_0$ is the same in all velocity regions, we obtain the following expressions for the matrix elements $a_{k\ell}^{so}$, $b_{k\ell}^{so}$ and $c_{k\ell}^{so}$.

$$
\begin{aligned}
a_{11}^{so} &= \left(\sum_{m=1}^{3} \vec{W}_m W_m^2, \sum_{n=1}^{3} \vec{W}_n W_n^2 \right)_2 , \\
a_{12}^{so} &= \frac{7}{2} \left(\sum_{m=1}^{3} \vec{W}_m W_m^2, \sum_{n=1}^{3} \vec{W}_n W_n^2 \right)_2 - \frac{1}{2} \left(\sum_{m=1}^{3} \vec{W}_m W_m^2, \sum_{n=1}^{3} \vec{W}_n W_n^4 \right)_2 , \\
a_{21}^{so} &= \frac{7}{2} \left(\sum_{m=1}^{3} \vec{W}_m W_m^2, \sum_{n=1}^{3} \vec{W}_n W_n^2 \right)_2 - \frac{1}{2} \left(\sum_{m=1}^{3} \vec{W}_m W_m^4, \sum_{n=1}^{3} \vec{W}_n W_n^2 \right)_2 , \\
a_{22}^{so} &= \frac{49}{4} \left(\sum_{m=1}^{3} \vec{W}_m W_m^2, \sum_{n=1}^{3} \vec{W}_n W_n^2 \right)_2 - \frac{7}{4} \left(\sum_{m=1}^{3} \vec{W}_m W_m^2, \sum_{n=1}^{3} \vec{W}_n W_n^4 \right)_2 , \\
&\quad - \frac{7}{4} \left(\sum_{m=1}^{3} \vec{W}_m W_m^4, \sum_{n=1}^{3} \vec{W}_n W_n^2 \right)_2 + \frac{1}{4} \left(\sum_{m=1}^{3} \vec{W}_m W_m^4, \sum_{n=1}^{3} \vec{W}_n W_n^4 \right)_2 .
\end{aligned}
\tag{3.17}
$$

$$
\begin{aligned}
b_{00}^{SO} &= \left(\sum_{m=1}^{3} \vec{W}_m \circ \vec{W}_m, \sum_{n=1}^{3} \vec{W}_n \circ \vec{W}_n \right)_2 , \\
b_{01}^{SO} &= \frac{7}{2} \left(\sum_{m=1}^{3} \vec{W}_m \circ \vec{W}_m, \sum_{n=1}^{3} \vec{W}_n \circ \vec{W}_n \right)_2 - \left(\sum_{m=1}^{3} \vec{W}_m \circ \vec{W}_m, \sum_{n=1}^{3} \vec{W}_n \circ \vec{W}_n W_n^2 \right)_2 , \\
b_{10}^{SO} &= \frac{7}{2} \left(\sum_{m=1}^{3} \vec{W}_m \circ \vec{W}_m, \sum_{n=1}^{3} \vec{W}_n \circ \vec{W}_n \right)_2 - \left(\sum_{m=1}^{3} \vec{W}_m \circ \vec{W}_m W_m^2, \sum_{n=1}^{3} \vec{W}_n \circ \vec{W}_n \right)_2 , \\
b_{11}^{SO} &= \frac{49}{4} \left(\sum_{m=1}^{3} \vec{W}_m \circ \vec{W}_m, \sum_{n=1}^{3} \vec{W}_n \circ \vec{W}_n \right)_2 - \frac{7}{2} \left(\sum_{m=1}^{3} \vec{W}_m \circ \vec{W}_m, \sum_{n=1}^{3} \vec{W}_n \circ \vec{W}_n W_n^2 \right)_2 \\
&\quad - \frac{7}{2} \left(\sum_{m=1}^{3} \vec{W}_m \circ \vec{W}_m W_m^2, \sum_{n=1}^{3} \vec{W}_n \circ \vec{W}_n \right)_2 + \left(\sum_{m=1}^{3} \vec{W}_m \circ \vec{W}_m W_m^2, \sum_{n=1}^{3} \vec{W}_n \circ \vec{W}_n W_n^2 \right)_2 .
\end{aligned}
\tag{3.18}
$$

$$
\begin{aligned}
c_{00}^{SO} &= 2(\vec{W}_1, \vec{W}_1)_2 , \\
c_{01}^{SO} &= 5(\vec{W}_1, \vec{W}_1)_2 - 2(\vec{W}_1, \vec{W}_1 W_1^2)_2 , \\
c_{10}^{SO} &= 5(\vec{W}_1, \vec{W}_1)_2 - 2(\vec{W}_1 W_1^2, \vec{W}_1)_2 , \\
c_{11}^{SO} &= \frac{25}{2}(\vec{W}_1, \vec{W}_1)_2 - 5(\vec{W}_1, \vec{W}_1 W_1^2)_2 - 5(\vec{W}_1 W_1^2, \vec{W}_1)_2 \\
&\quad + 2(\vec{W}_1 W_1^2, \vec{W}_1 W_1^2)_2 .
\end{aligned}
\tag{3.19}
$$

Although a_{12}^{SO}, for example, is a sum of two integrals, we shall actually calculate it as the integral of a two-term integrand; this is possible since the integrating variables and domains are the same for both integrals, and is *desirable* since it allows a precise estimate of the uncertainty in a_{12}^{SO}. Essentially then, our task is to evaluate twelve integrals; four-each of $a_{k\ell}^{SO}$, $b_{k\ell}^{SO}$ and $c_{k\ell}^{SO}$ as shown in (3.17)-(3.19). All twelve integrals can be calculated in parallel, since the integrating variables and the domains are the same for all [cf. (3.14)].

Each integral in (3.17)-(3.19) has as an integrand some specific polynomial form in terms of the velocities $\vec{W}_1$, $\vec{W}_2$, $\vec{W}_3$. Our first step is to express these polynomial forms in terms of the variables $\vec{W}_0$, $\vec{W}_{21}$, $\vec{W}_{31}$ defined in (2.36). The $\vec{W}_0$-dependence of the integrands is then isolated, and the $\vec{W}_0$-integration in (3.14) can be done analytically. This process entails the application of various integral forms of the type found in Section 1.421 of Chapman and Cowling [1], as well as the performance of integrals of the type [cf. (3.14)]

$$\iiint_{\infty} d^3\vec{W}_0 \; W_0^n e^{-3W_0^2} = 4\pi \int_0^{\infty} dW_0 \; W_0^{n+2} e^{-3W_0^2} \quad ,$$

for various values of n. The integrals (3.14) are thereby reduced to 8-dimensional integrals, in which the integrands depend only on the velocities $\vec{W}_{21}$ and $\vec{W}_{31}$ in regions I, II and III. Note that, the velocities $\vec{W}_{21}(I)$, $\vec{W}_{31}(I)$ and $\vec{W}_{21}(III)$, $\vec{W}_{31}(III)$ are determined completely by the velocities $\vec{W}_{21}$ and $\vec{W}_{31}$ in region II and the collision vectors $\hat{k}_1$ and $\hat{k}_2$ [see (3.10)]; the collision vector $\hat{k}_2$ in turn is determined by $\vec{r}_{31}$ and $\vec{W}_{31}$ [see (3.9)].

The fact that $\vec{W}_0$ can be integrated out with relative ease is a consequence of the fact that the dynamics of the collision sequence is independent of the velocity of the center-of-mass of the three molecules. Another variable which does not affect the collision dynamics for hard sphere molecules is the scale with respect to which all the velocities are measured [this is because the angle of deflection for two colliding hard sphere molecules is independent of their velocities]. Suppose, in fact, we measure the two velocity variables $\vec{W}_{21}$ and $\vec{W}_{31}$ in units of W_{21}:

$$\left.\begin{aligned}\vec{W}_{21} &= W_{21}\hat{z}, \\ \vec{W}_{31} &= W_{21}\vec{w}\end{aligned}\right\} . \tag{3.20}$$

Essentially, this amounts to a change of variables in (3.14) of the form

$$(W_{21},W_{31}) \rightarrow (W_{21},\ w=W_{31}/W_{21}) \quad , \tag{3.21a}$$

with

$$dW_{21}dW_{31} = W_{21}dW_{21}dw \quad . \tag{3.21b}$$

The independence of the collision dynamics with respect to the velocity scale manifests itself in the following fact: If relations (3.20) are introduced into the various integrands, then every term in these integrands is found to be homogenous in W_{21}; that is, if $F(\vec{W}_{21},\vec{W}_{31})$ is a typical integrand term, then we discover that

$$F(\vec{W}_{21},\vec{W}_{31}) = F(W_{21}\hat{z},W_{21}\vec{w}) = W_{21}^{n}F(\hat{z},\vec{w}) \quad ,$$

with the value of n varying from term to term. We note in passing that $\hat{k}_2$ and $\Theta(\tau-\tau')$ are homogeneous in W_{21} of degree zero [cf. (3.6)-(3.9)], while E is homogeneous of degree two [cf. (2.39)]:

$$E = W_{21}^{2}E^{*}, \qquad E^{*} \equiv \frac{2}{3}(1+w^{2}-\hat{z}\cdot\vec{w}) \quad . \tag{3.22}$$

[Like E, $E^{*} \equiv E/W_{21}^{2}$ has the same value in all velocity regions.] Therefore, if $F(\vec{W}_{21},\vec{W}_{31})$ is a typical term in the integrand of (3.14), where we now assume that $\vec{W}_0$ has already been integrated out, then we can perform the W_{21}- integration analytically on a term-by-term basis:

$$\int_0^\infty dW_{31} W_{31}^3 \int_0^\infty dW_{21} W_{21}^4 \, e^{-E} F(\vec{W}_{21}, \vec{W}_{31})$$

$$= \int_0^\infty dw W_{21}^4 w^3 \int_0^\infty dW_{21} W_{21}^4 \, e^{-W_{21}^2 E^*} W_{21}^n F(\hat{z}, \vec{w})$$

$$= \int_0^\infty dw \, w^3 F(\hat{z}, \vec{w}) \int_0^\infty dW_{21} W_{21}^{8+n} e^{-W_{21}^2 E^*} \quad . \tag{3.23}$$

We note that the W_{21}-integration removes the factor e^{-E} and replaces it by the reciprocal of E^* raised to some half-odd-integer power.

Recapitulating, the integrals in (3.17)-(3.19) are dealt with in the following way: First, the integrand expressions involving $\vec{W}_1$, $\vec{W}_2$, $\vec{W}_3$ are converted to expressions involving $\vec{W}_0$, $\vec{W}_{21}$, $\vec{W}_{31}$ by means of (2.36). Next, the $\vec{W}_0$-integrations are performed analytically, thus reducing the integral forms $(\alpha,\beta)_2$ in (3.14) from 11 to 8 dimensions. The remaining velocity variables $\vec{W}_{21}$, $\vec{W}_{31}$ are then transformed to $\vec{W}_{21}$, $\vec{w}$ as prescribed in (3.20), and the integral over the magnitude W_{21} is performed analytically. The integral forms $(\alpha,\beta)_2$ in (3.14) then become 7-dimension integrals over the variables $\cos^3\theta$, ϕ_r, $\cos\theta_r$, r^4, ϕ_w, w, $\cos^2\theta_w$. The algebra involved in carrying out this program for the quantities in (3.17)-(3.19) is lengthy and complicated, and we shall only quote the results here. For this purpose we define the 7-dimensional integral form

$$(\alpha,\beta)_2 \equiv$$

$$\frac{7}{2^5\pi^2\sqrt{6}}\int_{-1}^{0} d\cos^3\theta \int_0^{2\pi} d\phi_r \int_0^{2\pi} d\phi_w \int_0^{\infty} dw\, w^3 \int_{1/2}^{1} d\cos\theta_r \int_1^{(2\cos\theta_r)^4} dr^4 \int_{1-r^{-2}}^{1} d\cos^2\theta_w \qquad (3.24)$$

$$\times \varepsilon E^{*-9/2}[\{\alpha(I)-\alpha(II)\}'*\{\beta(III)-\beta(II)\}'$$

$$+ \theta(\tau-\tau')\{\beta(I)-\beta(II)\}'*\{\alpha(III)-\alpha(II)\}'] \ ,$$

where τ is given by (3.6) with W_{31} replaced by w and τ' is given by (3.7) with $\vec{W}_{32}$ replaced by $\vec{w}-\hat{z}$, and where the primes are defined by (3.12) with $\vec{W}_{21}\cdot\hat{k}_1$ and $\vec{W}_{31}\cdot\hat{k}_2$ now replaced by $\hat{z}\cdot\hat{k}_1$ and $\vec{w}\cdot\hat{k}_2$, respectively. In terms of (3.24) the matrix elements (3.17)-(3.19) are

$$a_{11}^{so} = 3(\vec{\vec{L}}_1,\vec{\vec{L}}_1)_2 + \frac{99}{4}(\vec{K}_1,\vec{K}_1)_2 \ ,$$

$$a_{12}^{so} = 7(\vec{\vec{L}}_1,\vec{\vec{L}}_1)_2 + \frac{231}{4}(\vec{K}_1,\vec{K}_1)_2 + 33(\vec{\vec{L}}_1,\vec{\vec{L}}_2)_2 + \frac{1287}{8}(\vec{K}_1,\vec{K}_2)_2 \ ,$$

$$a_{21}^{so} = 7(\vec{\vec{L}}_1,\vec{\vec{L}}_1)_2 + \frac{231}{4}(\vec{K}_1,\vec{K}_1)_2 + 33(\vec{\vec{L}}_2,\vec{\vec{L}}_1)_2 + \frac{1287}{8}(\vec{K}_2,\vec{K}_1)_2 \ , \qquad (3.25)$$

$$a_{22}^{so} = \frac{77}{3}(\vec{\vec{L}}_1,\vec{\vec{L}}_1)_2 + 77(\vec{\vec{L}}_1,\vec{\vec{L}}_2)_2 + 77(\vec{\vec{L}}_2,\vec{\vec{L}}_1)_2 + 429(\vec{\vec{L}}_2,\vec{\vec{L}}_2)_2$$

$$+ \frac{1133}{4}(\vec{K}_1,\vec{K}_1)_2 + \frac{3003}{8}(\vec{K}_1,\vec{K}_2)_2 + \frac{3003}{8}(\vec{K}_2,\vec{K}_1)_2 + \frac{19305}{16}(\vec{K}_2,\vec{K}_2)_2$$

$$+ \frac{4719}{16}(S,S)_2 + 22(\vec{\vec{M}},\vec{\vec{M}})_2 \ .$$

$$
\begin{aligned}
b_{00}^{so} &= \frac{9}{2}(\vec{\vec{L}}_1, \vec{\vec{L}}_1)_2 \quad , \\
b_{01}^{so} &= \frac{21}{4}(\vec{\vec{L}}_1, \vec{\vec{L}}_1)_2 + \frac{99}{4}(\vec{\vec{L}}_1, \vec{\vec{L}}_2)_2 \quad , \\
b_{10}^{so} &= \frac{21}{4}(\vec{\vec{L}}_1, \vec{\vec{L}}_1)_2 + \frac{99}{4}(\vec{\vec{L}}_2, \vec{\vec{L}}_1)_2 \quad , \\
b_{11}^{so} &= \frac{301}{24}(\vec{\vec{L}}_1, \vec{\vec{L}}_1)_2 + \frac{231}{8}(\vec{\vec{L}}_1, \vec{\vec{L}}_2)_2 + \frac{231}{8}(\vec{\vec{L}}_2, \vec{\vec{L}}_1)_2 + \frac{1287}{8}(\vec{\vec{L}}_2, \vec{\vec{L}}_2)_2 \\
&\quad + 44(\vec{K}_1, \vec{K}_1)_2 + \frac{33}{2}(\vec{\vec{M}}, \vec{\vec{M}})_2 - \frac{429}{8}(S,S)_2 .
\end{aligned}
\tag{3.26}
$$

$$
\begin{aligned}
c_{00}^{so} &= (\vec{\ell}_1, \vec{\ell}_1)_2 \quad , \\
c_{01}^{so} &= \frac{5}{6}(\vec{\ell}_1, \vec{\ell}_1)_2 + \frac{9}{2}(\vec{\ell}_1, \vec{\ell}_2)_2 \quad , \\
c_{10}^{so} &= \frac{5}{6}(\vec{\ell}_1, \vec{\ell}_1)_2 + \frac{9}{2}(\vec{\ell}_2, \vec{\ell}_1)_2 \quad , \\
c_{11}^{so} &= \frac{55}{36}(\vec{\ell}_1, \vec{\ell}_1)_2 + \frac{15}{4}(\vec{\ell}_1, \vec{\ell}_2)_2 + \frac{15}{4}(\vec{\ell}_2, \vec{\ell}_1)_2 + \frac{99}{4}(\vec{\ell}_2, \vec{\ell}_2)_2 \\
&\quad + \frac{21}{4}(k,k)_2 + 3(\vec{\vec{m}}, \vec{\vec{m}})_2 \quad .
\end{aligned}
\tag{3.27}
$$

To define the symbols $\vec{K}_1$, $\vec{K}_2$, $\vec{\vec{L}}_1$, $\vec{\vec{L}}_2$, S, $\vec{\vec{M}}$, $\vec{\ell}_1$, $\vec{\ell}_2$, k and $\vec{\vec{m}}$ appearing in (3.25)-(3.27), some preliminary remarks must be made. First of all, the transformation (3.20), which "scales" the velocities in region II, also induces a scaling of velocities in regions I and III on account of (3.10). Thus, we have

$$\vec{z}(I) = \hat{z}-2\hat{z}\cdot\hat{k}_1\hat{k}_1 \quad , \qquad \vec{z}(III) = \hat{z}-\vec{w}\cdot\hat{k}_2\hat{k}_2 \quad ,$$
$$\vec{w}(I) = \vec{w}-\hat{z}\cdot\hat{k}_1\hat{k}_1 \quad , \qquad \vec{w}(III) = \vec{w}-2\vec{w}\cdot\hat{k}_2\hat{k}_2 \quad , \tag{3.28}$$

where, of course, $\vec{z}(II)\equiv\hat{z}$ and $\vec{w}(II)\equiv\vec{w}$. Now, it turns out to be more convenient to work with the *auxiliary* velocity variables [cf. (2.36)]

$$\begin{aligned}
\vec{w}_{10}(i) &\equiv -\tfrac{1}{3}[\vec{z}(i)+\vec{w}(i)] \\
\vec{w}_{20}(i) &\equiv -\tfrac{1}{3}[\vec{w}(i)-2\vec{z}(i)] \quad , \qquad i=I,II,III \quad . \\
\vec{w}_{30}(i) &\equiv -\tfrac{1}{3}[\vec{z}(i)-2\vec{w}(i)]
\end{aligned} \tag{3.29}$$

The velocities $\vec{w}_{10}$, $\vec{w}_{20}$, $\vec{w}_{30}$ are the velocities of spheres 1, 2 and 3 relative to the motion of the center of gravity. The expressions for the quantities $\vec{K}_1$, $\vec{K}_2$, $\vec{\vec{L}}_1$, etc. are now defined in terms of these auxiliary velocities $\vec{w}_{10}$, $\vec{w}_{20}$ and $\vec{w}_{30}$. Specifically for any region we have

$$\vec{K}_1 \equiv E^{*-1}\sum_{i=1}^{3}\vec{w}_{io}w_{io}^2 \quad , \tag{3.30a}$$

$$\vec{K}_2 \equiv E^{*-2}\sum_{i=1}^{3}\vec{w}_{io}w_{io}^4 \quad , \tag{3.30b}$$

$$\vec{\vec{L}}_1 \equiv E^{*-\frac{1}{2}}\sum_{i=1}^{3}\vec{w}_{io}\vec{w}_{io} \quad , \tag{3.30c}$$

$$\vec{\vec{L}}_2 \equiv E^{*-\frac{3}{2}}\sum_{i=1}^{3}\vec{w}_{io}\vec{w}_{io}w_{io}^2 \quad , \tag{3.30d}$$

$$S \equiv E^{*-\frac{3}{2}} \sum_{i=1}^{3} w_{io}^4 \quad , \tag{3.30e}$$

$$\vec{\vec{M}} \equiv E^{*-1} \sum_{i=1}^{3} \vec{w}_{io}\vec{w}_{io}\vec{w}_{io} \quad , \tag{3.30f}$$

$$\vec{\ell}_1 \equiv E^{*-0}\, \vec{w}_{10} \quad , \tag{3.30g}$$

$$\vec{\ell}_2 \equiv E^{*-1}\, \vec{w}_{10} w_{10}^2 \quad , \tag{3.30h}$$

$$k \equiv E^{*-\frac{1}{2}}\, w_{10}^2 \quad , \tag{3.30i}$$

$$\vec{\vec{m}} \equiv E^{*-\frac{1}{2}}\, \vec{w}_{10}\vec{w}_{10} \quad . \tag{3.30j}$$

We also note that

$$E^* = \sum_{i=1}^{3} w_{io}^2 \quad . \tag{3.30k}$$

From the expression (3.24) for the collision integrals we see that we need to evaluate the quantities $\{\alpha(I)-\alpha(II)\}' = \{\alpha(I)-\alpha(II)\}/\hat{z}.\hat{k}_1$ and $\{\alpha(III)-\alpha(II)\}' = \{\alpha(III)-\alpha(II)\}/\vec{w}.\hat{k}_2$ for all functions α defined in (3.30). With (3.28) and (3.29) we can express these quantities in terms of the vectors $\hat{z}$, $\vec{w}$, $\hat{k}_1$ and $\hat{k}_2$; the results are listed in Table V.

As a last step we need to express the vectors $\hat{z}$, $\vec{w}$, $\hat{k}_1$ and $\hat{k}_2$ in terms of the integration variables of (3.24). This step is not unique in that it depends upon which common frame one chooses to work in. In our calculations we worked in a frame in which the Z-axis pointed along $-\vec{r}_{31}$. The vectors $\vec{w}$ and $\vec{r}$ have a simple representation in this frame (see Fig. 11)

Table V

The Quantities $\{\alpha(I)-\alpha(II)\}'$ and $\{\alpha(III)-\alpha(II)\}'$ in the SO-Integrals

α	$\{\alpha(I)-\alpha(II)\}'$
$E^{*3/2}{}_S$	$2b(w_{20}^2-w_{10}^2+ab)$
$E^{*}\vec{K}_1$	$b\hat{z}-(w_{20}^2-w_{10}^2+2ab)\hat{k}_1$
$E^{*2}\vec{K}_2$	$b(-2w_{10}^2+ab)\vec{w}_{10}+b(2w_{20}^2+ab)\vec{w}_{20}-(w_{10}^2+w_{20}^2)(w_{20}^2-w_{10}^2+2ab)\hat{k}_1$
$E^{*1/2}\vec{\vec{L}}_1$	$2(a\hat{k}_1\hat{k}_1-\hat{z}\hat{k}_1)$
$E^{*3/2}\vec{\vec{L}}_2$	$b\vec{w}_{20}\vec{w}_{20}-b\vec{w}_{10}\vec{w}_{10}+a(w_{10}^2+w_{20}^2)\hat{k}_1\hat{k}_1+2w_{10}^2\vec{w}_{10}\hat{k}_1-2w_{20}^2\vec{w}_{20}\hat{k}_1+2ab\vec{w}_{30}\hat{k}_1$
$E^{*}\vec{\vec{M}}$	$3(\vec{w}_{10}\vec{w}_{10}\hat{k}_1-\vec{w}_{20}\vec{w}_{20}\hat{k}_1-a\vec{w}_{30}\hat{k}_1\hat{k}_1)$
$E^{*1/2}k$	$-b$
$\vec{\ell}_1$	$\hat{k}_1$
$E^{*}\ell_2$	$-b\vec{w}_{10}+(w_{10}^2-ab)\hat{k}_1$
$E^{*1/2}\vec{\vec{m}}$	$a\hat{k}_1\hat{k}_1+2\vec{w}_{10}\hat{k}_1$

Notes: 1) $\vec{w}_{10}=-\frac{1}{3}(\hat{z}+\vec{w})$, $\vec{w}_{20}=-\frac{1}{3}(\vec{w}-2\hat{z})$, $\vec{w}_{30}=-\frac{1}{3}(\hat{z}-2\vec{w})$, $a=\hat{z}\cdot\hat{k}_1$, $b=\vec{w}_{30}\cdot\hat{k}_1$.

2) $\vec{\vec{xy}} = \frac{1}{2}(\vec{x}\vec{y}+\vec{y}\vec{x})$; $\vec{\vec{\vec{xyz}}} = \frac{1}{6}(\vec{x}\vec{y}\vec{z} + \vec{x}\vec{z}\vec{y} + \vec{y}\vec{x}\vec{z} + \vec{y}\vec{z}\vec{x} + \vec{z}\vec{x}\vec{y} + \vec{z}\vec{y}\vec{x})$

3) $\{\alpha(III)-\alpha(II)\}'$ is obtained from $\{\alpha(I)-\alpha(II)\}'$ by the following transformation

$\hat{k}_1\to\hat{k}_2$, $\hat{z}\to\vec{w}$, $\vec{w}\to z$, $\vec{w}_{20}\to\vec{w}_{30}$, $\vec{w}_{30}\to\vec{w}_{20}$, $a\to a'$, $b\to b'$,

where $a' = \vec{w}\cdot\hat{k}_2$ and $b' = \vec{w}_{20}\cdot\hat{k}_2$

$$\vec{r}_{31} = \begin{bmatrix} 0 \\ 0 \\ -r \end{bmatrix} \quad , \quad \vec{w} = \begin{bmatrix} w\sin\theta_w \cos\phi_w \\ w\sin\theta_w \sin\phi_w \\ w\cos\theta_w \end{bmatrix} \quad . \tag{3.32}$$

The components of $\hat{z}$ and $\hat{k}_1$ are obtained by applying the appropriate rotation matrices, defined in Table IV, and the components of $\hat{k}_2$ are obtained by inserting (3.32a) and (3.32b) into (3.9).

$$\hat{z} = R_y(-(\pi-\theta_r)) \cdot R_z(\phi_r) \cdot R_y(\pi-\theta) \cdot \begin{bmatrix} 0 \\ 0 \\ 1 \end{bmatrix} =$$

$$= \begin{bmatrix} \sin\theta\cos\theta_r\cos\phi_r - \cos\theta\sin\phi_r \\ \sin\theta\sin\phi_r \\ \sin\theta\sin\theta_r\cos\phi_r + \cos\theta\cos\theta_r \end{bmatrix} , \tag{3.32c}$$

$$\hat{k}_1 = R_y(-(\pi-\theta_r)) \cdot R_z(\phi_r) \cdot \begin{bmatrix} 0 \\ 0 \\ -1 \end{bmatrix} = \begin{bmatrix} -\sin\theta_r \\ 0 \\ \cos\theta_r \end{bmatrix}, \tag{3.32d}$$

$$\hat{k}_2 = \begin{bmatrix} r(\varepsilon-1)\cos\theta_w \sin\theta_w \cos\phi_w \\ r(\varepsilon-1)\cos\theta_w \sin\theta_w \sin\phi_w \\ r(\varepsilon-1)\cos^2\theta_w + r \end{bmatrix} , \tag{3.32e}$$

with

$$\varepsilon \equiv \sqrt{1 - \frac{1-r^{-2}}{\cos^2\theta_w}} \quad . \tag{3.32f}$$

The remaining quantities in (3.24) are given by

$$E^* = \frac{2}{3}(1+w^2-\hat{z}\cdot\vec{w}) \quad , \tag{3.32g}$$

$$\tau = w^{-1} r (1-\varepsilon)\cos\theta_w \quad , \tag{3.32h}$$

$$\tau' = -\frac{(\vec{r}_{31}+\hat{k}_1)\cdot(\vec{w}-\hat{z})}{(\vec{w}-\hat{z})^2} + \frac{1}{(\vec{w}-\hat{z})^2}\sqrt{\{(\vec{r}_{31}+\vec{k}_1)\cdot(\vec{w}-\hat{z})\}^2+(\vec{w}-\hat{z})^2\{1-(\vec{r}_{31}+\hat{k}_1)^2\}} \quad , \tag{3.32i}$$

Substitution of the quantities of Table V into (3.24) and use of eqs. (3.32) completely specifies the SO-integrals in 7-dimensional form.

3.3 Evaluation of 7-Dimensional SO-Integrals

In the previous section we have reduced the SO-integrals to a 7-dimensional form (3.24) with the functions α and β defined in (3.30) and evaluated in Table V. Together with eqs. (3.32) the integrand is thus completely specified in terms of the integration variables.

In order to evaluate these 7-dimensional collision integrals we resort to a Monte Carlo integration procedure. However, the integral form in (3.24) *as it stands* is not yet analyzable by Monte Carlo techniques, because of the *infinite range* of the variable w. We must transform from the variable w to some variable u which has a *finite range*. One candidate for such a transformation is

$$u = (1+w^n)^{-1} \quad ,$$

which, for any $n \geq 1$, maps the infinite range $0 \leq w < \infty$ onto the finite range $0 \leq u \leq 1$. However, an important constraint on this or any such transformation is that its Jacobian must not cause the integrand to become unbounded as a function of u; for in a Monte Carlo procedure *both* the integrating domain and the integrand values must be strictly finite. Consequently, to make a suitable choice of n we must examine in detail the behavior of the integrand in (3.24) near w=0 (u=1) and $w=\infty$ (u=0). This is a rather laborius task; for not only does w enter into the integrand of (3.24) via the factor $w^3 E^{*-9/2}$, but it also enters through the primed differences in braces in (3.24) [cf. Table V]. Thus, *each term* in (3.25)-(3.27) must be examined in detail to determine its behavior near w=0 and $w=\infty$. It turns out that, for α and β equal to any of the quantities in (3.30), the primed differences in (3.24) all remain finite near w=0 and $w=\infty$. Since, asymptotically

$$w^3 E^{*-9/2} \equiv w^3 / \frac{2}{3}(w^2 - \hat{z}\cdot\vec{w} + 1)^{9/2} \sim w^3/(1+w^9) \ ,$$

then we consider the problem of integrating $w^3/(1+w^9)$ from w=0 to $w=\infty$. The proposed transformation $u=(1+w^n)^{-1}$ yields

$$\int_0^\infty \frac{w^3}{1+w^9}\, dw = \frac{1}{n} \int_0^1 \frac{(1-u)^{\frac{4-n}{n}} \cdot u^{\frac{5-n}{n}}}{[u^{9/n} + (1-u)^{9/n}]}\, du \ ,$$

from which we deduce that we must pick $n \leq 4$ to yield a bounded integrand. Since the highest value, n=4, should produce the smoothest behavior of the integrand (an important consideration in Monte Carlo applications),

we therefore choose for our w → u transformation

$$u = (1+w^4)^{-1} \quad . \tag{3.33}$$

Since (3.33) implies that

$$w^3 dw = -\frac{1}{4}\frac{du}{u^2} \quad ,$$

then (3.24) can now be written

$$(\alpha,\beta)_2 \equiv \frac{7}{2^7\pi^2\sqrt{6}} \int_{-1}^{0} d\cos^3\theta \int_{0}^{2\pi} d\phi_r \int_{0}^{2\pi} d\phi_w \int_{0}^{1} du \int_{1/2}^{1} d\cos\theta_r \int_{1}^{(2\cos\theta_r)^4} dr^4 \int_{1-r^{-2}}^{1} d\cos^2\theta_w$$

$$\times \frac{\varepsilon}{u^2 E^{*9/2}} \Big[\{\alpha(I)-\alpha(II)\}' * \{\beta(III)-\beta(II)\}'$$

$$+ \Theta(\tau-\tau')\{\beta(I)-\beta(II)\}' * \{\alpha(III)-\alpha(II)\}' \Big] , \tag{3.34}$$

where it is henceforth understood that the quantity w is given by the inverse of (3.33):

$$w = \left(\frac{1-u}{u}\right)^{1/4} \quad . \tag{3.35}$$

One final transformation of variables is needed to effect a Monte Carlo calculation. We wish to transform the 7-dimensional integrating region Ω,

$$\Omega \equiv \{(\cos^3\theta, \phi_r, \phi_w, u, \cos\theta_r, r^4, \cos^2\theta_w) \,||\, -1 \leq \cos^3\theta \leq 0 \ ,$$

$$0 \leq \phi_r \leq 2\pi,\ 0 \leq \phi_w \leq 2\pi,\ 0 \leq u \ll 1,\ \tfrac{1}{2} \leq \cos\theta_r \leq 1,$$

$$1 \leq r^4 < (2\cos\theta_r)^4,\ (1-r^{-2}) \leq \cos^2\theta_w \leq 1\}, \tag{3.36}$$

into a 7-dimensional unit cube

$$U_7 \equiv \{(\eta_1,\eta_2,\ldots,\eta_7) \,||\, 0\leq\eta_i\leq 1;\ i=1,2,\ldots,7\}. \tag{3.37}$$

This transformation would be easy if Ω were a rectangle; however, because the boundaries on the variable r^4 depend on the variable $\cos\theta_r$, while the boundaries on the variable $\cos^2\theta_w$ depend on the variable r^4, the method of effecting such a transformation is not so straightforward. This general problem is discussed in a separate technical report [15]. For the problem at hand we used the transformation scheme [5]

$$\cos^3\theta = -1+\eta_1 \ , \tag{3.38a}$$

$$\phi_r = 2\pi\eta_2 \ , \tag{3.38b}$$

$$\phi_w = 2\pi\eta_3 \ , \tag{3.38c}$$

$$u = \eta_4, \ w\equiv[(1-u)/u]^{1/4}, \tag{3.38d}$$

$$2\eta_5 = 4\cos^3\theta_r-3\cos\theta_r+1 \ , \tag{3.38e}$$

$$r^4 = [1+(4\cos^2\theta_r-1)\eta_6]^2, \tag{3.38f}$$

$$\cos^2\theta_w = (1-r^{-2})+r^{-2}\eta_7, \tag{3.38g}$$

where (3.38e) defines $\cos\theta_r$ in terms of η_5 through an implicit inversion. The rationale for eqs. (3.38a)-(3.38d) is obvious from (3.36), or equivalently from the ranges of the first four integration variables in (3.34). The unusual appearance of eqs. (3.38e)-(3.38g) is a consequence of the interdependence of these variables; these transformation equations were obtained

by a "successive conditioning method" discussed elsewhere [15]. Suffice it to say here that the transformation (3.38) is such that its Jacobian is equal to the volume of Ω, as may be verified directly:

$$\frac{\partial(\cos^3\theta, \phi_r, \phi_w, u, \cos\theta_r, r^4, \cos^2\theta_w)}{\partial(r_1, r_2, \ldots, r_7)} = |\Omega| = \frac{16\pi^2}{3} . \tag{3.39}$$

Thus, we may straightaway replace the integrating variables $\cos^3\theta, \phi_r, \ldots, \cos^2\theta_w$ in (3.34) by the variables $r_1, r_2, \ldots, r_7$, provided we multiply the integral by the constant factor in (3.39). Our *final formula* for $(\alpha,\beta)_2$ is therefore

$$(\alpha,\beta)_2 = \frac{7}{24\sqrt{6}} \int_0^1 dr_1 \int_0^1 dr_2 \cdots \int_0^1 dr_7 \, \frac{\varepsilon}{u^2 E^{*9/2}}$$

$$\times \Big[\{\alpha(I)-\alpha(II)\}' * \{\beta(III)-\beta(II)\}'$$

$$+ \theta(\tau-\tau') \{\beta(I)-\beta(II)\}' * \{\alpha(III)-\alpha(II)\}' \Big] . \tag{3.40}$$

We now summarize the definitions of, and relations between, the various quantities that enter into our calculation of the $\mu=2$ quantities in (2.22). We have by (2.22) and (3.15) and (3.16)

$$\lambda_{12}^*(N) = \frac{-1}{a_1(N)} \sum_{k=1}^{N} \sum_{\ell=1}^{N} a_k(N) a_\ell(N) a_{k\ell}^{SO} ,$$

$$\eta_{12}^*(N) = \frac{-1}{b_0(N)} \sum_{k=0}^{N-1} \sum_{\ell=0}^{N-1} b_k(N) b_\ell(N) b_{k\ell}^{SO} , \tag{3.41}$$

$$D_{12}^*(N) = \frac{-1}{c_0(N)} \sum_{k=0}^{N-1} \sum_{\ell=0}^{N-1} c_k(N) c_\ell(N) c_{k\ell}^{SO} .$$

The coefficients $a_k(N)$, $b_k(N)$ and $c_k(N)$ are given in Table III. The matrix elements $a^{so}_{k\ell}$, $b^{so}_{k\ell}$ and $c^{so}_{k\ell}$ are calculated from equations (3.25)-(3.27), and evidently involve evaluating integrals of the form $(\alpha,\beta)_2$. These integrals are defined by (3.40), where:

(i) the quantities $\cos\theta, \phi_r, \phi_w, u$ (and w), $\cos\theta_r, r, \cos\theta_w$ are obtained from the integrating variables $\lambda_1, \lambda_2, \ldots \lambda_7$ through eqs. (3.38),

(ii) the quantity $\varepsilon \equiv \sqrt{1-\frac{1-r^{-2}}{\cos^2\theta_w}}$ as given in (3.32f),

(iii) the vectors $\hat{z}, \vec{w}, \hat{k}_1, \hat{k}_2, \vec{r}_{31}$ are constructed in component form from the quantities, $\cos\theta, \phi_r, \phi_w, w, \cos\theta_r, r, \cos\theta_w$ through eqs. (3.32),

(iv) the quantities E^*, τ and τ' are given in (3.32g), (3.32h) and (3.32i) and $\Theta(\tau-\tau')$ is defined by

$$\Theta(\tau-\tau') = \begin{cases} 1 \text{ if } \tau>\tau' \\ 0 \text{ if } \tau<\tau' \end{cases},$$

(v) the quantities $\vec{K}_1, \vec{K}_2, \vec{\vec{L}}_1, \vec{\vec{L}}_2, S, \vec{\vec{M}}, \vec{\ell}_1, \vec{\ell}_2, k, \vec{\vec{m}}$ in (3.25)-(3.27) are calculated in regions I, II and III from the vectors $\hat{z}, \vec{w}, \hat{k}_1, \hat{k}_2$ through the chain of equations (3.30), (3.29) and (3.28),

(vi) for α = any of the quantities $\vec{K}_1, \vec{K}_2, \ldots, k, \vec{\vec{m}}$, the primed differences in (3.40) are calculated according to the rules

$$\{\alpha(I)-\alpha(II)\}' \equiv \{\alpha(I)-\alpha(II)\}/\hat{z}\cdot\hat{k}_1 ,$$

$$\{\alpha(III)-\alpha(II)\}' \equiv \{\alpha(III)-\alpha(II)\}/\vec{w}\cdot\hat{k}_2 ;$$

these quantities are given in Table V.

The Monte Carlo procedure for numerically calculating the quantities $a_{k\ell}^{so}$, $b_{k\ell}^{so}$, $c_{k\ell}^{so}$ is essentially to average the integrand in (3.40) over a set of points $\{P^i\}=\{(\eta_1^i,\eta_2^i,\ldots,\eta_7^i)\}$ picked from a random, uniform distribution in the 7-dimensional unit cube U_7 [cf. (3.37)];

$$(\alpha,\beta)_2 = \left\langle \frac{7}{24\sqrt{6}} \frac{\varepsilon}{u^2 E^{*9/2}} \left[\{\alpha(I)-\alpha(II)\}' * \{\beta(III)-\beta(II)\}' \right.\right. \qquad (3.42)$$

$$\left.\left. +\theta(\tau-\tau')\{\beta(I)-\beta(II)\}' * \{\alpha(III)-\alpha(II)\}' \right] \right\rangle_{U_7} .$$

The uncertainty in estimating this average with a *finite* set of points $\{P^1,P^2,\ldots,P^M\}$ is given by the r.m.s. deviation of the quantity being averaged, divided by $\sqrt{M}$. Hence, our computational algorithm is:

1° Generate 7 independent random numbers $\eta_1,\eta_2,\ldots,\eta_7$ from a uniform distribution in the unit interval.

2° Calculate the quantities $\cos\theta_r,\phi_r,\phi_w,u$ (and w), $\cos\theta_r,r,\cos\theta_w$ from Eqs. (3.38). In doing this, $\cos\theta_r$ is obtained from η_5 by numerically inverting (3.38e), and $\cos\theta_r$, r and $\cos\theta_w$ are obtained *in that order* from (3.38e), (3.38f) and (3.38g).

3° The appropriate integrands [i.e., the quantities in $\langle\ \rangle$ in (3.42) for α and β as prescribed by (3.25)-(3.27)] are evaluated at the given random point by following the procedures outlined in steps (ii)-(vi) above.

4° The computed value of the integrand, as well as its square (for calculating the variance in order to estimate the uncertainty), are added to respective running sums.

5° Steps 1°-4° are repeated as many times M as is practical, and then the running sums are converted to averages, thus yielding the estimates of $a_{k\ell}^{so}$, $b_{k\ell}^{so}$ and $c_{k\ell}^{so}$ along with the uncertainties in these estimates.

6° In order to precisely estimate the variances, each matrix element in (3.25)-(3.26) can be calculated as a *single* $(\alpha,\beta)_2$ integral by simply adding the appropriate integrands before averaging. Thus, for example a_{11}^{so} in (3.25) is calculated by averaging an integrand which is equal to: $3\times\{$integrand of $(\vec{L}_1,\vec{L}_1)_2\} + \frac{99}{4} \times \{$integrand of $(\vec{K}_1,\vec{K}_1)_2\}$. Similarly, $\lambda_{12}^{*}(N)$ in (3.41) is most efficiently calculated as the average of an integrand which is the indicated linear combination of the integrands of the $a_{k\ell}^{so}$ quantities.

In order to reduce the uncertainties in our results, we resorted to an empirically determined "importance sampling" procedure [15]. Instead of generating the variable η_i from the *uniform* density function $P(\eta_i)\equiv 1$, we generated η_i according to a *properly chosen non-uniform* density function $P(\eta_i)$, and included in the integrand the factor $1/P(\eta_i)$; the latter "corrects" for the non-uniform sampling, and "smooths" the integrand. A numerical examination of the extreme values of our integrands led to the use of the following specific importance sampling density functions (all defined on the unit interval):

$$P_1(\eta_1) \propto \exp[-3(1-\eta_1)], \tag{3.43a}$$

$$P_2(\eta_2) \propto 1+0.7*\sin(2\pi\eta_2), \tag{3.43b}$$

$$P_3(\eta_3) \propto 1+0.7*\sin(2\pi\eta_3), \tag{3.43c}$$

$$P_5(\eta_5) \propto \exp(-1.1\times\eta_5), \tag{3.43d}$$

$$P_6(\eta_6) \propto \exp(-0.8\times\eta_6), \tag{3.43e}$$

$$P_7(\eta_7) \propto \exp(-\eta_7). \tag{3.43f}$$

For a discussion of methods that generate random numbers from a prescribed non-uniform density function the reader is referred to a separate technical report [15].

One-variable importance sampling transformations of the kinds listed in (3.43) can be expected to reduce the variances by only a limited amount (even with due care in selecting an appropriate density function for each variable). Furthermore, as we are evaluating a total of 18 integrals simultaneously [12 for the matrix elements $a^{SO}_{k\ell}$ $b^{SO}_{k\ell}$, $c^{SO}_{k\ell}$ in (3.25)-(3.27), and 6 for $\lambda^*_{12}(N)$, $\eta^*_{12}(N)$, $D^*_{12}(N)$ in (3.41) for N=1 and 2], then we cannot expect a single set of importance sampling formulae to be optimum for all integrals. As it turned out, the quantities λ^*_{12} and η^*_{12} were more in need of help than D^*_{12}, and the formulae in (3.43) were chosen accordingly. The effect of this importance sampling procedure on the calculation of the SO-integrals was documented in AEDC-TR-71-51 [5]. The transformations (3.43) reduced the uncertainties in λ^*_{12} and η^*_{12} to approximately 2/5 of the uncertainties obtained with "straight" sampling; they also led to a slight reduction of the uncertainty in D^*_{12} by a factor 8/9. The uncertainty in a Monte Carlo calculation is directly proportional to the r.m.s. variation in the integrand and inversely proportional to the *square root* of the number of points sampled. The computer running time is essentially proportional to the number of points sampled, and is increased only very slightly by the incorporation of the importance sampling procedure of (3.43). As a result, a one-hour computer run *with* importance sampling produced results for λ^*_{12} and η^*_{12} comparable in accuracy to a five-hour computer run *without* importance sampling.

The results of our calculations of the single-overlap collision integrals thus obtained will be presented and discussed in Section 3.5.

3.4 Evaluation of 11-Dimensional SO-Integrals

In the previous two sections we considered those matrix elements $a_{k\ell}^{so}$, $b_{k\ell}^{so}$ and $c_{k\ell}^{so}$ that are needed to determine the coefficients $\lambda_{12}^*(N)$, $\eta_{12}^*(N)$ and $D_{12}^*(N)$ in (2.22) up to the *second* Sonine approximation N=2. However, preliminary calculations of these collision integrals showed that the second Sonine approximation $\lambda_{12}^*(2)$ for the thermal conductivity coefficient λ_{12}^* modified the first Sonine approximation $\lambda_{12}^*(1)$ by a significant amount [5]. It thus appeared desirable to make a more careful study of the rate of convergence of the expansion (2.22) for λ_{12}^*, η_{12}^* and D_{12}^*. For this purpose we need to consider matrix elements corresponding to higher order Sonine approximations (N>2).

In view of the algebraic complexities encountered in the last section for N=2, calculations for N>2 by that method are out of the question, and besides, this would not test the correctness of our calculations for N<2. Any attempt to *reduce* the dimensionality of our integrals below 7 would just compound the algebraic complexities, and could clearly not correct any previously made errors. As an alternate procedure we attempted to perform the single-overlap calculations directly from the 11-dimensional integral form (3.14). From an "orthodox" Monte Carlo standpoint this strategy appeared to be rather foolish, since it violated a cardinal rule of proceeding as far as possible *analytically* before resorting to a Monte Carlo procedure; furthermore, the infinite

ranges in (3.14) of the variables $\vec{W}_0$, W_{21} and W_{31} would seem to doom such a procedure anyway. Nevertheless, our strategy proved to be quite successful, as our results in Section 3.4 will show. In this section we shall give the specifics of our calculation of the 11-dimensional collision integrals.

We shall evaluate the coefficients $\eta^*_{12}(N)$ and $D^*_{12}(N)$ up to the third Sonine approximation N=3 and the coefficient $\lambda^*_{12}(N)$ up to the fourth Sonine approximation N=4. The expressions for the matrix elements to be considered are given in Tables VI-VIII.

In these expressions we have deleted terms with $\sum_{n=1}^{3} W_n$ and $\sum_{n=1}^{3} W_n^2$, since they contribute nothing. The first four elements in Tables VI-VIII were given earlier in (3.17)-(3.19). However, our object is now to calculate the matrix elements in the 11-dimensional form (3.14).

We begin by specifying the vector $\vec{W}_0$ in the polar form (W_0,θ_0,ϕ_0), where the polar angle θ_0 and azimuthal angle ϕ_0 are defined relative to the coordinate frame shown in Fig. 11. Thus,

$$d^3\vec{W}_0 = W_0^2 dW_0 d\cos\theta_0 d\phi_0.$$

Further, from the definition of E in (2.39) we have

$$e^{-E} = e^{-\frac{2}{3}W_{21}^2} \cdot e^{-\frac{2}{3}W_{31}^2} \cdot e^{+\frac{2}{3}\vec{W}_{21}\cdot\vec{W}_{31}}.$$

Thus, the integral form in (3.14) can be written

Table VI

The Matrix Elements $a_{k\ell}^{so}$

$$a_{11}^{so} = \left(\sum_{m=1}^{3} \vec{W}_m W_m^2, \sum_{n=1}^{3} \vec{W}_n W_n^2 \right)_2$$

$$a_{12}^{so} = \left(\sum_{m=1}^{3} \vec{W}_m W_m^2, \sum_{n=1}^{3} \vec{W}_n \left(\frac{7}{2} W_n^2 - \frac{1}{2} W_n^4\right) \right)_2$$

$$a_{21}^{so} = \left(\sum_{m=1}^{3} \vec{W}_m \left(\frac{7}{2} W_m^2 - \frac{1}{2} W_m^4\right), \sum_{n=1}^{3} \vec{W}_n W_n^2 \right)_2$$

$$a_{13}^{so} = \left(\sum_{m=1}^{3} \vec{W}_m W_m^2, \sum_{n=1}^{3} \vec{W}_n \left(\frac{63}{8} W_n^2 - \frac{9}{4} W_n^4 + \frac{1}{6} W_n^6\right) \right)_2$$

$$a_{31}^{so} = \left(\sum_{m=1}^{3} \vec{W}_m \left(\frac{63}{8} W_m^2 - \frac{9}{4} W_m^4 + \frac{1}{6} W_m^6\right), \sum_{n=1}^{3} \vec{W}_n W_n^2 \right)_2$$

$$a_{23}^{so} = \left(\sum_{m=1}^{3} \vec{W}_m \left(\frac{7}{2} W_m^2 - \frac{1}{2} W_m^4\right), \sum_{n=1}^{3} \vec{W}_n \left(\frac{63}{8} W_n^2 - \frac{9}{4} W_n^4 + \frac{1}{6} W_n^6\right) \right)_2$$

$$a_{32}^{so} = \left(\sum_{m=1}^{3} \vec{W}_m \left(\frac{63}{8} W_m^2 - \frac{9}{4} W_m^4 + \frac{1}{6} W_m^6\right), \sum_{n=1}^{3} \vec{W}_n \left(\frac{7}{2} W_n^2 - \frac{1}{2} W_n^4\right) \right)_2$$

$$a_{33}^{so} = \left(\sum_{m=1}^{3} \vec{W}_m \left(\frac{63}{8} W_m^2 - \frac{9}{4} W_m^4 + \frac{1}{6} W_m^6\right), \sum_{n=1}^{3} \vec{W}_n \left(\frac{63}{8} W_n^2 - \frac{9}{4} W_n^4 + \frac{1}{6} W_n^6\right) \right)_2$$

Table VI (continued)

$$a_{14}^{so} = \left(\sum_{m=1}^{3} \tilde{W}_m W_m^2, \sum_{n=1}^{3} \tilde{W}_n \left(\frac{231}{16}W_n^2 - \frac{99}{16}W_n^4 + \frac{11}{12}W_n^6 - \frac{1}{24}W_n^8\right) \right)_2$$

$$a_{41}^{so} = \left(\sum_{m=1}^{3} \tilde{W}_m \left(\frac{231}{16}W_m^2 - \frac{99}{16}W_m^4 + \frac{11}{12}W_m^6 - \frac{1}{24}W_m^8\right), \sum_{n=1}^{3} \tilde{W}_n W_n^2 \right)_2$$

$$a_{24}^{so} = \left(\sum_{m=1}^{3} \tilde{W}_m \left(\frac{7}{2}W_m^2 - \frac{1}{2}W_m^4\right), \sum_{n=1}^{3} \tilde{W}_n \left(\frac{231}{16}W_n^2 - \frac{99}{16}W_n^4 + \frac{11}{12}W_n^6 - \frac{1}{24}W_n^8\right) \right)_2$$

$$a_{42}^{so} = \left(\sum_{m=1}^{3} \tilde{W}_m \left(\frac{231}{16}W_m^2 - \frac{99}{16}W_m^4 + \frac{11}{12}W_m^6 - \frac{1}{24}W_m^8\right), \sum_{n=1}^{3} \tilde{W}_n \left(\frac{7}{2}W_n^2 - \frac{1}{2}W_n^4\right) \right)_2$$

$$a_{34}^{so} = \left(\sum_{m=1}^{3} \tilde{W}_m \left(\frac{63}{8}W_m^2 - \frac{9}{4}W_m^4 + \frac{1}{6}W_m^6\right), \sum_{n=1}^{3} \tilde{W}_n \left(\frac{231}{16}W_n^2 - \frac{99}{16}W_n^4 + \frac{11}{12}W_n^6 - \frac{1}{24}W_n^8\right) \right)_2$$

$$a_{43}^{so} = \left(\sum_{m=1}^{3} \tilde{W}_m \left(\frac{231}{16}W_m^2 - \frac{99}{16}W_m^4 + \frac{11}{12}W_m^6 - \frac{1}{24}W_m^8\right), \sum_{n=1}^{3} \tilde{W}_n \left(\frac{63}{8}W_m^2 - \frac{9}{4}W_m^4 + \frac{1}{6}W_m^6\right) \right)_2$$

$$a_{44}^{so} = \left(\sum_{m=1}^{3} \tilde{W}_m \left(\frac{231}{16}W_m^2 - \frac{99}{16}W_m^4 + \frac{11}{12}W_m^6 - \frac{1}{24}W_m^8\right), \sum_{n=1}^{3} \tilde{W}_n \left(\frac{231}{16}W_n^2 - \frac{99}{16}W_n^4 + \frac{11}{12}W_n^6 - \frac{1}{24}W_n^8\right) \right)_2$$

Note: $(\alpha,\beta)_2$ is defined in (3.14).

Table VII

The Matrix Elements $b_{k\ell}^{so}$

$$b_{00}^{so} = \left(\sum_{m=1}^{3} \vec{W}_m \vec{W}_m , \sum_{n=1}^{3} \vec{W}_n \vec{W}_n \right)_2$$

$$b_{01}^{so} = \left(\sum_{m=1}^{3} \vec{W}_m \vec{W}_m , \sum_{n=1}^{3} \{ \vec{W}_n \vec{W}_n (\tfrac{7}{2} - W_n^2) + \tfrac{1}{3} \vec{\vec{I}} W_n^4 \} \right)_2$$

$$b_{10}^{so} = \left(\sum_{m=1}^{3} \{ \vec{W}_m \vec{W}_m (\tfrac{7}{2} - W_m^2) + \tfrac{1}{3} \vec{\vec{I}} W_m^4 \} , \sum_{n=1}^{3} \vec{W}_n \vec{W}_n \right)_2$$

$$b_{11}^{so} = \left(\sum_{m=1}^{3} \{ \vec{W}_m \vec{W}_m (\tfrac{7}{2} - W_m^2) + \tfrac{1}{3} \vec{\vec{I}} W_m^4 \} , \sum_{n=1}^{3} \{ \vec{W}_n \vec{W}_n (\tfrac{7}{2} - W_n^2) + \tfrac{1}{3} \vec{\vec{I}} W_n^4 \} \right)_2$$

$$b_{02}^{so} = \left(\sum_{m=1}^{3} \vec{W}_m \vec{W}_m , \sum_{n=1}^{3} \{ \vec{W}_n \vec{W}_n (\tfrac{63}{8} - \tfrac{9}{2} W_n^2 + \tfrac{1}{2} W_n^4) + \tfrac{1}{3} \vec{\vec{I}} (\tfrac{9}{2} W_n^4 - \tfrac{1}{2} W_n^6) \} \right)_2$$

$$b_{20}^{so} = \left(\sum_{m=1}^{3} \{ \vec{W}_m \vec{W}_m (\tfrac{63}{8} - \tfrac{9}{2} W_m^2 + \tfrac{1}{2} W_m^4) + \tfrac{1}{3} \vec{\vec{I}} (\tfrac{9}{2} W_m^4 - \tfrac{1}{2} W_m^6) \} , \sum_{n=1}^{3} \vec{W}_n \vec{W}_n \right)_2$$

$$b_{12}^{so} = \left(\sum_{m=1}^{3} \{ \vec{W}_m \vec{W}_m (\tfrac{7}{2} - W_m^2) + \tfrac{1}{3} \vec{\vec{I}} W_m^4 \} , \sum_{n=1}^{3} \{ \vec{W}_n \vec{W}_n (\tfrac{63}{8} - \tfrac{9}{2} W_n^2 + \tfrac{1}{2} W_n^4) + \tfrac{1}{3} \vec{\vec{I}} (\tfrac{9}{2} W_n^4 - \tfrac{1}{2} W_n^6) \} \right)_2$$

$$b_{21}^{so} = \left(\sum_{m=1}^{3} \{ \vec{W}_m \vec{W}_m (\tfrac{63}{8} - \tfrac{9}{2} W_m^2 + \tfrac{1}{2} W_m^4) + \tfrac{1}{3} \vec{\vec{I}} (\tfrac{9}{2} W_m^4 - \tfrac{1}{2} W_m^6) \} , \sum_{n=1}^{3} \{ \vec{W}_n \vec{W}_n (\tfrac{7}{2} - W_n^2) + \tfrac{1}{3} \vec{\vec{I}} W_n^4 \} \right)_2$$

$$b_{22}^{so} = \left(\sum_{m=1}^{3} \{ \vec{W}_m \vec{W}_m (\tfrac{63}{8} - \tfrac{9}{2} W_m^2 + \tfrac{1}{2} W_m^4) + \tfrac{1}{3} \vec{\vec{I}} (\tfrac{9}{2} W_m^4 - \tfrac{1}{2} W_m^6) \} , \sum_{n=1}^{3} \{ \vec{W}_n \vec{W}_n (\tfrac{63}{8} - \tfrac{9}{2} W_n^2 + \tfrac{1}{2} W_n^4) + \tfrac{1}{3} \vec{\vec{I}} (\tfrac{9}{2} W_n^4 - \tfrac{1}{2} W_n^6) \} \right)_2$$

Note: $(\alpha, \beta)_2$ is defined in (3.14); $\vec{\vec{I}}$ is the unit tensor.

Table VIII

The Matrix Elements $c_{k\ell}^{so}$.

$$c_{00}^{so} = 2\left(\vec{W}_1, \vec{W}_1\right)_2$$

$$c_{01}^{so} = 2\left(\vec{W}_1, \vec{W}_1\left(\frac{5}{2}-W_1^2\right)\right)_2$$

$$c_{10}^{so} = 2\left(\vec{W}_1\left(\frac{5}{2}-W_1^2\right), \vec{W}_1\right)_2$$

$$c_{11}^{so} = 2\left(\vec{W}_1\left(\frac{5}{2}-W_1^2\right), \vec{W}_1\left(\frac{5}{2}-W_1^2\right)\right)_2$$

$$c_{02}^{so} = 2\left(\vec{W}_1, \vec{W}_1\left(\frac{35}{8}-\frac{7}{2}W_1^2+\frac{1}{2}W_1^4\right)\right)_2$$

$$c_{20}^{so} = 2\left(\vec{W}_1\left(\frac{35}{8}-\frac{7}{2}W_1^2+\frac{1}{2}W_1^4\right), \vec{W}_1\right)_2$$

$$c_{12}^{so} = 2\left(\vec{W}_1\left(\frac{5}{2}-W_1^2\right), \vec{W}_1\left(\frac{35}{8}-\frac{7}{2}W_1^2+\frac{1}{2}W_1^4\right)\right)_2$$

$$c_{21}^{so} = 2\left(\vec{W}_1\left(\frac{35}{8}-\frac{7}{2}W_1^2+\frac{1}{2}W_1^4\right), \vec{W}_1\left(\frac{5}{2}-W_1^2\right)\right)_2$$

$$c_{22}^{so} = 2\left(\vec{W}_1\left(\frac{35}{8}-\frac{7}{2}W_1^2+\frac{1}{2}W_1^4\right), \vec{W}_1\left(\frac{35}{8}-\frac{7}{2}W_1^2+\frac{1}{2}W_1^4\right)\right)_2$$

Note: $(\alpha,\beta)_2$ is defined in (3.14).

$$(\alpha,\beta)_2 = \frac{1}{5\sqrt{2}\pi^4} \int_0^\infty dW_0 W_0^2 e^{-3W_0^2} \int_0^\infty dW_{21} W_{21}^4 e^{-\frac{2}{3}W_{21}^2} \int_0^\infty dW_{31} W_{31}^3 e^{-\frac{2}{3}W_{31}^2}$$

$$\times \int_0^{2\pi} d\phi_0 \int_0^{2\pi} d\phi_w \int_0^{2\pi} d\phi_r \int_{-1}^{1} d\cos\theta_0 \int_{-1}^{0} d\cos^3\theta \int_{1/2}^{1} d\cos\theta_r$$

$$\times \int_1^{(2\cos\theta_r)^4} dr^4 \int_{1-r^{-2}}^{1} d\cos^2\theta_w \; \varepsilon \exp\left(\tfrac{2}{3}\vec{W}_{21}\cdot\vec{W}_{31}\right)$$

$$\times \Big[\{\alpha(I)-\alpha(II)\}' * \{\beta(III)-\beta(II)\}'$$

$$+\theta(\tau-\tau')\{\beta(I)-\beta(II)\}' * \{\alpha(III)-\alpha(I)\}' \Big]. \qquad (3.44)$$

The basic vectors, namely the velocities $\vec{W}_0$, $\vec{W}_{21}$, $\vec{W}_{31}$ in region II and the vectors $\hat{k}_1$ and $\vec{r}_{31}$, may be written in component form by referring to Figure 11 and applying the necessary rotation matrices defined in Table IV. Thus, we have relative to the coordinate frame indicated in Fig. 11,

$$\vec{W}_0 = \begin{bmatrix} W_0\sin\theta_0\cos\phi_0 \\ W_0\sin\theta_0\sin\phi_0 \\ W_0\cos\theta_0 \end{bmatrix}, \qquad (3.45a)$$

$$\vec{W}_{21} = \begin{bmatrix} 0 \\ 0 \\ W_{21} \end{bmatrix}, \qquad (3.45b)$$

$$\vec{W}_{31} = R_y(-(\pi-\theta)) \cdot R_z(-\phi_r) \cdot R_y(\pi-\theta_r) \cdot \begin{bmatrix} W_{31}\sin\theta_w\cos\phi_w \\ W_{31}\sin\theta_w\sin\phi_w \\ W_{31}\cos\theta_w \end{bmatrix} , \qquad (3.45c)$$

$$\hat{k}_1 = \begin{bmatrix} -\sin\theta \\ 0 \\ \cos\theta \end{bmatrix} , \qquad (3.45d)$$

$$\vec{r}_{31} = R_y(-(\pi-\theta)) \cdot \begin{bmatrix} r\sin\theta_r\cos\phi_r \\ r\sin\theta_r\sin\phi_r \\ r\cos\theta_r \end{bmatrix} . \qquad (3.45e)$$

In addition, the component representation of $\hat{k}_2$ is found by inserting (3.45c) and (3.45e) into (3.9), which we repeat here for convenience:

$$\hat{k}_2 = -\vec{r}_{31} - r\hat{W}_{31}(1-\varepsilon)\cos\theta_w . \qquad (3.45f)$$

The differences between these component formulae and those in (3.32) which were used in the 7-dimensional calculation are due simply to the fact that we are using different coordinate frames in the two cases. This is permissible since the final answers are scalars, and hence can depend only on the vector dot products, which are the same in all coordinate frames.

Eqs. (3.45a)-(3.45c) express the region II velocities $\vec{W}_0$, $\vec{W}_{21}$, $\vec{W}_{31}$ in terms of the integrating variables in (3.44), and eqs. (3.45d)-(3.45f) do the same for the collision vectors $\hat{k}_1$ and $\hat{k}_2$. With these quantities we may calculate the velocities $\vec{W}_0(i)$, $\vec{W}_{21}(i)$, $\vec{W}_{31}(i)$ in regions i=I and III by means of eqs. (3.10), and the velocities $\vec{W}_1(i)$, $\vec{W}_2(i)$, $\vec{W}_3(i)$ are then calculated from (2.36):

$$\left.\begin{aligned}
\vec{W}_1(i) &= \vec{W}_0 - \tfrac{1}{3}[\vec{W}_{21}(i) + \vec{W}_{31}(i)] \quad , \\
\vec{W}_2(i) &= \vec{W}_0 - \tfrac{1}{3}[\vec{W}_{31}(i) - 2\vec{W}_{21}(i)] \quad , \\
\vec{W}_3(i) &= \vec{W}_0 - \tfrac{1}{3}[\vec{W}_{21}(i) - 2\vec{W}_{31}(i)] \quad ,
\end{aligned}\right\} \quad i=I,II,III \ . \tag{3.46}$$

Thus, starting from a set of prescribed values for the eleven integrating variables in (3.44), we see that we may calculate the velocities $\vec{W}_1(i)$, $\vec{W}_2(i)$, $\vec{W}_3(i)$ for all regions i=I,II,III. This enables us to calculate the primed differences in (3.44) where α and β are any of the specific velocity functions appearing in the expressions for the matrix elements in Tables VI-VIII. Since τ, τ' and ε are also known in terms of the integrating variables [cf.(3.6), (3.7) and (3.8)], then it would appear that we have everything needed to calculate the quantities $a^{so}_{k\ell}$, $b^{so}_{k\ell}$ and $c^{so}_{k\ell}$, and hence the quantities $\lambda^*_{12}(N)$, $\eta^*_{12}(N)$ and $D^*_{12}(N)$ in (3.41).

The difficulty with (3.44) from a Monte Carlo standpoint is the infinite ranges associated with the variables W_0, W_{21}, and W_{31}. Our method of getting around this difficulty is as follows:

For a fixed integer n>0 and real a>0, define the function

$$P(x;n,a) \equiv A(n,a)x^n e^{-ax^2} , \tag{3.47a}$$

where A(n,a) is such that

$$\int_0^\infty P(x;n,a)dx = 1 \ . \tag{3.47b}$$

Using standard integral tables, one finds that the required formula for A(n,a) is

$$A(n,a) \equiv \begin{cases} \frac{2}{\sqrt{\pi}} a^{1/2} , & n=0 \\ \frac{2}{\sqrt{\pi}} \frac{2^{n/2} a^{(n+1)/2}}{1 \cdot 3 \cdot 5 \cdots (n-1)} , & n=2,4,6,\ldots \\ 2\, a^{(n+1)/2} \Big/ \left(\frac{n-1}{2}\right)! , & n=1,3,5,\ldots \end{cases} . \qquad (3.47c)$$

We now consider the transformation $x \to u$ defined by

$$u = \int_0^x P(x';n,a)dx' \equiv F(x;n,a) . \qquad (3.48a)$$

Since $P(x;n,a)>0$ on $0<x<\infty$, and since $F(0;n,a)=0$ while $F(\infty;n,a)=1$ [cf. (3.47b)], then (3.48a) defines an invertible mapping of the interval $0 \leq x < \infty$ onto the interval $0 \leq u \leq 1$. Formally, we write the inverse of (3.48a) as

$$x = F^{-1}(u;n,a). \qquad (3.48b)$$

The Jacobian of the transformation (3.48a) is evidently such that $du = P(x;n,a)dx$, or, using (3.47a),

$$x^n e^{-ax^2} dx = A^{-1}(n,a)du. \qquad (3.48c)$$

Returning now to (3.44), we introduce the transformations $W_0 \to u_0$, $W_{21} \to u_{21}$, $W_{31} \to u_{31}$ according to

$$\left.\begin{aligned} u_0 &= F(W_0,2,3) \quad , \\ u_{21} &= F(W_{21},4,\tfrac{2}{3}) \quad , \\ u_{31} &= F(W_{31},3,\tfrac{2}{3}) \quad . \end{aligned}\right\} \tag{3.49}$$

This implies, by (3.48c), that

$$W_0^2 e^{-3W_0^2} dW_0 \cdot W_{21}^4 e^{-\frac{2}{3}W_{21}^2} dW_{21} \cdot W_{31}^3 e^{-\frac{2}{3}W_{31}^2} dW_{31} =$$

$$= A^{-1}(2,3)du_0 \cdot A^{-1}(4,\tfrac{2}{3})du_{21} \cdot A^{-1}(3,\tfrac{2}{3})du_{31}$$

$$= \left(\frac{\pi}{\sqrt{2}}\,\frac{3^4}{2^{10}}\right)du_0 du_{21} du_{31} \quad , \tag{3.50}$$

where we have used the explicit formulae in (3.47c). Inserting (3.50) into (3.44), we thus obtain

$$(\alpha,\beta)_2 = \frac{3^4}{5\pi^3 2^{11}} \int_0^1 du_0 \int_0^1 du_{21} \int_0^1 du_{31} \int_0^{2\pi} d\phi_0 \int_0^{2\pi} d\phi_w \int_0^{2\pi} d\phi_r \int_{-1}^{1} d\cos\theta_0$$

$$\times \int_{-1}^{0} d\cos^3\theta \int_{1/2}^{1} d\cos\theta_r \int_1^{(2\cos\theta_r)^4} dr^4 \int_{1-r^{-2}}^{1} d\cos^2\theta_w \; \varepsilon \; e^{\frac{2}{3}\hat{W}_{21}\cdot\hat{W}_{31}}$$

$$\times \; [\{\alpha(I)-\alpha(II)\}'*\{\beta(III)-\beta(II)\}'$$

$$+ \Theta(\tau-\tau')\{\beta(I)-\beta(II)\}'*\{\alpha(III)-\alpha(II)\}'] \quad , \tag{3.51}$$

where it is henceforth understood that the quantities W_0, W_{21}, W_{31} are to be obtained from the following formulae [cf. (3.49) and (3.48b)]:

$$W_0 = F^{-1}(u_0;2,3) \ , \tag{3.52a}$$

$$W_{21} = F^{-1}(u_{21};4,\tfrac{2}{3}), \tag{3.52b}$$

$$W_{31} = F^{-1}(u_{31};3,\tfrac{2}{3}). \tag{3.52c}$$

We assume for the present that it is possible to calculate and invert the functions F, as required by (3.52); we shall consider the details of how this is to be accomplished later.

The formula for $(\alpha,\beta)_2$ in (3.51) is now expressed as an integral over the *finite* 11-dimensional volume Ω', defined by

$$\begin{aligned}\Omega' \equiv \{ &(u_0,u_{21},u_{31},\phi_0,\phi_w,\phi_r,\cos\theta_0,\cos^3\theta,\cos\theta_r,r^4,\cos^2\theta_w) \,|\, \\ &0\leq u_0\leq 1,\ 0\leq u_{21}\leq 1,\ 0\leq u_{31}\leq 1,\ 0<\phi_0\leq 2\pi, \\ &0\leq\phi_w\leq 2\pi,\ 0\leq\phi_r\leq 2\pi,\ -1\leq\cos\theta_0\leq 1,\ -1\leq\cos^3\theta<0, \\ &\tfrac{1}{2}\leq\cos\theta_r\leq 1,\quad 1\leq r^4\leq(2\cos\theta_r)^4,\ (1-r^{-2})\leq\cos^2\theta_w\leq 1\} \ . \end{aligned} \tag{3.53}$$

For Monte Carlo purposes, it is convenient to change variables in such a way that the volume Ω' is transformed into an 11-dimensional unit cube

$$U_{11} \equiv \{(\eta_1,\eta_2,\ldots,\eta_{11}) \,|\, 0\leq\eta_i\leq 1;\ i=1,2,\ldots,11\} \ . \tag{3.54}$$

We choose to do this by essentially the same transformation (3.38) which carried the 7-dimensional region Ω in (3.36) into a 7-dimensional cube U_7 in (3.37):

$$u_0 = \kappa_1, \tag{3.55a}$$

$$u_{21} = \kappa_2, \tag{3.55b}$$

$$u_{31} = \kappa_3, \tag{3.55c}$$

$$\phi_0 = 2\pi\kappa_4, \tag{3.55d}$$

$$\phi_w = 2\pi\kappa_5, \tag{3.55e}$$

$$\phi_r = 2\pi\kappa_6, \tag{3.55f}$$

$$\cos\theta_0 = -1+2\kappa_7, \tag{3.55g}$$

$$\cos^3\theta = -1+\kappa_8, \tag{3.55h}$$

$$2\kappa_9 = 4\cos^3\theta_r - 3\cos\theta_r + 1, \tag{3.55i}$$

$$r^4 = [1+(4\cos^2\theta_r - 1)\kappa_{10}]^2, \tag{3.55j}$$

$$\cos^2\theta_w = (1-r^{-2})+r^{-2}\kappa_{11}. \tag{3.55k}$$

The first 8 transformation formulae here are obvious from (3.51) and the last three transformation formulae are identical to the last three formulae in (3.38); note that (3.55i) defines $\cos\theta_r$ in terms of κ_9 through an implicit inversion. As in the 7-dimensional case, the Jacobian of this transformation is simply equal to the volume of Ω':

$$\frac{\partial(u_0, u_{21}, u_{31}, \phi_0, \ldots, \cos^2\theta_w)}{\partial(\kappa_1, \kappa_2, \kappa_3, \ldots, \kappa_{11})} = |\Omega'| = \frac{64\pi^3}{3}. \tag{3.56}$$

Thus, we may straightaway replace the integrating variables in (3.51) by the variables $\eta_1,\eta_2,\ldots,\eta_{11}$, provided we multiply the integral by the constant factor in (3.56). Our *final formula* for $(\alpha,\beta)_2$ is therefore

$$(\alpha,\beta)_2 = \frac{27}{160}\int_0^1 d\eta_1 \int_0^1 d\eta_2 \cdots \int_0^1 d\eta_{11}\, \varepsilon \exp\left(\frac{2}{3}\vec{W}_{21}\cdot\vec{W}_{31}\right) \tag{3.57}$$

$$\times \Big[\{\alpha(I)-\alpha(II)\}'*\{\beta(III)-\beta(II)\}'$$

$$+\theta(\tau-\tau')\{\beta(I)-\beta(II)\}'*\{\alpha(III)-\alpha(II)\}'\Big].$$

In summary, the calculation of the 11-dimensional integrals proceeds in the following way:

(i) The quantities $u_0,u_{21},u_{31},\phi_0,\phi_w,\phi_r,\cos\theta_0,\cos\theta,\cos\theta_r,r,\cos\theta_w$ are obtained from the integrating variables $\eta_1,\eta_2,\ldots,\eta_{11}$ through eqs. (3.55) [with an implied inversion in (3.55i)].

(ii) The quantities W_0,W_{21},W_{31} are obtained from u_0,u_{21},u_{31} through eqs. (3.52) [cf. discussion below].

(iii) The vectors $\vec{W}_0,\vec{W}_{21},\vec{W}_{31},\hat{k}_1,\vec{r}_{31}$ are obtained from (3.45), using the matrices in Table IV.

(iv) The quantities $\varepsilon,\tau,\tau',\hat{k}_2$ are calculated from eqs. (3.6)-(3.9), and $\theta(\tau-\tau')$ is set to 1 if $\tau>\tau'$ or 0 if $\tau\leqslant\tau'$.

(v) From the region II velocities $\vec{W}_0,\vec{W}_{21}$ and $\vec{W}_{31}$, and the collision vectors $\hat{k}_1$ and $\hat{k}_2$, the velocities $\vec{W}_1(i)$, $\vec{W}_2(i)$, $\vec{W}_3(i)$ in regions i=I,II,III are calculated via eqs. (3.10) and (3.46).

(vi) The primed differences in (3.57) are then calculated according to the definitions (3.12) for the quantities α and β appearing in the expressions for the matrix elements in Tables VI-VIII.

(vii) The various matrix elements $a^{so}_{k\ell}$, $b^{so}_{k\ell}$, $c^{so}_{k\ell}$ are calculated by evaluating the integrals $(\alpha,\beta)_2$ in Tables VI-VIII; the coefficients $\lambda^*_{12}(N)$, $\eta^*_{12}(N)$, $D^*_{12}(N)$ are computed from (3.41) using the coefficients given in Table III.

We now describe how the crucial calculations in (3.52) were carried out. The function F(x;n,a) is defined in (3.48a). Using the definitions of P(x;n,a) and A(n,a) in eqs. (3.47), one can derive by a somewhat tedious induction argument the following explicit expression for F(x;n,a):

$$F(x;n,a,) = \begin{cases} \operatorname{erf}(x\sqrt{a}) - \frac{2}{\sqrt{\pi}} e^{-ax^2} x\sqrt{a} \sum_{\nu=1}^{n/2} \frac{(2ax^2)^{\nu-1}}{1\cdot 3\cdot 5\cdots(2\nu-1)}, & n \text{ even}, \\ 1 - e^{-ax^2} \sum_{\nu=0}^{(n-1)/2} \frac{(ax^2)^{\nu}}{\nu!}, & n \text{ odd}. \end{cases} \tag{3.58}$$

Here, erf(x) is the "error function",

$$\operatorname{erf}(x) \equiv \frac{2}{\sqrt{\pi}} \int_0^x e^{-t^2} dt \quad (x \geq 0), \tag{3.59}$$

and $F(x;n=0,a)=\operatorname{erf}(x\sqrt{a})$. Now, for fixed values of n and a, eq. (3.58) allows us to evaluate

$$u=F(x;n,a),$$

for any *given* x in $(0,\infty)$. Thus, by using a numerical inversion technique on the computer, it is possible, for fixed values of n and a, to *find* the value of x which satisfies the above relation for a *given* value of u in

(0,1). This is precisely the procedure that we used. We employed an alternating "successive bisection/inverse linear interpolation" method to accomplish the numerical inversion [the inverse linear interpolation procedure by itself will not converge for values of u near 1, since $dx/du \to \infty$ as $u \to 1$]. The evaluation of F(x;n,a) for a given x was always carried out in double-precision to minimize computer round-off error. This procedure required a double-precision error function subroutine for even values of n†. The double-precision error function calculation is rather involved, with the result that inversions of u=F(x;n,a) for n even are considerably slower than for n odd. In the actual calculations, we found it convenient to *modify* (3.44) by changing $W_0^2 \to W_0^3$ and $W_{21}^4 \to W_{21}^5$, and then incorporating into the integrand a factor $1/W_0 W_{21}$). Then the n-values in (3.49) are all odd, so that the inversions required by (3.52) are more rapidly accomplished (but note that the factor in (3.50) must be modified accordingly).

An important point which was *not* investigated analytically was the boundedness of the integrand in (3.51), especially for $W_0, W_{21}, W_{31} \to \infty$. The boundedness of the integrand in the original integral (3.44) was assured by the exponentials multiplying dW_0, dW_{21} and dW_{31}, but it is quite possible that, in transforming from an infinite to a finite integration region by means of (3.49), we rendered the integrand unbounded. Certainly, the factor $\exp(\frac{2}{3}\vec{W}_{21} \cdot \vec{W}_{31})$ in (3.51) as well as the Sonine polynomials used for α and β are unbounded functions of W_{21} and W_{31}.

---

† We are indebted to I. Stegun and R. Zucker of the National Bureau of Standards for providing us with a double-precision error function subroutine (subroutine ERRINT).

Essentially, we proceeded blindly in the hope that the intricasies of the integrand (i.e., the differences and scalar products that are taken) would work to counteract these features and keep things bounded. The final answers for $\lambda^*_{12}(N)$, $\eta^*_{12}(N)$ and $D^*_{12}(N)$ seemed satisfactory in this respect.

The Monte Carlo algorithm for numerically calculating the quantities $a^{so}_{k\ell}$, $b^{so}_{k\ell}$, $c^{so}_{k\ell}$ is to evaluate (3.57) for the required functions α and β by averaging its integrand over a set of points $\{P^i\}=\{\eta^i_1,\eta^i_2,\ldots,\eta^i_{11})\}$ picked from a random, uniform distribution in the 11-dimensional unit cube U_{11} [cf. (3.54)]:

$$(\alpha,\beta)_2 = \left\langle \frac{27}{160}\ \varepsilon \exp\left(\frac{2}{3}\vec{w}_{21}\cdot\vec{w}_{31}\right)\left[\{\alpha(I)-\alpha(II)\}'*\{\beta(III)-\beta(II)\}'\right.\right.$$
$$\left.\left. + \theta(\tau-\tau')\{\beta(I)-\beta(II)\}'*\{\alpha(III)-\alpha(II)\}'\right]\right\rangle_{U_{11}} . \qquad (3.60)$$

The uncertainty in estimating this average with a *finite* set of points $\{P^1,P^2,\ldots,P^M\}$ is given by the r.m.s. deviation of the quantity being averaged, divided by $\sqrt{M}$. Hence, the Monte Carlo algorithm is:

1° Generate 11 independent random numbers $\eta_1,\eta_2,\ldots,\eta_{11}$ from a uniform distribution in the unit interval.

2° Using the steps (i)-(vii)[following eq. (3.57)], evaluate the various integrands at the point $(\eta_1,\eta_2,\ldots,\eta_{11})$.

3° Add the values of these integrands, and also the squares of these values (for computing the r.m.s. deviations), to respective running sums.

4° Repeat steps 1°-3° as many times M as is practical, and then convert the running sums to averages, thus yielding the estimates of the integrals along with the uncertainties in these estimates.

As in the calculations of the 7-dimensional integrals, we again used an empirically determined, single-variable importance sampling procedure to reduce the uncertainties in our results. The specific importance sampling functions used were as follows:

$$P_1(r_1) \propto 1+0.45\cos(2\pi r_1), \tag{3.61a}$$

$$\left.\begin{matrix}P_2(r_2)\\ P_3(r_3)\end{matrix}\right\} \propto \begin{cases}\text{piecewise linear function}\\ \text{through points } (0.0,1.0),\\ (0.8,1.0),\ (0.9,1.5),(0.95,\\ 2.0),(0.98,4.0),(1.0,9.0)\end{cases} \tag{3.61b}$$

$$P_4(r_4) \propto 1+.0.45\cos(2\pi r_4), \tag{3.61c}$$

$$P_5(r_5) \propto 1+.0.65\cos(2\pi r_5), \tag{3.61d}$$

$$P_6(r_6) \propto 1+0.65\cos(2\pi r_6), \tag{3.61e}$$

$$P_7(r_7) \propto \exp(-r_7), \tag{3.61f}$$

$$P_8(r_8) \propto \exp[-3(1-r_6)], \tag{3.61g}$$

$$P_9(r_9) \propto \exp(-2r_9) \tag{3.61h}$$

$$P_{10}(r_{10}) \propto \exp(-r_{10}), \tag{3.61i}$$

$$P_{11}(r_{11}) \propto \exp(-2r_{11}). \tag{3.61j}$$

This importance sampling proceedure reduced the r.m.s. variation in the key integrands by a factor of nearly 4, and thus reduced the running time required for a given level of accuracy by a factor of roughly 4^2=16.

3.5 Single-Overlap Results

The single-overlap collision integrals derived in Section 3.2 were computed in a 7-dimensional form according to the procedure described in Section 3.3 by a computer program called Subroutine OVRLAP. Those collision integrals were evaluated that determine the contribution to the transport coefficients in the first (N=1) and second (N=2) Sonine approximations. The values thus obtained for the coefficients λ^*_{12}, η^*_{12}, D^*_{12} are presented in Table i.† At the same time we calculated the values of the individual matrix elements $a^{so}_{k\ell}$, $b^{so}_{k\ell}$, $c^{so}_{k\ell}$; the values obtained for these matrix elements are presented in Table ii.

For each quantity we show the results of four "runs" of Subroutine OVRLAP on the University of Maryland 1108 computer. Each run used 200,000 random points in the 7-dimensional unit cube, and required about 40 minutes of "c.p.u. time" or 22 minutes of "core time" [computer charges are calculated on the basis of *core* time]. The uncertainties in each *run* represent one standard deviation (~65% confidence limits) and become two standard deviations (~95% confidence limits) in the *averages*. This procedure, of performing each calculation as four independent "runs" and then averaging the results, was followed in almost all our calculations. It is to be preferred over making a single long run [i.e. in this case the "averages" are equivalent to *one* run with 800,000 random points in the 7-dimensional unit cube], because it allows one to insure that the fluctuations in the results are indeed of the same order of magnitude as

† Tables of three-particle collision integrals are headed with lower case Roman numerals and are placed in the Appendix.

the r.m.s. deviations predict. This procedure was also used as a precaution against having a single long computer run totally invalidated by a computer fault.

Monte Carlo estimates for these single-overlap collision integrals were first reported in AEDC-TR-71-51 [5]. The earlier results were obtained with the same subroutine, but were based on 50,000 random points. A comparison between the new and earlier results is presented in Table iii. As can be seen from this table, we have now reduced the uncertainty in these collision integrals by a factor 4 to 5.

In order to interpret the results we remind the reader of the fact that the coefficients λ^*_{12}, η^*_{12} and D^*_{12} represent the first (μ=2) corrections to the value *unity* predicted by the theory of Enskog [cf.(2.21)]. From Table i we conclude that in the first Sonine approximation†

$$\begin{aligned} \lambda^*_{12}(1) &= -0.0303\pm0.0003 \\ \eta^*_{12}(1) &= -0.0633\pm0.0004 \\ D^*_{12}(1) &= -0.1195\pm0.0005 \end{aligned} \quad , \tag{3.62}$$

and in the second Sonine approximation

$$\begin{aligned} \lambda^*_{12}(2) &= -0.0248\pm0.0003 \\ \eta^*_{12}(2) &= -0.0621\pm0.0004 \\ D^*_{12}(2) &= -0.1160\pm0.0005 \end{aligned} \quad . \tag{3.63}$$

† All uncertainties quoted in the text represent two standard deviations (95% confidence limits).

The single-overlap collisions are thus seen to *reduce* the excluded volume effect (unity) predicted by the theory of Enskog.

It was also inferred from these calculations, that the differences between the second and first Sonine approximations are

$$\begin{aligned} \lambda^*_{12}(2)-\lambda^*_{12}(1) &= +0.0055\pm0.0001 \quad , \\ \eta^*_{12}(2)-\eta^*_{12}(1) &= +0.0012\pm0.0001 \quad , \\ D^*_{12}(2)-D^*_{12}(1) &= +0.0035\pm0.0001 \quad . \end{aligned} \tag{3.64}$$

The second Sonine approximations $\lambda_0(2)$, $\eta_0(2)$ and $D_0(2)$ for the transport coefficients in the *low density limit* (2.13) modify the first Sonine approximations $\lambda_0(1)$, $\eta_0(1)$ and $D_0(1)$ by about 2% as can be seen from Table III. On comparing (3.64) and (3.62) we note that the second Sonine approximations $\eta^*_{12}(2)$ and $D^*_{12}(2)$ modify the first Sonine approximations again by a few percent; however the coefficient $\lambda^*_{12}(2)$ for the thermal conductivity differs from $\lambda^*_{12}(1)$ by as much as 18%. This phenomenon was noted earlier in AEDC-TR-71-51 [5] and it motivated us to conduct a study of the rate of convergence of the Sonine expansion (3.41) for the coefficients λ^*_{12}, η^*_{12} and D^*_{12}.

For a study of the higher Sonine approximations we used the 11-dimensional Monte Carlo procedure described in Section 3.4. From the results quoted in (3.63)-(3.64) we see that the uncertainties in the differences $\lambda^*_{12}(2)-\lambda^*_{12}(1)$, $\eta^*_{12}(2)-\eta^*_{12}(1)$, $D^*_{12}(2)-D^*_{12}(1)$ are smaller than the uncertainties in the individual coefficients (3.62) and (3.64), owing to a strong positive correlation between the first and the second Sonine approximation integrands. Similarly, in order to determine the effect of the higher order approximations a higher precision can be obtained by calculating the differences $\lambda^*_{12}(N)-\lambda^*_{12}(N-1)$, $\eta^*_{12}(N)-\eta^*_{12}(N-1)$, $D^*_{12}(N)-D^*_{12}(N-1)$ directly.

We have computed these differences up to the third Sonine approximation (N=3) for η^*_{12} and D^*_{12} and up to the fourth Sonine approximation (N=4) for λ^*_{12}. The results were obtained by the 11-dimensional Monte Carlo procedure using a computer program called Subroutine OVLP11; the results are presented in Table iv. Again each quantity was determined from four independent runs of Subroutine OVLP11. For the thermal conductivity quantities each of the four runs used 100,000 random points in the 11-dimensional unit cube and required 22 minutes of c.p.u. time or 17 minutes of core time. For the other quantities, each of the four runs used 30,000 random points in the 11-dimensional unit cube and required about 11 minutes of c.p.u. time or 9 minutes of core time. The values obtained simultaneously for the individual matrix elements $a^{so}_{k\ell}$, $b^{so}_{k\ell}$, $c^{so}_{k\ell}$ are presented in Table v.

For the collision integrals that determine the first and second Sonine approximations to λ^*_{12}, η^*_{12}, D^*_{12} we can make a comparison between the numerical estimates obtained with the 7-dimensional and 11-dimensional Monte Carlo procedures. Such a comparison is presented in Table vi; it turns out that the results of the two different integration procedures are in excellent agreement. Considering the relative complexities of the 7-dimensional and the 11-dimensional integrals we judge the 11-dimensional approach to be the more appropriate computational scheme for determining the higher order Sonine approximations.

Another consistency check on our calculations is provided by the symmetry relations (3.15)

$$a^{so}_{k\ell} = a^{so}_{\ell k}, \quad b^{so}_{k\ell} = b^{so}_{\ell k}, \quad c^{so}_{k\ell} = c^{so}_{\ell k}. \tag{3.65}$$

Our programs deliberately avoided assuming these relations. Thus the fact that all the relations (3.65) are held in Tables ii and v to within the calculated uncertainties constitutes another check of the consistency of these computations.

The data in Tables i and iv enable us to determine the rate of convergence of the Sonine expansion (3.41) for the contributions λ_{12}^*, η_{12}^*, D_{12}^* from the single-overlap collisions. The results are summarized in Table IX. It turns out that the rate of convergence, in particular for the thermal conductivity, is lower than the rate of convergence of the corresponding expansion (2.13) for the transport coefficients λ_0, η_0, D_0 from the linearized Boltzmann equation. In order to determine the coefficients λ_0, η_0, D_0 to within one percent it is sufficient to terminate the expansion (2.13) after the second Sonine approximation. However, if one wants to determine the coefficients λ_{12}^*, η_{12}^*, D_{12}^* to within one percent, it is necessary to evaluate $\eta_{12}^*(N)$ $D_{12}^*(N)$ up to the third Sonine approximation, and $\lambda_{12}^*(N)$ up to the fourth Sonine approximation. Note that all higher order Sonine approximations have the effect of reducing the difference with the value unity estimated by the theory of Enskog.

An independent attempt to evaluate the effect of the overlap collisions on the first density correction to the transport properties was made by Condiff and coworkers [16,17]. For this purpose, they evaluated a contribution to the transport coefficients classified as λ_{EVD}^*, η_{EVD}^* and D_{EVD}^*. The abbreviation "EVD" indicates that these terms incorporate excluded volume as well as dynamical effects. However, as pointed out in Part I [3], the EVD term of Condiff et al. does not account for all

Table IX

Rate of Convergence of Sonine Expansion for the Single-Overlap Contributions.

	Absolute value [a]	Percentage [b]
$\lambda^*_{12}(1)$	-0.0303±0.0003	100
$\lambda^*_{12}(2)-\lambda^*_{12}(1)$	+0.0055±0.0001	-18
$\lambda^*_{12}(3)-\lambda^*_{12}(2)$	+0.0014±0.0001	-5
$\lambda^*_{12}(4)-\lambda^*_{12}(3)$	+0.00035±0.00003	-1
$\eta^*_{12}(1)$	-0.0633±0.0004	100
$\eta^*_{12}(2)-\eta^*_{12}(1)$	+0.0012±0.0001	-2
$\eta^*_{12}(3)-\eta^*_{12}(2)$	+0.00038±0.00006	-0.6
$D^*_{12}(1)$	-0.1195±0.0005	100
$D^*_{12}(2)-D^*_{12}(1)$	+0.0035±0.0001	-3
$D^*_{12}(3)-D^*_{12}(2)$	+0.0011±0.0001	-0.9

[a] Uncertainties represent two standard deviations.

[b] Change in going from the N^{th} to the $(N+1)^{th}$ Sonine approximation in percentage of the value for N=1.

single-overlap contributions; it includes the SS-collisions and SN-collisions in Fig. 3 but does not incorporate the NS-collision sequence. Thus Condiff et al. did not evaluate the full collision integrals $\{\psi,\chi\}_2^{(3)}$ and $\{\psi,\chi\}_2^{\tilde{(3)}}$ defined in (2.25) but considered instead

$$\begin{aligned} \{\psi,\chi\}_{EVD}^{(3)} &\equiv \{\psi,\chi\}_{SS}^{(3)} + \{\psi,\chi\}_{SN}^{(3)} \quad , \\ \{\psi,\chi\}_{EVD}^{\tilde{(3)}} &\equiv \{\psi,\chi\}_{SS}^{\tilde{(3)}} + \{\psi,\chi\}_{SN}^{\tilde{(3)}} \quad . \end{aligned} \tag{3.66}$$

[The additional collision integral corresponding to the NS-collision sequence was incorporated by Condiff et al. in a term called TC1 as discussed in AEDC-TR-72-142 [3]] . On comparing (3.66) with (2.26) and (3.1) we see that the EVD contributions may be calculated by our computational procedure provided that we replace $\Theta(\tau-\tau')$ by zero for all values of τ and τ'.

We have thus calculated the coefficients λ_{EVD}^*, η_{EVD}^* and D_{EVD}^* up to the second Sonine approximation using again our subroutine OVRLAP. The results are presented in Table vii. Each run involved 100,000 points in the 7-dimensional unit cube and required about 20 minutes of c.p.u. time or 11 minutes core time. Condiff et al. have evaluated the coefficients $\lambda_{EVD}^*(1)$, $\eta_{EVD}^*(1)$ and $D_{EVD}^*(1)$ in the first Sonine approximation. Since they did not include the quantity $\Theta(\tau-\tau')$ in (3.1) they were able to evaluate their results as 3-dimensional integrals using a Gaussian-Legendre numerical technique. Thus a comparison of our values for $\lambda_{EVD}^*(1)$, $\eta_{EVD}^*(1)$ and $D_{EVD}^*(1)$ with those obtained by Condiff et al. yields another consistency check of our Monte Carlo procedure. The results obtained for λ_{EVD}^*, η_{EVD}^* and D_{EVD}^* by the two investigations are

summarized in Table X. The numerical estimates for the first Sonine approximations are in excellent agreement. In addition, our program enables us to determine the effect of the higher order Sonine approximations to the coefficients λ^*_{EVD}, η^*_{EVD} and D^*_{EVD}. It appears that the rate of convergence of the Sonine expansion for the EVD terms is the same as that for the total contribution from the single-overlap collisions, shown in Table IX; the second Sonine approximation $\lambda^*_{EVD}(2)$, $\eta^*_{EVD}(2)$, $D^*_{EVD}(2)$ again modify the first approximation by 18%, 2% and 3%, respectively.

Table X

EVD Integrals

	7-dimensional Monte Carlo [a]	Condiff et al. [16,17]
$\lambda^*_{EVD}(1)$	-0.0261±0.0004	-0.026228±0.000001
$\lambda^*_{EVD}(2)-\lambda^*_{EVD}(1)$	+0.0046±0.0001	
$\eta^*_{EVD}(1)$	-0.0527±0.0004	-0.052707±0.000001
$\eta^*_{EVD}(2)-\eta^*_{EVD}(1)$	+0.0011±0.0001	
$D^*_{EVD}(1)$	-0.0947±0.0004	-0.09442±0.00002
$D^*_{EVD}(2)-D^*_{EVD}(1)$	+0.0032±0.0001	

[a] Uncertainties represent two standard deviations.

Chapter IV

SEQUENCES OF THREE SUCCESSIVE COLLISIONS

4.1 Introduction

In order to determine the contribution of sequences of three successive collisions (μ=3) we need to consider the collision integrals (2.30)

$$\{\psi,\chi\}_3^{(3)} = \sum_{\nu=1}^{3} \{\psi,\chi\}_{3\nu}^{(3)} ,$$
$$\{\psi,\chi\}_3^{(\tilde{3})} = \sum_{\nu=1}^{3} \{\psi,\chi\}_{3\nu}^{(\tilde{3})} , \qquad (4.1)$$

where $\{\psi,\chi\}_{3\nu}^{(3)}$ and $\{\psi,\chi\}_{3\nu}^{(\tilde{3})}$ are defined in (2.31). It is again convenient to introduce a notation that covers both the collision integrals $\{\psi,\chi\}_3^{(3)}$ and $\{\psi,\chi\}_3^{(\tilde{3})}$. For this purpose we define in analogy to (3.3)

$$(\alpha,\beta)_{3\nu} = (-1)^{\nu-1} \frac{3\sqrt{2}}{10\pi^6} \int_{\Omega_{3\nu}} d\Omega\, e^{-(W_1^2+W_2^2+W_3^2)}$$
$$* \{\alpha(I)-\alpha(II)\} * \{\beta(IV_\nu)-\beta(III_\nu)\} , \qquad (4.2)$$

where the Roman numerals refer to the velocity regions in the diagrams of Fig. 7.

A more detailed representation of these collision sequences is given in Fig. 12. The velocities $\vec{W}_i=\vec{W}_i(II)$ are the velocities *after* the first collision. The collision vector of the first collision is indicated by $\hat{k}_1$ and that of the second collision by $\hat{k}_2$. The integrand is completely specified by the variables $\vec{W}_1$, $\vec{W}_2$, $\vec{W}_3$, $\hat{k}_1$, $\hat{k}_2$ and the time τ between the

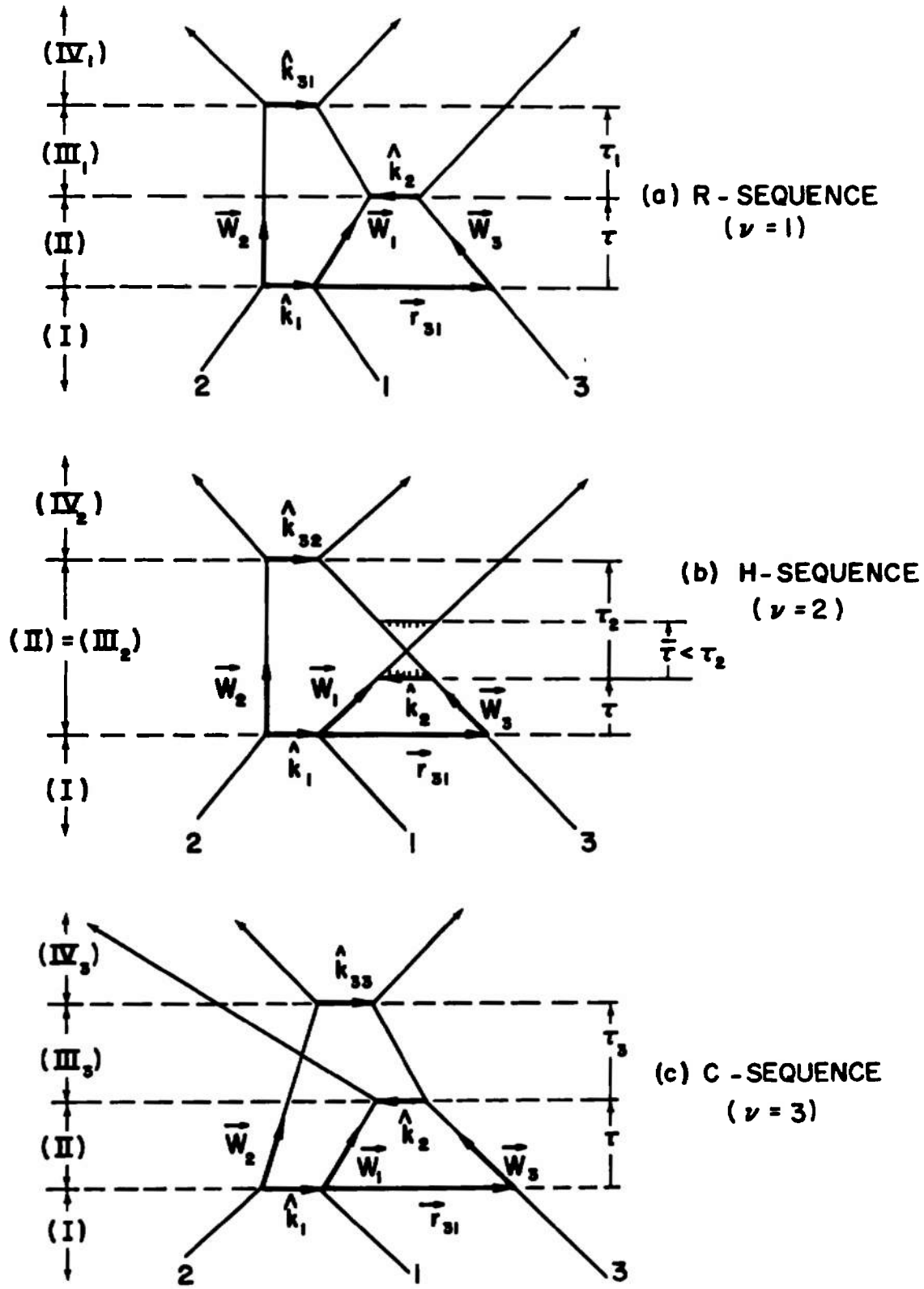

Figure 12. Diagrams associated with $\{\psi,\chi\}_3^{(3)}$ and $\{\psi,\chi\}_3^{\tilde{(3)}}$.

first and the second collision. The initial velocities $\vec{W}_i(I)$ are given by

$$\begin{aligned} \vec{W}_1(I) &= \vec{W}_1+\vec{W}_{21}\cdot\hat{k}_1\hat{k}_1 \quad , \\ \vec{W}_2(I) &= \vec{W}_2-\vec{W}_{21}\cdot\hat{k}_1\hat{k}_1 \quad , \\ \vec{W}_3(I) &= \vec{W}_3 \quad . \end{aligned} \tag{4.3}$$

The formulae for the velocities $\vec{W}_i(III)$ and $\vec{W}_i(IV)$ in regions III and IV, and also the formulae for the collision vector $\hat{k}_3$ of the third collision and the time τ_ν between the second and third collisions, depend upon whether we consider the R(ν=1), H(ν=2) or C(ν=3) diagrams. We thus write $\vec{W}_i(III_\nu)$, $\vec{W}_i(IV_\nu)$, $\hat{k}_{3\nu}$ and τ_ν to distinguish these quantities for the different diagrams, as indicated in Fig. 12. The velocities $\vec{W}_i(III_\nu)$ and $\vec{W}_i(IV_\nu)$ are given by

$$(\nu=1)\begin{cases} \vec{W}_1(III_1) = \vec{W}_1+\vec{W}_{31}\cdot\hat{k}_2\hat{k}_2 \\ \vec{W}_2(III_1) = \vec{W}_2 \\ \vec{W}_3(III_1) = \vec{W}_3-\vec{W}_{31}\cdot\hat{k}_2\hat{k}_2 \end{cases} \tag{4.4}$$

$$\begin{cases} \vec{W}_1(IV_1) = \vec{W}_1(III_1)+\vec{W}_{21}(III_1)\cdot\hat{k}_{31}\hat{k}_{31} \\ \vec{W}_2(IV_1) = \vec{W}_2(III_1)-\vec{W}_{21}(III_1)\cdot\hat{k}_{31}\hat{k}_{31} \\ \vec{W}_3(IV_1) = \vec{W}_3(III_1) \end{cases} \tag{4.5}$$

$$(\nu=2)\begin{cases}\vec{W}_1(III_2) = \vec{W}_1 \\ \vec{W}_2(III_2) = \vec{W}_2 \\ \vec{W}_3(III_2) = \vec{W}_3 \end{cases} \tag{4.6}$$

$$(\nu=2)\begin{cases}\vec{W}_1(IV_2) = \vec{W}_1 \\ \vec{W}_2(IV_2) = \vec{W}_2+\vec{W}_{32}\cdot\hat{k}_{32}\hat{k}_{32} \\ \vec{W}_3(IV_2) = \vec{W}_3-\vec{W}_{32}\cdot\hat{k}_{32}\hat{k}_{32} \end{cases} \tag{4.7}$$

$$(\nu=3)\begin{cases}\vec{W}_1(III_3) = \vec{W}_1+\vec{W}_{31}\cdot\hat{k}_2\hat{k}_2 \\ \vec{W}_2(III_3) = \vec{W}_2 \\ \vec{W}_3(III_3) = \vec{W}_3-\vec{W}_{31}\cdot\hat{k}_2\hat{k}_2 \end{cases} \tag{4.8}$$

$$(\nu=3)\begin{cases}\vec{W}_1(IV_3) = \vec{W}_1(III_3) \\ \vec{W}_2(IV_3) = \vec{W}_2(III_3)+\vec{W}_{32}(III_3)\cdot\hat{k}_{33}\hat{k}_{33} \\ \vec{W}_3(IV_3) = \vec{W}_3(III_3)-\vec{W}_{32}(III_3)\cdot\hat{k}_{33}\hat{k}_{33} \end{cases} \tag{4.9}$$

In terms of the definition (4.2) we may rewrite the collision integrals (4.1) as

$$\{\psi,\chi\}^{(3)}_{3\nu} = (\Psi,X)_{3\nu} \quad . \tag{4.10}$$

where $\Psi=\sum_{m=1}^{3}\psi_m$ and $X=\sum_{n=1}^{3}\chi_n$ as in (2.42), and

$$\{\psi,\chi\}^{(\tilde{3})}_{3\nu} = 2\sum_{n=1}^{3}(\psi_n,\chi_n)_{3\nu} \quad . \tag{4.11}$$

From Fig. 12 we note that, for $\nu=2$ and $\nu=3$, only particle 2 participates in *both* the first and the third collisions; hence, for $\nu=2$ and $\nu=3$ only the term n=2 contributes to (4.11). However, for $\nu=1$, particles 1 and 2 participate in the first and third collisions; hence, for this diagram the two terms n=1 and n=2 contribute to (4.11). The collision integrals (4.11) for the self-diffusion thus reduce to

$$\{\psi,\chi\}^{(3)}_{3\nu} = 2(\psi_2,\chi_2)_{3\nu} + 2\delta_{1,\nu}(\psi_1,\chi_1)_{3\nu}, \tag{4.12}$$

where $\delta_{1,\nu}$ is the Kronecker delta.

In determining the effects of three and four successive collisions on the transport coefficients λ_1, η_1, D_1 we shall consider only the first Sonine approximation N=1 in (2,21). The consequences of this limitation will be discussed in Section 6.1. We thus consider the collision integrals

$$\begin{aligned}
\lambda^*_{13}(1) &= \sum_{\nu=1}^{3} \lambda^*_{13\nu}(1) \quad , \\
\eta^*_{13}(1) &= \sum_{\nu=1}^{3} \eta^*_{13\nu}(1) \quad , \\
D^*_{13}(1) &= \sum_{\nu=1}^{3} D^*_{13\nu}(1) \quad .
\end{aligned} \tag{4.13}$$

where

$$\begin{aligned}
\lambda^*_{13\nu}(1) &= -\left[\sum_{m=1}^{3} S^{(1)}_{3/2}(W_m^2)\vec{W}_m, \sum_{n=1}^{3} S^{(1)}_{3/2}(W_n^2)\vec{W}_n\right]_{3\nu} , \\
\eta^*_{13\nu}(1) &= -\left[\sum_{m=1}^{3} S^{(0)}_{5/2}(W_m^2)\vec{W}_m\circ\vec{W}_m, \sum_{n=1}^{3} S^{(0)}_{5/2}(W_n^2)\vec{W}_n\circ\vec{W}_n\right]_{3\nu} ,
\end{aligned} \tag{4.14}$$

$$D^{*}_{13\nu}(1)=-2\left[S^{(0)}_{3/2}(W_2^2)\vec{W}_2,\ S^{(0)}_{3/2}(W_2^2)\vec{W}_2\right]_{3\nu}$$
$$-2\delta_{1,\nu}\left[S^{(0)}_{3/2}(W_1^2)\vec{W}_1, S^{(0)}_{3/2}(W_1^2)\vec{W}_1\right]_{3\nu} \quad . \qquad \text{(4.14 cont.)}$$

In these expressions we may insert the explicit forms of the Sonine polynomials (see Table I). Using the fact that $\sum_n \vec{W}_n$ and $\sum_n W_n^2$ do not change in a collision, the collision integrals (4.14) reduce to

$$\lambda^{*}_{13\nu}(1)= -\left[\sum_{m=1}^{3}\vec{W}_m W_m^2, \sum_{n=1}^{3}\vec{W}_n W_n^2\right]_{3\nu} \quad ,$$
$$\eta^{*}_{13\nu}(1)= -\left[\sum_{m=1}^{3}\vec{W}_m\vec{W}_m, \sum_{n=1}^{3}\vec{W}_n\vec{W}_n\right]_{3\nu} \quad , \qquad (4.15)$$
$$D^{*}_{13\nu}(1)= -\ 2[1+\delta_{1,\nu}]\left[\vec{W}_2,\vec{W}_2\right]_{3\nu} \quad .$$

In the last equation for the self-diffusion coefficient $D^{*}_{13\nu}(1)$ we have made use of the fact that

$$\{\vec{W}_1(I)-\vec{W}_1(II)\}\cdot\{\vec{W}_1(IV_1)-\vec{W}_1(III)_1)\}$$
$$=\{\vec{W}_2(I)-\vec{W}_2(II)\}\cdot\{\vec{W}_2(IV_1)-\vec{W}_2(III_1)\} \quad ,$$

as follows immediately from (4.3) and (4.5).

In order to evaluate the collision integrals (4.15) we shall proceed as follows. In Sections 4.2 and 4.3 we shall develop a uniform approach for the three different collision sequences (R, H and C). We shall thus formulate a method in which the R-, H-, and C-collision integrals are computed simultaneously. In addition we shall develop in Section 4.4 a different procedure especially designed for the R-collision integrals. This additional special method will be presented for the following two reasons.

First, by comparing the results of the two calculation procedures for the R-collision integrals we shall obtain a strong consistency check on our computation methods. Secondly, this special method for the R-collision integrals will form the basis of our analysis of the collision integrals associated with sequences of four collisions to be discussed in Chapter V. The results for the collision integrals associated with three successive collisions will be presented in Section 4.5.

4.2 Analysis of R-, H- and C-Collision Sequences

The collision integrals (4.15) are all defined in terms of the integral form (4.2). Using (2.40) we thus consider

$$(\alpha,\beta)_{3\nu} = (-1)^{\nu-1}\frac{3\sqrt{2}}{10\pi^6}\int_{\Omega_{3\nu}} d\vec{W}_0 d\vec{W}_{21} d\vec{W}_{31} d\hat{k}_1 d\hat{k}_2 d\tau |\vec{W}_{21}\cdot\hat{k}_1||\vec{W}_{31}\cdot\hat{k}_2|$$

$$\times\ e^{-3W_0^2}\ e^{-E\{\alpha(I)-\alpha(II)\}}*\{\beta(IV_\nu)-\beta(III_\nu)\}, \quad (4.16)$$

where the velocities $\vec{W}_0$, $\vec{W}_{21}$ and $\vec{W}_{31}$ are defined in (2.36). The velocity $\vec{W}_0$ is the same in all velocity regions between collisions. The expressions for the relative velocities in the various regions follow from (4.3)-(4.9).

The formulae (4.5), (4.7) and (4.9) for the region IV_ν velocities naturally involve (and assume the existence of) the third collision vectors $\hat{k}_{3\nu}$. To obtain the formulae for $\hat{k}_{3\nu}$, and the times τ_ν between the second and third collisions, we proceed as follows. First, denoting by $\vec{\rho}_{ij}$ the position

vector of i relative to j at the instant of the *second* collision (with collision vector $\hat{k}_2$), it will be seen from Fig. 12 that, for any of the ν-diagrams,

$$\vec{\rho}_{21} = -\hat{k}_1+\vec{W}_{21}\tau \ ,$$
$$\vec{\rho}_{32} = \hat{k}_{12}-\vec{W}_{21}\tau \ , \tag{4.17}$$

where

$$\vec{k}_{12} \equiv \hat{k}_1-\hat{k}_2 \ . \tag{4.18}$$

In terms of these relative position vectors $\vec{\rho}_{ij}$ at the second collision, it is seen from Fig. 12 that the *third* collision vectors $\hat{k}_{3\nu}$ are given by

$$\hat{k}_{31} = -\vec{\rho}_{21}-\vec{W}_{21}(III_1)\tau_1 \ , \tag{4.19a}$$
$$\hat{k}_{32} = \vec{\rho}_{32}+\vec{W}_{32}(III_2)\tau_2 \ , \tag{4.19b}$$
$$\hat{k}_{33} = \vec{\rho}_{32}+\vec{W}_{32}(III_3)\tau_3 \ . \tag{4.19c}$$

where the corresponding times τ_ν between the second and third collisions are obtained as the smaller (earlier) solutions of the quadratic equations

$$|\vec{\rho}_{21}+\vec{W}_{21}(III_1)\tau_1|^2=1 \ ,$$
$$|\vec{\rho}_{32}+\vec{W}_{32}(III_2)\tau_2|^2=1 \ , \tag{4.20}$$
$$|\vec{\rho}_{32}+\vec{W}_{32}(III_3)\tau_3|^2=1 \ .$$

(The equations (4.20) which determine τ_ν are just the requirements $|\hat{k}_{3\nu}|^2=1$.) In summary, the third collision vectors $\hat{k}_{3\nu}$ are obtained from the integrating variables $\vec{W}_{21}$, $\vec{W}_{31}$, $\hat{k}_1$, $\hat{k}_2$ and τ in the following way: First, the vectors $\vec{\rho}_{21}$ and $\vec{\rho}_{32}$ are calculated according to (4.17);

next, the region III_ν velocities are calculated according to (4.4), (4.6) and (4.8); then the times τ_ν are calculated by solving eqs. (4.20); and finally, the vectors $\hat{k}_{3\nu}$ are obtained from eqs. (4.19).

One other dynamical quantity of interest in Fig. 12 is the time $\bar{\tau}$ between the 1-3 penetrating and separating collisions in the H-diagram. Since the position vector of 3 relative to 1 at a time t after the penetrating collision is evidently $-\hat{k}_2 + \vec{W}_{31}t$, then $\bar{\tau}$ is obtained simply by solving the equation

$$|-\hat{k}_2+\vec{W}_{31}\bar{\tau}|^2=1 \quad .$$

Expanding, and discarding the solution $\bar{\tau}=0$ (which corresponds to the penetrating rather than the separating collision), we obtain

$$\bar{\tau} = \frac{2\hat{W}_{31}\cdot\hat{k}_2}{W_{31}} \quad . \tag{4.21}$$

In order to evaluate (4.16) we adopt the coordinate system shown in Fig. 13. This is the rest frame of 1 between the first and second collisions (the figure shows the centers of 1, 2 and 3 at the moment of the first collision), with $\vec{W}_{21}$ defining the Z-axis and $\hat{k}_1$ defining the XZ-plane. We have just seen how all the dynamical quantities in each ν-diagram can be calculated from the "basic" variables $\vec{W}_{21}$, $\vec{W}_{31}$, $\hat{k}_1$, $\hat{k}_2$, τ. In the frame shown in Fig. 13, the basic vectors have the representations:†

$$\hat{W}_{21} = \begin{pmatrix} 0 \\ 0 \\ 1 \end{pmatrix} , \tag{4.22a}$$

† The angle θ_1 in this chapter is the same angle as θ in the preceding chapter.

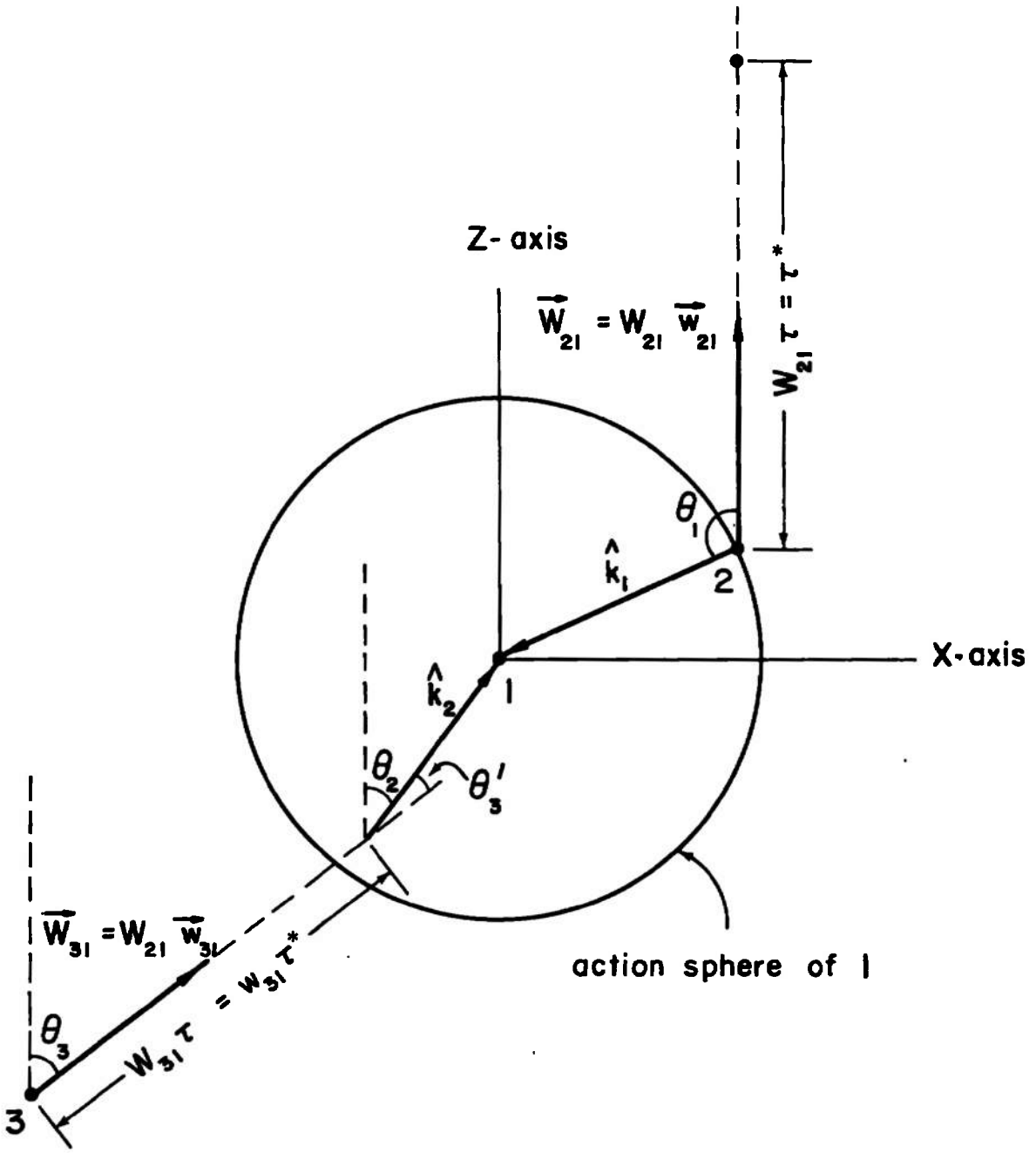

Figure 13. Schematic representation of the integration variables used in the calculations of the μ=3 (R,C, and H) integrals. The figure shows the rest frame of 1 *just after* the first collision, with $\hat{W}_{21}$ in the Z-direction and $\hat{k}_1$ in the XZ-plane.

$$\hat{k}_1 = \begin{pmatrix} -\sin\theta_1 \\ 0 \\ \cos\theta_1 \end{pmatrix} , \tag{4.22b}$$

$$\hat{k}_2 = \begin{pmatrix} \sin\theta_2\cos\phi_2 \\ \sin\theta_2\sin\phi_2 \\ \cos\theta_2 \end{pmatrix} , \tag{4.22c}$$

$$\hat{W}_{31} = \begin{pmatrix} \sin\theta_3\cos(\phi_2+\phi_3) \\ \sin\theta_3\sin(\phi_2+\phi_3) \\ \cos\theta_3 \end{pmatrix} . \tag{4.22d}$$

Note from (4.22d) that the azimuthal angle ϕ_3 of $\hat{W}_{31}$ is defined relative to an initial plane through $\hat{k}_2$ and the Z-axis (thus, when $\phi_3=0$ the vectors $\hat{W}_{31}$, $\hat{W}_{21}$ and $\hat{k}_2$ are coplanar). The reason for doing this will become apparent later. With the angles θ_1, θ_2, θ_3, ϕ_2, ϕ_3 thus defined, and with the angular integrations on $\vec{W}_{21}$ and the azimuthal integration on $\hat{k}_1$ having been trivially carried out in accordance with (2.41), (4.16) becomes

$$(\alpha,\beta)_{3\nu} = (-1)^{\nu-1}\,\frac{12\sqrt{2}}{5\pi^4}\iiint_{\infty} d^3\vec{W}_0\; e^{-3W_0^2}\int_0^{\infty} dW_{21}W_{21}^2\int_{-1}^{0} d\cos\theta_1$$

$$\times\int_0^{\pi} d\theta_2\sin\theta_2\int_0^{2\pi} d\phi_2\int_0^{\infty} dW_{31}W_{31}^2\int_0^{\pi} d\theta_3\sin\theta_3\int_0^{2\pi} d\phi_3\int_0^{\infty} d\tau \tag{4.23}$$

$$\times\,\Theta_{3\nu}|\vec{W}_{21}\cdot\hat{k}_1||\vec{W}_{31}\cdot\hat{k}_2|\,e^{-E\{\alpha(I)-\alpha(II)\}*\{\beta(IV_\nu)-\beta(III_\nu)\}} .$$

Here, the quantity $\Theta_{3\nu}$ is defined to be unity whenever the integrating variables are such that the ν-diagram collision sequence can be realized, and zero otherwise.

Note from Fig. 13 that

$$\begin{aligned} \vec{W}_{21}\cdot\hat{k}_1 &= W_{21}\cos\theta_1 \ , \\ \vec{W}_{31}\cdot\hat{k}_2 &= W_{31}\cos\theta_3' \ , \end{aligned} \tag{4.24}$$

where θ_3' is defined to be the angle between $\vec{W}_{31}$ and $\hat{k}_2$, and is given in terms of the integrating variables by the formula

$$\cos\theta_3' = \cos\theta_2\cos\theta_3+\sin\theta_2\sin\theta_3\cos\phi_3 \ , \tag{4.25}$$

as may be seen by calculating $\hat{W}_{31}\cdot\hat{k}_2$ from (4.22c) and (4.22d). Now, it is clear from Fig. 13 that the only condition imposed by the first collision is

$$\cos\theta_1 < 0 \ , \tag{4.26a}$$

and that the only condition imposed by the second collision [other than the condition $\tau>0$, which has already been taken care of in (4.23)] is

$$\cos\theta_3' > 0 \ . \tag{4.26b}$$

Hence, (4.23) can be written

$$\begin{aligned} (\alpha,\beta)_{3\nu} = (-1)^{\nu}\,\frac{12\sqrt{2}}{5\pi^4}\int_{\infty}\!\!\int\!\!\int\!\!\int d^3\vec{W}_0 e^{-3W_0^2}\int_0^{\infty} dW_{21}W_{21}^3\int_0^{\infty} dW_{31}W_{31}^3\int_0^{\infty} d\tau \\ \times\int_{-1}^{0} d\cos\theta_1\int_0^{\pi} d\theta_2\int_0^{\pi} d\theta_3\int_0^{2\pi} d\phi_2\int_0^{2\pi} d\phi_3\ \Theta(\cos\theta_3') \\ \times\ \Theta_{3\nu}\ \sin\theta_2\sin\theta_3\cos\theta_1\cos\theta_3''\ e^{-E\{\alpha(I)-\alpha(II)\}*\{\beta(IV_\nu)-\beta(III_\nu)\}} \ , \end{aligned} \tag{4.27}$$

where *now* $\Theta_{3\nu}$=1 or 0 according to whether the integrating variables do or do not permit the third collision to occur. That is, Θ_ν now concerns *only the third collision* in diagram ν, since the first and second collisions are now assured through the limits of integration on $\cos\theta_1$ and τ and the theta function on $\cos\theta'_3$. [For the H diagram only, Θ_2 must *also* require $\tau_2 > \overline{\tau}$.]

We next impose upon (4.27) a change of variables $(W_{31},\tau)\rightarrow(w_{31},\tau^*)$, according to

$$\left.\begin{aligned} w_{31} &= W_{31}/W_{21} \\ \tau^* &= W_{21}\tau \end{aligned}\right\} \quad . \tag{4.28}$$

This transformation is evidently such that $dW_{31}d\tau = dw_{31}d\tau^*$, and is made in anticipation of a later analytical integration over the variable W_{21}. In essence, this transformation induces a scaling of the velocities in all regions, henceforth denoted by a *lower case* w, and a scaling of all times between collisions, henceforth denoted by an *asterisk*. We shall also use a *prime* to denote velocity region III for the R- and C-diagrams; note from (4.4) and (4.8) that the velocities in region III for the R- and C-diagrams bear indeed the same relationships to the integration variables. The region III velocities for the H-diagram are simply the (unprimed) region II velocities, as shown in (4.6). We now rewrite the relative velocities in the various regions as follows. With

$$\left.\begin{aligned} \vec{w}_{21} &\equiv \vec{W}_{21}/W_{21} = \hat{W}_{21} \\ \vec{w}_{31} &\equiv \vec{W}_{31}/W_{21} = w_{31}\hat{W}_{31} \end{aligned}\right\} \quad , \tag{4.29}$$

$$\left.\begin{aligned} \vec{w}'_{21} &\equiv \vec{w}_{21} - \vec{w}_{31}\cdot\hat{k}_2\hat{k}_2 \\ \vec{w}'_{31} &\equiv \vec{w}_{31} - 2\vec{w}_{31}\cdot\hat{k}_2\hat{k}_2 \end{aligned}\right\} , \tag{4.30}$$

the scaled velocities in the various regions of the R-, C- and H-diagrams are:

$$\left.\begin{aligned} \vec{w}_{21}(II) &\equiv \vec{W}_{21}(II)/W_{21} = \vec{w}_{21} \\ \vec{w}_{31}(II) &\equiv \vec{W}_{31}(II)/W_{21} = \vec{w}_{31} \end{aligned}\right\} , \tag{4.31}$$

$$\left.\begin{aligned} \vec{w}_{21}(I) &\equiv \vec{W}_{21}(I)/W_{21} = \vec{w}_{21} - 2\vec{w}_{21}\cdot\hat{k}_1\hat{k}_1 \\ \vec{w}_{31}(I) &\equiv \vec{W}_{31}(I)/W_{21} = \vec{w}_{31} - \vec{w}_{21}\cdot\hat{k}_1\hat{k}_1 \end{aligned}\right\} , \tag{4.32}$$

$(\nu=1)$

$$\left.\begin{aligned} \vec{w}_{21}(III_1) &\equiv \vec{W}_{21}(III_1)/W_{21} = \vec{w}'_{21} \\ \vec{w}_{31}(III_1) &\equiv \vec{W}_{31}(III_1)/W_{21} = \vec{w}'_{31} \end{aligned}\right\} , \tag{4.33}$$

$$\left.\begin{aligned} \vec{w}_{21}(IV_1) &\equiv \vec{W}_{21}(IV_1)/W_{21} = \vec{w}'_{21} - 2\vec{w}'_{21}\cdot\hat{k}_{31}\hat{k}_{31} \\ \vec{w}_{31}(IV_1) &\equiv \vec{W}_{31}(IV_1)/W_{21} = \vec{w}'_{31} - \vec{w}'_{21}\cdot\hat{k}_{31}\hat{k}_{31} \end{aligned}\right\} , \tag{4.34}$$

$(\nu=2)$

$$\left.\begin{aligned} \vec{w}_{21}(III_2) &\equiv \vec{W}_{21}(III_2)/W_{21} = \vec{w}_{21} \\ \vec{w}_{31}(III_2) &\equiv \vec{W}_{31}(III_2)/W_{21} = \vec{w}_{31} \end{aligned}\right\} , \tag{4.35}$$

$$\left.\begin{aligned} \vec{w}_{21}(IV_2) &\equiv \vec{W}_{21}(IV_2)/W_{21} = \vec{w}_{21} + \vec{w}_{32}\cdot\hat{k}_{32}\hat{k}_{32} \\ \vec{w}_{31}(IV_2) &\equiv \vec{W}_{31}(IV_2)/W_{21} = \vec{w}_{31} - \vec{w}_{32}\cdot\hat{k}_{32}\hat{k}_{32} \end{aligned}\right\} , \tag{4.36}$$

$$(\nu=3)\begin{cases} \vec{w}_{21}(III_3) \equiv \vec{W}_{21}(III_3)/W_{21} = \vec{w}'_{21} \\ \vec{w}_{31}(III_3) \equiv \vec{W}_{31}(III_3)/W_{21} = \vec{w}'_{31} \end{cases}, \tag{4.37}$$

$$\begin{cases} \vec{w}_{21}(IV_3) \equiv \vec{W}_{21}(IV_3)/W_{21} = \vec{w}'_{21} + \vec{w}'_{32}\cdot\hat{k}_{33}\hat{k}_{33} \\ \vec{w}_{31}(IV_3) \equiv \vec{W}_{31}(IV_3)/W_{21} = \vec{w}'_{31} - \vec{w}'_{32}\cdot\hat{k}_{33}\hat{k}_{33} \end{cases}. \tag{4.38}$$

In (4.36) $\vec{w}_{32}=\vec{w}_{31}-\vec{w}_{21}$ and in (4.38) $\vec{w}'_{32}=\vec{w}'_{31}-\vec{w}'_{21}$. The relative positions (4.17) at the instant of the second collision may be written

$$\begin{aligned} \vec{\rho}_{21} &= -\hat{k}_1+\vec{w}_{21}\tau^* \quad , \\ \vec{\rho}_{32} &= \vec{k}_{12}-\vec{w}_{21}\tau^* \quad , \end{aligned} \tag{4.39}$$

where $\hat{k}_{12}$ is defined in (4.18). The third collision vectors $\hat{k}_{3\nu}$ are given by [see (4.19)]

$$\begin{aligned} \hat{k}_{31} &= -\vec{\rho}_{21}-\vec{w}'_{21}\tau_1^* \quad , \\ \hat{k}_{32} &= \vec{\rho}_{32}+\vec{w}_{32}\tau_2^* \quad , \\ \hat{k}_{33} &= \vec{\rho}_{32}+\vec{w}'_{32}\tau_3^* \quad , \end{aligned} \tag{4.40}$$

where the scaled times τ_ν^* between the second and third collisions are the (earlier) solutions of the quadratic equations [see (4.20)]

$$\begin{aligned} |\vec{\rho}_{21} + \vec{w}'_{21}\tau_1^*|^2=1 \quad , \\ |\vec{\rho}_{32} + \vec{w}_{32}\tau_2^*|^2=1 \quad , \\ |\vec{\rho}_{32} + \vec{w}'_{32}\tau_3^*|^2=1 \quad . \end{aligned} \tag{4.41}$$

And finally, the scaled time between the penetrating and separating collisions in the H-diagram is seen from (4.21) to be

$$\bar{\tau}^* \equiv w_{21}\bar{\tau} = \frac{2\hat{w}_{31}\cdot\hat{k}_2}{w_{31}} \quad . \tag{4.42}$$

After the scaling transformation (4.28) the integral (4.27) becomes

$$(\alpha,\beta)_{3\nu} = (-1)^{\nu}\frac{12\sqrt{2}}{5\pi^4}\iiint_{\infty} d^3\vec{w}_0 e^{-3w_0^2}\int_0^{\infty} dw_{21} w_{21}^6 e^{-w_{21}^2 E^*}\int_0^{\infty} dw_{31} w_{31}^3\int_0^{\infty} d\tau^*$$

$$\times \int_{-1}^{0} d\cos\theta_1 \int_0^{\pi} d\theta_2 \int_0^{\pi} d\theta_3 \int_0^{2\pi} d\phi_2 \int_0^{2\pi} d\phi_3 \; \Theta(\cos\theta_3')\Theta_{3\nu}$$

$$\times \sin\theta_2 \sin\theta_3 \cos\theta_1 \cos\theta_3' \{\alpha(\mathrm{I})-\alpha(\mathrm{II})\}^*\{\beta(\mathrm{IV}_\nu)-\beta(\mathrm{III}_\nu)\} \; , \tag{4.43}$$

where we have defined a "scaled E" [see (2.39) and note from (4.29) that $w_{21}^2 = 1$]:

$$E^* \equiv \frac{2}{3}(1+w_{31}^2-\vec{w}_{21}\cdot\vec{w}_{31}) \; . \tag{4.44}$$

The $\vec{w}_0$ and w_{21} integrations in (4.43) will eventually be performed analytically. The remaining 7-dimensional integral will be evaluated by Monte Carlo methods, but for this it will be necessary to first get rid of the infinite integration limits on the two variables w_{31} and τ^*. The variable w_{31} can be handled similarly to the variable w in the single overlap calculation [see (3.33)]. However, the variable τ^* presents a more serious problem, the solution of which is very intimately connected with the behavior of the quantities $\Theta_{3\nu}$, i.e., with the conditions imposed

by the existence of the third collisions. We shall now consider this matter in detail.

According to the diagrams in Fig. 12, the third collisions are all interacting. Thus, a first requirement for the existence of the third collision is that the colliding particles be separated (non-overlapping) at the instant of the *second* collision. Hence, we require

$$\left.\begin{array}{ll} |\vec{\rho}_{21}|^2 > 1 & \text{for } \nu=1 \\ |\vec{\rho}_{32}|^2 > 1 & \text{for } \nu=2 \text{ and } 3 \end{array}\right\} . \tag{4.45}$$

Given that the particles involved in the third collision are not overlapping at the instant of the second collision, it remains only to require that $\hat{k}_{3\nu}$ exist, i.e., that $\hat{k}_{3\nu}$ be calculable as a real vector from (4.40). For this, it is necessary and sufficient that the corresponding quadratic equation in (4.41) yield for τ^*_ν a *real* , *positive* number. Each of these quadratic equations is evidently of the form

$$|\vec{\rho} + \vec{w}\tau^*_\nu|^2=1 ,$$

where $\rho^2>1$ because of (4.45). It is straightforward to show that, given $\rho^2>1$, a real, positive solution τ^*_ν exists if and only if

$$\left.\begin{array}{l} \vec{w}\cdot\vec{\rho}<0 \\ (\vec{w}\times\vec{\rho})^2-w^2<0 \end{array}\right\} \quad \text{and} .$$

Therefore, the necessary and sufficient conditions for the third collisions to occur are as follows:

$$R(\nu=1) \quad \begin{cases} \rho_{21}^2 > 1 \ , \\ \vec{w}'_{21} \cdot \vec{\rho}_{21} < 0 \ , \\ (\vec{w}'_{21} \times \vec{\rho}_{21})^2 - w'^2_{21} < 0 \ , \end{cases} \tag{4.46}$$

$$H(\nu=2) \quad \begin{cases} \rho_{32}^2 > 1 \ , \\ \vec{w}_{32} \cdot \vec{\rho}_{32} < 0 \ , \\ (\vec{w}_{32} \times \vec{\rho}_{32})^2 - w_{32}^2 < 0 \ , \end{cases} \tag{4.47}$$

$$C(\nu=3) \quad \begin{cases} \rho_{32}^2 > 1 \ , \\ \vec{w}'_{32} \cdot \vec{\rho}_{32} < 0 \ , \\ (\vec{w}'_{32} \times \vec{\rho}_{32})^2 - w'^2_{32} < 0 \ . \end{cases} \tag{4.48}$$

When these conditions are satisfied, eqs. (4.41) will have two positive roots (as expected), and we must evidently take τ_ν^* to be the smaller root:

$$\begin{aligned} \tau_1^* &= \left[-\vec{w}'_{21} \cdot \vec{\rho}_{21} - \sqrt{(\vec{w}'_{21} \cdot \vec{\rho}_{21})^2 - w'^2_{21}(\rho_{21}^2 - 1)} \right] \Big/ w'^2_{21} \ , \\ \tau_2^* &= \left[-\vec{w}_{32} \cdot \vec{\rho}_{32} - \sqrt{(\vec{w}_{32} \cdot \vec{\rho}_{32})^2 - w_{32}^2(\rho_{32}^2 - 1)} \right] \Big/ w_{32}^2 \ , \\ \tau_3^* &= \left[-\vec{w}'_{32} \cdot \vec{\rho}_{32} - \sqrt{(\vec{w}'_{32} \cdot \vec{\rho}_{32})^2 - w'^2_{32}(\rho_{32}^2 - 1)} \right] \Big/ w'^2_{32} \ . \end{aligned} \tag{4.49}$$

The corresponding vectors $\hat{k}_{3\nu}$ are then obtained from (4.40), (4.39). and (4.49).

For a given ν, $\Theta_{3\nu}$ will be unity if all three inequalities in (4.46), (4.47) or (4.48) are satisfied [and, for ν=2, if the condition $\tau_2^* > \bar{\tau}^*$ is also satisfied]; otherwise, $\Theta_{3\nu}$ will be zero. Now, in order to resolve

the problem of the infinite range on τ^* in (4.43), it is necessary to express the conditions (4.46)-(4.48) directly in terms of τ^*, and to then analyze them into *new* conditions which yield expressions for *upper limits* on τ^*.

The τ^* dependence in (4.46)-(4.48) enters via the quantities $\vec{\rho}_{21}$ and $\vec{\rho}_{32}$ in (4.39). Substituting (4.39) into (4.46)-(4.48) we find after some algebra (note $\vec{w}_{21} \equiv \hat{w}_{21}$):

$$(\nu=1)\begin{cases} \tau^{*2} - 2\tau^* (\hat{w}_{21} \cdot \hat{k}_1) > 0 \quad , & (4.50a) \\ \tau^* (\hat{w}'_{21} \cdot \hat{w}_{21}) < \hat{w}'_{21} \cdot \hat{k}_1 \quad , & (4.50b) \\ A_1 \tau^{*2} - 2B_1 \tau^* - C_1 < 0 \quad , & (4.50c) \end{cases}$$

$$(\nu=2,3)\begin{cases} \tau^{*2} - 2\tau^* (\hat{w}_{21} \cdot \vec{k}_{12}) - (1-k_{12}^2) > 0 \quad , & (4.51a) \\ \tau^* F_\nu > G_\nu \quad , & (4.51b) \\ A_\nu \tau^{*2} - 2B_\nu \tau^* - C_\nu < 0 \quad , & (4.51c) \end{cases}$$

where A_ν, B_ν, C_ν, F_ν, G_ν are defined by

$$\left.\begin{aligned} A_1 &\equiv (\hat{w}'_{21} \times \hat{w}_{21})^2 \\ B_1 &\equiv (\hat{w}'_{21} \times \hat{w}_{21}) \cdot (\hat{w}'_{21} \times \hat{k}_1) \\ C_1 &\equiv (\hat{w}'_{21} \cdot \hat{k}_1)^2 \end{aligned}\right\} \quad , \qquad (4.52)$$

$$\left.\begin{aligned} A_2 &\equiv (\hat{w}_{32}\times\hat{w}_{21})^2 \\ B_2 &\equiv (\hat{w}_{32}\times\hat{w}_{21})\cdot(\hat{w}_{32}\times\vec{k}_{12}) \\ C_2 &\equiv (\hat{w}_{32}\cdot\vec{k}_{12})^2+(1-k_{12}^2) \\ F_2 &\equiv \hat{w}_{32}\cdot\hat{w}_{21} \\ G_2 &\equiv \hat{w}_{32}\cdot\vec{k}_{12} \end{aligned}\right\} , \tag{4.53}$$

$$\left.\begin{aligned} A_3 &\equiv (\hat{w}'_{32}\times\hat{w}_{21})^2 \\ B_3 &\equiv (\hat{w}'_{32}\times\hat{w}_{21})\cdot(\hat{w}'_{32}\times\vec{k}_{12}) \\ C_3 &\equiv (\hat{w}'_{32}\cdot\vec{k}_{12})^2+(1-k_{12}^2) \\ F_3 &\equiv \hat{w}'_{32}\cdot\hat{w}_{21} \\ G_3 &\equiv \hat{w}'_{32}\cdot\vec{k}_{21} \end{aligned}\right\} . \tag{4.54}$$

The third conditions, (4.50c) and (4.51c), evidently require that a certain quadratic form in τ^* be negative; it will be convenient to denote the roots of these quadratic forms (when they exist) by t_ν^+ and t_ν^-:

$$t_\nu^\pm \equiv \left[B_\nu \pm \sqrt{B_\nu^2+A_\nu C_\nu}\right]\Big/A_\nu . \tag{4.55}$$

The requirements (4.50) for the R-diagram are somewhat simpler than the requirements (4.51) for the H and C diagrams, and will be considered first. Since $\hat{w}_{21}\cdot\hat{k}_1=\cos\theta_1$, then because $\cos\theta_1<0$ in (4.43) it is seen that requirement (4.50a) is *always* satisfied.

Furthermore, using the conditions $\hat{w}_{21}\cdot\hat{k}_1<0$, $\hat{w}_{31}\cdot\hat{k}_2>0$ and $\tau^*>0$, the remaining two requirements (4.50b) and (4.50c) may be shown to be equivalent with

$$(\nu=1)\begin{cases} \hat{k}_1\cdot\hat{k}_2<0 & , \quad (4.56a) \\ \hat{w}_{31}\cdot\hat{k}_2 > (\hat{w}_{21}\cdot\hat{k}_1)/(\hat{k}_1\cdot\hat{k}_2) & , \quad (4.56b) \\ 0<\tau^*<t_1^+ & . \quad (4.56c) \end{cases}$$

The conditions (4.56a) and (4.56b) were first noted by Weinstock [18]. Since (4.56a) and (4.56b) do not involve conditions on τ^*, then (4.56c) implies that the infinite upper limit on the τ^* integration in (4.43) can be replaced by t_1^+, as defined by (4.55) and (4.52):

$$\nu=1: \quad \int_0^{\infty} d\tau^* \rightarrow \int_0^{t_1^+} d\tau^* \quad .$$

With requirement (4.56c) thus met, the quantity Θ_{31} is then 1 or 0 according to whether the two requirements (4.56a) and (4.56b) are or are not both satisfied.

We turn now to the more difficult task of analyzing the requirements (4.51) for the H- and C-diagrams. Here we find that it is not possible to obtain a single condition on τ^* analogous to (4.56c); instead all three inequalities will provide conditions on τ^*, as well as requirements independent of τ^*.

Consider first (4.51a), which requires that a certain quadratic form in τ^* be positive. Since this quadratic form is concave up, then

if it has no real roots it will indeed always be positive. However, if the roots to the quadratic do exist,

$$t^{\pm} \equiv \hat{w}_{21}\cdot\vec{k}_{12} \pm \sqrt{(\hat{w}_{21}\cdot\vec{k}_{12})^2+(1-k_{12}^2)} \quad , \tag{4.57}$$

then the quadratic form will be positive only if either $\tau^*<t^-$ or $\tau^*>t^+$ An examination of the discriminant of the quadratic form in (4,51a), taking cognizance of the fact that τ^* in any case is restricted to positive values, leads to the following restrictions:

- If $k_{12}^2\leq 1$, then require $\tau^*>t^+$.
- If $k_{12}^2>1$, and $\hat{w}_{21}\cdot\vec{k}_{12}>0$ and $(\hat{w}_{21}\cdot\vec{k}_{12})^2>k_{12}^2-1$, then require either $\tau^*<t^-$ or $\tau^*>t^+$.

(4.58)

Consider next (4.51b). If F_ν and G_ν both have the same sign, then (4.51b) implies that τ^* must be bounded by the quantity

$$t_\nu^\circ \equiv G_\nu/F_\nu \quad (>0) \quad . \tag{4.59}$$

However, the mere fact that τ^* is positive evidently prohibits the combination $F_\nu<0$ and $G_\nu>0$. Thus, (4.51b) leads to the following restrictions:

- If $F_\nu\leq 0$, then require $G_\nu<0$.
- If $F_\nu<0$ and $G_\nu<0$, then require $\tau^*<t_\nu^\circ$.
- If $F_\nu>0$ and $G_\nu>0$, then require $\tau^*>t_\nu^\circ$.

(4.60)

Finally, we consider (4.51c). From (4.53) and (4.54) it is seen that $A_\nu>0$. In the special case $A_\nu=0$, it is seen that we will also have $B_\nu=0$, and (4.51c) reduces to the simple requirement that $C_\nu>0$. In the usual case where $A_\nu>0$, then (4.51c) evidently requires that a certain concave-up quadratic form in τ^* be negative. Thus, the roots $t_\nu^\pm$ [see (4.55)] to this quadratic form *must* exist, and τ^* must lie between them subject to the condition $\tau^*>0$. Therefore, (4.51c) leads to the following restrictions:

- If $A_\nu=0$, then require $C_\nu>0$,
- If $A_\nu\neq0$ and $B_\nu>0$, then require $C_\nu > -B_\nu^2/A_\nu$,
- If $A_\nu\neq0$ and $B_\nu\leq0$, then require $C_\nu>0$,
- If $A_\nu\neq0$ then require $\text{Max}(0,t_\nu^-) < \tau^* < t_\nu^+$.

(4.61)

We see, then, that the existence of the third collision for $\nu=1$ requires only the satisfaction of (4.56), whereas for $\nu=2$ and 3 we must satisfy (4.58), (4.60) and (4.61). Nevertheless, we have derived a set of conditions which determines whether $\Theta_{3\nu}$ is 1 or 0, and which when $\Theta_{3\nu}=1$ provides lower and upper bounds, say $T_\nu^{(1)}$ and $T_\nu^{(2)}$, on τ^*. The requirements for $\Theta_{3\nu}=1$, and the consequent formulae for $T_\nu^{(1)}$ and $T_\nu^{(2)}$, are summarized in Table XI. Again, $\Theta_{3\nu}$ in (4.43) is 1 if all the ν requirements in Table XI are satisfied, and $\Theta_{3\nu}$ is zero otherwise. Furthermore, from the quantities $T_\nu^{(1)}$ and $T_\nu^{(2)}$ found by the prescription in Table XI, the τ^* integration in (4.43) can be dealt with in the following manner:

Table XI

Requirements for $\Theta_{3\nu}=1$ and Formulae for $T_\nu^{(1)}$ and $T_\nu^{(2)}$

ν=1 (R diagram)

Require $\hat{k}_1\cdot\hat{k}_2<0$ and $\vec{w}_{31}\cdot\hat{k}_2>\dfrac{\hat{w}_{21}\cdot\hat{k}_1}{\hat{k}_1\cdot\hat{k}_2}$.

Put $T_1^{(1)}=0$ and $T_1^{(2)}=t_1^+$.

ν=2 and 3 (H- and C-diagrams)

1° If $B_\nu>0$: Require $C_\nu>-B_\nu^2/A_\nu$.

If $B_\nu<0$: Require $C_\nu>0$.

Either way, put $T_\nu^{(1)}=\text{Max}(0,t_\nu^-)$ and $T_\nu^{(2)}=t_\nu^+$.

2° If $F_\nu<0$: Require $G_\nu<0$ and $T_\nu^{(1)}<t_\nu^\circ$,

and reset $T_\nu^{(2)}=\text{Min}(T_\nu^{(2)},t_\nu^\circ)$

If $F_\nu>0$ and $G_\nu>0$: Require $T_\nu^{(2)}>t_\nu^\circ$

and reset $T_\nu^{(1)}=\text{Max}(T_\nu^{(1)},t_\nu^\circ)$.

3° If $k_{12}^2<1$: Require $T_\nu^{(2)}>t^+$,

and reset $T_\nu^{(1)}=\text{Max}(T_\nu^{(1)},t^+)$.

If $k_{12}^2>1$ and $\hat{w}_{21}\cdot\vec{k}_{12}>0$ and $(\hat{w}_{21}\cdot\vec{k}_{12})^2>k_{12}^2-1$, *and*

(i) if $T_\nu^{(1)}>t^-$: Require $T_\nu^{(2)}>t^+$,

and reset $T_\nu^{(1)}=\text{Max}\,(T_\nu^{(1)},t^+)$.

(ii) if $T_\nu^{(1)}<t^-$ and $T_\nu^{(2)}<t^+$: Reset $T_\nu^{(2)}=\text{Min}(T_\nu^{(2)},t^-)$.

(iii) if $T_\nu^{(1)}<t^-$ and $T_\nu^{(2)}>t^+$: With $\tau^*=T_\nu^{(1)}+(T_\nu^{(2)}-T_\nu^{(1)})\tilde{\tau}$

and $0<\tilde{\tau}<1$, require either $\tau^*<t^-$ or $\tau^*>t^+$.

4° For ν=2 only, require $\bar{\tau}^*<\tau_2^*$.

$$\int_0^{\infty} d\tau^* = \int_{T_\nu^{(1)}}^{T_\nu^{(2)}} d\tau^* = \Delta_\nu \int_0^1 d\tilde{\tau} \quad , \tag{4.62}$$

where $$\Delta_\nu \equiv T_\nu^{(2)} - T_\nu^{(1)} \quad , \tag{4.63}$$

and $$\tau^* = T_\nu^{(1)} + \Delta_\nu \tilde{\tau} \quad , \tag{4.64}$$

It is important to notice here that a given value of the variable $\tilde{\tau}$ produces *different* values of τ^* for ν=1,2 and 3; in other words, the transformation $\tilde{\tau} \to \tau^*$ is different for each ν

In terms of this new variable $\tilde{\tau}$, (4.43) can be written

$$(\alpha,\beta)_{3\nu} = (-1)^\nu \frac{12\sqrt{2}}{5\pi^4} \iiint_{\infty} d^3\vec{W}_0 e^{-3W_0^2} \int_0^{\infty} dW_{21} W_{21}^6 e^{-W_{21}^2 E^*} \int_0^{\infty} dw_{31} w_{31}^3 \int_0^1 d\tilde{\tau}$$

$$\times \int_{-1}^{0} d\cos\theta_1 \int_0^{\pi} d\theta_2 \int_0^{\pi} d\theta_3 \int_0^{2\pi} d\phi_2 \int_0^{2\pi} d\phi_3 \; \Theta(\cos\theta_3') \; \Theta_{3\nu} \cos\theta_1 \tag{4.65}$$

$$\times \Delta_\nu \sin\theta_2 \sin\theta_3 \cos\theta_3' \; \{\alpha(\mathrm{I}) - \alpha(\mathrm{II})\} * \{\beta(\mathrm{IV}_\nu) - \beta(\mathrm{III}_\nu)\} \quad ,$$

where $\Theta_{3\nu}$ and Δ_ν are determined from Table XI with the quantities A_ν, B_ν, C_ν, F_ν, G_ν, $t_\nu^{\pm}$, $t^{\pm}$, t_ν° defined through (4.52)-(4.55), (4.57), (4.59).

In transforming from τ^* to $\tilde{\tau}$ in (4.62) we transformed a possibly infinite range $(T_\nu^{(1)}, T_\nu^{(2)})$ into the finite range (0,1), which of course was our intention. However, in so doing we introduced a possibly infinite

factor $T_\nu^{(2)} - T_\nu^{(1)} = \Delta_\nu$ into the integrand. We must therefore investigate to see if any divergences $\Delta_\nu \to \infty$ are adequately controlled by approaches to zero of other factors in the integrand of (4.65). This problem was analyzed earlier in AEDC-TR-69-68 [4,7].

To begin with, we note from Table XI that t_ν^+ is *always* an upper bound for Δ_ν. For $\nu=1$ we have $\Delta_\nu = t_\nu^+$; however, for $\nu=2$ and 3, Δ_ν may be less than t_ν^+, not only because $T_\nu^{(1)}$ may be positive, but also because $T_\nu^{(2)}$ may be determined not by t_ν^+ but rather by t_ν° or t^- [see Table XI]. But in any case, we should first investigate when and how $t_\nu^+ \to \infty$, since this will give us a definite bound on the behavior of Δ_ν.

t_ν^+ is defined in (4.55), and from the definitions of the quantities A_ν, B_ν, C_ν in (4.52)-(4.54), it is clear that the numerator in (4.55) is strictly finite, so that the only way for t_ν^+ to become infinite is for A_ν to vanish. Furthermore, as each B_ν is proportional to $\sqrt{A_\nu}$, it is clear that the divergences in t_ν^+ are of the type

$$\lim_{A_\nu \to 0} t_\nu^+ \propto A_\nu^{-1/2} \quad .$$

From the definitions of A_1, A_2, A_3 in (4.52)-(4.54) one calculates

$$A_1^{-1/2} = \frac{\left[w_{31}^2 \cos^2\theta_3' - 2w_{31}\cos\theta_3'\cos\theta_2 + 1\right]^{1/2}}{w_{31}\cos\theta_3'\sin\theta_2} \quad , \tag{4.66a}$$

$$A_2^{-1/2} = \frac{\left[w_{31}^2 - 2w_{31}\cos\theta_3 + 1\right]^{1/2}}{w_{31}\sin\theta_3} \quad , \tag{4.66b}$$

$$A_3^{-1/2} = \frac{\left[w_{31}^2 \sin^2\theta_3' + 2w_{31}(\cos\theta_2\cos\theta_3' - \cos\theta_3) + 1\right]^{1/2}}{w_{31}\left[\sin^2\theta_3 + \sin\theta_2\cos\theta_3'(\sin\theta_2\cos\theta_3' - 2\sin\theta_3\cos\phi_3)\right]^{1/2}} \quad . \tag{4.66c}$$

From (4.66a) we see that Δ_1 can become infinite only if $\cos\theta_3'$ or $\sin\theta_2$ vanish, in which cases Δ_1 diverges like $(\cos\theta_3'\sin\theta_2)^{-1}$; however, since the integrand in (4.65) contains Δ_1 multiplied by $(\cos\theta_3'\sin\theta_2)$, then the integrand will always be bounded. [This need for $\sin\theta_2$ is the reason why we write $\sin\theta_2 d\theta_2$ instead of $d\cos\theta_2$ in (4.65).]

From (4.66b) we see that Δ_2 can become infinite only if $\sin\theta_3$ vanishes, in which case Δ_2 may diverge like $(\sin\theta_3)^{-1}$; however, since the integrand in (4.65) contains Δ_2 multiplied by $(\sin\theta_3)$, then the integrand will always be bounded. [This need for $\sin\theta_3$ is the reason why we write $\sin\theta_3 d\theta_3$ instead of $d\cos\theta_3$ in (4.65).]

The situation for Δ_3 is more complicated. A detailed analysis of the denominator of $A_3^{-1/2}$ in (4.66c) yields the following conclusions: In varying circumstances this denominator can go to zero like either $\sin\theta_3$ or $(\sin\theta_2\cos\theta_3')$; in either case the integrand in (4.65) clearly remains bounded. The only other way in which the denominator in (4.66c) can approach zero, with Δ_3 determined by the diverging t_3^+ and *not* by t_3° or $t^\pm$, is in the *double limit* $\theta_2 \to \pi/2$ and $\phi_3 \to 0$; in this case it is found that the denominator in (4.66c) approaches zero like $\left[(\frac{\pi}{2}-\theta_2)^2\cos^2\theta_3+\phi_3^2\sin^2\theta_3\right]^{1/2}$. Thus

$$\lim_{\substack{\theta_2\to\pi/2\\ \phi_3\to 0}} \Delta_3 \propto \lim_{\substack{\theta_2\to\pi/2\\ \phi_3\to 0}} \left[(\tfrac{\pi}{2}-\theta_2)^2\cos^2\theta_3 + \phi_3^2\sin^2\theta_3\right]^{-1/2} . \tag{4.67}$$

In this case only will the integrand in (4.65) become unbounded.

To eliminate this divergence for the C-diagram, we transform variables $(\theta_2,\phi_3) \to (r,x)$ by

$$\left.\begin{aligned} r\cos x &= \pi - 2\theta_2 \\ r\sin x &= \phi_3/2 \end{aligned}\right\} . \tag{4.68}$$

Under this transformation,

$$\int_0^{\pi} d\theta_2 \int_0^{2\pi} d\phi_3 = \int_0^{\pi} dx \int_0^{r_0(x)} r\,dr \ , \tag{4.69}$$

where

$$r_0(x) \equiv \text{Min}\left[\frac{\pi}{\sin x}, \frac{\pi}{|\cos x|}\right] . \tag{4.70}$$

The double limit $\theta_2 \to \pi/2$, $\phi_3 \to 0$ is equivalent to the single limit $r \to 0$, so the divergence of the quantity in brackets in (4.65) now has the following character:

$$\lim_{\substack{\theta_2 \to \pi/2 \\ \phi 3 \to 0}} \frac{(\sin\theta_2 \cos\theta_3 \sin\theta_3)\,(d\theta_2 d\phi_3)}{\left[\left(\frac{\pi}{2}-\theta_2\right)^2 \cos^2\theta_3 + \phi_3^2 \sin^2\theta_3\right]^{1/2}} =$$

$$= \lim_{r \to 0} \frac{(\sin^2\theta_3)\,(r\,dr\,dx)}{\left[\frac{1}{4} r^2 \cos^2 x \cos^2\theta_3 + 4r^2 \sin^2 x \sin^2\theta_3\right]^{1/2}} =$$

$$= \frac{\sin^2\theta_3 \; dr\,dx}{\left[\frac{1}{4}\cos^2 x \cos^2\theta_3 + 4\sin^2 x \sin^2\theta_3\right]^{1/2}} \ ,$$

where we have used the fact that $\cos\theta_3' \to \sin\theta_3$ in the indicated limit. Evidently, the denominator can now vanish either if ($x \to \pi/2$, $\theta_3 \to 0$) or if ($x \to 0$, $\theta_3 \to \pi/2$). In the former case the denominator goes to zero like $\sin\theta_3$, which clearly causes no problems; in the latter case it can be shown that, if the C-diagram is dynamically possible at all, then Δ_3 is determined by t^- [which is always bounded] and *not* by t_3^+. In conclusion, the transformation (4.68) indeed removes the divergence of the integrand for $\nu=3$. We remark that the behavior of Δ_3 with respect to ϕ_3 as analyzed above was the reason for measuring ϕ_3 relative to an initial plane through $\hat{k}_2$ and the Z-axis, rather than the XZ-plane of Fig. 13.

It is convenient to introduce a further scaling transformation on the variable r in (4.68) by

$$\tilde{r} = r/r_0(x) \quad , \tag{4.71}$$

The integral (4.65) thus transforms to†

$$(\alpha,\beta)_{3\nu} = (-1)^\nu \frac{12\sqrt{2}}{5\pi^4} \iiint_\infty d^3\vec{W}_0 e^{-3W_0^2} \int_0^\infty dW_{21} W_{21}^6 e^{-W_{21}^2 E^*} \int_0^\infty dW_{31} W_{31}^3$$

$$\times \int_0^1 d\tilde{\tau} \int_{-1}^0 d\cos\theta_1 \int_0^\pi d\theta_3 \int_0^{2\pi} d\phi_2 \int_0^\pi dx \int_0^{\dot{1}} d\tilde{r}\ \Theta(\cos\theta_3')\ \Theta_{3\nu}\ \cos\theta_1 \tag{4.72}$$

$$\times \left[\Delta_\nu \tilde{r}\ r_0^2(x) \sin\theta_2 \cos\theta_3' \sin\theta_3\right] \{\alpha(I)-\alpha(II)\} * \{\beta(IV_\nu)-\beta(III_\nu)\} \cdot$$

† The variable r is the same as the variable ρ in ref. [4,7]. There is a misprint in these references: In eq. (2.7-24) of ref.[4] and in eq. (8.24) of ref.[7] ρ_{max} should read ρ_{max}^2.

Here E^* is given by (4.44), $\theta_{3\nu}$ and Δ_ν are determined through Table XI, $r_0(x)$ is given by (4.70), and the angles θ_2 and ϕ_3 are *now* defined in terms of $\tilde{r}$ and x by

$$\left.\begin{aligned} \theta_2 &\equiv \tfrac{1}{2}[\pi - \tilde{r}\, r_0(x)\cos x] \\ \phi_3 &\equiv 2\tilde{r}\, r_0(x)\sin x \end{aligned}\right\} . \tag{4.73}$$

4.3 Parallel Evaluation of R-, H- and C-Integrals

The collision integrals to be considered are given by (4.15) in terms of the 11-dimensional integral form (4.72). We can reduce this integral to a 7-dimensional integral, just as the 11-dimensional SO-integral (3.14) was reduced to the 7-dimensional SO-integral (3.24). That is, we integrate analytically over $\vec{W}_0$ and W_{21}. Then the collision integrals (4.15) reduce to integrals that are closely analogous to (3.25), (3.26) and (3.27).

$$\lambda^*_{13\nu}(1) = -3(\vec{L}_1,\vec{L}_1)_{3\nu} - \frac{99}{4}(\vec{K}_1,\vec{K}_1)_{3\nu} , \tag{4.74}$$

$$\eta^*_{13\nu}(1) = -\frac{9}{2}(\vec{L}_1,\vec{L}_1)_{3\nu} , \tag{4.75}$$

$$D^*_{13\nu}(1) = -2[1+\delta_{1,\nu}](\vec{w}_{20},\vec{w}_{20})_{3\nu} , \tag{4.76}$$

where $\vec{K}_1$ and $\vec{L}_1$ are again the functions defined in (3.30a) and (3.30c):

$$\vec{K}_1 \equiv E^{*-1} \sum_{i=1}^{3} \vec{w}_{io} w_{io}^2 \quad , \tag{4.77a}$$

$$\vec{\vec{L}}_1 \equiv E^{*-1/2} \sum_{i=1}^{3} \vec{w}_{io} \vec{w}_{io} \quad , \tag{4.77b}$$

with

$$\left.\begin{aligned} \vec{w}_{10}(i) &= -\tfrac{1}{3}[\vec{w}_{21}(i)+\vec{w}_{31}(i)] \\ \vec{w}_{20}(i) &\equiv -\tfrac{1}{3}[\vec{w}_{31}(i)-2\vec{w}_{21}(i)] \\ \vec{w}_{30}(i) &\equiv -\tfrac{1}{3}[\vec{w}_{21}(i)-2\vec{w}_{31}(i)] \end{aligned}\right\} \quad (i=I,II,III_\nu,IV_\nu) \quad , \tag{4.78}$$

and where now

$$(\alpha,\alpha)_{3\nu} = (-1)^\nu \frac{7\sqrt{6}}{8\pi^2} \int_0^\infty dw_{31} w_{31}^3 \int_0^1 d\tilde{\tau} \int_{-1}^{0} d\cos\theta_1 \int_0^\pi d\theta_3 \int_0^{2\pi} d\phi_2 \int_0^\pi dx \int_0^1 d\tilde{r}$$

$$\times\ \Theta(\cos\theta_3') \Theta_{3\nu} \cos^2\theta_1 d_\nu E^{*-9/2} \tag{4.79}$$

$$\times\ [\Delta_\nu r_0^2(x) \tilde{r} \sin\theta_2 \cos\theta_3' \sin\theta_3] \{\alpha(I)-\alpha(II)\}' * \{\alpha(IV_\nu)-\alpha(III_\nu)\}' \quad .$$

In this equation we have introduced *primed* differences $\{\alpha(I)-\alpha(II)\}'$ and $\{\alpha(IV_\nu)-\alpha(III_\nu)\}'$ which are defined in analogy to (3.12), as

$$\{\alpha(I)-\alpha(II)\}' \equiv \{\alpha(I)-\alpha(II)\}/\vec{w}_{21} \cdot \hat{k}_1 \quad , \tag{4.80a}$$

$$\{\alpha(IV_\nu)-\alpha(III_\nu)\}' \equiv \{\alpha(IV_\nu)-\alpha(III_\nu)\}/d_\nu \quad , \tag{4.80b}$$

where

$$d_\nu \equiv \begin{cases} \vec{w}'_{21}\cdot\hat{k}_{31} & \text{for } \nu=1 \ , \\ \vec{w}_{32}\cdot\hat{k}_{32} & \text{for } \nu=2 \ , \\ \vec{w}'_{32}\cdot\hat{k}_{33} & \text{for } \nu=3 \ . \end{cases} \tag{4.81}$$

This is done in recognition of the fact, that for the functions α that appear in (4.74)-(4.76), $\alpha(I)-\alpha(II)$ is proportional to $\vec{w}_{21}\cdot\hat{k}_1$ and $\alpha(IV_\nu)-\alpha(III_\nu)$ is proportional to d_ν. The primed differences (4.80) can be calculated explicitly in terms of the velocities $\vec{w}_{ij}$ and $\vec{w}'_{ij}$ [see (4.30)] and the collision vectors $\hat{k}_1$ and $\hat{k}_{3\nu}$; the results are presented in Table XII.

The 7-dimensional integrals (4.79) will be evaluated by a Monte Carlo procedure in very much the same way as the evaluation of the 7-dimensional SO-integrals described in Section 3.3. For this purpose we reduce again the w_{31}-integration to a finite interval by the transformation (3.33)†

$$u=(1+w^4)^{-1} \ , \tag{4.82}$$

for which $w_{31}^2 dw_{31}=-\frac{1}{4}du/u^2$. In addition, the form of (4.79) also suggests the transformation

$$\int_{-1}^{0} d\cos\theta_1 \cos^2\theta_1 = \frac{1}{3}\int_{-1}^{0} d\cos^3\theta_1 \ . \tag{4.83}$$

† A review made (at the time of this writing) of the logic leading to (4.82) suggests that for the integrals (4.79) a more suitable choice would have been $u=(1+w^3)^{-1}$.

Table XII

The Quantities $\{\alpha(I)-\alpha(II)\}'$ and $\{\alpha(IV_\nu)-\alpha(III_\nu)\}'$ in the Three-Collision Integrals.

$$\alpha=\frac{1}{2}E^{*1/2}\vec{\vec{L}}_1$$

$$\{\alpha(I)-\alpha(II)\}' = (\vec{w}_{21}\cdot\hat{k}_1)\hat{k}_1\hat{k}_1 - \overline{\overline{\vec{w}_{21}\hat{k}_1}}$$

$$\{\alpha(IV_1)-\alpha(III_1)\}' = (\vec{w}'_{21}\cdot\hat{k}_{31})\hat{k}_{31}\hat{k}_{31} - \overline{\overline{\vec{w}'_{21}\hat{k}_{31}}}$$

$$\{\alpha(IV_2)-\alpha(III_2)\}' = (\vec{w}_{32}\cdot\hat{k}_{32})\hat{k}_{32}\hat{k}_{32} - \overline{\overline{\vec{w}_{32}\hat{k}_{32}}}$$

$$\{\alpha(IV_3)-\alpha(III_3)\}' = (\vec{w}'_{32}\cdot\hat{k}_{33})\hat{k}_{33}\hat{k}_{33} - \overline{\overline{\vec{w}'_{32}\hat{k}_{33}}}$$

$$\alpha=3E^{*}\vec{\vec{K}}_1$$

$$\{\alpha(I)-\alpha(II)\}' = \vec{w}_{21}[2(\vec{w}_{31}\cdot\hat{k}_1)-(\vec{w}_{21}\cdot\hat{k}_1)]$$

$$+ \hat{k}_1[-1+2(\vec{w}_{21}\cdot\vec{w}_{31})-2(\vec{w}_{21}\cdot\hat{k}_1)\{2(\vec{w}_{31}\cdot\hat{k}_1)-(\vec{w}_{21}\cdot\hat{k}_1)\}]$$

$$\{\alpha(IV_1)-\alpha(III_1)\}' = \vec{w}'_{21}[2(\vec{w}'_{31}\cdot\hat{k}_{31})-(\vec{w}'_{21}\cdot\hat{k}_{31})]$$

$$+ \hat{k}_{31}[-\vec{w}'^{2}_{21}+2(\vec{w}'_{21}\cdot\vec{w}'_{31})-2(\vec{w}'_{21}\cdot\hat{k}_{31})\{2(\vec{w}'_{31}\cdot\hat{k}_1)-(\vec{w}'_{21}\cdot\hat{k}_{31})\}]$$

$$\{\alpha(IV_2)-\alpha(III_2)\}' = \vec{w}_{21}[2(\vec{w}_{31}\cdot\hat{k}_{32})-(\vec{w}_{32}\cdot\hat{k}_{32})]$$

$$- \vec{w}_{31}[2(\vec{w}_{21}\cdot\hat{k}_{32})+(\vec{w}_{32}\cdot\hat{k}_{32})]$$

$$+ \hat{k}_{32}[1-\vec{w}^{2}_{31}+2(\vec{w}_{32}\cdot\hat{k}_{32})\{\vec{w}_{31}\cdot\hat{k}_{32}+\vec{w}_{21}\cdot\hat{k}_{32}\}]$$

$$\{\alpha(IV_3)-\alpha(III_3)\}' = \vec{w}'_{21}[2(\vec{w}'_{31}\cdot\hat{k}_{33})-(\vec{w}'_{32}\cdot\hat{k}_{33})]$$

$$- \vec{w}'_{31}[2(\vec{w}'_{21}\cdot\hat{k}_{33})+(\vec{w}'_{32}\cdot\hat{k}_{33})]$$

$$+ \hat{k}_{33}[w'^{2}_{21}-w'^{2}_{31}+2(\vec{w}'_{32}\cdot\hat{k}_{33})\{\vec{w}'_{31}\cdot\hat{k}_{33}+\vec{w}'_{21}\cdot\hat{k}_{33}\}]$$

Table XII (continued)

$\alpha=\bar{w}_{20}$
$\{\alpha(I)-\alpha(II)\}' = -\hat{k}_1$
$\{\alpha(IV_1)-\alpha(III_1)\}' = -\hat{k}_{31}$
$\{\alpha(IV_2)-\alpha(III_2)\}' = +\hat{k}_{32}$
$\{\alpha(IV_3)-\alpha(III_3)\}' = +\hat{k}_{33}$

Note: $\bar{w}_{21} = \hat{w}_{21}$ is a unit vector in accordance with (4.29).

We thus rewrite (4.79) as

$$(\alpha,\alpha)_{3\nu} = (-1)^{\nu}\frac{7}{2^4\pi^2\sqrt{6}}\int_0^{\pi}d\theta_3\int_0^{1}d\tilde{r}\int_0^{\pi}dx\int_{-1}^{0}d\cos^3\theta_1\int_0^{2\pi}d\phi_2\int_0^{1}du\int_0^{1}d\tilde{\tau}$$

$$\times\,\Theta(\cos\theta_3')\Theta_{3\nu}\,\frac{\Delta_\nu d_\nu \tilde{r}r_0^2(x)\sin\theta_2\cos\theta_3'\sin\theta_3}{u^2E^{*9/2}} \tag{4.84}$$

$$\times\,\{\alpha(I)-\alpha(II)\}'*\{\alpha(IV_\nu)-\alpha(III_\nu)\}' \quad ,$$

where it is henceforth understood that w_{31} is given by the inverse of (4.82)

$$w_{31} = \left(\frac{1-u}{u}\right)^{1/4} \quad . \tag{4.85}$$

One final transformation of variables is needed to simplify the Monte Carlo formulae. Namely, we want to transform the 7-dimensional "box", which forms the integrating region in (4.84), into a 7-dimensional "cube". This is easily accomplished by putting

$$\begin{aligned}
\theta_3 &= \pi\eta_1 \quad , \\
\tilde{r} &= \eta_2 \quad , \\
x &= \pi\eta_3 \quad , \\
\cos^3\theta_1 &= (-1+\eta_4) \quad , \\
\phi_2 &= 2\pi\eta_5 \quad , \\
u &= \eta_6, \quad w_{31}=[(1-u)/u]^{1/4} \quad , \\
\tilde{\tau} &= \eta_7 \quad .
\end{aligned} \tag{4.86}$$

Since the Jacobian of this transformation is evidently

$$\frac{\partial(\theta_3,\tilde{r},x,\cos^3\theta_1,\phi_2,u,\tilde{\tau})}{\partial(\eta_1,\eta_2,\ldots,\eta_7)} = 2\pi^3 \quad , \tag{4.87}$$

then we obtain our *final formula* for the integral form $(\alpha,\alpha)_{3\nu}$

$$(\alpha,\alpha)_{3\nu} = (-1)^{\nu}\frac{7\pi}{8\sqrt{6}}\int_0^1 d\eta_1\int_0^1 d\eta_2\ldots\int_0^1 d\eta_7\ \Theta(\cos\theta_3')\ \Theta_{3\nu}$$

$$\times\ \frac{\Delta_\nu d_\nu \tilde{r}r_0^2(x)\sin\theta_2\cos\theta_3'\sin\theta_3}{u^2E^{*9/2}}\{\alpha(I)-\alpha(II)\}'*\{\alpha(IV_\nu)-\alpha(III_\nu)\}' \ . \tag{4.88}$$

Thus, in terms of the integral form (4.88), we can calculate the desired three-collision quantities in (4.13), (4.74), (4.75) and (4.76). The Monte Carlo procedure for numerically evaluating the integral (4.88) is, of course, to average the integrand over a set of points $\{P_i\} = \{(\eta_1^i,\eta_2^i,\ldots,\eta_7^i)\}$ picked from a random, uniform distribution in the 7-dimensional unit cube U_7:

$$(\alpha,\alpha)_{3\nu} = \left\langle (-1)^{\nu}\frac{7\pi}{8\sqrt{6}}\Theta(\cos\theta_3')\Theta_{3\nu}\ \frac{\Delta_\nu d_\nu \tilde{r}r_0^2(x)\sin\theta_2\cos\theta_3'\sin\theta_3}{u^2E^{*9/2}}\right.$$

$$\left.\times\ \{\alpha(I)-\alpha(II)\}'*\{\alpha(IV_\nu)-\alpha(III_\nu)\}'\right\rangle_{U_7} \ . \tag{4.89}$$

The uncertainty in estimating this average with a *finite* set of points $\{P^1,P^2,\ldots,P^M\}$ is given by the r.m.s. deviation of the quantity being averaged, divided by $\sqrt{M}$. Hence, our computational algorithm is:

1° Generate 7 independent random numbers $\mathcal{R}_1,\mathcal{R}_2,\ldots,\mathcal{R}_7$ from a uniform distribution in the unit interval.

2° Calculate the quantities θ_3, $\tilde{r}$, x, θ_1, ϕ_2, u (and w_{31}) and $\tilde{\tau}$ from equation (4.86).

3° Calculate $r_0(x)$ from (4.70), and calculate θ_2 and ϕ_3 from (4.73).

4° Calculate $\cos\theta_3'$ from (4.25), and so evaluate the theta function $\Theta(\cos\theta_3')$.

5° Construct the vectors $\vec{w}_{21}\equiv\hat{w}_{21}$, $\vec{w}_{31}\equiv w_{31}\hat{w}_{31}$, $\hat{k}_1$ and $\hat{k}_2$ from (4.22).

6° Calculate E^* from (4.44).

7° From the velocities $\vec{w}_{21},\vec{w}_{31},\vec{w}_{32}\equiv\vec{w}_{31}-\vec{w}_{21}$, and the collision vector $\hat{k}_2$, calculate the velocities $\vec{w}_{21}',\vec{w}_{31}',\vec{w}_{32}'\equiv\vec{w}_{31}'-\vec{w}_{21}'$ from (4.30). [Not necessary for ν=2.]

8° Calculate the quantities A_ν, B_ν, C_ν, F_ν, G_ν from (4.52)-(4.54), where $\vec{k}_{12}\equiv\hat{k}_1-\hat{k}_2$. Then calculate the quantities $t_\nu^{\pm}$, $t^{\pm}$, t_ν° from (4.55), (4.57), (4.59).

9° Determine $\Theta_{3\nu}$, $T_\nu^{(1)}$ and $T_\nu^{(2)}$ in accordance with the prescription given in Table XI. (For ν=2, defer checking requirement 4° in Table XI until step 11°.)

10° Calculate τ^* from (4.64) and obtain the vectors $\vec{\rho}_{21}$ and $\vec{\rho}_{31}$ defined in (4.39). Note that τ^* depends on the index ν of the diagram. Thus

$$\vec{\rho}_{21} = -\hat{k}_1 + \vec{w}_{21}(T_\nu^{(1)}+\Delta_\nu\tilde{\tau}) \quad , \qquad \vec{\rho}_{32} = \vec{k}_{12} - \vec{w}_{21}(T_\nu^{(1)}+\Delta_\nu\tilde{\tau}) \quad , \tag{4.90}$$

are different for the three diagrams! Next, calculate τ_ν^* from (4.49) and then the collision vectors $\hat{k}_{3\nu}$ from (4.40). Finally, calculate the quantities d_ν from (4.81).

11° For ν=2, calculate $\bar{\tau}^*$ from (4.42) and check requirement 4° in Table XI.

12° Calculate the primed differences (4.80) as given in Table XII.

13° Using the values found in the preceding steps, evaluate the required quantities in angular brackets in (4.89) and also the squares of these quantities (for computing the variances), and add these to respective cumulating sums.

14° Return to 1° and repeat for as many times M as is practical. Then convert the sums to averages, and so obtain Monte Carlo estimates of the three-collision quantities in (4.74)-(4.76), and (4.13), together with the uncertainties in these estimates.

In order to obtain a correct estimate of the uncertainty in a *sum* of integrals, such as in (4.74) and (4.13), we add the integrands first, rather than the integrals last.

If the $\cos\theta_3'$ test in 4° fails, i.e., if $\Theta(\cos\theta_3')$=0, then all integrands can be set to zero and we may immediately go to 14°. Likewise, if and when

any of the $\theta_{3\nu}$ requirements in Table XI (see steps 9° and 11°) are found *not* to be satisfied, the corresponding ν integrand may be immediately set to zero.

One practical difficulty arises, when the unit vector $\hat{k}_{3\nu}$ is computed as a difference between two possibly very large vectors [see (4.40), and note that the quantities ρ_{ij} and τ_ν^* can become very large]. Among the precautions taken to circumvent this problem was the use of the double-precision computation mode on the Univac 1108 for all calculations of dynamical quantities. In addition, we found it advantageous to first calculate the impact vectors $\vec{b}_{3\nu}$

$$\begin{aligned} \vec{b}_{31} &= -\vec{\rho}_{21} + \hat{w}'_{21}(\hat{w}'_{21}\cdot\vec{\rho}_{21}) \quad , \\ \vec{b}_{32} &= \vec{\rho}_{32} - \hat{w}_{32}(\hat{w}_{32}\cdot\vec{\rho}_{32}) \quad , \\ \vec{b}_{33} &= \vec{\rho}_{32} - \hat{w}'_{32}(\hat{w}'_{32}\cdot\vec{\rho}_{32}) \quad , \end{aligned} \tag{4.91}$$

and then calculate the collision vectors $\hat{k}_{3\nu}$ from

$$\begin{aligned} \hat{k}_{31} &= \vec{b}_{31} + \hat{w}'_{21}\sqrt{1-b_{31}^2} \quad , \\ \hat{k}_{32} &= \vec{b}_{32} - \hat{w}_{32}\sqrt{1-b_{32}^2} \quad , \\ \hat{k}_{33} &= \vec{b}_{33} - \hat{w}'_{32}\sqrt{1-b_{33}^2} \quad , \end{aligned} \tag{4.92}$$

instead of from (4.40).

As was done with the single-overlap calculations, an empirically-determined "importance sampling" procedure was used to decrease the uncertainties in the Monte Carlo calculations. For the record, the following importance sampling distributions were used [cf. (3.43) and the discussion thereof]:

$$P_1(\eta_1) \propto \exp(-3\eta_1) \quad , \quad , \tag{4.93a}$$

$$P_2(\eta_2) \propto \exp[-2(1-\eta_2)] \quad , \quad , \tag{4.93b}$$

$$P_4(\eta_4) \propto \exp[-1.5(1-\eta_4)] \quad , \tag{4.93c}$$

$$P_5(\eta_5) \propto 1+0.6\cos(2\pi\eta_5) \quad , \tag{4.93d}$$

$$P_6(\eta_6) \propto \exp(-3.8\,\eta_1) \quad . \tag{4.93e}$$

We note that (4.93e) produces a sharp bias towards values of u near 1, or w_{31} near 0. The need for such a transformation indicates that the magnitudes of the integrands were becoming large for values of w_{31} near 0 and is quite probably a reflection of the fact that the transformation in (4.82) used the exponent 4 instead of 3[†]. Had we used the exponent 3, the optimum form of P_6 would undoubtedly be different from (4.93e)

The results of these calculations for the R-, H- and C- integrals are presented and discussed in Section 4.5.

For many points in the 7-dimensional unit cube U_7 the conditions for $\Theta_{3\nu}$=1 (i.e. the condition that either/or a R-, H- and C-collision is dynamically possible) are not satisfied and the corresponding integrand will be zero. The fraction of the unit cube where the integrand is non-vanishing is the efficiency ratio. This efficiency ratio depends, of course, on the importance sampling used. For the importance sampling (4.93) the efficiency ratio turns out to be 15% for the R-integrals, 10% for the H-integrals and 5% for the C-integrals.

[†] Cf. footnote on page 129.

4.4 Special Evaluation of R-Integrals

The R-collision sequence is dynamically simpler than the H- and C-collision sequences. It thus lends itself more readily to a treatment in which the efficiency ratio is appreciably larger than the efficiency ratio of 15% connected with the method of the previous section.

We work in the rest frame of particle 2 between the first and third collisions [in this section we need not append the subscript ν to the quantities $\hat{k}_3$, III and IV, since $\nu=1$ is always understood]. We take the center of particle 2 as the origin, $\vec{W}_{12}(II)\equiv\vec{W}_{12}$ in the +Z-direction, and $\hat{k}_1$ in the first quadrant of the YZ-plane. The situation is as shown in Fig. 14. The center of 1 is at point P_{11} at the first collision, moves up to point P_{12} for the second collision, and then comes back to point P_{13} for the third collision. For fixed P_{11} it is seen that, as point P_{12} varies from infinitesimally above P_{11} to infinitely far above P_{11}, the *possible locations for* P_{13} on the action sphere of 2 vary from an infinitesimal neighborhood of P_{11} to the entire +Z-hemisphere; however, in *no* case can P_{13} ever lie in the -Z-hemisphere. The following is also true: For any fixed $\hat{k}_1$ satisfying

$$0 \leq \theta_1 < \pi/2 \quad , \tag{4.94}$$

and for any fixed $\hat{k}_3$ in the +Z-hemisphere, i.e.,

$$\left.\begin{array}{l} 0 < \theta_3 < \pi/2 \\ 0 < \phi_3 < 2\pi \end{array}\right\} \quad , \tag{4.95}$$

it is always possible to find a "critical point" P_c above P_{11} such that $\overline{P_{11}P_{12}}$ must be larger than $\overline{P_{11}P_c}$ in order that a recollision with perihelion

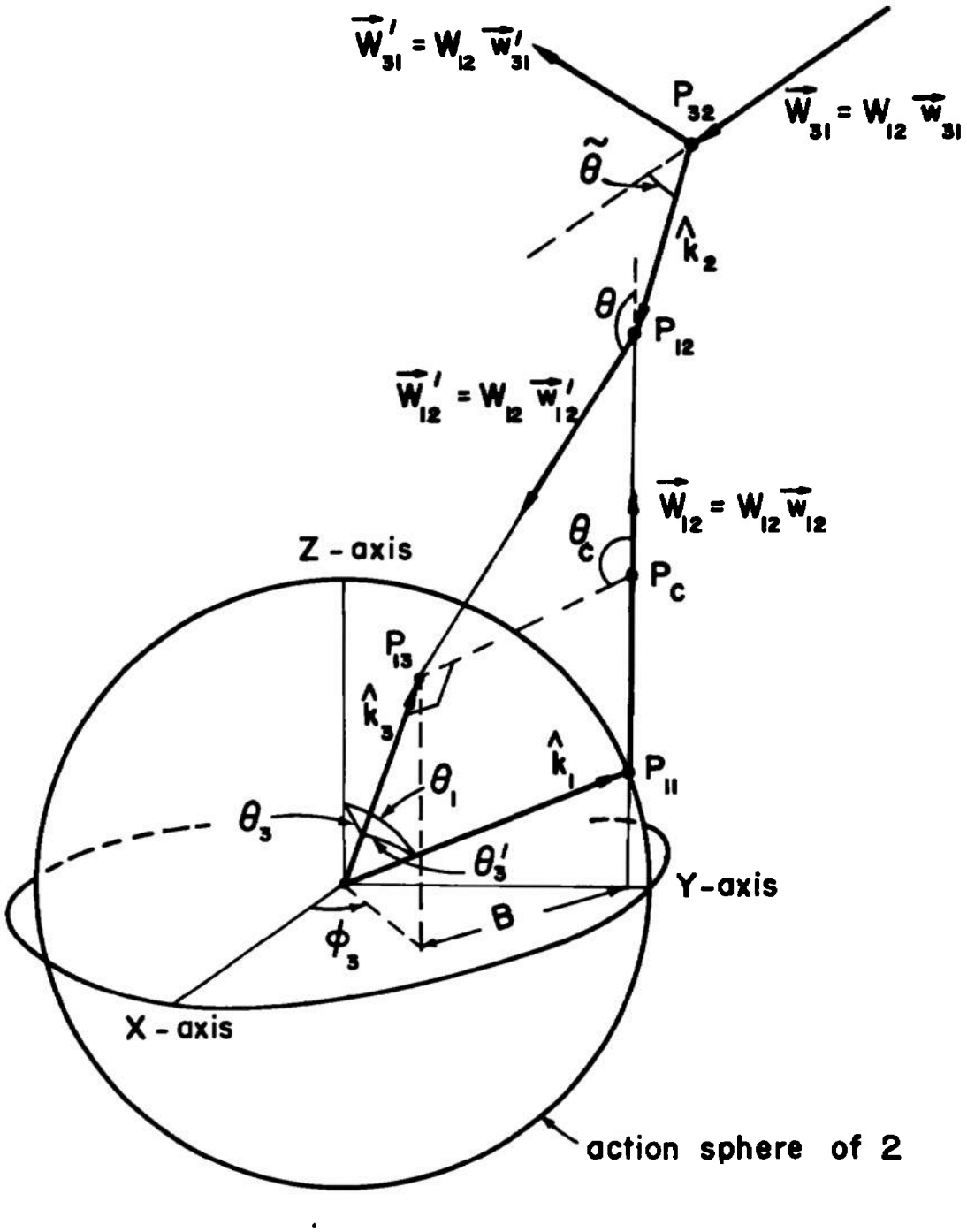

Figure 14. Schematic representation of the integration variables used in the special calculation of the R-integrals. The origin is the center of 2 between the first and third collisions, with $\vec{W}_{12}(II) \equiv \vec{W}_{12}$ in the +Z-direction and $\hat{k}_1$ in the first quadrant of the YZ-plane.

vector $\hat{k}_3$ is possible. The point P_c is in fact the intersection of the line extending from P_{11} in the +Z-direction with the plane tangent to the action sphere of 2 at P_{13} (i.e., the plane through the tip of and perpendicular to $\hat{k}_3$).

Instead of dealing directly with the distances $\overline{P_{11}P_{12}}$ and $\overline{P_{11}P_c}$, both of which can become infinitely large, we consider the velocity of 1 relative to 2 following the second collision, $\vec{W}_{12}(III) \equiv \vec{W}'_{12}$; let θ and ϕ denote, respectively, the polar and azimuthal angles of this vector. For fixed $\hat{k}_1$ and $\hat{k}_3$ satisfying (4.94) and (4.95), it is clear from Fig. 14 that the azimuthal angle ϕ of $\vec{W}'_{12}$ is completely determined, while the condition $\overline{P_{11}P_{12}} > \overline{P_{11}P_c}$ is equivalent to requiring the polar angle θ to be greater than a certain critical angle θ_c, which is also completely determined. A somewhat intricate analysis of the geometry of Fig. 14 reveals that the azimuthal angle ϕ and critical polar angle θ_c of $\vec{W}'_{12}$ are given in terms of the angles θ_1, θ_3, ϕ_3 by the following formulae: For the azimuthal angle we have

$$\left.\begin{aligned} \cos\phi &= \sin\theta_3\cos\phi_3/B \\ \sin\phi &= (\sin\theta_3\sin\phi_3-\sin\theta_1)/B \end{aligned}\right\} , \tag{4.96}$$

where

$$B \equiv [(\sin\theta_3\cos\phi_3)^2 + (\sin\theta_3\sin\phi_3-\sin\theta_1)^2]^{1/2} , \tag{4.97}$$

is the projection of $\overline{P_{12}P_{13}}$ onto the XY-plane, as shown in Fig. 14. For the critical polar angle θ_c we find

$$\cos\theta_c = \frac{\sin\theta_3(\sin\theta_1\sin\phi_3-\sin\theta_3)}{\left[(1-\sin\theta_1\sin\theta_3\sin\phi_3)^2-\cos^2\theta_1\cos^2\theta_3\right]^{1/2}} . \tag{4.98}$$

Thus, with $\hat{k}_1$ and $\hat{k}_3$ specified according to (4.94) and (4.95), $\vec{W}'_{12}$ is specified by fixing its azimuthal angle according to (4.96), and requiring that its polar angle satisfy the condition

$$-1 < \cos\theta < \cos\theta_c \quad . \tag{4.99}$$

The magnitudes of both $\vec{W}_{12}$ and $\vec{W}'_{12}$ are evidently unrestricted:

$$0 < W_{12} < \infty \quad , \tag{4.100}$$

$$0 < W'_{12} < \infty \quad . \tag{4.101}$$

With $\vec{W}_{12}$, $\vec{W}'_{12}$, $\hat{k}_1$ and $\hat{k}_3$ fixed, it remains only to specify the vectors $\hat{k}_2$ and $\vec{W}_{31}(II) \equiv \vec{W}_{31}$. We let θ_2 and ϕ_2 denote the polar and azimuthal angles of $\hat{k}_2$; and we let $\tilde{\theta}$ and $\tilde{\phi}$ denote the polar and azimuthal angles of $\vec{W}_{31}$ *relative to a coordinate system with* $\hat{k}_2$ *in the +Z-direction.* By definition we have

$$\hat{W}_{31} \cdot \hat{k}_2 = \cos\tilde{\theta} \quad , \tag{4.102}$$

and an obvious requirement for the second collision to occur at all is [see Fig. 14]

$$0 < \cos\tilde{\theta} < 1 \quad . \tag{4.103}$$

Apart from requirement (4.103), the only other condition on $\vec{W}_{31}$ and $\hat{k}_2$ is that they be such as to satisfy the velocity-change equation

$$\vec{W}'_{12} = \vec{W}_{12} + \vec{W}_{31} \cdot \hat{k}_2 \hat{k}_2 \quad , \tag{4.104}$$

for *fixed* vectors $\vec{W}_{12}$ and $\vec{W}'_{12}$. In fact, (4.104), together with (4.103), is seen to determine *completely* the vector $\hat{k}_2$ according to

$$\hat{k}_2 = (\vec{W}'_{12}-\vec{W}_{12})/|\vec{W}'_{12}-\vec{W}_{12}| \quad , \tag{4.105}$$

and also the magnitude of $\vec{W}_{31}$ according to

$$W_{31} = |\vec{W}'_{12}-\vec{W}_{12}|/\cos\tilde{\theta} \quad . \tag{4.106}$$

The polar angle $\tilde{\phi}$ of $\vec{W}_{31}$ is evidently unrestricted:

$$0 < \tilde{\phi} < 2\pi \quad . \tag{4.107}$$

It follows from the foregoing observations that, in addition to the four variables $\vec{W}_0$ and W_{12}, the following set of seven variables can serve as integrating variables for the R-integrals:

$$\left.\begin{array}{ll} \cos\theta_1 & \text{in } (0,1) \\ \cos\theta_3 & \text{in } (0,1) \\ \phi_3 & \text{in } (0,2\pi) \\ \cos\theta & \text{in } (-1,\cos\theta_c) \\ W'_{12} & \text{in } (0,\infty) \\ \cos\tilde{\theta} & \text{in } (0,1) \\ \tilde{\phi} & \text{in } (0,2\pi) \end{array}\right\} \quad . \tag{4.108}$$

The attractive feature of these variables is that only one of them has a non constant limit [the upper limit on $\cos\theta$ is the complicated *but bounded* function of θ_1, θ_3, ϕ_3 in (4.98)], and only one variable has an infinite range [the upper limit on W'_{12} is ∞].

Before attempting to express the integral form $(\alpha,\beta)_{31}$ in (4.2) as an integral over the variables in (4.108), let us collect the formulae giving all the quantities of dynamical interest in terms of these new variables.

In anticipation of the subsequent analytical "scaling integration" over the variable W_{12}, we shall express all velocities $\vec{W}_{ij}$ in terms of their "scaled" values,

$$\vec{w}_{ij} \equiv \vec{W}_{ij}/W_{12}. \tag{4.109}$$

In the coordinate frame of Fig. 14 we have

$$\vec{w}_{12} = \begin{bmatrix} 0 \\ 0 \\ 1 \end{bmatrix} , \tag{4.110a}$$

$$\hat{k}_1 = \begin{bmatrix} 0 \\ \sin\theta_1 \\ \cos\theta_1 \end{bmatrix} , \tag{4.110b}$$

$$\hat{k}_3 = \begin{bmatrix} \sin\theta_3\cos\phi_3 \\ \sin\theta_3\sin\phi_3 \\ \cos\theta_3 \end{bmatrix} , \tag{4.110c}$$

$$\vec{w}'_{12} = w'_{12}\begin{bmatrix} \sin\theta\cos\phi \\ \sin\theta\sin\phi \\ \cos\theta \end{bmatrix} , \tag{4.110d}$$

where ϕ is defined in (4.96) and (4.97);

$$\hat{k}_2 = \begin{bmatrix} \sin\theta_2\cos\phi \\ \sin\theta_2\sin\phi \\ \cos\theta_2 \end{bmatrix} , \tag{4.110e}$$

where we have used (4.105) to deduce that the azimuthal angle of $\hat{k}_2$ is the same as that of $\vec{w}'_{12}$, while the polar angle of $\hat{k}_2$ is given by

$$\left.\begin{aligned} \cos\theta_2 &= (w'_{12}\cos\theta - 1)/\delta \\ \sin\theta_2 &= w'_{12}\sin\theta/\delta \end{aligned}\right\} , \tag{4.111}$$

with

$$\delta \equiv |\vec{w}'_{12}-\vec{w}_{12}| = \sqrt{w'^2_{12}-2w'_{12}\cos\theta+1} \quad , \tag{4.112}$$

$$\vec{w}_{31} = R_z(-\phi)\cdot R_y(-\theta_2)\cdot\begin{bmatrix} w_{31}\sin\tilde{\theta}\cos\tilde{\phi} \\ w_{31}\sin\tilde{\theta}\sin\tilde{\phi} \\ w_{31}\cos\tilde{\theta} \end{bmatrix} \quad , \tag{4.113}$$

where the rotation matrices (defined in Table IV) transform the components of $\vec{w}_{31}$ out of the frame defined relative to $\hat{k}_2$ as polar axis, and where w_{31} is given by [cf. (4.106) and (4.112)]

$$w_{31} = \delta/\cos\tilde{\theta} \quad . \tag{4.114}$$

In terms of the above quantities, the scaled relative velocities in the various regions are as follows [cf. (4.31)-(4.34)]:

$$\begin{aligned} \vec{w}_{12}(II) &= \vec{w}_{12} \\ \vec{w}_{31}(II) &= \vec{w}_{31} \end{aligned} \tag{4.115}$$

$$\begin{aligned} \vec{w}_{12}(III) &= \vec{w}'_{12} \\ \vec{w}_{31}(III) &= \vec{w}'_{31} \equiv \vec{w}_{31} - 2\vec{w}_{31}\cdot\hat{k}_2\hat{k}_2 \end{aligned} \quad , \tag{4.116}$$

$$\begin{aligned} \vec{w}_{12}(I) &= \vec{w}_{12} - 2\vec{w}_{12}\cdot\hat{k}_1\hat{k}_1 \\ \vec{w}_{31}(I) &= \vec{w}_{31} + \vec{w}_{12}\cdot\hat{k}_1\hat{k}_1 \end{aligned} \quad , \tag{4.117}$$

$$\begin{aligned} \vec{w}_{12}(IV) &= \vec{w}'_{12} - 2\vec{w}'_{12}\cdot\hat{k}_3\hat{k}_3 \\ \vec{w}_{31}(IV) &= \vec{w}'_{31} + \vec{w}'_{12}\cdot\hat{k}_3\hat{k}_3 \end{aligned} \quad . \tag{4.118}$$

It is clear, then, that the set of variables, $\vec{W}_0$, W_{12}, and the ones listed in (4.108) [with W'_{12} replaced by $w'_{12} \equiv W'_{12}/W_{12}$], indeed constitutes a viable set of integrating variables for the integrals $(\alpha,\beta)_{31}$ given in (4.2). However, the transformation from the set of variables in (2.28) and (4.2) to our new set is not altogether trivial. We now direct our attention to this problem.

To begin with, we make a change of variables similar to (2.35) except we use $\vec{W}_{12}$ instead of $\vec{W}_{21}$:

$$\left.\begin{aligned} \vec{W}_0 &= \tfrac{1}{3}(\vec{W}_1+\vec{W}_2+\vec{W}_3) \\ \vec{W}_{12} &= \vec{W}_1-\vec{W}_2 \\ \vec{W}_{31} &= \vec{W}_3-\vec{W}_1 \end{aligned}\right\} \quad \text{or} \quad \left\{\begin{aligned} \vec{W}_1 &= \vec{W}_0+\tfrac{1}{3}(\vec{W}_{12}-\vec{W}_{31}) \\ \vec{W}_2 &= \vec{W}_0-\tfrac{1}{3}(2\vec{W}_{12}+\vec{W}_{31}) \\ \vec{W}_3 &= \vec{W}_0+\tfrac{1}{3}(2\vec{W}_{31}+\vec{W}_{12}) \end{aligned}\right. \tag{4.119}$$

so that

$$W_1^2+W_2^2+W_3^2 = 3W_0^2+E \quad , \tag{4.120}$$

with

$$E \equiv \tfrac{2}{3}(W_{12}^2+W_{31}^2+\vec{W}_{I2}\cdot\vec{W}_{31}) \quad . \tag{4.121}$$

Introducing this transformation into (4.2) and introducing also the transformation (2.34) we have

$$(\alpha,\beta)_{31} = \frac{3\sqrt{2}}{10\pi^6} \int_{\Omega_R} d\vec{W}_0 d\vec{W}_{12} d\vec{W}_{31} d\hat{k}_1 d\hat{k}_2 d\tau \, |\vec{W}_{12}\cdot\hat{k}_1||\vec{W}_{31}\cdot\hat{k}_2| e^{-3W_0^2-E}$$

$$\times \{\alpha(I)-\alpha(II)\}*\{\beta(IV)-\beta(III)\} \quad . \tag{4.122}$$

Here, Ω_R is the integration region appropriate to the R(ν=1)-diagram in Fig. 12; the velocity regions refer, of course, also to this diagram. Taking $\vec{W}_{12}$ along the Z-axis and $\hat{k}_1$ in the YZ-plane performs three trivial integrations and introduces an overall factor of $8\pi^2$ in accordance with (2.41). Using the previously defined angular variables, and noting that the occurrence of the first and second collisions requires

$$\vec{W}_{12}\cdot\hat{k}_1 = w_{12}\cos\theta_1 > 0 \ , \tag{4.123}$$

$$\vec{W}_{31}\cdot\hat{k}_2 = w_{31}\cos\tilde{\theta} > 0 \ , \tag{4.124}$$

we may write (4.122) as

$$(\alpha,\beta)_{31} = \frac{12\sqrt{2}}{5\pi^4}\int\int\int_{\infty} d^3\vec{W}_0 \int_0^{\infty} dW_{21}W_{21}^3 \int_0^1 d\cos\theta_1 \int_0^1 d\cos\tilde{\theta} \int_0^{2\pi} d\tilde{\phi}$$

$$\times \int\int\int\int dW_{31}W_{31}^3 d\cos\theta_2 d\phi_2 d\tau\ \Theta_R \cos\theta_1 \cos\tilde{\theta} e^{-3W_0^2-E^*}$$

$$\times\{\alpha(I)-\alpha(II)\}*\{\beta(IV)-\beta(III)\} \ . \tag{4.125}$$

In (4.125) we have put the upper limits on the variables $\cos\theta_1$, $\cos\tilde{\theta}$, $\tilde{\phi}$ as required by (4.108). However, the limits on the variables W_{31}, $\cos\theta_2$, ϕ_2 and τ are not known at the moment; therefore, we have introduced the quantity Θ_R which is 1 or 0 depending on whether the requirements for the R-collision are or are not satisfied. If we now introduce the scaling transformation

$$\begin{aligned} W_{31} &\rightarrow w_{31}=W_{31}/W_{21} \\ \tau &\rightarrow \tau^*=W_{12}\tau \end{aligned} \ , \tag{4.126}$$

and define

$$E^* \equiv \frac{2}{3}(1+w_{31}^2+\vec{w}_{12}\cdot\vec{w}_{31}) \quad , \tag{4.127}$$

then (4.125) becomes

$$(\alpha,\beta)_{31} = \frac{12\sqrt{2}}{5\pi^4}\int_{\infty}\int_{\infty}\int_{\infty} d^3\vec{w}_0 e^{-3w_0^2}\int_0^{\infty} dw_{12} w_{12}^6 e^{-w_{12}^2 E^*}\int_0^1 d\cos\theta_1\int_0^1 d\cos\tilde{\theta}\int_0^{2\pi} d\tilde{\phi}$$

$$\times\int\int\int\int dw_{31}\, d\cos\theta_2\, d\phi_2\, d\tau^*\, \Theta_R\, w_{31}^3\cos\theta_1\cos\tilde{\theta}$$

$$\times\{\alpha(I)-\alpha(II)\}*\{\beta(IV)-\beta(III)\} \quad . \tag{4.128}$$

Our task now is to transform the variables $(w_{31},\cos\theta_2,\phi_2,\tau^*)$ into the "desired" variables $(w'_{12},\cos\theta_3,\phi_3,\cos\theta)$; note that we may then omit the quantity Θ_R in (4.128) by simply inserting the integration limits on these new variables as indicated in (4.108). The difficult part of this task is to compute the Jacobian of this transformation:

$$J \equiv \frac{\partial(w_{31},\cos\theta_2,\phi_2,\tau^*)}{\partial(w'_{12},\cos\theta_3,\phi_3,\cos\theta)} \quad . \tag{4.129}$$

For this purpose we note from (4.111), (4.112) and (4.114) that w_{31} and $\cos\theta_2$ are given by

$$w_{31} = \left[w'^2_{12}-2w'_{12}\cos\theta + 1\right]^{1/2}/\cos\tilde{\theta} \tag{4.130a}$$

$$\cos\theta_2 = (w'_{12}\cos\theta-1)/[w'^2_{12}-2w'_{12}\cos\theta + 1]^{1/2} \quad . \tag{4.130b}$$

Further, since $\phi_2=\phi$, then we have from (4.96)

$$\phi_2 = \arctan\left(\frac{\sin\theta_3\sin\phi_3-\sin\theta_1}{\sin\theta_3\cos\phi_3}\right) . \qquad (4.130c)$$

Finally, to calculate an expression for τ^* we need only to observe that

$$\tau^* \equiv w_{12}\tau\,\overline{P_{11}P_{12}} \quad .$$

Hence, an analysis of the geometry of Fig. 14 yields the expression [cf. (4.97)]

$$\tau^* = -\cot\theta[(\sin\theta_3\cos\phi_3)^2+(\sin\theta_3\sin\phi_3-\sin\theta_1)^2]^{1/2} + \cos\theta_3 - \cos\theta_1 . \qquad (4.130d)$$

Equations (4.130) evidently permit us to calculate the Jacobian (4.129). This computation is rather lengthy, but yields the result

$$J = \frac{-w'_{12}\vec{w}'_{12}\cdot\hat{k}_3}{\delta^2 B\sin\theta\cos\tilde{\theta}} \quad , \qquad (4.131)$$

where δ and B are defined in (4.112) and (4.97), and where the minus sign appears because the only negative quantity on the right side of (4.131) is the inner product $\vec{w}'_{12}\cdot\hat{k}_3$ [see Fig. 14].

We now insert in (4.128) the transformation

$$\iiiint dw_{31}d\cos\theta_2 d\phi_2 d\tau^*\ \Theta_R = \int_0^\infty dw'_{12}\int_0^1 d\cos\theta_3\int_0^{2\pi} d\phi_3\int_{-1}^{\cos\theta_c} d\cos\theta\ J \quad .$$

Writing J as in (4.131) and w_{31} as in (4.114), we obtain the result

$$(\alpha,\beta)_{31} = -\frac{12\sqrt{2}}{5\pi^4}\iiint_{\infty} d^3\vec{W}_0 e^{-3W_0^2}\int_0^{\infty} dW_{12} W_{12}^6 e^{-W_{12}^2 E^*}$$

$$\times \int_0^1 d\cos\theta_1 \int_0^1 d\cos\tilde{\theta} \int_0^{2\pi} d\tilde{\phi} \int_0^{\infty} dw'_{12} \int_0^1 d\cos\theta_3 \int_0^{2\pi} d\phi_3 \int_{-1}^{\cos\theta_c} d\cos\theta$$

$$\times \frac{\delta w'_{12}\vec{w}'_{12}\cdot\hat{k}_3\cos\theta_1}{B\cos^3\tilde{\theta}\sin\theta}\{\alpha(I)-\alpha(II)\}*\{\beta(IV)-\beta(III)\} \quad . \tag{4.132}$$

We can eliminate the singularity at $\sin\theta=0$ by changing variables from $\cos\theta$ to θ. Thus,

$$(\alpha,\beta)_{31} = -\frac{12\sqrt{2}}{5\pi^4}\iiint_{\infty} d^3\vec{W}_0 e^{-3W_0^2}\int_0^{\infty} dW_{12} W_{12}^6 e^{-W_{12}^2 E^*}$$

$$\times \int_0^1 d\cos\theta_1 \int_0^1 d\cos\theta_3 \int_0^{2\pi} d\phi_3 \int_0^{\pi} d\theta \int_0^1 d\cos\tilde{\theta} \int_0^{2\pi} d\tilde{\phi} \int_0^{\infty} dw'_{12}$$

$$\times \Theta(\theta-\theta_c)\frac{\delta w'_{12}\vec{w}'_{12}\cdot\hat{k}_3\cos\theta_1}{B\cos^3\tilde{\theta}}\{\alpha(I)-\alpha(II)\}*\{\beta(IV)-\beta(III)\} \quad , \tag{4.133}$$

where the theta function $\Theta(\theta-\theta_c)$ is unity if $\cos\theta \ll \cos\theta_c$ [see (4.99)] and is zero otherwise.

Using this integral form we want to evaluate again the recollision contributions (4.15) to the transport coefficients

$$\lambda^*_{131}(1) = -\left(\sum_{m=1}^{3} \vec{W}_m W_m^2, \sum_{n=1}^{3} \vec{W}_n W_n^2\right)_{31} ,$$

$$\eta^*_{131}(1) = -\left(\sum_{m=1}^{3} \vec{W}_m \vec{W}_m, \sum_{n=1}^{3} \vec{W}_n \vec{W}_n\right)_{31} , \qquad (4.134)$$

$$D^*_{131}(1) = -4\left(\vec{W}_2, \vec{W}_2\right)_{31} .$$

Each integral of (4.134) contains a specific polynomial in $\vec{W}_1, \vec{W}_2, \vec{W}_3$. We express these polynomials in terms of the variables $\vec{W}_0, \vec{W}_{12}, \vec{W}_{31}$ according to (4.119). The $\vec{W}_0$-dependence is thereby rendered explicit, and the $\vec{W}_0$-integration in (4.133) can then be carried out analytically. The polynomials now involve only the velocities $\vec{W}_{12}$ and $\vec{W}_{31}$. Scaling according to (4.126) will then render the W_{12} dependence explicit, and the W_{12}-integration in (4.133) can be carried out analytically. These operations leave us with 7-dimensional integral expressions for the quantities in (4.134). It is found that, after the W_{12}-dependence has been integrated out, the quantity $\{\alpha(I)-\alpha(II)\}$ always contains the factor $\vec{w}_{12}\cdot\hat{k}_1$, while the quantity $\{\beta(IV)-\beta(III)\}$ always contains the factor $\vec{w}'_{12}\cdot\hat{k}_3$, for all functions α and β with which we shall be concerned. Hence we introduce again the primed differences

$$\{\alpha(I)-\alpha(II)\}' \equiv \{\alpha(I)-\alpha(II)\} \Big/ \hat{w}_{12}\cdot\hat{k}_1 , \qquad (4.135a)$$

$$\{\alpha(IV)-\alpha(III)\}' \equiv \{\alpha(IV)-\alpha(III)\} \Big/ \vec{w}'_{12}\cdot\hat{k}_3 . \qquad (4.135b)$$

If we carry out the $\vec{W}_0$- and W_{12}-integrations, we obtain [c.f.(4.74)-(4.76)]

$$\lambda^*_{131}(1) = -3(\vec{\vec{L}}_1,\vec{\vec{L}}_1)_{31} - \frac{99}{4}(\vec{K}_1,\vec{K}_1)_{31} \quad , \tag{4.136}$$

$$\eta^*_{131}(1) = -\frac{9}{2}(\vec{\vec{L}}_1,\vec{\vec{L}}_1)_{31} \quad , \tag{4.137}$$

$$D^*_{131}(1) = -4(\vec{w}_{20},\vec{w}_{20})_{31} \quad , \tag{4.138}$$

where the functions $\vec{K}_1$ and $\vec{\vec{L}}_1$ are again defined by (4.77) with

$$\left.\begin{aligned} \vec{w}_{10}(i) &= \frac{1}{3}[\vec{w}_{12}(i)-\vec{w}_{31}(i)] \\ \vec{w}_{20}(i) &= -\frac{1}{3}[2\vec{w}_{12}(i)+\vec{w}_{31}(i)] \quad (i=1,II,III,IV) \\ \vec{w}_{30}(i) &= \frac{1}{3}[2\vec{w}_{31}(i)+\vec{w}_{12}(i)] \end{aligned}\right\} \quad , \tag{4.139}$$

and where $(\alpha,\alpha)_{31}$ is now given by

$$(\alpha,\alpha)_{31} = -\frac{7\sqrt{6}}{8\pi^2}\int_0^1 d\cos\theta_1 \int_0^1 d\cos\theta_3 \int_0^{2\pi} d\phi_3 \int_0^{\pi} d\theta \int_0^1 d\cos\tilde{\theta} \int_0^{2\pi} d\tilde{\phi} \int_0^{\infty} dw'_{12}$$

$$\times\, \Theta(\theta-\theta_c)\frac{\delta w'^3_{12}(\hat{w}'_{12}\cdot\hat{k}_3)^2\cos^2\theta_1}{E^{*9/2}B\cos^3\tilde{\theta}}\{\alpha(I)-\alpha(II)\}'*\{\alpha(IV)-\alpha(III)\}' \tag{4.140}$$

The integrand $\{\alpha(I)-\alpha(II)\}'*\{\alpha(IV)-\alpha(III)\}'$ may again be obtained from the formulas presented in Table XII.

At this point we might compare the above expression for $(\alpha,\alpha)_{31}$ with the expression (4.79). In (4.79) we had to concern ourselves with the

dependence of the integrand on w_{31}, in order to effect a suitable change of variable $w_{31} \rightarrow u$ which transformed the infinite range $0<w_{31}<\infty$ into a finite range $0<u<1$. In (4.140) we face a similar problem with the infinitely ranging variable w'_{12}, but it is the case that the asymptotic behavior of the integrand in (4.140) on w'_{12} is *not* the same as the asymptotic behavior of the integrand in (4.79) on w_{31}; thus, a full investigation of the w'_{12}-dependence of the integrand in (4.140) for the functions α required by (4.136)-(4.138) is necessary. Both (4.140) and (4.79) involve the factor $E^{*-9/2}$, and this causes no boundedness problems since E^* can never approach zero [from (4.127), $E^* > \frac{2}{3}\{(w_{31}-1)^2+w_{31}\}>0$]. However, in (4.79) we had to investigate the unbounded behavior of Δ_ν in order to be certain that the quantities multiplying Δ_ν always kept the integrand bounded. In (4.140) we must similarly concern ourselves with the behavior of the integrand when $B \rightarrow 0$ and when $\cos\tilde{\theta} \rightarrow 0$.

The analysis of the behavior of the integrand in (4.140) for the cases $w'_{12} \rightarrow 0$, $w'_{12} \rightarrow \infty$, $\cos\tilde{\theta} \rightarrow 0$ and $B \rightarrow 0$ is quite lengthy, and we shall give only a brief summary of the results here.

A detailed investigation of the w'_{12} behavior of all integrands of interest leads to the conclusion that the transformation

$$u = (1+w'^4_{12})^{-1} \quad , \tag{4.141a}$$

with

$$w'^3_{12} dw'_{12} = -\frac{1}{4}\frac{du}{u^2} \quad , \tag{4.141b}$$

maps the infinite w'_{12}-range onto the unit interval in such a way as to keep all integrands smooth and bounded at the limits $w'_{12}\to 0\,(u\to 1)$ and $w'_{12}\to\infty\,(u\to 0)$. With this transformation, (4.140) becomes

$$(\alpha,\alpha)_{31} = -\frac{7\sqrt{6}}{32\pi^2}\int_0^1 d\cos\theta_1 \int_0^1 d\cos\theta_3 \int_0^{2\pi} d\phi_3 \int_0^{\pi} d\theta \int_0^1 d\cos\tilde{\theta} \int_0^{2\pi} d\tilde{\phi} \int_0^1 du$$

$$\times\,\theta(\theta-\theta_c)\left(\frac{\delta(\hat{w}'_{12}\cdot\hat{k}_3)^2}{u^2 E^{*9/2}\cos^3\tilde{\theta}}\right)\left(\frac{\cos^2\theta_1}{B}\right)\{\alpha(I)-\alpha(II)\}'*\{\alpha(IV)-\alpha(III)\}' \,, \tag{4.142}$$

where it is henceforth understood that w'_{12} is given by

$$w'_{12} = \left(\frac{1-u}{u}\right)^{1/4} . \tag{4.143}$$

Next, we investigate the boundedness of the first factor in parenthesis in the integrand of (4.142). For this purpose it is useful to eliminate $\tilde{w}_{31}$ from the expression for E^* in (4.127). It turns out that this leads to

$$E^* = \varepsilon/\cos^2\tilde{\theta} \,, \tag{4.144a}$$

where

$$\varepsilon \equiv \frac{2}{3}\left[w'^2_{12} + w'_{12}\{\cos\tilde{\theta}(\cos\theta\cos\tilde{\theta}-\sin\theta\sin\tilde{\theta}\cos\phi)-2\cos\theta\} + 1\right] . \tag{4.144b}$$

Thus we have

$$\frac{\delta(\hat{w}'_{12}\cdot\tilde{k}_3)^2}{u^2E^{*9/2}\cos^3\tilde{\theta}} = \frac{\delta(w'_{12}\cdot\hat{k}_3)^2\cos^6\tilde{\theta}}{u^2\varepsilon^{9/2}} \qquad (4.145)$$

Now the limit $u\to 0$ need not concern us, since the u (or w'_{12}) behavior of the integrand has already been judged acceptable. However, we must look at the possibility of $\varepsilon\to 0$. A detailed analysis of (4.144b) reveals that $\varepsilon=0$ if and only if $w'_{12}=1$ *and* $\sin\theta=0$ *and* $\cos\tilde{\theta}=0$. Further analysis shows that

for $w'_{12}=1$, θ near 0, $\tilde{\theta}$ near $\pi/2$:

$$\varepsilon\approx\frac{2}{3}(\sin^2\theta+\cos^2\tilde{\theta}-\sin\theta\cos\tilde{\theta}\cos\tilde{\phi}),$$

$$\delta\approx\sin\theta, \qquad (4.146)$$

$$|\hat{w}_{12}\cdot\hat{k}_3|\lesssim\sin\theta \quad .$$

Therefore, when ε is near zero we have

$$\frac{\delta(\hat{w}'_{12}\cdot\hat{k}_3)^2\cos^6\tilde{\theta}}{\varepsilon^{9/2}} \lesssim \frac{\sin\theta\ \sin^2\theta\ \cos^6\tilde{\theta}}{\mathrm{Max}(\sin^9\theta,\cos^9\tilde{\theta})} \sim 1 \quad , \qquad (4.147)$$

which shows that the first factor in parenthesis in the integrand of (4.142) is always bounded.

Finally, we investigate the boundedness of the second factor in parenthesis in (4.142). The problem here, of course, is with the case B=0, where B is defined by (4.97). The geometrical meaning of B is indicated in Fig. 14.

Since, according to Fig. 14, B is the distance from the tip of $\hat{k}_3$ to the line extending vertically upwards from the tip of $\hat{k}_1$, it is convenient to introduce a polar representation (θ_3', ϕ_3') of $\hat{k}_3$ in a frame having $\hat{k}_1$ as its polar axis. Such a frame is obtained simply by rotating the frame in Fig. 14 about the X-axis through an angle $-\theta_1$. The angles (θ_3', ϕ_3') and (θ_3, ϕ_3) are thus related by

$$\begin{bmatrix} \sin\theta_3\cos\phi_3 \\ \sin\theta_3\sin\phi_3 \\ \cos\theta_3 \end{bmatrix} = R_x(+\theta_1) \begin{bmatrix} \sin\theta_3'\cos\phi_3' \\ \sin\theta_3'\sin\phi_3' \\ \cos\theta_3' \end{bmatrix} \tag{4.148}$$

where the rotation matrix $R_x(\theta_1)$ is defined in Table IV. Eq. (4.148) shows how the components of $\hat{k}_3$ in the coordinate frame of Fig. 14 (i.e., the angles θ_3 and ϕ_3) are obtained from the components of $\hat{k}_3$ in a frame whose Z-axis points along $\hat{k}_1$ (i.e., the angles θ_3' and ϕ_3'). In particular, one calculates from (4.148) that

$$\cos\theta_3 = -\sin\theta_1\sin\theta_3'\sin\phi_3' + \cos\theta_1\cos\theta_3' \quad . \tag{4.149}$$

With (4.148) we can express B in (4.97) in terms of $\theta_1, \theta_3', \phi_3'$ as follows:

$$B = [2(1-\cos\theta_3') - \{\sin\theta_3'\sin\theta_1\sin\phi_3' + (1-\cos\theta_3')\cos\theta_1\}^2]^{1/2} \quad . \tag{4.150}$$

From this expression (and the geometry of Fig. 14) it may be deduced that B=0 is and only if $\theta_3'=0$. A more detailed analysis reveals that the most rapid approach of $B\to 0$ with $\theta_3'\to 0$ occurs when we also have $\phi_1\to\pi/2$; specifically, we have for

$\phi_3' = \pi/2$, θ_3' near 0, θ_1 near $\pi/2$:

$$B \sim \sqrt{\frac{1}{2}}\, \sin\theta_3' \cos^2\theta_1 \quad , \tag{4.151}$$

whence

$$\left(\frac{\cos^2\theta_1}{B}\right) \sim \frac{\sqrt{2}}{\sin\theta_3'} \quad .$$

Consequently, the second factor in parenthesis in the integrand of (4.142) can blow up like $1/\sin\theta_3'$ in the limit $\theta_3' \to 0$. To circumvent this problem, we change variables $(\cos\theta_3, \phi_3) \to (\theta_3', \phi_3')$ according to

$$d\cos\theta_3 d\phi_3 = d\cos\theta_3' d\phi_3' = \sin\theta_3' d\theta_3' d\phi_3' \quad . \tag{4.152}$$

Since this transformation introduces a factor $\sin\theta_3'$, it clearly solves our problems when $B \to 0$. However, the limits on θ_3' and ϕ_3', will be rather complicated, since the lower limit on $\cos\theta_3$ was 0 and not -1. The simplest way to proceed is to let θ_3' and ϕ_3' vary over their full limits, and to insert a theta function requiring the quantity in (4.149) to be positive. Thus, our expression for $(\alpha,\alpha)_{31}$ in (4.142) now becomes

$$(\alpha,\alpha)_{31} = -\frac{7\sqrt{6}}{32\pi^2} \int_0^1 d\cos\theta_1 \int_0^{\pi} d\theta_3' \int_0^{2\pi} d\phi_3' \int_{-\pi}^{0} d\theta \int_0^1 d\cos\tilde{\theta} \int_0^{2\pi} d\tilde{\phi} \int_0^1 du$$

$$\times \Theta(\cos\theta_3) \Theta(\cos\theta_c - \cos\theta) \left(\frac{\delta(\hat{w}_{12}' \cdot \hat{k}_3)^2}{u^2 E^{*9/2} \cos^3\tilde{\theta}}\right) \left(\frac{\sin\theta_3' \cos^2\theta_1}{B}\right)$$

$$\times \{\alpha(I) - \alpha(II)\}' * \{\alpha(IV) - \alpha(III)\}' \quad . \tag{4.153}$$

where now the integrand is a bounded function of the integrating variables for all functions α of interest, and where it is henceforth understood that the angles θ_3 and ϕ_3 are given by (4.148).

A final trivial transformation of variables is made to simplify the Monte Carlo evaluation of $(\alpha,\alpha)_{31}$. Namely, we transform the 7-dimensional "box" which forms the integrating region for (4.153), into a 7-dimensional unit "cube":

$$\cos\theta_1 = r_1 \quad , \tag{4.154a}$$

$$\theta_3' = \pi r_2 \quad , \tag{4.154b}$$

$$\phi_3' = 2\pi(r_3+0.25) \quad , \tag{4.154c}$$

$$\theta = \pi r_4 \quad , \tag{4.154d}$$

$$\cos\tilde{\theta} = r_5 \quad , \tag{4.154e}$$

$$\tilde{\phi} = 2\pi r_6 \quad , \tag{4.154f}$$

$$u = r_7, \quad w_{12}' = [(1-u)/u]^{1/4} \quad . \tag{4.154g}$$

Since the Jacobian of this transformation is

$$\frac{\partial(\cos\theta_1,\theta_3',\phi_3',\theta,\cos\tilde{\theta},\tilde{\phi},u)}{\partial(r_1,r_2,\ldots,r_7)} = 4\pi^4 \quad , \tag{4.155}$$

then we obtain our *final formula* for $(\alpha,\alpha)_{31}$:

$$(\alpha,\alpha)_{31} = -\frac{7\sqrt{6}\pi^2}{8}\int_0^1 d\mathcal{R}_1\int_0^1 d\mathcal{R}_2\cdots\int_0^1 d\mathcal{R}_7\;\Theta(\cos\theta_3)\;\Theta(\cos\theta_c-\cos\theta)$$

$$\left(\frac{\delta(\hat{w}'_{12}\cdot\hat{k}_3)^2}{u^2E^{*9/2}\cos^3\tilde{\theta}}\right)\left(\frac{\sin\theta'_3\cos^2\theta_1}{B}\right)\{\alpha(I)-\alpha(II)\}'*\{\alpha)IV)-\alpha(III)\}' \quad . \quad (4.156)$$

Using the integral form (4.156) we may now calculate the R-collision integrals (4.136)-(4.138). The Monte Carlo procedure for numerically evaluating the integral (4.156) is to average the integrand over a set of points $\{P^i\}\equiv\{\mathcal{R}_1^i,\mathcal{R}_2^i,\ldots,\mathcal{R}_7^i\}$ picked from a random, uniform distribution in the 7-dimensional unit cube U_7:

$$(\alpha,\alpha)_{31} = \left\langle -\frac{7\sqrt{6}\pi^2}{8}\Theta(\cos\theta_3)\;\Theta(\cos\theta_c-\cos\theta)\left(\frac{\delta(\hat{w}'_{12}\cdot\hat{k}_3)^2}{u^2E^{*9/2}\cos^3\tilde{\theta}}\right)\left(\frac{\sin\theta'_3\cos^2\theta_1}{B}\right)\right.$$

$$\left.\times\{\alpha(I)-\alpha(II)\}'*\{\alpha(IV)-\alpha(III)\}'\right\rangle_{U_7} \quad . \quad (4.157)$$

The uncertainty in estimating this average with a *finite* set of points $\{P^1,P^2,\ldots,P^M\}$ is given by the r.m.s. deviation of the quantity being averaged, divided by $\sqrt{M}$. Hence, our computational algorithm is as follows:

1° Generate 7 independent random numbers $\eta_1,\eta_2,\ldots,\eta_7$ from a uniform distribution in the unit interval.

2° Calculate the quantities $\theta_1,\theta_3',\phi_3',\theta,\tilde{\theta},\tilde{\phi},u$ (and w_{12}') from eqs. (4.154).

3° From θ_1,θ_3' and ϕ_3', calculate θ_3 and ϕ_3 from (4.148). Set the first theta function in (4.157) to 0 or 1 according to whether $\cos\theta_3$ [see (4.149)] is negative or positive. If $\cos\theta_3<0$ proceed to step 11° with all integrands equal to zero, noting that the coordinates $\eta_4,\eta_5,\eta_6,\eta_7$ have not been used and need not be regenerated for the next point.

4° From θ_1,θ_3, and ϕ_3, calculate $\cos\theta_c$ from (4.98), and set the second theta function in (4.157) to 0 or 1 according to whether $\cos\theta$ is greater than or less than $\cos\theta_c$. If $\cos\theta>\cos\theta_c$ proceed to step 11° with all integrands equal to zero, noting that the coordinates η_5,η_6,η_7 have not been used and need not be regenerated for the next point.

5° Calculate B and ϕ according to (4.97) and (4.96). Calculate δ,θ_2 and w_{31} according to (4.112), (4.111) and (4.114).

6° Calculate the vectors $\hat{k}_1$, $\hat{k}_2$ and $\hat{k}_3$ according to (4.110b), (4.110e) and (4.110c). Calculate the velocities $\vec{w}_{12}$ and $\vec{w}_{12}'$ according to (4.110a) and (4.110d). Calculate the velocity $\vec{w}_{31}$ according to (4.113), and calculate the velocity $\vec{w}_{31}'$ according to the definition in (4.116).

7° Using the above vectors, calculate E^* according to (4.127), and also calculate $\hat{w}_{12}'\cdot\hat{k}_3$.

8° From the region II velocities $\vec{w}_{12}$ and $\vec{w}_{31}$ and the collision vector $\hat{k}_1$, calculate the region I velocities according to (4.117). Similarly, from the region III velocities $\vec{w}'_{12}$ and $\vec{w}'_{31}$ and the collision vector $\hat{k}_3$, calculate the region IV velocities according to (4.118).

9° Evaluate the velocities $\vec{w}_{10}$, $\vec{w}_{20}$ and $\vec{w}_{30}$ in all velocity regions according to (4.139). Then evaluate the quantities $\vec{K}_1$ and $\vec{L}_1$ in all velocity regions according to (4.77a) and (4.77b).

10° Using the definitions (4.135), calculate the primed differences in (4.157) for the functions α appearing in (4.136)-(4.138) (see Table XII).

11° Using the values found in the preceeding steps, evaluate the required integrands in angular brackets in (4.157), and also the squares of these integrands (for computing the variances), and add these to respective cumulating sums.

12° Return to 1°, and repeat for as many times M as is practical. Then convert the sums to averages, and so obtain the Monte Carlo estimates of the quantities in (4.136)-(4.138), together with the uncertainties in these estimates.

In the actual calculations, steps 8°-10° were combined by calculating the primed differences in quantities $\vec{K}_1$, $\vec{L}_1$ and $\vec{w}_{20}$ analytically in terms of the velocities in regions II and III and the other integrating variables as indicated in Table XII. The computer calculations were carried out in

double-precision to minimize the effects of round-off errors on certain critical dynamical quantities.

Again, an empirically determined importance sample procedure was used to effect a substantial reduction in the uncertainties without increasing the number of sampling points M. This time the following importance sampling distributions were used [cf. (3.43) and the discussion thereof]:

$$P_2(\eta_2) \propto \exp(-9\eta_2) \quad , \tag{4.158a}$$

$$P_3(\eta_3) \propto [(\eta_3-0.5)^2 + (0.15)^2]^{-1} , \tag{4.158b}$$

$$P_5(\eta_5) \propto \exp[-3(1-\eta_5)] \quad , \tag{4.158c}$$

$$P_6(\eta_6) \propto 1+0.65 \cos(2\pi\eta_6) \quad . \tag{4.158d}$$

The heavy bias in (4.158a) toward low η_2-values indicates, according to (4.154b) and Fig. 14, that the configurations for which $\hat{k}_1$ and $\hat{k}_3$ are close together contribute strongly to the R-integrals. The additive constant 0.25 in (4.154c) was inserted to simplify the importance sampling on the η_3 variable in (4.158b).

The results of these special calculations for the R-integrals are presented and discussed in the next section.

4.5 Three-Collision Results

The "parallel calculations" of the R-, H- and C-integrals described in Section 4.3 were carried out by means of a computer program called Subroutine RHC. The "special calculation" of the R-integrals as described in Section 4.4 was carried out by means of a computer program called Subroutine RECOLL.

The results of the calculations of the R-integral are presented in Table viii. Eight runs were made with subroutine RHC and four runs were made with subroutine RECOLL. Each RHC run used 500,000 random points [with approximately 15% of them actually satisfying the conditions for non-zero theta functions $\Theta(\cos\theta_3')$ and Θ_{31} in eq. (4.89)], and required about 36 minutes of "cpu time", or 18 minutes of chargeable "core time", on the Univ. of Md. Univac 1108 Computer. Each RECOLL run used 200,000 random points [with approximately 52% of them actually satisfying the conditions for non-zero theta functions $\Theta(\cos\theta_c-\cos\theta)$ and $\Theta(\cos\theta_3)$ in eq. (4.157)], and required about 13 minutes of "cpu time", or 5 minutes of chargeable "core time", on the same computer. The agreement between the RHC results and the RECOLL results is seen to be quite satisfactory; in view of the considerable difference between the computation schemes outlined in Sections 4.3 and 4.4, this constitutes a very strong consistency check on our R-collision integrals. We take for our "best values" the averages of all twelve runs in Table viii; the uncertainties quoted in these "grand averages" evidently represent a conservative estimate of the 95% confidence limits.

The first four RHC runs listed in Table viii actually calculated the R-, H- and C-integrals simultaneously. The H- and C-results are presented in Tables ix and x. Like numbered runs in Tables ix, x and xi and in the

upper part of Table viii refer to the same physical computer run. We mentioned that each of these four runs used 500,000 random points in the 7-dimensional unit cube, and required about 36 minutes of "cpu time", or 18 minutes of chargeable "core time", on the Univ. of Md. Univac 1108 Computer. The percentages of the 500,000 points which satisfy the theta function requirements (i.e., the dynamical conditions) of the various diagrams were approximately as follows:

15.5% satisfied R ,
9.3% satisfied H ,
4.5% satisfied C ,

11.9% satisfied R only ,
3.6% satisfied H only ,
2.3% satisfied C only ,

3.6% satisfied R and H only ,
0.03%satisfied R and C only ,
2.1% satisfied H and C only ,
0.04% satisfied R and H and C.

Little objective significance can be attached to the above figures, since they will vary drastically with whether or not importance sampling is employed; these figures are for the importance sampling scheme described in eqs. (4.93).

Concerning the results obtained for the R-, H-, and C-collision integrals, we may note the following features.

1° The *sign* of the contribution from a given diagram is *usually* $(-1)^N$, where N is the number of non-interacting collisions

required by the diagram (N=0 for the R- and C-diagrams, N=1 for the H-diagram). Note that this rule holds for the Enskog (N=2) and SO(N=1) contributions as well. The *only exceptions* to this rule seem to be the H-diagram contribution to the viscosity (which is positive instead of negative) and the C-diagram contribution to the viscosity (which is evidently consistent with zero).

2° The C-diagram contributes least of the three-collision diagrams.

3° For the thermal conductivity and the viscosity, the H-diagram contributes more strongly than the R-diagram.

4° For the self-diffusion, the R- and H-contributions are both large and of comparable size, but are of opposite sign. Thus, the R- and H-contributions largely cancel each other for the self-diffusion.

Results obtained for the total contributions from the sequences of three successive collisions are shown in Table xi. The totals $\lambda^*_{13}(1)$, $\eta^*_{13}(1)$ and $D^*_{13}(1)$ were calculated as separate averages of the *sums* of the R-, H- and C-integrands in the four main runs, i.e., first four runs, of Subroutine RHC. Since about 25% of the points which satisfied some one diagram also satisfied at least one other diagram, this procedure allowed us to incorporate whatever correlations were present in deducing error estimates for the total contributions. Thus the errors in the totals, such as $\lambda^*_{13}(1)$, are somewhat less than the combined uncertainties in $\lambda^*_{131}(1)$,

$\lambda^*_{132}(1)$ and $\lambda^*_{133}(1)$, and similarly for the viscosity and self-diffusion.

The results for the three-collision contributions are summarized in Table XIII. For the final values of these collision integrals we have selected the average values for the H- and C-collision integrals in Tables ix and x and the grand average for the R-collision integral in Table viii. The error estimates for the total three-collision contributions are obtained from the four main results in Table xi as discussed above.

The most outstanding feature of the net three-collision results is that $\lambda^*_{13}(1)$ is negative whereas $\eta^*_{13}(1)$ and $D^*_{13}(1)$ are both positive. The difference in sign between $\lambda^*_{13}(1)$ and $\eta^*_{13}(1)$ is traceable to the difference in sign between their H-diagram contributions, which dominates in both cases. We note that if the R-diagram contribution to the self-diffusion had not been doubled by the fact that the same two particles participate in the first and last collisions [see (4.76)], then $D^*_{13}(1)$ would have been dominated by its negative H-diagram contribution just as $\lambda^*_{13}(1)$ was.

Evidently, the three-collision contribution to $\lambda^*_1(1)$ tends to reinforce the single-overlap contribution, whereas the three-collision contributions to $\eta^*_1(1)$ and $D^*_1(1)$ tend to offset the respective single-overlap contributions.

In Chapter III we calculated the single-overlap integrals in two different ways, thus providing a consistency check on our computer programs. In this chapter we have calculated the R-collision integrals by two different proceedures, thus testing the consistency of

Table XIII

Summary of Three-collision Results

Coef.	= R-contribution	+ H-contribution	+ C-contribution	= Total
$\lambda^*_{13}(1)$	+0.0128±0.0002	-0.0307±0.0004	+0.0051±0.0003	-0.0128±0.0005
$\eta^*_{13}(1)$	+0.0101±0.0003	+0.0276±0.0004	-0.0001±0.0002	+0.0376±0.0005
$D^*_{13}(1)$	+0.0980±0.0008	-0.0917±0.0008	+0.0282±0.0007	+0.0345±0.0013

Note: All uncertainties represent 95% confidence limits.

these results as well. We note that the H- and C-collision integrals are computed from Subroutine RHC by the same logic as the R-collision integrals. In addition, however, it is possible to make a consistency check relating the procedure for calculating the H-collision integrals with the single-overlap collision integrals. We shall refer to this check as the "H-SO Test."

The "H-SO Test" is obtained by considering the collision integrals that account for the contributions from the NS-collision sequence in (2.25)

$$\{\psi,\chi\}^{(3)}_{NS} = \{\chi,\psi\}^{(3)}_{SN}; \quad \{\psi,\chi\}^{(\tilde{3})}_{NS} = \{\chi,\psi\}^{(\tilde{3})}_{SN} \quad , \tag{4.159}$$

The SN- and NS-collision sequences are represented schematically in Fig. 15. The SN-collision sequence is the same as that shown in Fig. 6b. The NS-collision sequence is related to the SN-collision sequence by time reversal. As pointed out in Section 3.1, the SN-collision sequence is obtained from Fig. 10 if we require $\tau'<\tau$, where τ' is the time that particles 2 and 3 separate. Thus the collision integrals (4.159) are given by the single-overlap collision integrals (3.1), (3.3) or (3.42) if we replace the integrand $A+\theta(\tau-\tau')B$ with $\theta(\tau-\tau')B$. They may thus be obtained directly from Subroutine OVRLAP if we drop the first term of the integrand $A+\theta(\tau-\tau')B$ in (3.42).

On the other hand, the NS-collision sequence may also be obtained from Fig. 12b, if we replace the condition $\bar{\tau}<\tau_2$ with the condition $\bar{\tau}>\tau_2$. Thus the same collision integrals may also be computed from Subroutine RHC by evaluating (4.89) for $\nu=2$, when the condition $\bar{\tau}<\tau_2$ is replaced with the

condition $\bar{\tau} > \tau_2$. Both procedures should yield the same results, since it follows from (4.159) that in the first Enskog approximation

$$\lambda_{SN}(1) = \lambda_{NS}(1), \quad \eta_{SN}(1) = \eta_{NS}(1), \quad D_{SN}(1) = D_{NS}(1) \quad . \tag{4.160}$$

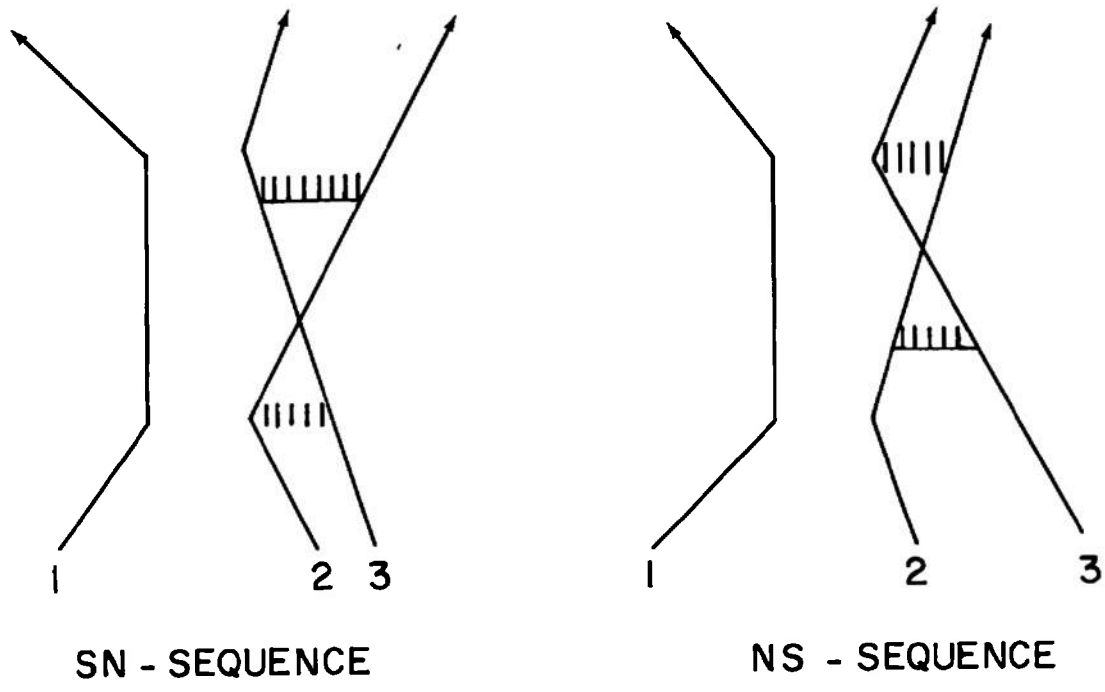

Fig. 15. The SN- and NS-collision sequences.

The results obtained for the SN-collision integrals (from Subroutine OVRLAP) and for the NS-collision integrals (from Subroutine RHC) are presented in Table xii. The agreement between the results obtained with the two different procedures is seen to be quite satisfactory.

The "H-SO Test" may also be formulated in the following way. If we drop the requirement $\bar{\tau}<\tau_2$ in the calculation of the H-collision integrals, Subroutine RHC yields the combined contributions from the H-collisions and NS-collisions. The results of these computations are given in Table xiii. The same results should be obtained if we add the H-collision integrals from Table ix to the NS-collision integrals obtained from Subroutine OVRLAP after replacing the integrand $A+\Theta B$ with ΘB. The latter values are presented in the last row of Table xiii. In view of the differences between the procedures used to evaluate the SO- and the H-integrals, this agreement constitutes almost as strong a check on our H-integrals in Subroutine RHC as Subroutine RECOLL did for the R-integrals.

Another attempt to calculate the three-collision integrals has been made by Condiff and coworkers [16,17]. As pointed out in AEDC-TR-72-142[3] they consider the collision integrals $\{\psi,\chi\}_R^{(3)}$, $\{\psi,\chi\}_{H+NS}^{(3)}$, $\{\psi,\chi\}_C^{(3)}$, together with the EVD-integrals defined in (3.66). Their results, therefore, should be compared with the numbers listed in Tables vii, viii, xiii and x. The computer results, found originally by Condiff and coworkers, differed in various aspects from the numerical results presented in this report. However, after making a comparison with our results they were able to locate some errors in their original calculations. At the time of this writing, Condiff has informed us that his group has now been able to confirm the results presented in this report [17].

CHAPTER V

SEQUENCES OF FOUR SUCCESSIVE COLLISIONS

5.1 Introduction

In this chapter we consider the contributions from four successive collisions among three molecules ($\mu=4$). The corresponding collision integrals

$$\{\psi,\chi\}_4^{(3)} = \sum_{\nu=1}^{2}\left[\{\psi,\chi\}_{4\nu}^{(3)} + \{\chi,\psi\}_{4\nu}^{(3)}\right] ,$$

$$\{\psi,\chi\}_4^{(\tilde{3})} = \sum_{\nu=1}^{2}\left[\{\psi,\chi\}_{4\nu}^{(\tilde{3})} + \{\chi,\psi\}_{4\nu}^{(\tilde{3})}\right] , \tag{5.1}$$

were defined in (2.32) and (2.33). They are related to the RH-collision sequence ($\nu=1$) and RC-collision sequence ($\nu=2$) shown in Fig. 8. We shall only evaluate the four-collision contribution to the transport coefficients in the first Sonine approximation. In this approximation $\psi=\chi$ so that we consider

$$\{\psi,\psi\}_4^{(3)} = 2\sum_{\nu=1}^{2}\{\psi,\psi\}_{4\nu}^{(3)} ,$$

$$\{\psi,\psi\}_4^{(\tilde{3})} = 2\sum_{\nu=1}^{2}\{\psi,\psi\}_{4\nu}^{(\tilde{3})} . \tag{5.2}$$

The geometry of the RH-collision sequence and the RC-collision sequence is shown schematically in Fig. 16. In analogy to the procedure followed in Chapter III and IV we define

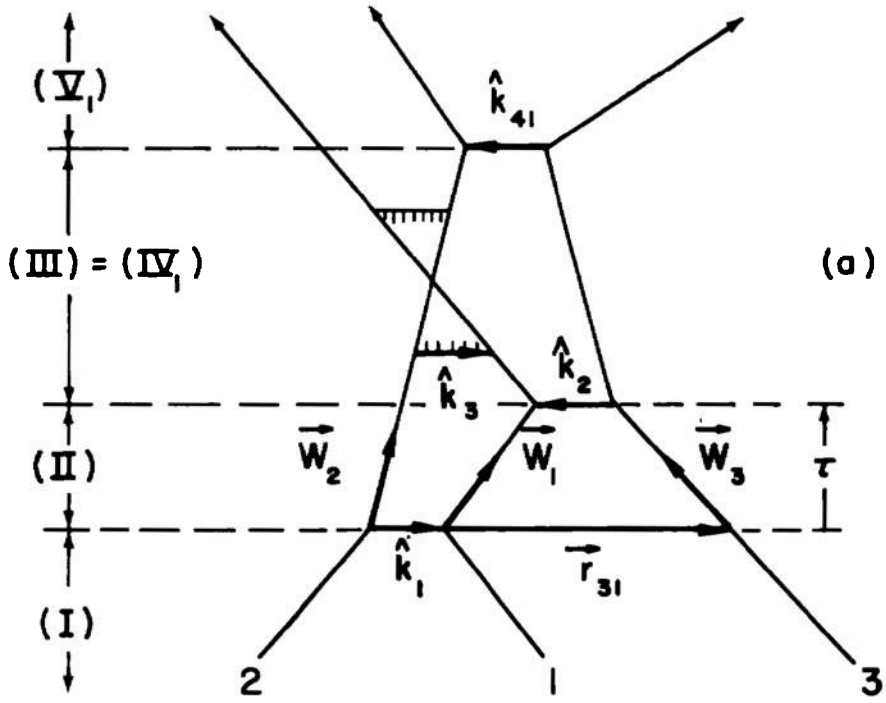

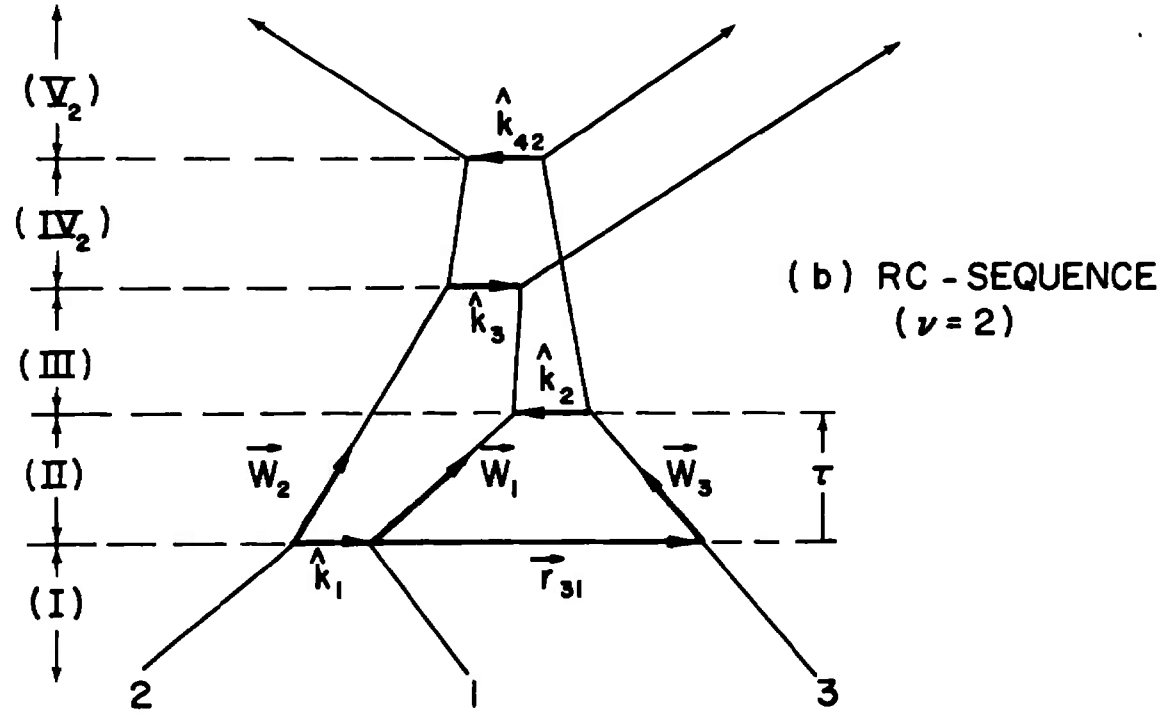

Figure 16. Diagrams associated with $\{\psi,\chi\}_4^{(3)}$ and $\{\psi,\chi\}_4^{(\tilde{3})}$.

$$(\alpha,\alpha)_{4\nu} \equiv (-1)^{\nu} \frac{6\sqrt{2}}{10\pi^6} \int_{\Omega_{4\nu}} d\vec{W}_0 d\vec{W}_{12} d\vec{W}_{31} d\hat{k}_1 d\hat{k}_2 d\tau \tag{5.3}$$

$$\times |\vec{W}_{12}\cdot\hat{k}_1||\vec{W}_{31}\cdot\hat{k}_2| e^{-3W_0^2-E}\{\alpha(I)-\alpha(II)\}*\{\alpha(V_\nu)-\alpha(IV_\nu)\},$$

where the integration variables $\vec{W}_0, \vec{W}_{12}, \vec{W}_{31}, \hat{k}_1, \hat{k}_2$ and the quantity E are the same as in Section 4.4 for the R-integrals. In terms of the integral form (5.2) we may rewrite the collision integrals (5.3) as

$$\{\psi,\psi\}_4^{(3)} = \sum_{\nu=1}^{2} (\Psi,\Psi)_{4\nu} \quad , \tag{5.4a}$$

where $\Psi = \sum_{m=1}^{3} \psi_m$ as in (2.42), and

$$\{\psi,\psi\}_4^{(\bar{3})} = 2 \sum_{\nu=1}^{2} (\psi_2,\psi_2)_{4\nu}. \tag{5.4b}$$

In (5.4b) we use the fact that only particle 2 is involved in both the first and last collisions; thus only the n=2 term in (2.33b) yields a non-vanishing contribution.

We observe from Fig. 16 that velocity regions I, II and III are the same for the RH- and RC-diagrams, and in fact coincide with the first three velocity regions of the R-diagram in Fig. 12. In other words, the functional dependence of the vectors $\vec{W}_{12}(I), \vec{W}_{31}(I), \vec{W}_{12}(III), \vec{W}_{31}(III)$ and $\hat{k}_3$ upon the

integrating variables $\vec{W}_{12}\equiv\vec{W}_{12}(II)$, $\vec{W}_{31}\equiv\vec{W}_{31}(II)$, $\hat{k}_1$, $\hat{k}_2$ and τ are the *same* for the RH-, RC- and R-diagrams; they are again given by (4.3), (4.4) and (4.19a). For the RH-diagram (ν=1) we want the third collision with perihelion vector $\hat{k}_3$ to be *non-interacting* and followed by an interacting collision between particles 2 and 3. For the RC-diagram we want the third collision with perihelion vector $\hat{k}_3$ to be *interacting* and followed by an interacting collision between particles 2 and 3. Clearly, then, the integrating volumes Ω_{41} and Ω_{42} in (5.3) are each *subvolumes* of Ω_R, the R-diagram integrating volume. Thus, we define theta functions $\Theta_{4\nu}$ by

$$\Theta_{4\nu} \equiv \begin{cases} 1, \text{ if } \vec{W}_0,\vec{W}_{12},\vec{W}_{31},\hat{k}_1,\hat{k}_2,\tau \text{ are such that, if the } \hat{k}_3 \text{ collision} \\ \quad \text{be made } \{\nu=1\text{: non-interacting}/\nu=2\text{: interacting}\}, \text{ then a} \\ \quad 2\text{-}3 \text{ collision will follow;} \\ 0, \text{ otherwise.} \end{cases} \tag{5.5}$$

Then (5.3) can be written as

$$(\alpha,\alpha)_{4\nu} = 2(-1)^{\nu}\frac{3\sqrt{2}}{10\pi^6}\int_{\Omega_R} d\vec{W}_0 d\vec{W}_{12} d\vec{W}_{31} d\hat{k}_1 d\hat{k}_2 d\tau\ |\vec{W}_{12}\cdot\hat{k}_1||\vec{W}_{31}\cdot\hat{k}_1| e^{-3W_0^2-E}$$

$$\times \Theta_{4\nu}\{\alpha(I)-\alpha(II)\}*\{\alpha(V_\nu)-\alpha(IV_\nu)\} \quad . \tag{5.6}$$

From eqs. (2.22), (2.23), (5.1) and (5.4) we see that the four-collision contribution to the transport coefficients is given by

$$\lambda^*_{14}(N) = \sum_{\nu=1}^{2} \lambda^*_{14\nu}(N) \quad ,$$

$$\eta^*_{14}(N) = \sum_{\nu=1}^{2} \eta^*_{14\nu}(N) \quad , \tag{5.7}$$

$$D^*_{14}(N) = \sum_{\nu=1}^{2} D^*_{14\nu}(N) \quad ,$$

where, for the first Sonine approximation (N=1),

$$\lambda^*_{14\nu}(1) = -\left(\sum_{m=1}^{3} S^{(1)}_{3/2}(W_m^2)\vec{W}_m, \sum_{n=1}^{3} S^{(1)}_{3/2}(W_n^2)\vec{W}_n \right)_{4\nu} \quad ,$$

$$\eta^*_{14\nu}(1) = -\left(\sum_{m=1}^{3} S^{(0)}_{5/2}(W_m^2)\vec{W}_m\vec{W}_m, \sum_{n=1}^{3} S^{(0)}_{5/2}(W_n^2)\vec{W}_n\vec{W}_n \right)_{4\nu} \quad , \tag{5.8}$$

$$D^*_{14\nu}(1) = -2\left(S^{(0)}_{3/2}(W_2^2)\vec{W}_2, S^{(0)}_{3/2}(W_2^2)\vec{W}_2 \right)_{4\nu} \quad .$$

In these last equations we may insert the explicit forms of the Sonine polynomials in Table I, and use the fact that $\Sigma_n \vec{W}_n$ and $\Sigma_n W_n^2$ do not change in a collision, to obtain the more explicit expressions

$$\lambda^*_{14\nu}(1) = -\left(\sum_{m=1}^{3} \vec{W}_m W_m^2, \sum_{n=1}^{3} \vec{W}_n W_n^2 \right)_{4\nu} \quad ,$$

$$\eta^*_{14\nu}(1) = -\left(\sum_{m=1}^{3} \vec{W}_m \vec{W}_m, \sum_{n=1}^{3} \vec{W}_n \vec{W}_n \right)_{4\nu} \quad , \tag{5.9}$$

$$D^*_{14\nu}(1) = -2\left(\vec{W}_2, \vec{W}_2 \right)_{4\nu} \quad ,$$

in terms of the integrals form (5.6).

5.2 Evaluation of RH- and RC-Integrals

According to (5.6) both the RH- and the RC-integrals may be formulated as integrals over the same region as the R-integrals. We therefore may adopt the same procedure as followed in evaluating the R-integrals. Of the two procedures for calculating the R-integrals described in Chapter IV, the special procedure described in Section 4.4 is better suited for this purpose, since it yields the higher efficiency ratio.

In view of the similarities between (5.6) and (4.122), it is clear that we may use the integrating variables specified in Fig. 14 and employ the same logic as that used in going from (4.122) to (4.133), to obtain

$$(\alpha,\alpha)_{4\nu} = -2(-1)^{\nu}\frac{12\sqrt{2}}{5\pi^4}\iiint_{\infty} d^3\vec{w}_o e^{-3w_0^2}\int_0^{\infty} dw_{12} w_{12}^6 e^{-w_{12}^2 E^*}$$

$$\times \int_0^1 d\cos\theta_1 \int_0^1 d\cos\theta_3 \int_0^{2\pi} d\phi_3 \int_0^{\pi} d\theta \int_0^1 d\cos\tilde{\theta} \int_0^{2\pi} d\tilde{\phi} \int_0^{\infty} dw'_{12}$$

$$\times \Theta(\theta-\theta_c)\frac{\delta w'^2_{12}\hat{w}'_{12}\cdot\hat{k}_3\cos\theta_1}{B\cos^3\tilde{\theta}}\Theta_{4\nu}\{\alpha(I)-\alpha(II)\}^*\{\alpha(V_\nu)-\alpha(IV_\nu)\} \quad . \qquad (5.10)$$

We recall from Section 4.4 that E^* is given by (4.127), θ_c is given by (4.98), δ is given by (4.112), B is given by (4.97), lower case w's denote velocities "scaled" according to (4.109), unprimed velocities refer to region II, primed velocities refer to region III, and the vectors $\hat{k}_1,\hat{k}_2,\hat{k}_3$, $\vec{w}_{12},\vec{w}'_{12}$ and $\vec{w}_{31}$ are given explicitly in terms of the integrating variables by (4.110)-(4.113). The velocities in regions I,II,III,IV_ν and V_ν are given in terms of the aforementioned vectors by the following equations [cf. (4.115)-(4.118) and Fig. 16]:

$$\begin{aligned} \vec{w}_{12}(I) &= \vec{w}_{12} - 2\vec{w}_{12}\cdot\hat{k}_1\hat{k}_1 \\ \vec{w}_{31}(I) &= \vec{w}_{31} + \vec{w}_{12}\cdot\hat{k}_1\hat{k}_1 \end{aligned} \quad , \tag{5.11}$$

$$\begin{aligned} \vec{w}_{12}(II) &= \vec{w}_{12} \\ \vec{w}_{31}(II) &= \vec{w}_{31} \end{aligned} \quad , \tag{5.12}$$

$$\begin{aligned} \vec{w}_{12}(III) &\equiv \vec{w}'_{12} \\ \vec{w}_{31}(III) &\equiv \vec{w}'_{31} \equiv \vec{w}_{31} - 2\vec{w}_{31}\cdot\hat{k}_2\hat{k}_2 \end{aligned} \quad , \tag{5.13}$$

$(\nu = 1)$

$$\begin{aligned} \vec{w}_{12}(IV_1) &= \vec{w}'_{12} \\ \vec{w}_{31}(IV_1) &= \vec{w}'_{31} \end{aligned} \quad , \tag{5.14}$$

$$\begin{aligned} \vec{w}_{12}(V_1) &= \vec{w}_{12}(IV_1) - \vec{w}_{32}(IV_1)\cdot\hat{k}_{41}\hat{k}_{41} \\ \vec{w}_{31}(V_1) &= \vec{w}_{31}(IV_1) - \vec{w}_{32}(IV_1)\cdot\hat{k}_{41}\hat{k}_{41} \end{aligned} \quad , \tag{5.15}$$

$(\nu = 2)$

$$\begin{aligned} \vec{w}_{12}(IV_2) &= \vec{w}'_{12} - 2\vec{w}'_{12}\cdot\hat{k}_3\hat{k}_3 \\ \vec{w}_{31}(IV_2) &= \vec{w}'_{31} + \vec{w}'_{12}\cdot\hat{k}_3\hat{k}_3 \end{aligned} \quad , \tag{5.16}$$

$$\begin{aligned} \vec{w}_{12}(V_2) &= \vec{w}_{12}(IV_2) - \vec{w}_{32}(IV_2)\cdot\hat{k}_{42}\hat{k}_{42} \\ \vec{w}_{31}(V_2) &= \vec{w}_{31}(IV_2) - \vec{w}_{32}(IV_2)\cdot\hat{k}_{42}\hat{k}_{42} \end{aligned} \quad . \tag{5.17}$$

We observe that the formulae (5.15) and (5.17) for the velocities in regions V_ν require the fourth collision vectors, $\hat{k}_{4\nu}$. The conditions for the existence of $\hat{k}_{4\nu}$ are of course precisely the conditions for $\Theta_{4\nu} = 1$ in (5.10), namely, that the positions and velocities of 2 and 3 immediately

following the third collision be such that 2 and 3 will indeed collide in the future. The position and velocity of 3 relative to 2 immediately following the third collision in diagram ν are as follows:

$$\vec{r} = \hat{k}_3 - \hat{k}_2 + (\vec{w}'_{31}/w'_{12})(B/\sin\theta) \quad , \tag{5.18a}$$

$$\vec{w}_\nu = \vec{w}_{31}(IV_\nu) + \vec{w}_{12}(IV_\nu) \quad . \tag{5.18b}$$

If we denote by τ' the time between the second and third collisions ($=\tau_1$ in Fig. 12), then (5.18a) follows from the two equations $w'_{12}\tau' = B/\sin\theta$ and $\vec{r} = \hat{k}_3 - \vec{w}'_{12}\tau' - \hat{k}_2 + \vec{w}'_{32}\tau'$, both of which can be deduced from the geometry of Fig. 14. We can be assured that $r^2 > 1$, i.e., that particles 2 and 3 are separated at the instant of the third collision, since otherwise the third collision would be an "overlap collision," in violation of the theorem which says that a collision sequence containing an overlap collision cannot contain more than three complete collisions [5,10].† Given $r^2 > 1$, the necessary and sufficient conditions for a future collision between 2 and 3 in diagram ν are [cf. eqs. (4.46)-(4.48)]:

$$\Theta_{4\nu}=1 \iff \begin{cases} \vec{w}_\nu \vec{r} < 0 \quad , \\ (\vec{w}_\nu \times \vec{r})^2 - w_\nu^2 < 0 \quad . \end{cases} \tag{5.19}$$

When both of these conditions are satisfied then the vector $\hat{k}_{4\nu}$ exists and is given by

---

†By the same theorem, we need not make sure that, in the RH-diagram, particles 1 and 2 separate before particles 2 and 3 collide in the fourth collision.

$$\hat{k}_{4\nu} = -r + \frac{\vec{w}_\nu \left[\vec{w}_\nu \cdot r + \sqrt{(\vec{w}_\nu \cdot r)^2 - w_\nu^2 (r^2-1)} \right]}{w_\nu^2} \tag{5.20}$$

We note in passing that the inner products appearing in the velocity change equations (5.15) and (5.17) can be shown from (5.18b) and (5.20) to be given by

$$\vec{w}_{32}(IV_\nu) \cdot \hat{k}_{4\nu} = + \sqrt{(\vec{w}_\nu \cdot \vec{r})^2 - w_\nu^2 (r^2-1)} \quad . \tag{5.21}$$

In summary, with $\vec{r}$ and $\vec{w}$ as defined in (5.18), $\Theta_{4\nu}$ in (5.10) is 1 or 0 according as conditions (5.19) are or are not both satisfied; further, if $\Theta_{4\nu} = 1$ then $k_{4\nu}$ is given by (5.20).

All quantities in the expression (5.10) for $(\alpha,\alpha)_{4\nu}$ are now well defined analytically. The functions α needed in (5.19) are polynomials in the velocities $\vec{w}_1$, $\vec{w}_2$, $\vec{w}_3$. Using the transformation equations (4.119), we now express these functions as polynomials in terms of the variables $\vec{w}_0$, $\vec{w}_{12}$ and $\vec{w}_{31}$. The $\vec{w}_0$-dependence is thereby rendered explicit, and the $\vec{w}_0$-integration in (5.10) can then be carried out analytically. The integrands will then involve only the velocities $\vec{w}_{12}$ and $\vec{w}_{31}$. Scaling according to (4.109) will then render the w_{21} dependence explicit, and the w_{12}-integration in (5.10) can then be carried out analytically. These operations transform eqs. (5.9) into [cf. (4.136)-(4.138)]

$$\lambda^*_{14\nu}(1) = -3(\vec{L}_1, \vec{L}_1)_{4\nu} - \frac{99}{4}(\vec{K}_1, \vec{K}_1)_{4\nu} \quad , \tag{5.22}$$

$$\eta^*_{14\nu}(1) = -\frac{9}{2}(\vec{L}_1, \vec{L}_1)_{4\nu} \quad , \tag{5.23}$$

$$D^*_{14\nu}(1) = -2(\vec{w}_{20}, \vec{w}_{20})_{4\nu} \quad , \tag{5.24}$$

where $\overleftrightarrow{L}_1$ and $\overleftarrow{K}_1$ are defined in (3.30) or (4.77), with the velocities $\overleftarrow{w}_{10}(i)$, $\overleftarrow{w}_{20}(i)$, $\overleftarrow{w}_{30}(i)$ given in the various regions i = I, II, III, IV_ν, V_ν according to (4.139), and where now $(\alpha,\alpha)_{4\nu}$ is given as the 7-dimensional integral form

$$(\alpha,\alpha)_{4\nu} = (-1)^{\nu-1}\frac{7\sqrt{6}}{4\pi^2}\int_0^1 d\cos\theta_1 \int_0^1 d\cos\theta_3 \int_0^{2\pi} d\phi_3 \int_0^{\pi} d\theta \int_0^1 d\cos\tilde{\theta} \int_0^{2\pi} d\tilde{\phi} \int_0^{\infty} dw'_{12}$$

$$\times\ \theta(\theta-\theta_c)\ \theta_{4\nu}\left(\frac{\delta w'^2_{12}(\hat{w}'_{12}\cdot\hat{k}_3)\cos\theta_1}{E^{*9/2}B\cos^3\tilde{\theta}}\right)\{\alpha(I)-\alpha(II)\}*\{\alpha(V_\nu)-\alpha(IV_\nu)\} \quad . \qquad (5.25)$$

The integral (5.25) is still not quite in a form suitable for evaluation by a Monte Carlo procedure. First, we have to choose a suitable change of variables $w'_{12} \to u$ which maps the infinite interval $0 < w'_{12} < \infty$ onto the finite interval $0 < u < 1$. After a detailed analysis of the w'_{12} behavior of the integrand in (5.25), it was determined that a suitable transformation is

$$u = \left(1 + w'^3_{12}\right)^{-1} \quad , \qquad (5.26a)$$

for which

$$w'^2_{12}dw'_{12} = -\frac{1}{3}\frac{du}{u^2} \quad . \qquad (5.26b)$$

Inserting this transformation into (5.25), we obtain

$$(\alpha,\alpha)_{4\nu} = (-1)^{\nu-1}\frac{7\sqrt{6}}{12\pi^2}\int_0^1 d\cos\theta_1 \int_0^1 d\cos\theta_3 \int_0^{2\pi} d\phi_3 \int_0^{\pi} d\theta \int_0^1 d\cos\tilde{\theta} \int_0^{2\pi} d\tilde{\phi} \int_0^1 du$$

$$\times\, \Theta(\cos\theta_c - \cos\theta)\; \Theta_{4\nu}\left(\frac{\delta(\hat{w}'_{12}\cdot\hat{k}_3)\cos\theta_1}{u^2 E^{9/2} B\cos^3\tilde{\theta}}\right) \{\alpha(I)-\alpha(II)\}*\{\alpha(V_\nu)-(IV_\nu)\} \quad , \qquad (5.27)$$

where it is henceforth understood that the variable w'_{12}

$$w'_{12} = \left(\frac{1-u}{u}\right)^{1/3} \quad . \qquad (5.28)$$

It remains now only to investigate the boundedness of the integrand in (5.27) with respect to the zeros of the quantities B and $\cos\tilde{\theta}$. This has essentially already been done in connection with the formula for $(\alpha,\alpha)_{31}$ in (4.142). However, it will be observed that the quantity in parenthesis in the integrand of (5.27) is *not* exactly the same as the product of the quantities in parentheses in the integrand of (4.142). The difference is due to the fact that, in (4.142), the velocity region differences are the *primed* differences defined in (4.135), whereas in (5.25) we have the ordinary unprimed differences. The point is that the extra factors $\cos\tilde{\theta}_1$ and $\hat{w}'_{12}\cdot\hat{k}_3$ in (4.142), which appeared respectively in the differences $\{\alpha(I)-\alpha(II)\}$ and $\{\beta(IV)-\beta(III)\}$, *both* played key roles in these boundedness considerations. Now, in (5.27), we will still get a factor of $\hat{w}'_{12}\cdot\hat{k}_1 = \cos\theta_1$ from the difference $\{\alpha(I)-\alpha(II)\}$; however, the quantity $\{\alpha(V_\nu)-\alpha(IV_\nu)\}$ will be proportional to $\hat{w}_{32}(IV_\nu)\cdot\hat{k}_{4\nu}$ instead of $\hat{w}'_{12}\cdot\hat{k}_3$. Hence, for (5.27) we need to examine the boundedness of the factor

$$\left(\frac{\delta(\hat{w}'_{12}\cdot\hat{k}_3)(\hat{w}_{32}(IV_\nu)\cdot\hat{k}_{4\nu})}{u^2E^{*9/2}\cos^3\tilde{\theta}}\right)\left(\frac{\cos^2\theta_1}{B}\right) \quad , \tag{5.29}$$

instead of what appears in (4.142).

The first factor in (5.29) differs from the first factor in (4.142) only in the replacement of one of the $\hat{w}'_{12}\cdot\hat{k}_3$ factors by $\hat{w}_{32}(IV_\nu)\cdot\hat{k}_{4\nu}$. Now, in analyzing the behavior of the first factor in (4.142), we found that the only possible divergence could occur for $\cos\tilde{\theta}$ near 0 *and* $\sin\theta$ near 0. A detailed analysis reveals that this situation can occur only when the first three collisions are all "grazing" collisions, in which the particles are always moving nearly parallel. From the RH- and RC-diagrams in Fig. 12, it is clear that in such a case the fourth collisions will necessarily be "grazing" collisions also, so that the $\hat{w}\cdot\hat{k}$ factor for that collision will likewise be very small. Therefore, we may expect the term $\hat{w}_{32}(IV_\nu)\cdot\hat{k}_{4\nu}$ to approach zero essentially as fast as $\hat{w}'_{12}\cdot\hat{k}_3$ approaches zero, at least, in the double limit $\tilde{\theta}\to\pi/2$ and $\theta\to 0$, so that the first factor in (5.29) should be always bounded just as the first factor in (4.142) was seen to be [cf. (4.147)].

The second factor in (5.29) is obviously the same as the second factor in (4.142). Now, in (4.151) we saw that this factor diverges like $1/\sin\theta'_3$ as $\theta'_3\to 0$, where θ'_3 is the angle between $\hat{k}_3$ and $\hat{k}_1$ [cf. Fig. 14]. We thus found it necessary to change variables from $(\cos\theta_3,\phi_3)$ to (θ'_3, ϕ'_3) according to (4.152). Eq. (5.27) then becomes

$$(\alpha,\alpha)_{4\nu} = (-1)^{\nu-1}\frac{7\sqrt{6}}{12\pi^2}\int_0^1 d\cos\theta_1 \int_0^{\pi} d\theta_3' \int_0^{2\pi} d\phi_3' \int_0^{\pi} d\theta \int_0^1 d\cos\tilde{\theta} \int_0^{2\pi} d\tilde{\phi} \int_0^1 du$$

$$\times \quad \Theta(\cos\theta_3)\,\Theta(\cos\theta_c-\cos\theta)\,\Theta_{4\nu}\left(\frac{\delta(\hat{w}_{12}'\cdot\hat{k}_3)\cos\theta_1\sin\theta_3'}{u^2E^{*9/2}B\cos^3\tilde{\theta}}\right)$$

$$\times \quad \{\alpha(I)-\alpha(II)\}*\{\alpha(V_\nu)-\alpha(IV_\nu)\} \quad , \tag{5.30}$$

where it is henceforth understood that the angles θ_3 and ϕ_3 are given by (4.148), and where the new theta function insures that the condition $\cos\theta_3 > 0$ will be fulfilled as was required by (5.27) [see also eq. (4.149)]. We shall not use primed differences in (5.30) as we did in (4.153), but it is clear that the integrand in (5.30) *taken as a whole* is a bounded function of all the integrating variables.

One last transformation of variables is made in preparation for the Monte Carlo calculations. In this transformation, we transform the 7-dimensional integrating region in (5.30) into a 7-dimensional unit cube according to [cf. (4.154)]

$$\cos\theta_1 = \eta_1 \quad , \tag{5.31a}$$

$$\theta_3' = \pi\eta_2 \quad , \tag{5.31b}$$

$$\phi_3' = 2\pi(\eta_3+0.25) \quad , \tag{5.31c}$$

$$\theta = \pi\eta_4 \quad , \tag{5.31d}$$

$$\cos\tilde{\theta} = \eta_5 \quad , \tag{5.31e}$$

$$\tilde{\phi} = 2\pi\eta_6 \quad , \tag{5.31f}$$

$$u = \eta_7, \; w_{12}'=[(1-u)/u]^{1/3} \quad . \tag{5.31g}$$

[The additive constant in (5.31c) is inserted to simplify the importance sampling procedure later.] The Jacobian of this transformation is $4\pi^4$ [cf. (4.155)], so we obtain as our *final formula* for $(\alpha,\alpha)_{4\nu}$

$$(\alpha,\alpha)_{4\nu} = (-1)^{\nu-1}\,\frac{7\sqrt{6}\pi^2}{3}\int_0^1 d\mathcal{R}_1\int_0^1 d\mathcal{R}_2\ \ldots\int_0^1 d\mathcal{R}_7$$

$$\times\ \Theta(\cos\theta_3)\ \Theta(\cos\theta_c-\cos\theta)\ \Theta_{4\nu}\left(\frac{\delta\hat{w}'_{12}\cdot\hat{k}_3\ \cos\theta_1\sin\theta'_3}{u^2_{E^*}{}^{9/2}B\cos^3\tilde{\theta}}\right)$$

$$\times\ \{\alpha(I)-\alpha(II)\}*\{\alpha(V_\nu)-\alpha(IV_\nu)\}\qquad . \tag{5.32}$$

Before summarizing the Monte Carlo computation algorithm for the four collision integrals, we first describe a trick which we used to essentially double the efficiency of our computational procedure. The philosophy of our computation of the RH- and RC-diagrams has obviously been to first construct an R-collision sequence [cf. Fig. 12], and then, by making the third collision {non-interacting/interacting}, to simply inquire as to whether or not particles 2 and 3 will subsequently collide, in which case we will have an {RH/RC} collision sequence. Our "trick" to increase our computing efficiency follows from the symmetry of the R-diagram and the invariance of all our integrals to a change in sign of all velocities: we could equally well place the fourth collision *before* the first collision in the R-diagram, provided we allow this collision with perihelion vector $\hat{k}_1$ to be non-interacting as well as interacting. In other words, once we have set up the collision vectors $\hat{k}_1$, $\hat{k}_2$ and $\hat{k}_3$, we can attempt to construct a four-collision sequence *either* by checking to see if 2 and 3 collide *after* the third collision with collision vector $\hat{k}_3$ *or* by checking to see if 2 and 3

collide *before* the first collision with collision vector $\hat{k}_1$. In the former case we make the check with the $\hat{k}_3$ collision penetrating as well as interacting, in order to check for both the RH- and RC-diagrams. In the latter case we make the check with the $\hat{k}_1$ collision separating as well as interacting for the same reason. In Part I of this series we have referred to the collision sequences thus obtained as HR- and CR-collision sequences [3]. It is thus possible to evaluate concurrently the RH- and RC-collision integrals as well as the HR- and CR-collision integrals. Since [3]

$$\{\psi\ \psi\}^{(3)}_{RH} = \{\psi,\psi\}^{(3)}_{HR} \quad , \qquad (5.33)$$

$$\{\psi\ \psi\}^{(3)}_{RC} = \{\psi,\psi\}^{(3)}_{CR} \quad ,$$

with a similar identity for the self-diffusions collision integrals, the two sets of integrals should be equal. By thus calculating *both* the RH- and RC-integrals *and* the HR- and CR-integrals, we obtain not only an important consistency check, but also two separate numerical estimates for the same collision integrals.

The relationship between these collision sequences is made more clear in Fig. 17. Fig. 17a shows schematically how the RH- and RC-collision sequences are constructed according to the treatment outlined thus far in this section. The regions between the first and third collisions are constructed from the R-diagram mathematically by setting the integration variables in (5.30) subject to the requirements imposed by the theta functions on $\cos\theta_3$ and $\cos\theta$. The region before the first collision is then determined, as is also the region after the third collisions. Of course, in the region after the third collision, we have *two situations* to investigate, namely, for the third collision non-interacting (ν=1) and interacting (ν=2)†. In each case we construct the velocity $\vec{w}_\nu$ and position vector $\vec{r}$ of 3 relative to 2 immediately after the third collision [cf. (5.18)], and, if conditions (5.19) are satisfied, we then construct the fourth collision vector $\hat{k}_{4\nu}$, thereby completing the RH- and/or RC diagram.

But there is another way of constructing sequences of four successive collisions and this method is illustrated by the diagram of Fig. 17b. We shall refer to this diagram as the "reversed" diagram to distinguish it from the "direct" diagram of Fig. 17a. In the reversed diagram, we shall denote the collision vectors by $\hat{\kappa}_i$ instead of $\hat{k}_i$, the scaled velocities by $\vec{\omega}_{ij}$ instead of $\vec{w}_{ij}$, and the velocity regions by lower case instead of upper case Roman numerals. The reversed diagram is "reversed" in the sense that it is of precisely the same structure as the direct diagram except for a reversal of all velocities; this may be seen by imagining the reversed

---

† For this reason we have not schematized the velocities of 1 and 2 in region IV_ν in Fig. 17a.

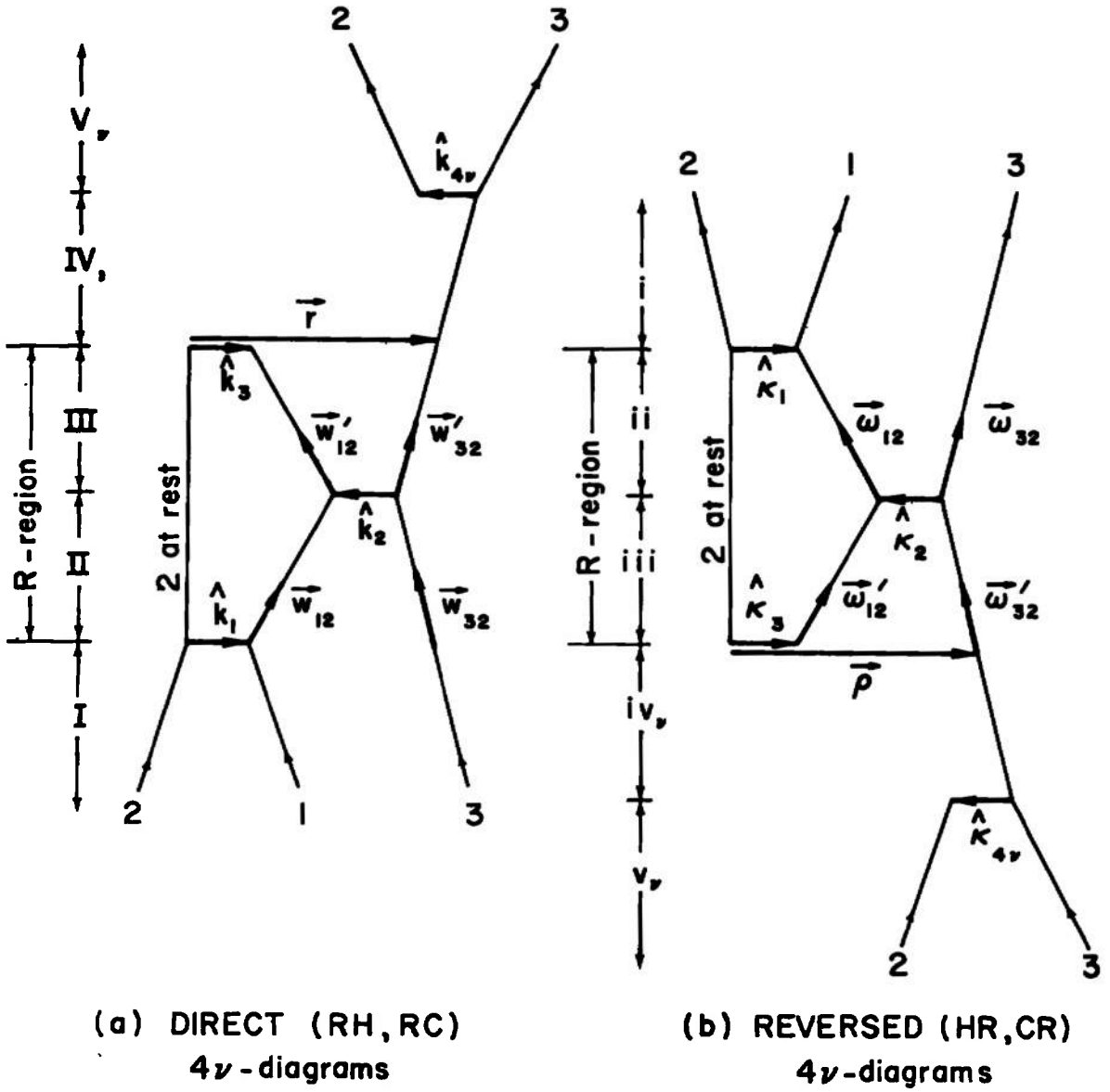

(a) DIRECT (RH, RC) 4ν-diagrams

(b) REVERSED (HR, CR) 4ν-diagrams

Figure 17. Relationship between RH- and RC-collisions (Fig. 17a) and HR- and CR-collisions (Fig. 17b).

diagram in Fig. 17b, together with its velocity region designations, to be turned upside down. Now, it is seen from the figure that some simple, direct relationships exist between the dynamical variables in the first four velocity regions of the two diagrams. Specifically, once the basic R-diagram has been set up, i.e., once a set of values for the integrating variables in (5.30) have been found which satisfy the theta function conditions on $\cos\theta_3$ and $\cos\theta$, then the dynamical variables in the first four velocity regions of the "reversed" diagram are obtained from those of the "direct" diagram according to the following formulae:

$$\hat{\kappa}_1 = \hat{k}_3 \quad , \tag{5.34a}$$

$$\hat{\kappa}_2 = \hat{k}_2 \quad , \tag{5.34b}$$

$$\hat{\kappa}_3 = \hat{k}_1 \quad , \tag{5.34c}$$

$$\left.\begin{aligned}
&\vec{\omega}_{ij}(\mathrm{i}) = \vec{w}_{ij}(\mathrm{IV}_2) && (5.35a)\\
&\vec{\omega}_{ij}(\mathrm{ii}) \equiv \vec{\omega}_{ij} = \vec{w}'_{ij} && (5.35b)\\
&\vec{\omega}_{ij}(\mathrm{iii}) \equiv \vec{\omega}'_{ij} = \vec{w}_{ij} && (5.35c)\\
&\vec{\omega}_{ij}(\mathrm{iv}_1) = \vec{\omega}'_{ij} = \vec{w}_{ij} && (5.35d)\\
&\vec{\omega}_{ij}(\mathrm{iv}_2) = \vec{w}_{ij}(\mathrm{I}) && (5.35e)
\end{aligned}\right\} \quad ij = 12,31 \quad .$$

We may then investigate whether the fourth collision occurs in the reversed diagram by a procedure similar to that used for the direct diagram [cf. the discussion of equations (5.18) - (5.20)]. Thus, letting $\vec{\rho}$ and $\vec{\omega}_\nu$ denote the position and velocity of 3 relative to 2 at the instant of the $\hat{\kappa}_3$ collision in the reversed ν-diagram, we have

$$\vec{\rho} = \hat{k}_1 - \hat{k}_2 - \vec{w}_{31}(B\cot\theta + \cos\theta_3 - \cos\theta_1) \tag{5.36a}$$

$$\vec{\omega}_\nu = \vec{w}_{31}(I) + \vec{w}_{12}(I) \quad . \tag{5.36b}$$

Since $\vec{\rho}$ is the position of 3 relative to 2 at the instant of the $\hat{k}_1$ collision, and since the scaled time τ^* between the $\hat{k}_1$ and $\hat{k}_2$ collisions is given by (4.130d) and (4.97), then (5.36a) follows directly from the relation $\vec{\rho} = \hat{k}_1 + \vec{w}_{12}\tau^* - \hat{k}_2 - \vec{w}_{32}\tau^*$, which relation is easily read off from Fig. 14. Now, the conditions on $\vec{\rho}$ and $\vec{\omega}_\nu$ which insure the existence of $\hat{\kappa}_{4\nu}$ are the same as those on $\vec{r}$ and $\vec{w}_\nu$ in the direct diagram, except we must take into account the fact that all velocities are reversed. Hence, from (5.19), the necessary and sufficient conditions for the existence of the fourth collision in the reversed ν-diagram are

$$\textit{reversed} \qquad \Theta_{4\nu} = 1 \iff \begin{cases} \vec{\omega}_\nu \cdot \vec{\rho} > 0 \\ (\vec{\omega}_\nu \times \vec{\rho})^2 - \omega_\nu^2 < 0 \end{cases} , \tag{5.37}$$

When both of these conditions are satisfied, then the vector $\hat{\kappa}_{4\nu}$ exists and is given by [cf. (5.20)]

$$\hat{\kappa}_{4\nu} = -\vec{\rho} + \vec{\omega}_\nu \frac{\left[\vec{\omega}_\nu \cdot \vec{\rho} - \sqrt{(\vec{\omega}_\nu \cdot \vec{\rho})^2 - \omega_\nu^2(\rho^2 - 1)}\right]}{\omega_\nu^2} \quad . \tag{5.38}$$

The velocities in region v_ν are then given by [cf. (5.15) and (5.17)]

$$\left.\begin{aligned} \vec{\omega}_{12}(v_\nu) &= \vec{\omega}_{12}(iv_\nu) - \vec{\omega}_{32}(iv_\nu)\cdot\hat{\kappa}_{4\nu}\hat{\kappa}_{4\nu} \\ \vec{\omega}_{31}(v_\nu) &= \vec{\omega}_{31}(iv_\nu) - \vec{\omega}_{32}(iv_\nu)\cdot\hat{\kappa}_{4\nu}\hat{\kappa}_{4\nu} \end{aligned}\right\} , \tag{5.39}$$

where [cf. (5.21)]

$$\vec{\omega}_{32}(iv_\nu)\cdot\hat{\kappa}_{4\nu} = -\sqrt{(\vec{\omega}_\nu\cdot\vec{\rho})^2 - \omega_\nu^2(\rho^2-1)} \quad . \tag{5.40}$$

In evaluating $(\alpha,\alpha)_{4\nu}$ for the HR- and CR-diagrams, we use the same formula (5.30) as for the RH- and RC-diagrams, but with two exceptions: first, we replace the $\Theta_{4\nu}$ condition (5.19) by the condition (5.37); and second, we replace the velocity functions α in (5.30) by

$$\alpha(I) \equiv \alpha(\vec{w}_{12}(I), \vec{w}_{31}(I)) \to \alpha(i) \equiv \alpha(\vec{\omega}_{12}(i), \vec{\omega}_{31}(i)) \quad , \tag{5.41}$$

and similarly for II → ii, $IV_\nu \to iv_\nu$ and $V_\nu \to v_\nu$.

Calculating simultaneously the RH-, RC-collision integrals and the HR-, CR-collision integrals provide us with a strong consistency check. The independence of the two procedures is further enhanced by the fact that a given set of values for the integrating variables in (5.30) can *never* satisfy both a direct and a reversed diagram; otherwise we would have a collision sequence containing a total of five complete collisions, which is known to be dynamically impossible [10,11]. Of course, nothing prevents a given point in the integrating region of (5.30) from simultaneously satisfying the conditions for an RH- and an RC-diagram in the direct mode, or from simultaneously satisfying the conditions for an HR- and CR-diagram in the reverse mode.

Operationally, it is thus a fairly simple matter to graft onto the procedure for calculating $(\alpha,\alpha)_{4\nu}$ in (5.32) for the RH- and RC-integrals. The Monte Carlo procedure for numerically evaluating the integral (5.32) is to average the integrand over a set of points

$\{P^i\} \equiv \{\eta_1^i, \eta_1^i, \ldots, \eta_7^i\}$ picked from a random, uniform distribution in the 7-dimensional unit cube U_7:

$$(\alpha,\alpha)_{4\nu} = \left\langle (-1)^{\nu-1} \frac{7\sqrt{6}\pi^2}{3} \Theta(\cos\theta_3)\, \Theta(\cos\theta_3 - \cos\tilde{\theta})\, \Theta_{4\nu} \left(\frac{\delta(\hat{w}'_{12}\cdot\hat{k}_3)\cos\theta_1 \sin\theta'_3}{u^2 E^{*9/2} B \cos^3\tilde{\theta}} \right) \right.$$

$$\left. \times \{\alpha(I) - \alpha(II)\} * \{\alpha(V_\nu) - \alpha(IV_\nu)\} \right\rangle_{U_7} . \qquad (5.42)$$

The uncertainty in estimating this average with a *finite* set of points $\{P^1, P^2, \ldots, P^M\}$ is given by the r.m.s. deviation of the quantity being averaged, divided by $\sqrt{M}$. Hence, our computational algorithm is as follows:

1° Generate 7 independent random numbers $\eta_1, \eta_2, \ldots, \eta_7$ from a uniform distribution in the unit interval.

2° Calculate the quantities θ_1, θ'_3, ϕ'_3, θ, $\tilde{\theta}$, $\tilde{\phi}$, u (and w'_{12}) from equations (5.31).

3° From θ_1, θ'_3 and ϕ'_3, calculate θ_3 and ϕ_3 from (4.148). Set the first theta function in (5.42) to 0 or 1 according to whether $\cos\theta_3$ [see (4.149)] is negative or positive. If $\cos\theta_3 < 0$ proceed to step 14° with all integrands equal to zero, noting that the coordinates η_4, η_5, η_6, η_7 have not been used and need not be regenerated for the next point.

4° From θ_1, θ_3 and ϕ_3, calculate $\cos\theta_c$ from (4.98) and set the second theta function in (5.42) to 0 or 1 according to whether $\cos\theta$ is greater or less than $\cos\theta_c$. If $\cos\theta > \cos\theta_c$, proceed to step 14° with all integrands equal to zero, noting that the coordinates η_5, η_6, η_7 have not been used and need not be regenerated for the next point.

5° Calculate B and ϕ according to (4.97) and (4.96). Calculate δ, θ_2 and w_{31} according to (4.112), (4.111) and (4.114).

6° Calculate the vectors $\hat{k}_1$, $\hat{k}_2$ and $\hat{k}_3$ according to (4.110b,c,e) Calculate the velocities $\vec{w}_{12}$ and $\vec{w}'_{12}$ according to (4.110a) and (4.110d). Calculate the velocity $\vec{w}_{31}$ according to (4.113) and calculate the velocity $\vec{w}_{31}$ according to (5.13).

7° From the region II velocities $\vec{w}_{12}$ and $\vec{w}_{31}$ and the collision vector $\hat{k}_1$, calculate the region I velocities according to (5.11). Similarly, from the region III velocities $\vec{w}_{12}$ and $\vec{w}_{31}$ and the collision vector $\hat{k}_3$, calculate the velocities in region IV_1 and IV_2 according to (5.14) and (5.16).

8° Set up the equivalent HR- and CR-diagram quantities in (5.34) and (5.35). [On the computer this can be accomplished automatically by means of the "equivalencing" operation.]

9° Calculate the vectors $\vec{r}$ and $\vec{w}_\nu$ according to (5.18), and put the *direct* $\Theta_{4\nu}$ equal to 1 or 0 according to whether $\vec{r}$ and $\vec{w}_\nu$ do or do not satisfy both inequalities in (5.19). If the inequalities are satisfied for $\nu = 1$ and/or 2, calculate the corresponding collision vector $\hat{k}_{4\nu}$ from (5.20) and the corresponding region V_ν velocities from (5.15) and/or (5.17)

[making use of (5.21)]. If, on the other hand, Θ_{41} and/or Θ_{42} is found to be zero, put the corresponding RH- and/or RC-integrands to zero.

10° Calculate the vectors $\vec{\rho}$ and $\vec{\omega}_\nu$ according to (5.36), and put the *reversed* $\Theta_{4\nu}$ equal to 1 or 0 according to whether $\vec{\rho}$ and $\vec{\omega}_\nu$ do or do not satisfy both inequalities in (5.37). If the inequalities are satisfied for ν = 1 and/or 2, calculate the corresponding collision vector $\hat{\kappa}_{4\nu}$ from (5.38) and the corresponding region v_ν velocities from (5.39) [making use of (5.40)]. If, on the other hand, Θ_{41} and/or Θ_{42} is found to be zero, put the corresponding HR- and/or CR-integrands to zero.

11° If *none* of the direct diagrams (RH, RC) or the reversed diagrams (HR, CR) is satisfied, proceed immediately to step 14° with all integrands equal to zero. If *any* of the four diagrams are satisfied, calculate E* according to (4.127) so that all the quantities in parentheses in (5.42) are now known, and proceed to the next step.

12° For each of the satisfied diagrams, calculate the velocities $\vec{w}_{10}$, $\vec{w}_{20}$, $\vec{w}_{30}$ (or their reversed diagram counterparts $\vec{\omega}_{10}$, $\vec{\omega}_{20}$, $\vec{\omega}_{30}$ in all velocity regions according to (4.139). Then evaluate the quantities $\vec{K}_1$ and $\vec{L}_1$ in all velocity regions according to (4.77).

13° Calculate the differences $\{\alpha(I)-\alpha(II)\}$ and $\{\alpha(V_\nu)-\alpha(IV_\nu)\}$, or their reversed diagram counterparts $\{\alpha(i)-\alpha(ii)\}$ and $\{\alpha(v_\nu)-\alpha(iv_\nu)\}$, for the appropriate diagram and the functions α required by (5.22) - (5.24).

14° Using the values found in the preceeding steps, evaluate the required integrands in angular brackets in (5.42), and also the squares of these integrands (for computing the variances), and add these to respective cumulating sums.

15° Return to 1°, and repeat for as many times M as is practical. Then convert the cumulating sums to averages, and so obtain the Monte Carlo estimates of the quantities (5.22) - (5.24), as calculated for both the "direct" diagrams (RH, RC) and the "reversed" diagrams (HR, CR), together with the uncertainties in these estimates.

In the actual calculations extensive use was made of the "equivalence" feature of Fortran, in order to facilitate nearly simultaneous treatments of the direct (RH, RC) and the reversed (HR, CR) diagrams. In addition, the double-precision mode was utilized in order to minimize the effects of computer round-off in the calculation of certain critical dynamical quantities. The RH-, RC-, HR- and CR-averages were all computed separately. We also computed the sum RH+RC, as required by (5.7), as the average of the sum of the RH- and RC-integrands in order to correctly assess the uncertainties in the final answer for the four-collision contribution to the transport coefficients; again, the same procedure was used to evaluate the combined contribution from the HR- and CR-diagrams.

As in all our Monte Carlo calculations, an empirically-determined "importance sampling" procedure was used to effect a substantial reduction in the uncertainties without increasing the number of sampling points used. This time the following importance sampling distributions were used [cf. (3.43) and the discussion thereof]:

$$P_1(\eta_1) \propto \exp(-5\eta_1) \quad , \qquad (5.43a)$$

$$P_2(\eta_2) \propto \exp(-10\eta_2) \quad , \qquad (5.43b)$$

$$P_3(\eta_3) \propto [(\eta_3-0.5)^2 + (0.05)^2]^{-1} \quad , \qquad (5.43c)$$

$$P_4(\eta_4) \propto \exp(-2.5\eta_4) \quad , \qquad (5.43d)$$

$$P_5(\eta_5) \propto \exp[-(1-\eta_5)] \quad , \qquad (5.43e)$$

$$P_6(\eta_6) \propto \exp[-2(1-\eta_6)] \quad , \qquad (5.43f)$$

$$P_7(\eta_7) \propto 1 + 0.85 \cos(2\pi\eta_7) \quad , \qquad (5.43g)$$

On the basis of preliminary computer runs made without importance sampling, we estimate that this procedure improved the efficiency of our calculations by a factor of roughly 200; i.e., we would have had to run on the computer for approximately 200 hours *without* importance sampling to obtain results comparable in accuracy to a 1 hour computer run *with* importance sampling. It is interesting to compare the above importance sampling scheme to that used in the special calculation of the R-diagram in (4.158), inasmuch as that calculation of the R-diagram forms the basis for our present calculation of the RH- and RC-diagrams. We note that we still employ a strong bias in favor of low η_2- values and values of η_3 near 1/2; but in addition, we have added a bias in favor of low η_1- values, and an oscillatory bias on η_7.

On the basis of the above importance sampling transformations, we have deduced that the following configurations contribute most strongly to the 4-collision integrals [cf. Fig. 14]:

- $\hat{k}_1$ very close to the Y-axis.
- $\hat{k}_3$ very close to $\hat{k}_1$, lying just above $\hat{k}_1$ in the YZ-plane.
- θ small
- w'_{12} very large for the "direct" diagrams and very small for the "reversed" diagrams.

The last point reveals that (5.43g) actually represents a "compromise" between the direct and reversed calculations. We might add that the realization of the R-diagram *alone* requires only the above condition on $\hat{k}_3$, and indeed favors values of θ near π over values near zero.

The results of our four-collision calculations are presented in the next section.

5.3 Four-Collision Results

The calculations of both the RH-, RC- and the HR-, CR-integrals were carried out in the manner described in the preceding sections by means of a computer program called Subroutine FOUR. In Tables xiv, xv, and xvi we present the results of four separate runs of Subroutine FOUR. Each run used 250,000 random points in the 7-dimensional unit cube, and required approximately 18 minutes of c.p.u. time on the NWC Univac 1108 Computer. The uncertainties in these tables represent again one standard deviation for the "runs" and two standard deviations for the "averages".

The results of the runs are statistically rather ragged, as is evidenced not only by the fluctuations in the *averages* from run to run,

but even more by the fluctuations in the *uncertainties* associated with these averages. In this respect, the results would have been considerably improved by a ten-fold increase in the number of sampling points used. However, what is most significant about these results is that they are five to six orders of magnitude smaller than the Enskog contribution (which is unity in our units); moreover, compared to the three-collision results in Table XIII, we have

$$\begin{aligned} |\lambda^*_{14}(1)| &\sim (0.2 \times 10^{-4}) \times |\lambda^*_{13}(1)| \quad , \\ |\eta^*_{14}(1)| &\sim (0.3 \times 10^{-4}) \times |\eta^*_{13}(1)| \quad , \\ |D^*_{14}(1)| &\sim (1.3 \times 10^{-4}) \times |D^*_{14}(1)| \quad . \end{aligned} \tag{5.44}$$

Thus, the four-collision contributions are roughly four orders of magnitude smaller than the three-collision contributions, and can therefore be neglected for all practical purposes. This can be regarded as the chief result of our four-collision calculations. From earlier preliminary studies of sequences of four successive collisions by Foch and Cohen [19] and by Sengers [4] it could be anticipated that the effect of these collision sequences on the transport coefficients would be small. The study reported here has now definitely established the order of magnitude of these correction terms.

Some remarks should perhaps be made concerning the handling of the uncertainties in Tables xiv, xv and xvi. We note that the total contributions presented in Table xvi are in each case equal to the sum of the individual terms:

$$\lambda^*_{14}(1) = \sum_{\nu=1}^{2} \lambda^*_{14\nu}(1), \; \eta^*_{14}(1) = \sum_{\nu=1}^{2} \eta^*_{14\nu}(1) \text{ and } D^*_{14}(1) = \sum_{\nu=1}^{2} D^*_{14\nu}(1) \quad .$$

However, it is seen that the uncertainties in $\lambda^*_{14}(1)$, $\eta^*_{14}(1)$ and $D^*_{14}(1)$ are *less* than what might be expected from the uncertainties in the separate contributions. It is emphasized, though, that the uncertainties in $\lambda^*_{14}(1)$, $\eta^*_{14}(1)$, $D^*_{14}(1)$ were calculated *directly* in the Monte Carlo program, by the device of averaging an integrand which was the sum of the integrands of the two separate terms (ν=1,2). The fact that the summed integrands had smaller uncertainties than expected merely indicates the presence of fluctuations in the separate integrands which were negatively correlated. We shall see how this came about more clearly below, but our point here is that the uncertainties quoted for $\lambda^*_{14}(1)$, $\eta^*_{14}(1)$, and $D^*_{14}(1)$ in Table xvi were honestly obtained. In calculating the uncertainties in the *averages* in Tables xiv, xv, and xvi, we used again the rule that the two-standard deviation uncertainty in the average of four repeated Monte Carlo runs is equal to the square root of the average of the *squares* of the *one*-standard deviations which were found in the runs. This is a generalization of the usual rule (namely, that the *constant* one-standard deviation found in four repeated runs can be regarded as two standard deviations for the average of the four runs) to cover the case in which the uncertainties in the repeated runs *vary* from run to run.

The crucial check on our calculations lies in comparing the results for the RH- and RC-integrals (top part of Tables xiv and xv) with the results for the HR- and CR-integrals, respectively (bottom part of Tables xiv and xv). The agreement is seen to be quite good, considerably better, in fact, than the agreement between different runs. This constitutes a very strong consistency check on our calculations of the four-collision integrals.

Our final results for the four-collision contributions are summarized in Table XIV.. These values were obtained by regarding the runs represented in Table xvi as eight independent, statistically equivalent runs. We note that the RH- (= HR-) integrals are all negative and that the RC- (= CR-) integrals are all positive. The RH-integrals yield the dominant contributions; the resultant four-collision contributions are thus all negative, although in the case of the thermal conductivity our statistics will evidently admit a small positive value, or even the null value. Again, in view of the extreme smallness of these four-collision quantities, their precise values are not terribly important.

We conclude with a few remarks concerning the efficiencies of these four-collision calculations:

1° Of the one million points sampled in the four runs, 48% were found to satisfy the basic R-diagram. Of these, 0.48% satisfied at least one of the direct diagrams, while 0.51% satisfied at least one of the reversed diagrams.

2° The percentage breakdown of all the points that satisfied either an RH- or an RC-diagram was (rather surprisingly) essentially the same as that of the points that satisfied either an HR-or a CR-diagram. This percentage was as follows:

99.9% satisfied RH ,
71% satisfied RC ,

29% satisfied RH only ,
0.1% satisfied RC only ,

71% satisfied RH and RC .

Table XIV

Summary of Four-Collision Results

Coef.	= RH-contribution	+ RC-contribution	= Total
$\lambda_{14}^{*}(1)$	$(-0.06\pm0.07)\times10^{-5}$	$(+0.04\pm0.03)\times10^{-5}$	$(-0.02\pm0.06)\times10^{-5}$
$\eta_{14}^{*}(1)$	$(-0.21\pm0.04)\times10^{-5}$	$(+0.11\pm0.03)\times10^{-5}$	$(-0.10\pm0.03)\times10^{-5}$
$D_{14}^{*}(1)$	$(-0.69\pm0.09)\times10^{-5}$	$(+0.25\pm0.04)\times10^{-5}$	$(-0.44\pm0.08)\times10^{-5}$

Note: All uncertainties represent 95% confidence limits.

What is noteworthy about these figures is that they imply that the RC-integrating region is about 7/10 the size of the RH-integrating region, and is *almost wholly contained inside* the RH-integrating region This large overlap between the RH- and RC-integrating regions is what allowed, e.g., the uncertainty in $\lambda^{\dagger}_{14}(1)$ to be considerably less that the combined uncertainties in $\lambda^{*}_{141}(1)$ and $\lambda^{*}_{142}(1)$.

While the foregoing efficiency figures are interesting, one ought not to read too much into them, since they are all relative to the particular set of dynamical variables used as well as the nature of the importance sampling procedures employed. The point is that the *size* of an integrating region can be changed simply by changing the integrating variables: only the *full integral* is invariant with respect to which set of integrating variables is employed.

Chapter VI

CONCLUSIONS

6.1 Summary of Results

We may now collect and combine the results of the calculations in the preceding three sections to obtain the *net* three-body contributions to the linear density transport coefficients in the first Sonine approximation. These final results are given in Table XV. In considering Table XV we recall from (2.21) that the kinetic contributions to the first density coefficients can be written in the Nth Sonine approximations as

$$\lambda_1^{KK}(N) = -\frac{5}{12}\pi\sigma^3\,\lambda_0(N)\sum_{\mu=1}^{4}\lambda_{1\mu}^*(N) \quad ,$$

$$\eta_1^{KK}(N) = -\frac{5}{12}\pi\sigma^3\,\eta_0(N)\sum_{\mu=1}^{4}\eta_{1\mu}^*(N) \quad , \tag{6.1}$$

$$D_1^{KK}(N) = -\frac{5}{12}\pi\sigma^3\,D_0(N)\sum_{\mu=1}^{4}D_{1\mu}^*(N) \quad .$$

Here $\lambda_0(N)$, $\eta_0(N)$ and $D_0(N)$ are the N^{th} Sonine approximation to the transport coefficients in the dilute limit as given by the Boltzmann equation, and σ is the diameter of the hard sphere molecules.

In these equations, the μ=1 terms are the "double-overlap" contributions which we have previously shown to be identical with the contributions estimated by Enskog [3]. Our definitions are such that these μ=1 terms are unity in all Sonine approximations. The remaining terms, the μ=2 "single-overlap' contributions, the μ=3 "three-collision" contributions, and the μ=4 "four-collision" contributions, are the

Table XV

Summary of Three-Particle Collision Contributions to the Transport Coefficients in the First Sonine Approximation

Coef.	(μ=1)	(μ=2)	(μ=3)	(μ=4)	Total
$\lambda^*_{1\mu}(1)$	1	-0.0303±0.0003	-0.0128±0.0005	(-0.02±0.06) × 10^{-5}	1 - (0.0431±0.0006)
$\eta^*_{1\mu}(1)$	1	-0.0633±0.0004	+0.0376±0.0005	(-0.10±0.03) × 10^{-5}	1 - (0.0257±0.0007)
$D^*_{1\mu}(1)$	1	-0.1195±0.0005	+0.0345±0.0013	(-0.44±0.08) × 10^{-5}	1 - (0.0850±0.0014)

Note: Uncertainties represent 95% confidence limits.

values tabulated in Table XV in the first Sonine approximation. From (2.18) and Table XV we thus conclude

$$\lambda_1^{KK}(1) = -\frac{5}{12}\pi\sigma^3 \lambda_0 [1-(0.0431 \pm 0.0006)]$$
$$\eta_1^{KK}(1) = -\frac{5}{12}\pi\sigma^3 \eta_0 [1-(0.0257 \pm 0.0007)] \qquad (6.2)$$
$$D_1(1) = -\frac{5}{12}\pi\sigma^3 D_0 [1-(0.0850 \pm 0.0014)]$$

We see that the net effect of the μ=2,3,4 contributions is to *decrease* the Enskog value by roughly 4.3% for the thermal conductivity, 2,6% for the viscosity, and 8.5% for the self-diffusion, in the first Sonine approximation.

The values quoted in Table XV all correspond to the first Sonine approximation . This approximation is entirely adequate to determine the relative contributions of the various three-particle collisions to the transport properties. With respect to the absolute value of these contributions, we found in Chapter III that the results for μ=2 changed somewhat when going to higher Sonine approximations, namely, by 3% for the viscosity η_{12}^*, 4% for the self-diffusion D_{12}^* and around 24% for the thermal conductivity λ_{12}^*. It is reasonable to expect that the higher Sonine approximation could affect the three-collision results (η_{13}^*, D_{13}^*, λ_{13}^*) by a similar amount. The contributions due to four successive collisions (μ=4) have been definitely established to be negligibly small.

An announcement of these results was included in a paper presented at the International Symposium "100 Years Boltzmann Equation" in Vienna [20].

It should be noted that (6.2) represents only the effect of three-particle collisions on the first density corrections to the transport properties. The full first density coefficients are given by (1.2) and (1.3).

$$\lambda_1 = \pi\sigma^3\lambda_0\left[\frac{4}{5} - \frac{5}{12}\{1 + \sum_{\mu=2}^{4} \lambda_{1\mu}^*\}\right] \quad ,$$

$$\eta_1 = \pi\sigma^3\eta_0\left[\frac{8}{15} - \frac{5}{12}\{1 + \sum_{\mu=2}^{4} \lambda_{1\mu}^*\}\right] \quad , \tag{6.3}$$

or

$$\lambda_1 = \frac{23}{60}\pi\sigma^3\lambda_0\left[1 - \frac{25}{23}\sum_{\mu=2}^{4} \lambda_{1\mu}^*\right] \quad ,$$

$$\eta_1 = \frac{7}{60}\pi\sigma^3\eta_0\left[1 - \frac{25}{7}\sum_{\mu=2}^{4} \eta_{1\mu}^*\right] \quad , \tag{6.4}$$

and

$$D_1 = -\frac{5}{12}\pi\sigma^3\lambda_0\left[1 + \sum_{\mu=2}^{4} D_{1\mu}^*\right] \quad . \tag{6.5}$$

The factors in front of the brackets in (6.4) and (6.5) represent the predictions of the theory of Enskog. Using the values of Table XV we conclude that the actual first density coefficients are

$$\boxed{\begin{aligned} \lambda_1(1) &= \frac{23}{60}\pi\sigma^3\lambda_0\,[1 + (0.0468 \pm 0.0007)] \quad , \\ \eta_1(1) &= \frac{7}{60}\pi\sigma^3\eta_0\,[1 + (0.0918 \pm 0.0025)] \quad , \\ D_1(1) &= -\frac{5}{12}\pi\sigma^3 D_0\,[1 + (0.0850 \pm 0.0014)] \quad , \end{aligned}} \tag{6.6}$$

where the numbers refer again to the first Sonine approximation. Thus the sequences of 2, 3, and 4 successive collisions modify the Enskog values for the *total* first density coefficients by 4.7% for the thermal conductivity, 9.2% for the viscosity and 8.5% for the self-diffusion.

6.2 Discussion of Results

Our results, presented in (6.2) and (6.6), show that the theory of Enskog accounts for over 90% of the total three-particle collision contribution. In Chapter I we mentioned that the theory of Enskog [$\mu=1$ in (6.1)] incorporates only excluded volume effects. The next term ($\mu=2$) contains some excluded volume effects via the single-overlap collisions and some dynamical effects via sequences of two successive collisions; from Table XV we see that the magnitude of this term is of the order of 10% or less compared to the Enskog value. The contributions from sequences of three successive collisions ($\mu=3$) is even slightly smaller, while the contributions from sequences of four successive collisions ($\mu=4$) appears to be negligible. As mentioned in Chapter I, the $\mu=3$ and $\mu=4$ terms represent effects that are of a purely dynamical nature.

The density dependence of the equilibrium properties of a gas of hard spheres is completely determined by excluded volume effects. We conclude that the density dependence of non-equilibrium properties, such as the transport properties, is dominated by the same excluded volume effects. The terms accounting for dynamical correlations due to sequences of successive collisions can profitably be treated as correction terms to the theory of Enskog.

A first attempt to estimate the effect of three-particle collisions on the transport coefficients was made by Sengers. He concluded from preliminary results [4,6,7,21]

$$\lambda_1^{KK}(1) = -\frac{5}{12}\pi\sigma^3\lambda_0\,[1-(0.05 \pm 0.02)] \quad ,$$

$$\eta_1^{KK}(1) = -\frac{5}{12}\pi\sigma^3\eta_0\,[1-(0.04 \pm 0.01)] \quad , \qquad (6.7)$$

$$D_1(1) = -\frac{5}{12}\pi\sigma^3 D_0\,[1-(0.09 \pm 0.04)] \quad .$$

These results were obtained before the three-particle collision integrals were separated according to the number of successive collisions. Our new more precise results in (6.2) evidently are in agreement with and improve upon these earlier preliminary estimates.

In principle, it is also possible to compute the transport coefficients as a function of density by molecular dynamics computations. For a gas of hard spheres such a study was made by Alder and coworkers [22,23]. However, while this method has been rather successful at high densities, molecular dynamics calculations become inaccurate at low densities and they do not yield accurate predictions for the first density coefficients λ_1, η_1, and D_1. In practice, therefore, our results complement the molecular dynamics work of Alder et al. by providing accurate estimates for the transport properties at moderate densities.

APPENDIX

TABLES OF THREE-PARTICLE COLLISION INTEGRALS

Table i

The Coefficients λ_{12}^*, η_{12}^* and D_{12}^* from 7-Dimensional Monte Carlo

First Sonine approximation: N=1			
Run	$\lambda_{12}^*(1)$	$\eta_{12}^*(1)$	$D_{12}^*(1)$
1	-0.0297±0.0003	-0.0629±0.0004	-0.1192±0.0004
2	-0.0300±0.0003	-0.0632±0.0004	-0.1201±0.0004
3	-0.0307±0.0003	-0.0636±0.0004	-0.1196±0.0005
4	-0.0307±0.0003	-0.0634±0.0004	-0.1192±0.0005
AVG	-0.0303±0.0003	-0.0633±0.0004	-0.1195±0.0005
Second Sonine approximation: N=2			
Run	$\lambda_{12}^*(2)$	$\eta_{12}^*(2)$	$D_{12}^*(2)$
1	-0.0242±0.0003	-0.0618±0.0004	-0.1157±0.0004
2	-0.0245±0.0003	-0.0621±0.0004	-0.1166±0.0004
3	-0.0251±0.0003	-0.0624±0.0004	-0.1159±0.0005
4	-0.0252±0.0003	-0.0622±0.0004	-0.1156±0.0005
AVG	-0.0248±0.0003	-0.0621±0.0004	-0.1160±0.0005

Note: Uncertainties in "runs" represent one standard deviation and uncertainties in "averages" represent two standard deviations.

Table ii

Matrix Elements $a_{k\ell}^{so}$, $b_{k\ell}^{so}$, $c_{k\ell}^{so}$ from 7-Dimensional Monte Carlo

Run	a_{11}^{so}	a_{12}^{so}	a_{21}^{so}	a_{22}^{so}
1	+0.0297±0.0003	-0.0330±0.0002	-0.0329±0.0002	-0.0260±0.0006
2	+0.0300±0.0003	-0.0329±0.0002	-0.0329±0.0002	-0.0255±0.0006
3	+0.0307±0.0003	-0.0333±0.0002	-0.0335±0.0002	-0.0245±0.0006
4	+0.0307±0.0003	-0.0328±0.0002	-0.0330±0.0002	-0.0244±0.0006
AVG	+0.0303±0.0003	-0.0330±0.0002	-0.0331±0.0002	-0.0251±0.0006
Run	b_{00}^{so}	b_{01}^{so}	b_{10}^{so}	b_{11}^{so}
1	+0.0629±0.0004	-0.0192±0.0002	-0.0191±0.0002	+0.0666±0.0007
2	+0.0632±0.0004	-0.0192±0.0002	-0.0193±0.0002	+0.0666±0.0007
3	+0.0636±0.0004	-0.0198±0.0002	-0.0198±0.0002	+0.0677±0.0007
4	+0.0634±0.0004	-0.0195±0.0002	-0.0196±0.0002	+0.0673±0.0007
AVG	+0.0633±0.0004	-0.0194±0.0002	-0.0195±0.0002	+0.0671±0.0007
Run	c_{00}^{so}	c_{01}^{so}	c_{10}^{so}	c_{11}^{so}
1	+0.1192±0.0004	-0.0396±0.0003	-0.0393±0.0003	-0.0324±0.0008
2	+0.1201±0.0004	-0.0400±0.0003	-0.0399±0.0003	-0.0332±0.0008
3	+0.1196±0.0005	-0.0406±0.0003	-0.0402±0.0003	-0.0305±0.0008
4	+0.1192±0.0005	-0.0399±0.0003	-0.0401±0.0003	-0.0307±0.0008
AVG	+0.1195±0.0005	-0.0400±0.0003	-0.0399±0.0003	-0.0317±0.0008

Note: Uncertainties in "runs" represent one standard deviation and uncertainties in "averages" represent two standard deviations.

Table iii

Comparison with Previous Single-Overlap Results

	AEDC-TR-71-51[5]	This work
a_{11}^{so}	+0.028±0.002	+0.0303±0.0003
a_{12}^{so}	-0.033±0.001	-0.0330±0.0002
a_{21}^{so}	-0.033±0.001	-0.0331±0.0002
a_{22}^{so}	-0.028±0.003	-0.0251±0.0006
b_{00}^{so}	+0.063±0.002	+0.0633±0.0004
b_{01}^{so}	-0.019±0.001	-0.0194±0.0002
b_{10}^{so}	-0.020±0.001	-0.0195±0.0002
b_{11}^{so}	+0.063±0.004	+0.0671±0.0007
c_{00}^{so}	+0.118±0.002	+0.1195±0.0005
c_{01}^{so}	-0.039±0.001	-0.0400±0.0003
c_{10}^{so}	-0.040±0.001	-0.0399±0.0003
c_{11}^{so}	-0.032±0.003	-0.0317±0.0008
$\lambda_{12}^{*}(1)$	-0.028±0.002	-0.0303±0.0003
$\lambda_{12}^{*}(2)$	-0.023±0.002	-0.0248±0.0003
$\eta_{12}^{*}(1)$	-0.063±0.002	-0.0633±0.0004
$\eta_{12}^{*}(2)$	-0.062±0.002	-0.0621±0.0004
$D_{12}^{*}(1)$	-0.118±0.002	-0.1195±0.0005
$D_{12}^{*}(2)$	-0.115±0.002	-0.1160±0.0005

Note: Uncertainties represent two standard deviations or 95% confidence limits.

Table iv

Successive Sonine Approximations from 11-Dimensional Monte Carlo

Run	$\lambda_{12}^{*}(1)$	$\lambda_{12}^{*}(2)-\lambda_{12}^{*}(1)$	$\lambda_{12}^{*}(3)-\lambda_{12}^{*}(2)$	$\lambda_{12}^{*}(4)-\lambda_{12}^{*}(3)$
1	-0.029±0.001	+0.0058±0.0003	+0.0015±0.0001	+0.00038±0.00003
2	-0.029±0.001	+0.0057±0.0003	+0.0013±0.0001	+0.00034±0.00004
3	-0.032±0.001	+0.0060±0.0004	+0.0014±0.0001	+0.00036±0.00003
4	-0.031±0.001	+0.0054±0.0003	+0.0014±0.0001	+0.00031±0.00003
AVG	-0.030±0.001	+0.0057±0.0003	+0.0014±0.0001	+0.00035±0.00003

Run	$\eta_{12}^{*}(1)$	$\eta_{12}^{*}(2)-\eta_{12}^{*}(1)$	$\eta_{12}^{*}(3)-\eta_{12}^{*}(2)$
1	-0.066±0.001	+0.0010±0.0003	+0.00034±0.00006
2	-0.062±0.001	+0.0013±0.0002	+0.00032±0.00005
3	-0.063±0.001	+0.0013±0.0002	+0.00044±0.00006
4	-0.062±0.001	+0.0012±0.0002	+0.00041±0.00006
AVG	-0.063±0.001	+0.0012±0.0003	+0.00038±0.00006

Run	$D_{12}^{*}(1)$	$D_{12}^{*}(2)-D_{12}^{*}(1)$	$D_{12}^{*}(3)-D_{12}^{*}(2)$
1	-0.120±0.002	+0.0040±0.0004	+0.0011±0.0001
2	-0.117±0.002	+0.0039±0.0003	+0.0011±0.0001
3	-0.117±0.002	+0.0034±0.0003	+0.0011±0.0001
4	-0.121±0.002	+0.0028±0.0004	+0.0009±0.0001
AVG	-0.119±0.002	+0.0035±0.0004	+0.0011±0.0001

Note: Uncertainties in "runs" represent one standard deviation and uncertainties in "averages" represent two standard deviations.

Table v

Matrix Elements $a^{so}_{k\ell}$, $b^{so}_{k\ell}$, $c^{so}_{k\ell}$ from 11-Dimensional Monte Carlo

$a^{so}_{11} = +0.030 \pm 0.001$	$b^{so}_{00} = +0.063 \pm 0.001$	$c^{so}_{00} = +0.119 \pm 0.002$
$a^{so}_{12} = -0.034 \pm 0.002$	$b^{so}_{01} = -0.020 \pm 0.003$	$c^{so}_{01} = -0.039 \pm 0.003$
$a^{so}_{21} = -0.034 \pm 0.002$	$b^{so}_{10} = -0.020 \pm 0.003$	$c^{so}_{10} = -0.040 \pm 0.003$
$a^{so}_{22} = -0.027 \pm 0.006$	$b^{so}_{11} = +0.061 \pm 0.007$	$c^{so}_{11} = -0.026 \pm 0.008$
$a^{so}_{13} = -0.017 \pm 0.003$	$b^{so}_{02} = -0.011 \pm 0.004$	$c^{so}_{02} = -0.018 \pm 0.004$
$a^{so}_{31} = -0.015 \pm 0.003$	$b^{so}_{20} = -0.011 \pm 0.004$	$c^{so}_{20} = -0.020 \pm 0.004$
$a^{so}_{23} = -0.094 \pm 0.009$	$b^{so}_{12} = -0.11 \pm 0.02$	$c^{so}_{12} = -0.16 \pm 0.01$
$a^{so}_{32} = -0.095 \pm 0.009$	$b^{so}_{21} = -0.12 \pm 0.02$	$c^{so}_{21} = -0.16 \pm 0.01$
$a^{so}_{33} = -0.12 \pm 0.02$	$b^{so}_{22} = -0.09 \pm 0.05$	$c^{so}_{22} = -0.18 \pm 0.02$
$a^{so}_{14} = -0.005 \pm 0.003$		
$a^{so}_{41} = -0.007 \pm 0.003$		
$a^{so}_{24} = -0.07 \pm 0.01$		
$a^{so}_{42} = -0.06 \pm 0.01$		
$a^{so}_{34} = -0.15 \pm 0.02$		
$a^{so}_{43} = -0.16 \pm 0.02$		
$a^{so}_{44} = -0.21 \pm 0.03$		

Note: Uncertainties represent two standard deviations.

Table vi

Comparison Between 7-Dimensional and 11-Dimensional Monte Carlo Results

matrix elements	7-dimensional Monte Carlo	11-dimensional Monte Carlo
a_{11}^{so}	+0.0303±0.0003	+0.030±0.001
a_{12}^{so}	-0.0330±0.0002	-0.034±0.002
a_{21}^{so}	-0.0331±0.0002	-0.034±0.002
a_{22}^{so}	-0.0251±0.0006	-0.027±0.006
b_{00}^{so}	+0.0633±0.0004	+0.063±0.001
b_{01}^{so}	-0.0194±0.0002	-0.020±0.003
b_{10}^{so}	-0.0195±0.0002	-0.020±0.003
b_{11}^{so}	+0.0671±0.0007	+0.061±0.007
c_{00}^{so}	+0.1195±0.0005	+0.119±0.002
c_{01}^{so}	-0.0400±0.0003	-0.039±0.003
c_{10}^{so}	-0.0399±0.0003	-0.040±0.003
c_{11}^{so}	-0.0317±0.0008	-0.026±0.008
$\lambda_{12}^{*}(2)-\lambda_{12}^{*}(1)$	+0.0055±0.0001	+0.0057±0.0003
$\eta_{12}^{*}(2)-\eta_{12}^{*}(1)$	+0.0012±0.0001	+0.0012±0.0003
$D_{12}^{*}(2)-D_{12}^{*}(1)$	+0.0035±0.0001	+0.0035±0.0004

Note: Uncertainties represent two standard deviations.

Tabel vii

EVD Collision Collision from 7-Dimensional Monte Carlo

First Sonine approximation: N=1			
Run	$\lambda^*_{EVD}(1)$	$\eta^*_{EVD}(1)$	$D^*_{EVD}(1)$
1	-0.0260±0.0004	-0.0525±0.0004	-0.0949±0.0004
2	-0.0264±0.0004	-0.0532±0.0004	-0.0948±0.0004
3	-0.0261±0.0004	-0.0529±0.0004	-0.0946±0.0004
4	-0.0260±0.0004	-0.0522±0.0004	-0.0945±0.0004
AVG	-0.0261±0.0004	-0.0527±0.0004	-0.0947±0.0004
Second Sonine approximation: N=2			
Run	$\lambda^*_{EVD}(2)$	$\eta^*_{EVD}(2)$	$D^*_{EVD}(2)$
1	-0.0214±0.0004	-0.0514±0.0004	-0.0917±0.0004
2	-0.0219±0.0004	-0.0520±0.0004	-0.0916±0.0004
3	-0.0215±0.0004	-0.0517±0.0004	-0.0914±0.0004
4	-0.0214±0.0004	-0.0511±0.0004	-0.0913±0.0004
AVG	-0.0215±0.0004	-0.0516±0.0004	-0.0915±0.0004

Note: Uncertainties in "runs" represent one standard deviation and uncertainties in "averages" represent two standard deviations.

Table viii

R-Collision Integrals

Run	$\lambda^*_{131}(1)$	$\eta^*_{131}(1)$	$D^*_{131}(1)$
results from Subroutine RHC			
1	+0.0127±0.0002	+0.0102±0.0003	+0.0968±0.0007
2	+0.0129±0.0002	+0.0105±0.0003	+0.0978±0.0007
3	+0.0129±0.0002	+0.0096±0.0003	+0.0972±0.0008
4	+0.0128±0.0002	+0.0104±0.0003	+0.0979±0.0007
5	+0.0128±0.0002	+0.0101±0.0003	+0.0986±0.0008
6	+0.0127±0.0002	+0.0103±0.0003	+0.0992±0.0008
7	+0.0128±0.0002	+0.0102±0.0003	+0.0982±0.0008
8	+0.0127±0.0002	+0.0098±0.0003	+0.0968±0.0008
AVG	+0.0128±0.0002	+0.0101±0.0003	+0.0978±0.0008
results from Subroutine RECOLL			
1	+0.0129±0.0002	+0.0095±0.0003	+0.0986±0.0008
2	+0.0127±0.0002	+0.0099±0.0003	+0.0978±0.0008
3	+0.0128±0.0002	+0.0102±0.0003	+0.0984±0.0008
4	+0.0127±0.0002	+0.0102±0.0003	+0.0986±0.0008
AVG	+0.0128±0.0002	+0.0100±0.0003	+0.0984±0.0008
averages of all runs above			
GRAND AVG	+0.0128±0.0002	+0.0101±0.0003	+0.0980±0.0008

Note: Uncertainties in "runs" represent one standard deviation, and uncertainties in "averages" represent two standard deviations.

Table ix

H-Collision Integrals

Run	$\lambda^*_{132}(1)$	$\eta^*_{132}(1)$	$D^*_{132}(1)$
1	-0.0304±0.0004	+0.0272±0.0004	-0.0914±0.0008
2	-0.0307±0.0004	+0.0274±0.0004	-0.0912±0.0008
3	-0.0312±0.0004	+0.0280±0.0004	-0.0918±0.0008
4	-0.0306±0.0004	+0.0276±0.0004	-0.0924±0.0008
AVG	-0.0307±0.0004	+0.0276±0.0004	-0.0917±0.0008

Table x

C-Collision Integrals

Run	$\lambda^*_{133}(1)$	$\eta^*_{133}(1)$	$D^*_{133}(1)$
1	+0.0052±0.0003	-0.0003±0.0002	+0.0275±0.0006
2	+0.0050±0.0003	-0.0002±0.0002	+0.0287±0.0006
3	+0.0049±0.0004	-0.0002±0.0003	+0.0287±0.0011
4	+0.0055±0.0003	+0.0002±0.0002	+0.0277±0.0005
AVG	+0.0051±0.0003	-0.0001±0.0002	+0.0282±0.0007

Note: Uncertainties in "runs" represent one standard deviation, and uncertainties in "averages" represent two standard deviations.

Table xi

Total contributions from three successive collisions

Run	$\lambda^*_{13}(1)$	$\eta^*_{13}(1)$	$D^*_{13}(1)$
1	-0.0125±0.0005	+0.0371±0.0005	+0.0329±0.0012
2	-0.0129±0.0005	+0.0377±0.0005	+0.0352±0.0012
3	-0.0134±0.0006	+0.0373±0.0006	+0.0340±0.0015
4	-0.0123±0.0005	+0.0382±0.0005	+0.0333±0.0012
AVG	-0.0128±0.0005	+0.0376±0.0005	+0.0339±0.0013

Note: Uncertainties in "runs" represent one standard deviation, and uncertainties in "averages" represent two standard deviations.

Table xii

SN- and NS-Collision Integrals

SN-integrals from Subroutine OVRLAP			
Run	$\lambda^*_{SN}(1)$	$\eta^*_{SN}(1)$	$D^*_{SN}(1)$
1	-0.0038±0.0002	-0.0105±0.0003	-0.0250±0.0004
2	-0.0038±0.0002	-0.0102±0.0003	-0.0251±0.0004
3	-0.0038±0.0002	-0.0108±0.0003	-0.0249±0.0004
4	-0.0037±0.0002	-0.0101±0.0003	-0.0255±0.0004
AVG	-0.0038±0.0002	-0.0104±0.0003	-0.0251±0.0004

	NS-Integrals from Subroutine RHC		
Run	$\lambda^*_{NS}(1)$	$\eta^*_{NS}(1)$	$D^*_{NS}(1)$
1	-0.0041±0.0003	-0.0109±0.0004	-0.0251±0.0006
2	-0.0036±0.0003	-0.0105±0.0004	-0.0245±0.0006
3	-0.0040±0.0003	-0.0100±0.0004	-0.0243±0.0006
4	-0.0041±0.0003	-0.0105±0.0004	-0.0250±0.0006
AVG	-0.0040±0.0003	-0.0105±0.0004	-0.0247±0.0006

Note: Uncertainties in "runs" represent one standard deviation, and uncertainties in "averages" represent two standard deviations.

Table xiii

Combined Contributions from H- and NS-Collisions

Run	$\lambda_H^*(1)+\lambda_{NS}^*(1)$	$\eta_H^*(1)+\eta_{NS}^*(1)$	$D_H^*(1)+D_{NS}^*(1)$
from Subroutine RHC ignoring condition $\bar{\tau}<\tau_2$			
1	-0.0346±0.0007	+0.0180±0.0007	-0.1173±0.0013
2	-0.0342±0.0006	+0.0167±0.0007	-0.1180±0.0013
3	-0.0347±0.0006	+0.0170±0.0007	-0.1181±0.0013
4	-0.0338±0.0007	+0.0172±0.0007	-0.1158±0.0013
AVG	-0.0343±0.0007	+0.0172±0.0007	-0.1173±0.0013
from Subroutine RHC and Subroutine OVRLAP with integrand $A+\Theta B$ replaced with ΘB			
AVG	-0.0345±0.0006	+0.0172±0.0007	-0.1168±0.0012

Note: Uncertainties in "runs" represent one standard deviation, and uncertainties in "averages" represent two standard deviations.

Table xiv

RH- and HR-Integrals

RH-Integrals			
Run	$\lambda^*_{141}(1)\times10^5$	$\eta^*_{141}(1)\times10^5$	$D^*_{141}(1)\times10^5$
1	-0.07±0.11	-0.26±0.06	-0.80±0.14
2	-0.08±0.08	-0.23±0.04	-0.69±0.11
3	+0.05±0.06	-0.13±0.02	-0.42±0.05
4	-0.12±0.09	-0.24±0.06	-0.60±0.09
AVG	-0.08±0.09	-0.21±0.05	-0.63±0.10

HR-Integrals			
Run	$\lambda^*_{141}(1)\times10^5$	$\eta^*_{141}(1)\times10^5$	$D^*_{141}(1)\times10^5$
1	-0.20±0.06	-0.23±0.04	-0.67±0.09
2	-0.06±0.10	-0.24±0.06	-0.77±0.16
3	+0.16±0.14	-0.11±0.05	-0.82±0.19
4	-0.07±0.07	-0.22±0.05	-0.71±0.11
AVG	-0.04±0.10	-0.20±0.05	-0.75±0.14

Note: Uncertainties in "runs" represent one standard deviation and uncertainties in "averages" represent two standard deviations.

Table xv

RC- and CR-Integrals

RC-Integrals			
Run	$\lambda^*_{142}(1)\times10^5$	$\eta^*_{142}(1)\times10^5$	$D^*_{142}(1)\times10^5$
1	+0.04±0.04	+0.12±0.03	+0.28±0.06
2	+0.05±0.02	+0.09±0.02	+0.23±0.04
3	-0.02±0.04	+0.07±0.02	+0.20±0.03
4	+0.04±0.05	+0.13±0.04	+0.23±0.04
AVG	+0.03±0.04	+0.10±0.03	+0.24±0.04

CR-Integrals			
Run	$\lambda^*_{142}(1)\times10^5$	$\eta^*_{142}(1)\times10^5$	$D^*_{142}(1)\times10^5$
1	+0.07±0.03	+0.12±0.03	+0.23±0.05
2	+0.09±0.05	+0.16±0.05	+0.27±0.05
3	+0.04±0.03	+0.08±0.02	+0.30±0.07
4	+0.01±0.04	+0.11±0.04	+0.27±0.05
AVG	+0.05±0.04	+0.12±0.04	+0.27±0.06

Note: Uncertainties in "runs" represent one standard deviation and uncertainties in "averages" represent two standard deviations.

Table xvi

Total Contributions from Four Successive Collisions

RH + RC			
Run	$\lambda^*_{14}(1)\times10^5$	$\eta^*_{14}(1)\times10^5$	$D^*_{14}(1)\times10^5$
1	-0.03±0.10	-0.14±0.06	-0.52±0.13
2	-0.13±0.07	-0.14±0.04	-0.46±0.09
3	+0.03±0.04	-0.06±0.02	-0.22+0.03
4	-0.08±0.08	-0.11±0.03	-0.37±0.07
AVG	-0.05±0.08	-0.11±0.04	-0.39±0.09

HR + CR			
Run	$\lambda^*_{14}(1)\times10^5$	$\eta^*_{14}(1)\times10^5$	$D^*_{14}(1)\times10^5$
1	-0.13±0.05	-0.11±0.03	-0.44±0.07
2	+0.03±0.08	-0.08±0.04	-0.50±0.12
3	+0.20±0.13	-0.03±0.05	-0.52±0.17
4	-0.06±0.05	-0.11±0.03	-0.44±0.09
AVG	+0.01±0.08	-0.08±0.04	-0.48±0.12

Note: Uncertainties in "runs" represent one standard deviation and uncertainties in "averages" represent two standard deviations.

REFERENCES

1. S. Chapman and T. G. Cowling, *The Mathematical Theory of Non-uniform Gases,* (Cambridge Univ. Press, London and New York, 3rd. ed., 1970).
2. J. O. Hirschfelder, C. F. Curtiss and R. B. Bird, *Molecular Theory of Gases and Liquids,* (John Wiley, New York, 1954).
3. J. V. Sengers, M. H. Ernst and D. T. Gillespie, *Three-Particle Collision Integrals for Thermal Conductivity, Viscosity and Self-Diffusion of a Gas of Hard Spherical Molecules, Part I. Theory,* Technical Report AEDC-TR-72-142 (Arnold Engineering Development Center, Tenn., 1972). See also: J. V. Sengers, M. H. Ernst and D. T. Gillespie, J. Chem. Phys. 56, 5583 (1972).
4. J. V. Sengers, *Triple Collision Effects in the Thermal Conductivity and Viscosity of Moderately Dense Gases,* Technical Report AEDC-TR-69-68 (Arnold Engineering Development Center, Tenn., 1969).
5. D. T. Gillespie and J. V. Sengers, *Triple Collision Effects in the Thermal Conductivity and Viscosity of Moderately Dense Gases, Part II.,* Technical Report AEDC-TR-71-51 (Arnold Engineering Development Center, Tenn., 1971).
6. J. V. Sengers, in *Boulder Lectures in Theoretical Physics,* Vol. 9C, W. E. Brittin, ed. (Gordon and Breach, New York, 1967), pp. 335-374.
7. J. V. Sengers, in *Kinetic Equations,* R. L. Liboff and N. Rostoker, eds. (Gordon and Breach, New York, 1971), pp. 137-193.

8. E. A. Mason and T. H. Spurling, *The Virial Equation of State*, (Pergamon Press, New York, 1969).

9. D. T. Gillespie and J. V. Sengers, Proc. 5th Symposium on Thermophysical Properties, C. F. Bonilla, ed. (ASME, New York, 1970), pp. 42-54.

10. J. V. Sengers, D. T. Gillespie and W. R. Hoegy, Phys. Letters 32A, 387 (1970).

11. W. R. Hoegy and J. V. Sengers, Phys. Rev. A2, 2461 (1970).

12. J. V. Sengers, Phys. Fluids 9, 1333 (1966).

13. M. H. Ernst, J. R. Dorfmann, W. R. Hoegy and J. M. J. Van Leeuwen, Physica 45, 127 (1969).

14. D. Burnett, Proc. London Math. Soc. 39, 385 (1935).

15. D. T. Gillespie, *The Monte Carlo Method of Evaluating Integrals*, Technical Report (Earth and Planetary Sciences Division, Naval Weapons Center, China Lake, Cal., to be published).

16. W. D. Henline and D. W. Condiff, J. Chem. Phys. 54, 5346 (1971).

17. G. B. Brinser and D. W. Condiff, J. Chem. Phys. (in press).

18. J. Weinstock, Phys. Rev. 132, 470 (1963).

19. E. G. D. Cohen, in *Boulder Lectures in Theoretical Physics*, Vol. 8A (Univ. Colorado Press, 1966), Appendix I, p. 167.

20. J. V. Sengers, in *The Boltzmann Equation, Theory and Applications*, E. G. D. Cohen and W. Thirring, eds., Acta Physica Austriaca, Suppl. X, (Springer Verlag, Vienna and New York, 1973) pp. 177-208.

21. J. V. Sengers and F. W. Karriker, unpublished work (1966).

22. B. J. Alder, D. M. Gass and T. E. Wainwright, J. Chem. Phys. 53, 3813 (1970).

23. J. H. Dymond and B. J. Alder, Ber. Bunsenges. Phys. Chem, 75, 394 (1971).